Development and mathematical modelling of affinity system based on novel matrix

Onwuasoanya, Daniel I.

Award date:
1987

Awarding institution:
University of Bath

DEVELOPMENT AND MATHEMATICAL MODELLING OF AFFINITY SYSTEM BASED ON NOVEL MATRIX

A thesis submitted in partial fulfilment for the degree of

Doctor of Philosophy

in the School of Chemical Engineering

of the University of Bath

by

Daniel I. Onwuasoanya, (M.Sc.)

1987

ProQuest LLC
789 East Eisenhower Parkway
P.O. Box 1346
Ann Arbor, MI 48106-1346

DECLARATION

This thesis is based on work in the Department of Chemical Engineering (1984-1985) at the University College of Swansea/School of Chemical Engineering at the University of Bath (1985-1987) in partial fulfilment for the Degree of Doctor of Philosophy of the University of Bath. It is the original and independent work of the author except where specific references to other investigators are made.

No part of this thesis has been, or is currently being, submitted to any other University as a requirement for any degree.

Candidate.....

(D.I. Onwuasoanya)

Supervisor.....

(Prof. J.A. Howell)

Date 20/11/87.....

DEDICATION

To My Dad and Ifeka

ACKNOWLEDGEMENTS

I would like to thank Prof. J.A. Howell for his supervision of this work and Prof. W.J. Thomas for use of his computers.

Thanks are extended to the Federal Government of Nigeria for financial support and Bio-Isolates Ltd. for supply of raw materials.

The financial suport from ORS is gratefully acknowledged.

Finally, I would like to thank Mrs Judith Harbutt for typing this thesis.

CONTENTS

ABSTRACT

A novel and fast flow regenerated cellulose based support matrix was investigated for use in affinity separations. Separation performance and some of the factors affecting it were studied experimentally and theoretically with an aim of establishing the criteria for process scale prediction and optimization of its performance.

Two forms of the matrix support (membrane and sponge) to which Cibacron Blue 3GA has been attached (blue membrane and blue sponge) were used for separation of human serum albumin (HSA) from the human blood plasma. The performance of blue membrane (BM) and the sponge (BS) were found to be satisfactory in terms of capacity and product purity. Protein A-sponge capacity was comparable to other cellulosic matrix-protein A adsorbents.

Transport and bed parameters of the sponge packed in a column were investigated by means of tracer pulse response technique. This showed that the sponge had a high voidage and indicated relatively high but tolerable axial dispersion.

Mathematical modelling of the adsorption stage in column operation was carried out using non porous and axially dispersed plug flow models. It appeared from the comparison of experimental and predicted breakthrough curve (B.T.C.) that more than a single rate mechanism was involved in the determination of the shape of the B.T.C.

CHAPTER 1

INTRODUCTION

INTRODUCTION

Efficient and cost effective protein recovery and purification are very important for beneficial exploitation of commercially valuable proteins which are abundant in biological systems.

The most important sources of proteins are biological fluids such as blood, milk and urine; living cells such as plant and animal tissues; and microbial cells. Chase (1984a) has listed some compounds of commercial interest, including proteins, from biological sources. Recent advances in recombinant DNA technology have widened the range of commercially important proteins available from microbiological systems by opening up novel and important ways to use microbial cells to produce novel protein or proteins normally found only in higher organisms. Proteins as produced by biological sytems are present in dilute form and thus require large product streams. In addition, they are frequently only part of a complex mixture of similar materials or impurities, sensitive to a wide variety of environmental conditions such as high shear force, extreme pH, high temperatures and organic solvents. These factors have resulted in limited technological transfer from the well-established chemical engineering techniques to the relatively new downstream protein processing in biotechnology for production scale operations. For example, distillation and solvent extraction separation techniques well known in chemical industries have only limited applications in protein processing.

Protein recovery and purification are often complicated and can require multiple, separate operations. Because of this, the cost of the recovery and purification of proteins from recombinant DNA fermentations, for example, can contribute up to 90% of the overall processing cost (Dwyer , 1984). Various methods of protein recovery and purification have been used in laboratories for a long time. Some of the commonly used techniques include crossflow filtration, precipitation, molecular exclusion, electromigration and adsorption chromatography. Some of these protein processing techniques are discussed briefly below.

Crossflow filtration is a separation technique based on the ability of a membrane to pass some solution components and retard others on the basis of their molecular size. The system is arranged so that the flow of feed is parallel to the filter medium; the feed is re-circulated rapidly enough to prevent cake formation. Many different polymers are used and fabrication conditions are varied to make these membranes of different pore sizes. Ultrafiltration is one part of a spectrum of crossflow filtration techniques and has been applied to protein processing for some time. Ultrafiltration is mostly used in a protein purification scheme as a method for concentration and removal of salts and other smaller molecules from protein solutions. Concentration of up to 20% protein or more from very dilute protein solution and elimination of up to 99% of salt by this technique is typical. However, ultrafiltration technique can constitute a valuable means of achieving a purification of some desired proteins by exploiting differences in molecular weight (size) between required proteins and other unwanted proteins. For

example, plasma protein fractionation has been carried out using ultrafiltration-diafiltration (Mitra and Ng, 1986). Selectivity between protein mixtures, is however, low.

Protein recovery by precipitation is one of the earliest techniques for large-scale protein processing. Protein precipitation is caused by the aggregation of protein molecules caused by a change in their environment. Examples of such changes include increasing or decreasing ionic strength, changes of pH and changes in the dielectric constant of the solvent. Preparation of precipitate is achieved by the use of an agent, the precipitant. Commonly used precipitating agents include ammonium sulphate, especially for enzyme precipitation and alcohols. For large-scale work, the precipitation and concentration of proteins with solvents has been widely used. However, the flammable nature of the solvents together with a relatively high cost has led to a search for other methods, with the notable exception of serum fractionation. In this process, despite the introduction of other techniques, ethanol precipitation has reigned supreme since its introduction by Cohn et al. (1946). The selectivity of precipitation techniques is generally not high but for serum it offers the advantage of concurrent sterilisation.

Molecular exclusion of sieve chromatography fractionates proteins on the basis of molecular size. Gel filtration has been used for plasma protein fractionation (Curling, 1978). However, the major application of the gel chromatography in protein processing is mainly for desalting of protein solutions since the process is

in most cases slow for protein fractionation. The major drawbacks of gel chromatography are low capacity and low throughput.

Electromigration techniques for protein fractionation and purification depend on the migration of protein molecules through an electric field according to molecular size and charge. One important disadvantage of this method is the difficulty involved in scaled up processes. This is because heat generation depends on operating current; for large scale processes, unacceptable heat generation is inevitable and will not be conducive for processing of heat labile biostream.

Adsorption techniques now constitute the major purification methods for proteins. Adsorption techniques involve the selective removal of protein molecules from solution onto a solid phase from which they can be recovered by resolution into a second, appropriate solvent. These liquid-phase to solid-phase transfer processes include a variety of different techniques that are all characterized by a type of molecular interaction between the protein (solute) molecules and the surface of the adsorbing materials. McCormick (1987) has listed major types of liquid chromatography, including adsorption chromatography and the nature of interaction between solutes and adsorbing surface. Ion exchange and affinity techniques are the most commonly used fixed bed adsorption methods for protein processing. They are also the first and second most used techniques respectively for protein purification in general (Bonnerjea et al., 1986).

The ion exchange technique depends on the electrostatic interaction of proteins with surface modified by quarternary

aminoethyl (QAE), diethylaminoethyl (DEAE), sulfopropryl (SP), or carboxymethyl (CM) surface groups. Proteins are polyelectrolytes and can carry negative, positive or zero charges dependent upon the iso-electric point of the particular proteins, and the pH of the buffer containing it. This offers some possibility for selective adsorption of proteins on chosen ion exchangers. One advantage of ion-exchange techniques over other adsorption techniques such as affinity technique is relatively higher capacity, especially on the small scale. Selectivity is, however, not very high. One method with very high selectivity compared with any other method of protein purification is the affinity technique

The affinity technique is a form of adsorption specific to target molecules. Bioselective adsorption is based upon the complementary interaction of two molecules, for example, an enzyme and its immobilized substrate (ligand) or an antibody and a suitably immobilized ligand (an antigen). Affinity technique offers a means of obtaining very high purification of proteins in one step which would ordinarily require a multiple step application of other methods to achieve. It is a relatively new technique in comparison to the other aforementioned techniques; it offers the potential for innovative process development which is critical to the successful commercialization of biotechnology. Affinity technique is the subject of this thesis and will be discussed in greater detail in subsequent chapters.

In a typical protein purification scheme involving the recovery of proteins from crude product streams and subsequent purification, some or most of the above techniques may be involved

as unit operations in the overall process. Bonnerjea et al. (1986) have studied the sequence of the individual unit operations and found no strict sequence in studied numbers of purification schemes. However, they found that, for example, for protein isolation and purification from cells, homogenization is generally followed by precipitation, then ion-exchange chromatography, affinity separation, and finally, gel filtration. Ultrafiltration can be used in place of gel filtration or a pre-concentration stage before the application of ion-exchange and affinity steps in the above scheme. The sequence is a logical one (Bonnerjea et al, 1986). Precipitation can deal with large quantities of material and is less affected by interfering non-protein materials than adsorption and chromatography procedures. Affinity methods can be applied at an earlier stage, but the materials are very expensive, it makes sense to use less costly ion-exchange media first to reduce protein loads and remaining fouling materials. Gel filtration or diafiltration can be used to reduce salt concentration. A final concentration step using ultrafiltration can be applied to reduce bulk volume.

As has been mentioned earlier, efficient and cost effective protein purification is very important; affinity technique is a newer method and one which offers efficient and cost effective protein processing in biotechnology. To exploit the potentials of the affinity separation method, cheap matrix support, cheap and stable ligands, porous and fast flow matrix support are needed. In addition, information for the design and operation of large-scale affinity systems must be available. Cellulose based support matrix

is the cheapest source of support available but has the disadvantage of poor flow properties. The synthetic organic dyes as ligands are cheap and stable and therefore very suitable for large-scale applications; they have affinity for a variety of proteins. Information needed for a scaled-up process can be obtained from experimental observations and theoretical simulations based on appropriate models of the effect of important operating parameters on the performance of the affinity system under consideration.

The objective of this project is to investigate the use of a highly porous, fast flow cellulose based sponge support matrix in affinity separation. Special emphasis is on the use of Cibacron blue 3GA-sponge adsorbent for the separation of human serum albumin from human blood plasma. A model for the theoretical prediction of the affinity system performance will also be considered.

CHAPTER 2

REVIEW OF AFFINITY TECHNIQUE

2. AFFINITY TECHNIQUE: A REVIEW

2.1 DEVELOPMENT OF AFFINITY SEPARATION

The use of specific interactions of biological molecules as a means of purification or fractionation of proteins dates back to 1910 when a selective adsorption of amylase onto insoluble starch was carried out. This was followed by the immobilization of antigens on cellulose much later in 1951. The late adaptation of the affinity technique as a routine laboratory method for protein separations was due to the absence of suitable supports and lack of satisfactory techniques for immobilizing ligands onto matrices. The wide acceptance of affinity interactions as a powerful technique for the isolation and purification of biological macromolecules was due to the rapid development of the method from 1959 to 1968 and the refinements in the 1970s.

A rapid development of the technique resulted from the introduction of the first gel filtration of proteins by Porath and Flodin (1959) and especially so after Hjerten (1962) used agarose suspensions for chromatographic separations - agarose beads proved to be very good support. Further, Axen et al. (1967) and Porath et al. (1967) introduced simple and high yield techniques involving the activation of polysaccharide gels by means of cyanogen halides especially cyanogen bromide which made it easy to attach proteins or other ligands onto chromatographic supports. The problem of steric accessibility between immobilized ligand and the target molecule to be separated was resolved by Cuatrecsas et al. (1968) who introduced the concept of a spacer arm which interposes between the ligand and the support material. Further refinements were

carried out by Cuatrecasas et al. (1970) and Cuatrecasas (1970a,b).

Recent years have seen a marked increase in the use of affinity separation techniques in the biotechnological industry. This has resulted in a search for better adsorbent support materials to meet the requirements of large scale operations. The early works on affinity separations were carried out mainly with cellulose and later agarose matrices. The former has been criticized for its fibrous microcrystalline nature resulting in poor flow properties (high flow resistance and uneven flow distribution). Because of the cost attractiveness of a cellulose matrix attempts have been made (Peska, et al., 1976; Chen and Tsao, 1976; 1977) to prepare cellulose in bead-form which appears to be highly porous, chemically versatile and physically rigid. Chen and Tsao (1977) used the bead form for immobilization of glucoamylase and glucose isomerase and found an enzyme loading of 2-3 times that of commercially available cellulose. All these properties make cellulose bead a promising ideal candidate for a matrix support in affinity separations. However, the evidence of the wide use of cellulose beads in large-scale affinity separations after about a decade is yet to emerge. This is evident in almost complete absence of cellulose based support in commercially available adsorbents.

The agarose whose only unacceptable quality as an affinity support is low mechanical strength, is now available commercially as Sepharose which has been cross-linked to give mechanical strength.

Also commercially available are cross-linked dextran (with epichlorohydrin) as Sephadex, cross-linked polyacrylamide, porous

glass beads and porous silica beads.

The chemistry of the adsorbent preparation has also advanced a lot in the last decade. The isourea linkage resulting from the coupling of ligand or spacer arms onto matrices activated by the CNBr method encourages ionic adsorption on the matrix. This effect is non-specific and therefore undesirable for affinity separations. Another potential problem with cyanogen-bromide-activated polysaccharides is the stability of the isourea linkage. It was found that the coupled ligand or spacer arm continously leaks, especially under alkaline conditions (Yang and Tsao, 1982). Other methods of activation of affinity matrices have now emerged. The most notable of which are the carbonyldiimidazole method, periodate method, tosyl chloride method, bisepoxiranes and epichlorohydrin method, the hydrazine method and the benzoquinone method.

The small ligand affinity system of enzymes and other smaller proteins, metals, dyes and other substances have been added to the predominantly immunoaffinity systems of the early stages of development. As a result, a broad spectrum of affinity systems for the separation and purification of a large number of biological molecules are now available commercially.

The theoretical and analytical treatments which played little or no part in the early development of affinity separations are now quite common.

Despite the recent developments, the scale-up from the laboratories to the production plants has been slow. However, the recent upsurge in interest in biotechnology, especially in downstream processing seems set to remedy this situation in the near future.

2.2 THE BASIS OF AFFINITY SEPARATIONS

An affinity separation is based on the synthesis of an immobilised phase with specific activity for one particular compound or class of compounds and the use of this material in adsorption processes. A successful separation requires that a biospecific ligand is available and that it can be covalently attached to a chromatographic bed material, the matrix. It is also important that the immobilized ligand retains its specific binding affinity for the target molecules, and that methods are available for selectivity desorbing the bound substances in an active form, after washing away unbound material. The principle of affinity separation is depicted in Fig. 2.1.

Examples of affinity interactions most commonly encountered in affinity separations are shown as complementary partners in Table 2.1.Any one of the partners involved in an interaction process can either be used as a ligand or the target molecule to be separated specifically from a mixture of other biological compounds. It is necessary that the association constant between the ligand and the complementary molecules (adsorbate) is more than 10^3 M.

The matrix support shown in Fig. 2.1 does not necessarily have to be insoluble. In affinity adsorption the matrix support is insoluble, in affinity precipitation it is soluble, and in affinity partitioning it is soluble in one phase (usually water) but insoluble in the other of the two-phase systems.

Affinity adsorption is the subject of the present investigation.

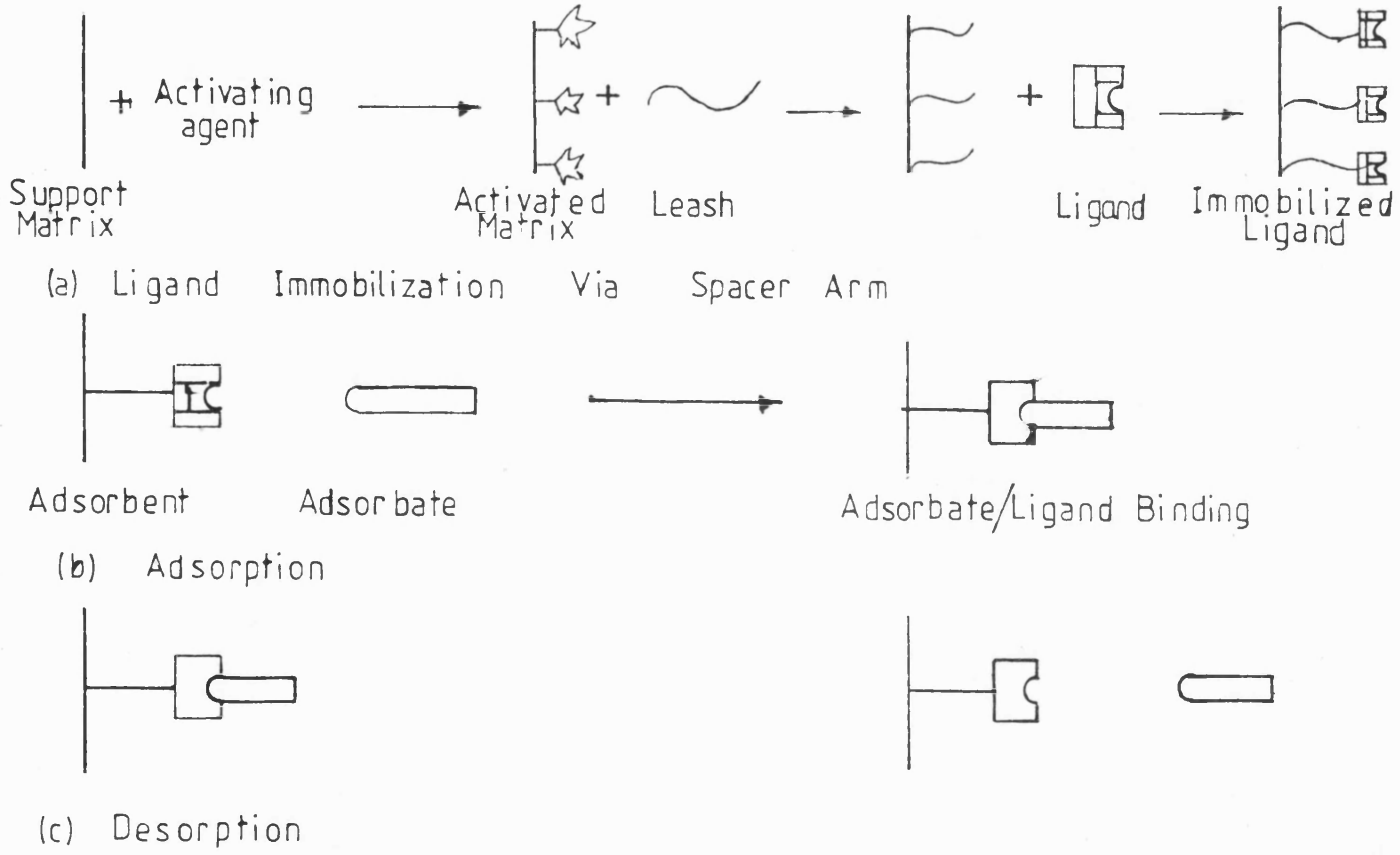

Fig. 2.1. Schematic Representation of Preparation of the Affinity System and the Main Steps in Affinity Separation.

Table 2.1. Principal Interacting Molecules Used in Affinity Separations.

BIOLOGICAL MATERIAL(S)	COMPLEMENTARY MOLECULE(S)
Enzymes	Substrate(s) analogue, inhibitor and cofactor
Antibodies	Antigen, virus, cell
Lectins	Polysaccharide, glycorprotein, cell surface receptor, cell
Nucleic acids	Histone, nucleic acid polymerase, binding protein and complementary base sequence
Receptors	Hormones, vitamins, toxins, growth factors
Aromatic groups containing macro molecules	Dyes
Metal interacting macromolecules	Metal ions

2.3 ADSORBENTS

In the majority of instances, an affinity adsorbent is composed of an inert support matrix, a spacer arm, and an immobilized ligand having affinity for the macromolecule under consideration. The types of adsorbents used in affinity separations are diverse. The diversity stems from the types of matrix support used for the immobilization of the ligands and the type of ligands immobilized. Also, the methods of attachment of the ligands to the

matrix supports vary because the functional groups via which the ligands are coupled, must not be those likely to be involved in the specific interaction which forms the basis of affinity separation. Different methods must therefore be used to couple ligands via thiol(-SH) groups or amino ($-NH_2$) groups onto the matrix support, for example.

The successful application of the affinity separation technique requires that the adsorbent has a number of favourable characteristics. These properties are conferred onto the adsorbent by the type of matrix support, method of matrix activation and ligand or spacer arm coupling, the dimensions and type of spacer arm, and the ligand concentration and type.

2.3.1 THE MATRIX SUPPORT

Angal and Dean (1977) among others, have shown that the nature of the matrix has a profound effect on the separation performance of an adsorbent in the affinity technique. The nature of the matrix determines its physical properties such as its mechanical strength and flow characteristics; its behaviour towards biological molecules and to a certain extent, its capacity. The properties of the ideal matrix for affinity separation have been discussed by several authors among whom are Cuatrecasas et al. (1968), Lowe and Dean (1974), and Yang and Tsao (1982). These favourable properties of a matrix are:

(i) The matrix should be hydrophilic and have no intrinsic charged group in order to prevent non-specific adsorption of proteins.

(ii) It should have good mechanical properties which are retained after chemical treatment to minimize flow resistance and assure an even flow pattern.

(iii) It should have good porosity with size large enough to allow an easy transfer of macromolecules inside the particle.

(iv) It should have a sufficient number of active groups that are amenable to the chemical functionalization and modification required in covalently linking ligand to it.

(v) It must be mechanically and chemically stable to the treatment of chemical modification and the varying operation conditions.

The conclusion of these authors seems to be that the polysaccharides, notably the agaroses, cross-linked dextrans and to some extent cellulose beads provide the best available matrix support for affinity separations. Commercially available matrix supports include cross-linked agarose (Sepharose-CL$^{(R)}$), cross-linked dextran (Sephadex$^{(R)}$), Spherosil$^{(R)}$.

2.3.2 THE LIGAND

Several factors influence ligand selection. Firstly, the ligand should have a dissociation constant less than 10^{-3}M or the binding constant greater than 10^{3} M^{-1} (Yang and Tsao, 1982). In addition to dissociation constant requirement, the ligand should have chemically modifiable groups which allow it to be attached to the matrix without destroying its binding activity. Furthermore, it should exhibit specific and reversible binding for the substance to be purified. Also stability during chemical modification and under

operating conditions is required.

The activation and coupling step in adsorbent preparation of the polysaccharide matrices depend on the functional groups of the ligand needed for covalent linkage with matrix support. Some of the available activation methods as a function of the ligand/ligand functional groups in common use are shown in Table 2.2.

Table 2.2. Some ligands and Activators in Common Use.

LIGANDS	FUNCTIONAL GROUP	REAGENTS USED IN ACTIVATION METHOD
Proteins, peptides, amino acids	amino ($-NH_2$)	carbonyldiimidazole, cyanogen bromide, peroxidate, hydrazine, epoxy-oxirane
Amino acids, keto acids, carboxylic acids	carboxyl (-COOH)	hexylamine
Proteins	Thiol (-SH)	Bisepoxirane, divinyl sulfone and epichlorohydrin
Sugar	hydroxyl (-OH)	Bisepoxirane, benzoquinone, epichlorohydrin, divinyl sulfone
Aldehydes	-CHO	adipic acid hydrazide
Heavy metal derivatives	heavy metals	divinylsulfone

The attached ligand is either monospecific or group specific. Concerning biospecificity, strictly monospecific ligands are very rare (Nishikawa, 1975). However, interaction between antigen and its antibody is quite specific, for example, and dissociation constants are commonly lower than 10^{-7}M. Because of such strong binding, drastic desorbing conditions used for removing the biologically active material from an immunosolvent frequently result in its inactivation.

In contrast to the high specificity in immunosorbents, there are numerous ligands which are group specific. They are specific for a functional class of enzymes or proteins. Group specific ligands have been used extensively in enzyme and protein isolation and purification (Yang and Tsao, 1982; Mosbach et al., 1972; Kopperschlager et al., 1982). An important advantage of a ligand with a broad biospecificity spectrum is that it is no longer obligatory to devise a new organic synthesis for every projected biospecific purification. The disadvantage is broad biospecificity in the adsorption step. Some group specific adsorbents available commercially include Blue Sepharose$^{(R)}$ CL-4B, ConA-Sepharose$^{(R)}$, immobilized lectins$^{(R)}$, 5'AMP-Sepharose$^{(R)}$ 4B, 2'5'ADP-Sepharose$^{(R)}$ (Pharmacia, 1983), Heparin-Ultrogel$^{(R)}$ 4R, SS DNA-Ultrogel$^{(R)}$ ALR and Blue-Trisacyl$^{(R)}$ (LKB, 1983).

The degree of substitution of the ligand on the matrix has an important bearing on the separation performance of the affinity system. Very low ligand density on the matrix results in low capacity. However, very high density of ligands cause non-specific adsorption and multipoint interaction effects (Trayer et al.,

1978). The degree of substitution depends on activation and coupling procedures; namely, quantity of activator, reaction time, pH of the medium, reaction temperature and ligand concentration.

2.3.3 SPACER ARM (LEASH)

The use of spacer arms has been discussed widely in the literature. Accessibility of the ligand attached to the matrix support of an adsorbent to its target molecule is the reason for the use of spacer arms. Irrespective of porosity of the matrix support, there appears to be some steric hindrance towards ligand-target molecule interaction if the ligand is attached directly to the support (Lowe and Dean, 1974). Use of a leash is especially important in systems where there is a problem of accessibility due, for example, to cross-linking. Also relatively low molecular weight ($< 5,000$) ligands often need to be spaced from the matrix with leashes.

Commonly used leashes are short chain hydrocarbons ($<C_{12}$). The length of the leash should be chosen carefully since the wrong length could create its own problems. It has been shown that leashes can not only introduce non-specific adsorption but can also cause localized steric hindrance or, in some cases, introduces cross-linking to the porous particles and significantly reduces the porosity of the matrices (Yang and Tsao, 1982). In spite of the advantages of the use of leashes Nishikawa (1975) has concluded on the basis of some of its disadvantages that indiscriminate usage in adsorbents should be avoided. It should be used only when it is absolutely necessary.

2.3.4 CHEMISTRY OF ADSORBENT PREPARATION

Much has been written in the literature about many varieties of chemical reactions employed to connect a leash or ligand to matrices. Lowe and Dean (1974), LKB (1983), and Yang and Tsao (1982) are good sources of information on this topic.

2.4 APPLICATIONS OF AFFINITY TECHNIQUE

Purification of biological materials, especially proteins, by conventional procedures which utilize the physical characteristics of the molecules such as size, charge and solubility are often laborious and incomplete, and the yields are often low. In contrast, affinity techniques offer relatively simple means of obtaining high yield and high purity materials from biological sources.

The main area of the application of affinity techiniques is by far the downstream processing of proteins. However, the affinity technique has been successfully applied to the separation of carbohydrates and glycoproteins by use of immobilized lectins (Soderman et al., 1973). Cells and nucleic acids have also been purified using affinity techniques (Parikh and Cuatrecasas, 1985). Applications of affinity chromatography are the subject of many reviews and reports (for example, Parikh and Cuatrecasas, 1985; Lowe and Dean, 1974; Walters, 1985).

In addition to preparative applications, the affinity technique has been used for analytical and investigative purposes. For example, O'Carra and Barry (1972) and Delaney and O'Carra (1974) have used the technique to study the kinetic mechanism of

enzyme-substrate binding. They demonstrated the compulsory-ordered kinetic mechanism of lactate dehydrogenase (LDH) in the binding with NADH and its substrates.

Depending on the way in which the ligand is derivatized and physically contained, affinity purification methods are classified as belonging to one of the following three categories: affinity adsorption, affinity precipitation and affinity partitioning (Janson, 1984). Janson has described these methods but affinity adsorption in which a ligand is attached to a solid phase is of main interest here. Protein recovery and purification is also the area of application of affinity adsorption that is of major interest in this review.

Although affinity adsorption, especially affinity chromatography, has been frequently employed on a laboratory scale, it has not been employed as frequently for the large-scale purification of proteins. The emphasis in biotechnology, at the moment, is on the scaling-up of the numerous affinity systems which are available for downstream processing of proteins.

Robinson et al. (1972, 1974) have discussed factors affecting production scale affinity separations. They used 1.8 litre (.15 m diameter) column of p-aminophenyl-β-D-galactosidase from E. coli. The process was carried out at a linear flow rate of 24 cmh^{-1} and a processing capacity of 5 g pure enzyme per 2 h cycle was obtained. Hanford et al. (1978) carried out a pilot-plant scale recovery of human serum albumin from Cohn Fraction IV using a column of Cibacron Blue 3GA-Sepharose CL-6B. Linear flow rate of 20-25 cm/h was used in the process; column dimension was 20 cm

(diameter) x 12 cm height. 0.3 g of HSA per litre of plasma in addition to that obtained by cold ethanol precipitation was recovered. Janson and Hedman (1982) have listed some twenty five examples of large scale applications of the affinity technique for protein recovery and purifications.

The factors affecting the scale up of the affinity techniques have been reviewed and discussed extensively in the literature; for example Janson and Hedman (1982), Janson (1984) and Chase (1985). The lack of ideal adsorbents seems to be one of the major problems. At the moment, the majority of affinity separations are carried out using an agarose based support matrix (Janson and Hedman, 1982), because it fulfils most of the criteria for an ideal matrix. However, for large-scale applications, agarose does have some drawbacks. Even with cross-linked agarose beads, the rigidity ideally required for large-scale operations is lacking to some extent; therefore, flow rate limitations are inevitable. In addition, the cost of agarose is very high. However, recent developments in media for large-scale chromatography of proteins based on hydrophilic synthetic organic polymers and on super cross-linked agarose (Janson and Hedman, 1987) have led to a situation where the limit for throughput is no longer set by flow resistance. Cost still remains to be considered.

Also, the long term stability of affinity media and hence re-use is often a problem. Ligand costs are often high and only several cycles of use can result in economic application of affinity adsorbents.

Recovery and purification of proteins from crude mixtures pose even more problems. For example, purification of an intracellular enzyme within a microbial cell will involve disintegration of cells either by high pressure homogenization or cell solubilization; this invariably results in a mixture of cell debris, other materials and the target protein. The application of such crude extracts to chromatographic columns often results in clogging and fouling of the column packings. This does not only reduce the capacity of the adsorbents but also shortens the lifetime of often very expensive adsorbents. Janson (1984) has listed batch types of affinity techniques which can be used in cases of this nature. These techniques help to preserve the one-step purification advantage of the affinity technique.

One group of ligands which do not suffer the disadvantages of other ligands is reactive dyestuffs. These synthetic dyes have affinity to a number of proteins and do not suffer from the denaturation very common with protein ligands. They are often stable and cheap. Reactive dyes are therefore well suited for large-scale affinity separation applications to protein purification in cases where their use is possible.

The uses of reactive dyes in protein purification have been reviewed by many authors. For example, Lowe and Stead (1985), Stead (1987), Lowe et al. (1981), Kopperschlager et al. (1982) and Small et al. (1983). Many types of reactive dyes are commercially available but the most important are the anthraquinone dyes such as procion H and Cibacron blue 3GA. Cibacron blue 3GA has been used extensively for the purification of NAD^+- and NADH-dependent

dehydrogenases, ATP-dependent kinases. The binding of these enzymes to dye matrix conjugates is regarded as a specific interaction of the dye with a typical structural element in these enzymes designated as "dinucleotide fold" (Birkenmeier and Kopperschlager, 1982). However, Cibacron blue binds very strongly to HSA which is thought to be due to the binding of the dye to the bilirubin binding sites of albumin (Leatherbarrow and Dean, 1980). The interaction of the other plasma proteins with the dye depends on the pH. For example, at pH below 8.0 almost all plasma proteins bind to the dye but only HSA can bind at pH8.0 or above.

2.5 THE OPERATIONS OF AFFINITY SEPARATIONS

Most affinity separations are carried out using packed columns. The process cycle can be divided into four stages; an adsorption stage in which feed containing the target molecule (adsorbate) is contacted with the solid phase to which a molecule which has affinity for the adsorbate has been attached (adsorbent). The adsorbate is picked up by the adsorbent and unadsorbed molecules pass through the column in the effluent, washing stage in which non-specifically adsorbed molecules are washed away, an elution or desorption stage during which specifically bound adsorbate is desorbed from the adsorbent by the disruption of specific interactions, and regeneration and/or equilibration stage during which the adsorbent is made ready for another cycle of operations. These operations are general in all affinity separations, whatever configuration of the adsorbent packing. They have been described extensively in the literature

(for example, Lowe and Dean (1974) and Chase (1984b)). A brief description is as follows.

2.5.1 ADSORPTION STEP

Most packed bed affinity separations are operated in frontal analysis mode (Chase, 1984c). This involves the continuous application of a constant feed stream of the adsorbate to the inlet of the bed until a "breakthrough" occurs, that is, the adsorbate is detected at the bed outlet. The feed flow is normally stopped at a pre-determined outlet concentration of the adsorbate. The plot of the effluent concentration of the adsorbate as a function of time or throughput volume is called the breakthrough curve (B.T.C.). The shape and position of the B.T.C. are important in the evaluation of the separation performance of an affinity system. They depend on a complex mix of equilibrium (adsorption isotherm) and non-equilibrium factors; (for example, mass transfer and axial disperson). Chase (1984a) has described the factors affecting the shape and position of B.T.C. in affinity separations as flow rate, the rate of mass transfer, the value of dissociation constant of affinity interactions, the inlet adsorbate concentration and the capacity of the bed. In addition, axial dispersion and particle size affect the B.T.C. Fig. 2.2 shows three B.T.C.s.

Generally, the area behind the breakthrough curves represent the maximum equilibrium capacity of the column. The amount of adsorbate that remains in the effluent is the area under the curve. For an adsorption step terminated at an effluent concentration CT, a given amount of the column capacity has been used and the rest unused, and some amount of feed has been wasted.

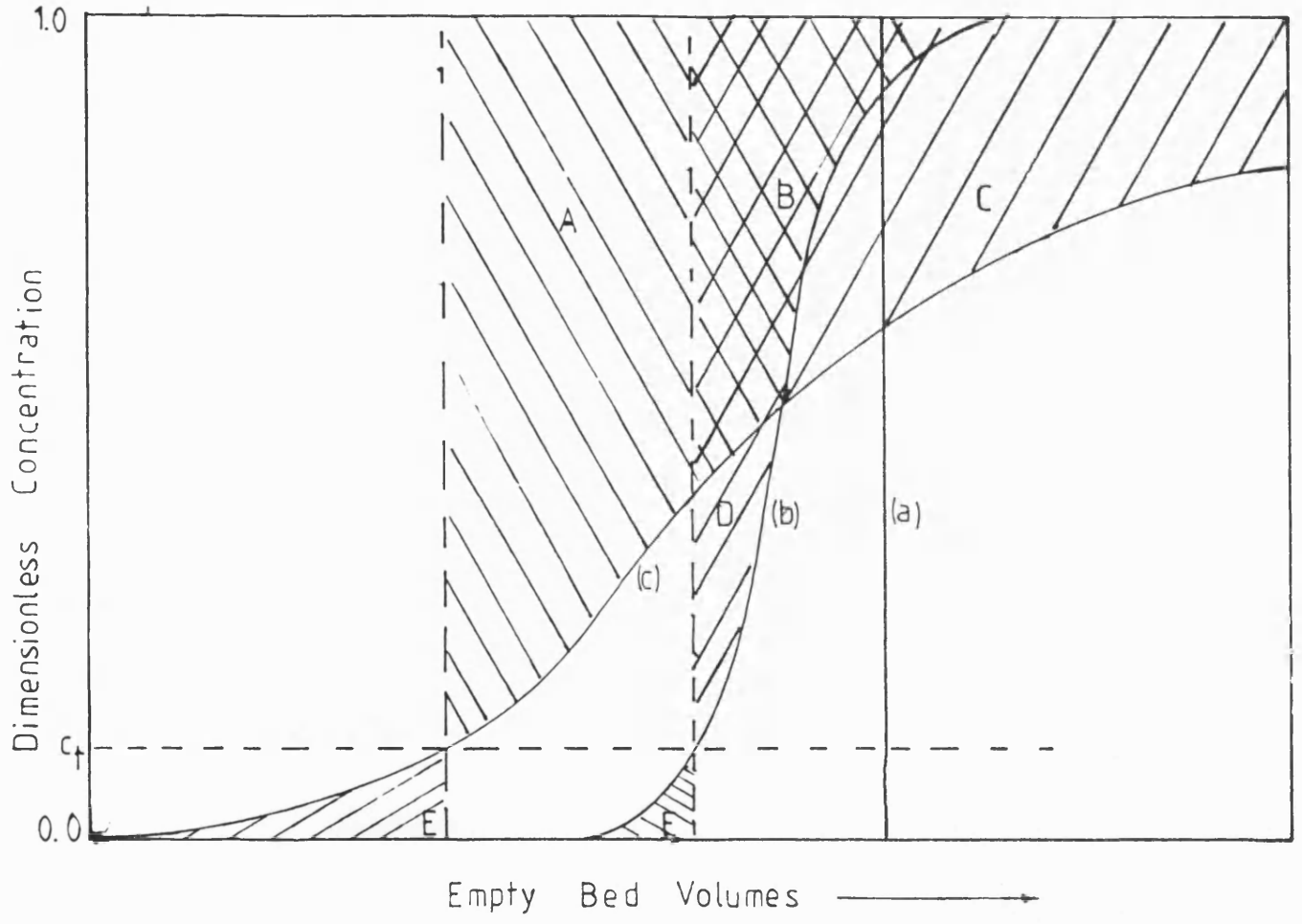

Fig. 2.2 a-b Breakthrough Curves.

Curve (a) is an idealised B.T.C. resulting from an infinite rate of mass transfer and absence of non-idealities in the column packing. In practice, this type of B.T.C. does not exist in affinity separations. Curves (b) and (c) represent B.T.C. due to finite mass transfer rates and some non-idealities in the column packing. The shaded areas, A, B and C represent the unused capacity of the bed for curve (c) while areas B and D represent the unused bed capacity for curve (b). Clearly curve (c) represents an inefficient use of the adsorbent. Also the shaded areas E and F for curves (c) and (b) respectively, are wasted feed. Obviously more feed is wasted in the former.

Sharp B.T.C., curve (b) results in greater utilization of the capacity of an adsorbent. The difference between curves (b) and (c) could be due to smaller axial dispersion, higher rate of mass transfer, higher initial adsorbate concentration, higher bed capacity and smaller particle size.

2.5.2 THE WASHING STEP

Once the adsorption step has been completed, the column is usually washed with the adsorption buffer until the level of contaminants has fallen to a pre-determined level. The function of the washing stage is to remove unbound and non-specifically bound materials. The washing conditions are chosen carefully to avoid the elution of specifically bound materials. Guidelines for choice of washing conditions have been given by Chase (1984b).

2.5.3 THE ELUTION STEP

Usually desorption of bound adsorbate can be effected by the use of two major approaches. Firstly, specific elution can be effected using a high concentration of the soluble ligand. Due to competition for the adsorbate between the immobilized ligand and the soluble ligand, the adsorbate will partition exclusively into the soluble phase if the soluble ligand is in excess. The soluble ligand is then separated from the adsorbate by exploiting the difference in molecular size of the two species. This method may be undesirable if the ligand cost is high. In the second case, the non-specific elution, the elution can be effected by a change in pH, use of protein denaturants such as guanidine chloride or urea, use of chaotropic agents such as sodium thiocyanate, use of polarity reducing agents such as dioxan, use of temperature effects and change in ionic strength or pH of eluting buffer. The elution mechanisms of these conditions have been discussed extensively in the literature.

Elution is normally carried out until a pre-determined level of the eluate has been reached.

2.5.6 REGENERATION/RE-EQUILIBRATION

After elution, the bed is usually washed with the adsorption buffer in order to rinse off the eluent. It is subsequently equilibriated with the adsorption buffer before the next adsorption cycle is carried out. When necessary, a complete regeneration of the bed is carried out using, for example, 0.1 M NaOH in order to remove irreversibly bound protein molecules. The regeneration

condition will depend very much on the type of adsorbent used but the above reagent is usually adequate.

2.6 FACTORS AFFECTING THE PERFORMANCE OF AFFINITY SEPARATION

Many factors act together at a given time to determine the performance of an affinity separation process. These factors are a complex mix of thermodynamic, rate and hydrodynamic phenomena. The identification of these factors and their optimization are very important in the successful application of the affinity technique in the recovery and purification of proteins, especially in production scale applications. Janson and Hedman (1987), Arnold et al. (1985a) and Chase (1984a) have discussed these factors especially as it applies to large-scale applications. In brief, the performance of an affinity separation can be measured in terms of dynamic capacity, throughput, selectivity and purity.

2.6.1 DYNAMIC CAPACITY

As has been mentioned earlier, the breakthrough curve (B.T.C.) provides the information necessary for the evaluation of the dynamic capacity of an affinity separation carried out in a column. The B.T.C. shape and position give an indication of separation efficiency and capacity respectively. The B.T.C. and other factors such as pH, temperature and ionic strength of adsorption buffer and how they affect dynamic capacity will be discussed.

2.6.1.1 THE BREAKTHROUGH CURVE

The breakthrough curve is a direct reflection of the adsorption or sorption processes taking place within the fixed bed. The nature of the adsorption processes and the effects of equilibrium and non-equilibrium processes can better be understood when the progress of the protein as it passes down an affinity column is followed.

When a protein solution, containing a constant amount of adsorbate, of concentration C_0 enters the inlet of an adsorbent column it contacts the adsorbent at the top of the bed. Adsorption occurs at the liquid/solid interface. The concentration of the feed falls to a low value in equilibrium with the fresh adsorbent over a finite length of fixed bed.

That length is termed the Adsorption Zone or Mass Transfer Zone as shown in Fig. 2.3a as Oa. As the adsorbent at the plane OC_o becomes saturated in equilibrium with C_o, the adsorption wave, $C_o a$, at time t_1 moves to the position cb at time t_2. For the time being, the liquid front moves ahead of the adsorption wave and contains no adsorbate. After a time, t_3, when the low concentration end of the adsorption wave has reached the exit of the bed, the adsorbate "breakthrough" occurs at t_3 and the adsorbate concentration in the effluent rises sharply until it reaches C_o. The plot of effluent concentration of the adsorbate as a function of time or volume (Fig. 2.3b) is called the breakthrough curve. The shaded portion of Fig. 2.3a is the unsaturated fraction of the adsorption zone before breakthrough occurs. As can be seen in Fig.2.3, the B.T.C. is a mirror image of the adsorption wave. The extent to which the adsorbent is utilized, especially if taken off- line at breakpoint

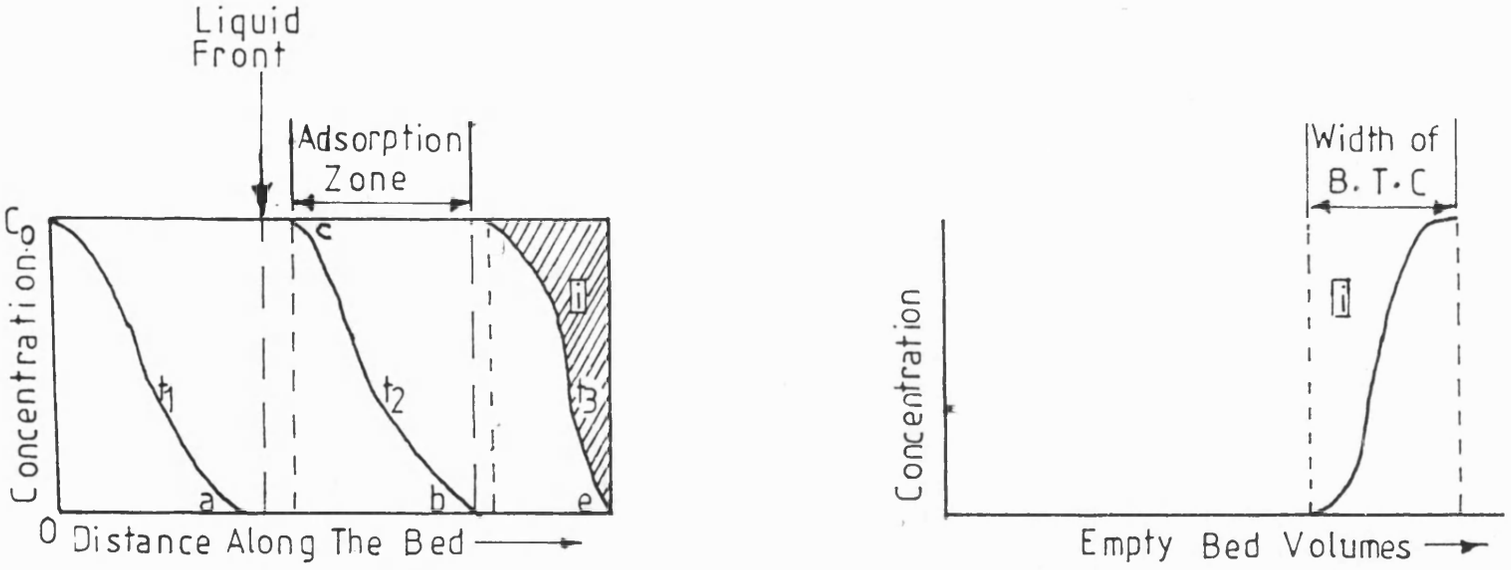

(a) Development and Progression of an Adsorption Wave Through a Bed

(b) Breakthrough Curve

Fig 2.3. The Distribution of Adsorbate Concentration in the Fluid Phase during flow of adsorbate solution through an Affinity Bed.

(t_3), depends on the shape of the adsorption wave which in turn depends upon the shape of the equilibrium isotherm.

In the absence of mass transfer resistances, instantaneous equilibrium between the liquid phase and the solid phase with respect to the adsorbate occurs. This would result in B.T.C. being a step function (Fig. 2.2), that is, there would be an instantaneous jump in the effluent concentration from zero to C_o at the moment the bed capacity was reached.

However, kinetic and other non-equilibrium processes tend to delay the time for attainment of equilibrium and hence, the increase in the width of the adsorption zone and that of B.T.C. The mass transfer rates are normally highest at the centre of the adsorption zone but lower at the tail end front due to high solid phase concentration and lower liquid concentration respectively.

2.6.1.2 ADSORPTION ISOTHERM

The equilibrium adsorption isotherm is normally obtained from the plot of solid phase and liquid phase distribution of an adsorbate at equilibrium given a constant temperature. Because the equilibrium isotherm determines the capacity of a given affinity adsorbent, it can be used sometimes as the basis for the selection of a suitable adsorbent for a given affinity separation.

There are three commonly known isotherm types in adsorption processes. They are classified according to shape, namely, favourable isotherm - isotherm is convex upwards, unfavourable isotherm - isotherm concave upwards, and linear isotherm (intermediate case) - isotherm is linear. These are shown in Fig. 2.4.

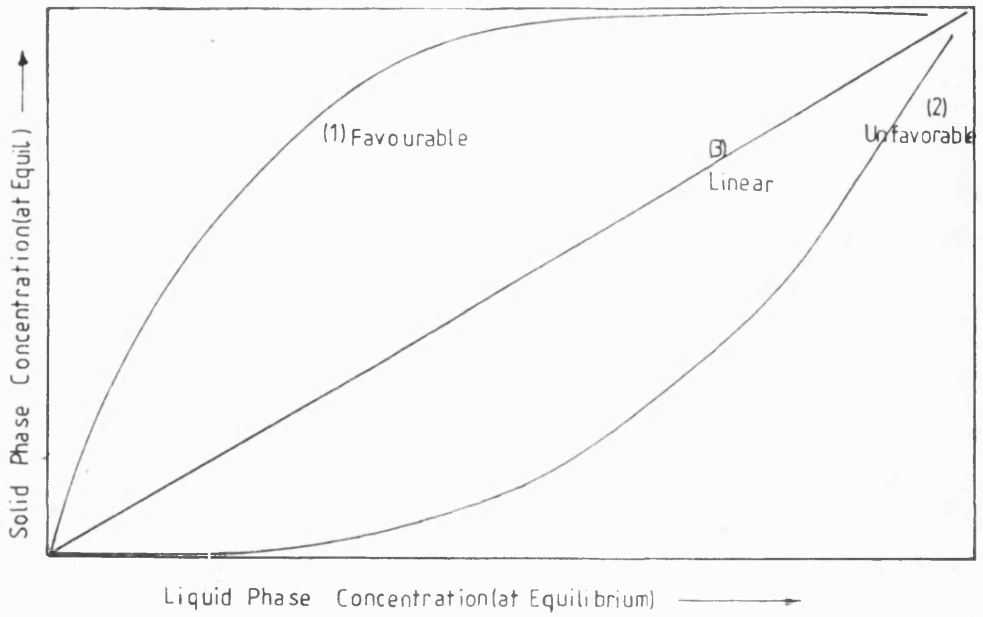

Fig. 2.4. Types of isotherms (1) favourable; (2) unfavourable; (3) linear

Vermeulen (1958) has examined these adsorption isotherm shapes and the effects they have on column performance. The equilibrium constant of favourable isotherms is usually more than that of unfavourable isotherms.

The favourable type isotherm is the most common in affinity systems (Tsao and Yang, 1982). Three types of favourable adsorption isotherms are common in adsorption systems. These are a Freundlich (1926), Brannamer, Emnett and Teller (BET, 1938) and Langmuir (1918). These will be discussed in more detail later.

2.6.1.3 ADSORPTION KINETICS

Several resistances to the transfer of adsorbate from the liquid phase to the adsorbent are normally encountered in affinity

separations. As was mentioned earlier, the effect of these resistances to mass transfer is to increase the relative width of the adsorption wave and hence the B.T.C. width. The resistances are due to diffusion through the bulk liquid, diffusion through the liquid film surrounding the adsorbent, the diffusion through the pores of the adsorbent, and sometimes adsorption of adsorbate unto the adsorbent. Usually one or more of these resistances will be the highest and is termed the rate-limiting step(s). In protein adsorption in affinity systems, the diffusion resistances are usually controlling (Tsao and Yang, 1982) although recent evidence suggests that in some cases as in protein adsorption using dye ligands, the adsorption step may be controlling (Chase, 1984a; Arnold, 1986).

Small particle size is favourable for reducing pore diffusion resistance. This is because of shortening the distance for diffusion within the adsorbent particles. However, in column operations pressure drop increases at a given flow rate as the particle gets finer. Usually a balance is struck between particle size and pressure drop. An additional advantage of small particles is the large area per unit volume which means an increase in dynamic capacity.

High flow rates act to lower the film mass transfer resistance. However, rigid packing is required to achieve very high flow rates. Also for normal size adsorbent particles (about 100 μm), high flow rate increases pore diffusion resistance. Therefore only a combination of the small particles and high flow rates can eliminate all diffusional resistances.

Southern and Hollis (1986) have developed a silica based matrix for application to fast affinity chromatography (FAC). The silica support is rigid (for high flow rate), small (< 5 μm). This meant that they could reduce mass transfer to almost zero and could increase the flow rate by 50 to more than 300 times to match kinetic rates of the affinity interaction which is now the controlling step.

The small particles of the sponge and its open structure are some of the reasons it has been chosen for study in this work.

2.6.1.4 IONIC STRENGTH OF THE BUFFER

The effect of ionic strength of a buffer on affinity systems is difficult to assess. For example, enzymes such as hexokinase isoenzymes and many dehydrogenases and other kinases are readily eluted from affinity adsorbents by high concentration of salts, such as KCl, at which they exhibit full enzyme activity in free solution; conditions under which one might expect binding to occur, (Trayer et al., 1978). Also, the action of salts in certain cases does appear to be specific, for example, myosin dissolved in 0.5M KCl will not bind to Sepharose-ADP conjugates, although if the Cl^- ions are replaced by acetate, then binding is very efficient. Sada et al. (1986) found that adsorption capacity of Sepharose 4B-anti- BSA decreased with decreasing pH on addition of NaCl; however, at higher ionic strength, the magnitude of the decrease in adsorption capacity was less.

Trayer et al. (1978) have recommended the highest possible salt concentration in affinity separations in order to limit non-

specific adsorption. Very high ionic strength undoubtedly leads to non-adsorption and is a method of elution of specifically bound adsorbates.

2.6.1.5 EFFECT OF pH

Like the ionic strength of the adsorption buffer, the effect of pH depends on the affinity system under consideration. At unfavourable pH, adsorption does not take place. This is one of the non-specific methods of elution. For example, all human blood plasma proteins bind to Cibacron blue-Sepharose at a pH under 8.0 but above this pH, only albumin binds. It needs at least 0.02 M KSCN (a chaotropic salt) to desorb albumin from this adsorbent. Unfavourable pH, therefore, results in lower capacity.

2.6.1.7 MATRIX COMPOSITION AND MATRIX PORE STRUCTURE

There is evidence that the matrix has an effect on the adsorption capcity. Angal and Dean (1977) have observed differences in capacity of different matrices - cellulose, Sepharose, and silicate - for the dye ligand adsorption of albumin. Chase (1984a) observed a similar effect with silica and Sepharose based adsorbents (similar pore sizes) for β-galactosidase adsorption.

2.6.1.8 TEMPERATURE

In general, adsorption decreases with increasing temperature (Lowe and Dean, 1974). This is because adsorption is essentially exothermic; the more exothermic the adsorption, the greater the decrease in adsorption for a given temperature

increment. Increased temperature decreased the binding of lactate dehydrogenase to N^6-(6-aminohexyl)-AMP-Sepharose especially at a temperature range of 5 - 10°C (Lowe and Dean, 1974). However, the increase in adsorption kinetics can offset this effect of temprature.

2.6.1.9 OTHER FACTORS

The other factors which can affect the adsorbent capacity include adsorbate size, degree of cross-linking and protein concentration.

The smaller the size of an adsorbate the faster its diffusion through the bulk liquid and the pores. Consequently, it reaches the ligands more easily than larger sized adsorbates.

Cross-linking is often necessary to achieve some mechanical strength with affinity adsorbents. However, over cross-linking can lead to a drastic reduction in pore size. This would normally lead to some steric hindrance and hence loss in capacity.

Within certain limits, protein capacity is a function of the equilibrium protein concentration. For a constant ligand concentration, in solutions of very high concentration, capacity becomes independent of initial protein concentration.

2.7 THROUGHPUT

In production scale protein recovery and purification, high throughput is very essential. This is even more important for the processing of biological fluids usually encountered in large, dilute volumes. Most important in determining throughput are the flow characteristics and the dynamic capacity of the adsorbent. Fast flow adsorbents are mechanically strong and have high

porosity. Super cross-linked Sepharose developed by Pharmacia and hydrophilic synthetic organic polymers like Trisacryl$^{(R)}$ developed by LKB (1983) are some of the examples of fast flow adsorbents now available. These will eventually lead to the elimination of the throughput bottleneck in large-scale protein purification. It would then mean that the throughput efficacy in industrial protein chromatography is no longer set by the flow rate resistance of the column packing, but rather by the overall kinetics of the chromatographic process (Janson and Hedman, 1987).

2.8 SELECTIVITY AND PURITY

One of the most important advantages of the affinity technique in protein recovery and purification is the very high achievable selectivity. Often a high purity is obtained in a single step which can only be achieved with multiple steps using conventional methods.

However, in the presence of other proteins and impurities selectivity and purity can be impaired. These effects are often due to non-specific adsorption, non-specific interference may result from hydrophobic or ionic interactions. Hydrophobic effects may be due to leash structure and/or high ligand concentration. Usually, a suitable choice of leash and ligand density on the matrix reduces this problem. Ionic interference can result from leash structure, matrix support, ligand or the coupling reagent (for example, cyanogen bromide). These ionic interferences can often be controlled by suitably high ionic strength of the adsorption buffer. Yang and Tsao (1982) have reviewed the causes of these

interferences and ways of reducing them.

2.9 SCALE-UP OF AFFINITY SEPARATION PROCESS

At present, most of the applications of the affinity technique have been confined to the laboratory scale. However, recent developments of adsorbent and more literature on the information required for optimal design and operation of fixed bed adsorption techniques, especially affinity chromatography indicate the acceleration from the laboratory to the production scale in the very near future. For example, Janson and Hedman (1982) have discussed important factors affecting large-scale recovery and purification of proteins by chromatographic methods. Recently, Jandson and Hedman (1987) have discussed factors important in the optimization of process chromatography of proteins. Various authors have reviewed and investigated the scale-up and operation of affinity separation systems - for example Chase (1984 a, b, c), Chase (1985), Arnold et al. (1985 a, b) and Robinson et al. (1972) and Robinson et al. (1974)

Although other methods of the affinity technique such as batch adsorption, affinity precipitation and affinity partitioning are available, affinity chromatography is by far the most widely used at present. Some of the most important advantages of affinity chromatography (or fixed bed adsorption) is the ease of scale-up and automation (Janson, 1984; Chase. 1986). Chase (1986) has automated the β-galactosidase production and discussed important developments needed to realise automation of many available affinity systems. Automation is often essential in the economic

operation of scaled-up processes.

In the laboratory scale affinity processes, protein purifications are often carried out in small columns of small diameters; optimization of the design and operation of protein separation is not often a worry provided the desired separation is achieved. However, in large-scale operations, important parameters affecting affinity separation must be optimized to achieve economic recovery of proteins. Given that the optimal height of the column has been established, and the parameters affecting performance optimized, scale-up simply involves the increase in diameter (Janson and Hedman, 1987). In addition, it is enough to keep the ratio of bed volumes and flow rates constant when scaling from small to large columns.

To obtain information necessary for the optimal design and operation of affinity separation, theoretical predictions as well as experimental data on the performance of the system are needed. This information is not yet readily available. Theoretical predictions using appropriate models describing the performance of an affinity system will give an indication of the effects of important parameters. Simulation of these effects will give important guidelines for the optimal design and operation of the scaled-up process. It is one of the objectives of this investigation to provide such a predictive model using blue-sponge. The blue- sponge is a particularly good candidate for scale-up affinity separation because of its fast flow structure, cheap and stable ligand, and cheap matrix.

CHAPTER 3

PREPARATION OF ADSORBENTS

3.1 PREPARATION OF THE CIBACRON BLUE 3GA - SPONGE AFFINITY ADSORBENT

3.1.1 APPARATUS

(a) IMPELLER

A gear driven Citenco F.H.P. Motors, Type K6TS9 from Citenco Ltd., Burehamwood, Herts, of 0-600 r.p.m. was used. A marine-type propeller or six blade turbine impellers normally mounted centrally through a shaft for axial mixing and radial mixing respectively were used. Impeller diameters were some 0.3 to 0.6 of the reaction vessel diameter.

(b) REACTION VESSELS

Copper reaction vessels of capacities 3 litre (12.5 cm diameter x 25 cm height) and 5 litres (12.5 cm x 40.75 cm) were equipped with baffles of dimensions 20 cm x 3 cm and 30 cm x 3 cm respectively.

(c) DELTA PUMP

A 12 r.p.m. speed (fixed) delta pump was used for the feed to column and to the U.V. detector.

(d) ULTRAVIOLET DETECTOR

An LKB U.V. detector model UVICORD II was used for on line monitoring of protein concentration at 280 nm. The protein solution flows through a continuous flow through cell of path dimension 10 mm path length 1 mm diameter.

(e) CHART RECORDER

A Servoscribe chart recorder was used in conjunction with the U.V. detector at a chart range setting of 20 mV.

(f) COLUMN

Amicon Wright borosilicate glass, adjustable length column, model GA 44 x 90 (44 mm diameter).

3.1.2 MATERIALS

(a) CIBACRON BLUE 3GA

Cibacron blue 3GA was kindly donated by the Ciba-Geigy Chemicals Ltd., Manchester. The commercial dyestuff is composed of water soluble anionic reactive dye (Cibacron blue 3GA) of the mono-chlor-triazinyl type, with simple diluents (e.g. common salt) and stabilizing agent. The dye was used as received.

(b) CELLULOSE SPONGE

The cellulose sponge was donated by Bio Isolates Ltd., Adelaide St., Swansea. The sponge was received in sheet form.

(e) BLUE MEMBRANE DISCS

Cellulose membranes (thickness about 0.5 mm) to which Cibacron blue dye has been attached was donated by Domnick Hunters Filters Ltd.

(d) HUMAN BLOOD PLASMA

Outdated human blood plasma was donated by the Singleton Hospital, Swansea. The plasma was received in frozen plastic packs.

(e) CHEMICALS

The chemicals used were AnalaR (Tris-HCl, HCl and sodium thiocyanate) or GPR (NaCl and Na_2CO_3) grade purchased from BDH Chemicals Ltd., Poole Street, Dorset. Crystallized and lyophilized human serum albumin powder was purchased from Sigma Chemicals Ltd.

3.1.3 EXPERIMENTAL

(a) BATCH IMMOBILIZATION REACTION

The covalent coupling of Cibacron Blue 3GA dye to the sponge matrix was effected by an ether linkage between the triazine ring and the hydroxyl (-OH-) group of the sponge matrix. The coupling reaction is shown in Fig. 3.1 below.

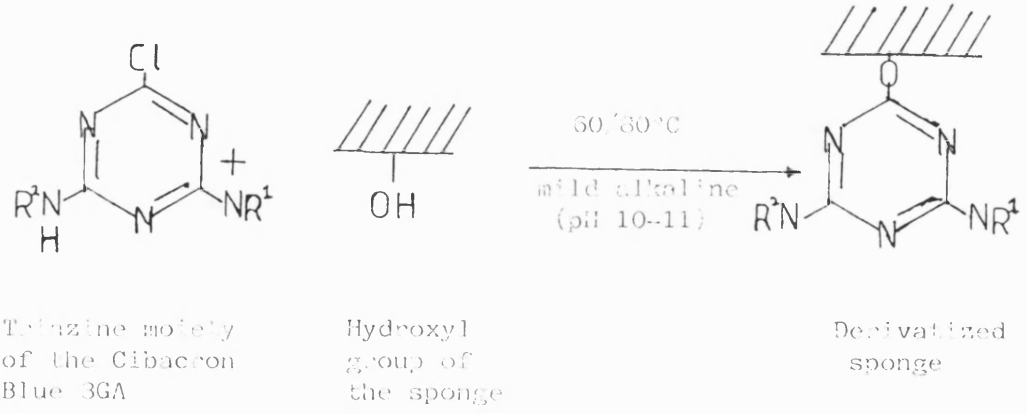

Fig. 3.1 Coupling of Cibacron Blue 3GA to Sponge

Because the standard methods used for the immobilization reaction with granular materials were difficult to use some modifications were made in order to suit the use with sponge. However, the immobilization reaction conditions (with respect to dye/matrix ratio, alkaline condition, sodium chloride concentration) were essentially the same as those described by Bohme et al. (1972).

It was noted from the literature that the laboratory method for the immobilization reaction as shown in Fig. 3.1 is essentially the same as that used in the industry for the dyeing of textile cotton materials (Ciba-Geigy, 1976). The basic principle involves the treatment of a polysaccharide material (with -OH groups with some 0.2-0.4% w/v dye solution at a mild alkaline condition (pH 10-11, achieved by addition of NaOH or Na_2CO_3, Ca 0.02% Na_2CO_3). Temperature conditions are either low (40-50°C, method of Heyns and Demor, 1974) or high (60-80°C, Bohme et al., 1972). The dye to matrix weight ratio depends on the amount of coupling required, usually 1:100 to 1:2. The total reaction time depends on the temperature range of the reaction used, usually 3½ hrs to 40 hrs.

Based on the information above on the reaction conditions, a solution (pH 10.8) of 0.3% (w/v) Cibacron Blue 36A, 60 g/l NaCl and 20 g/l Na_2CO_3 was used in all reactions. The dye/sponge weight ratio was kept at about 1:5.

The experimental set-ups for the derivatization of the sponge are shown in Fig. 3.2 a-b. Fig. 3.2a shows the set up for derivatization reaction for disc sponge. A disc of stainless steel

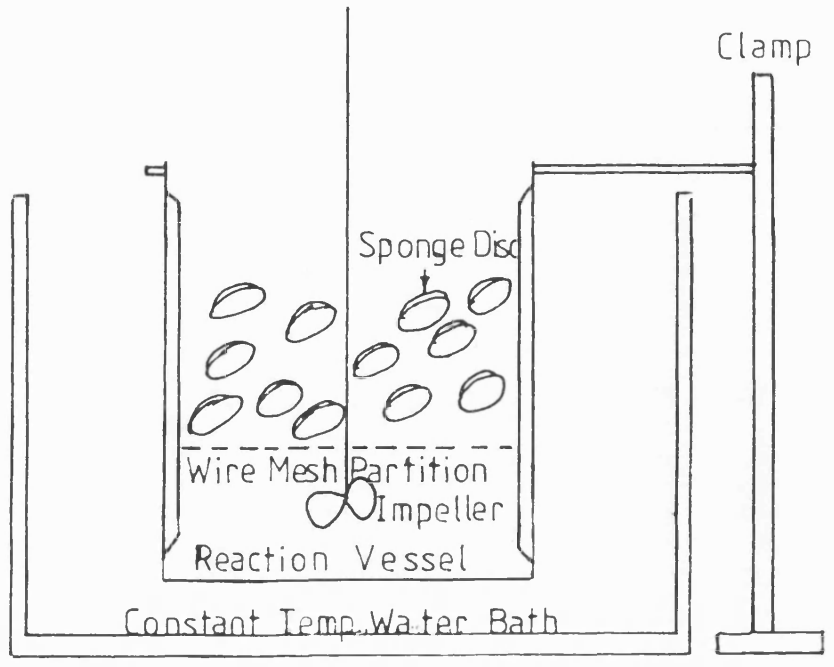

(a) Sponge Disc

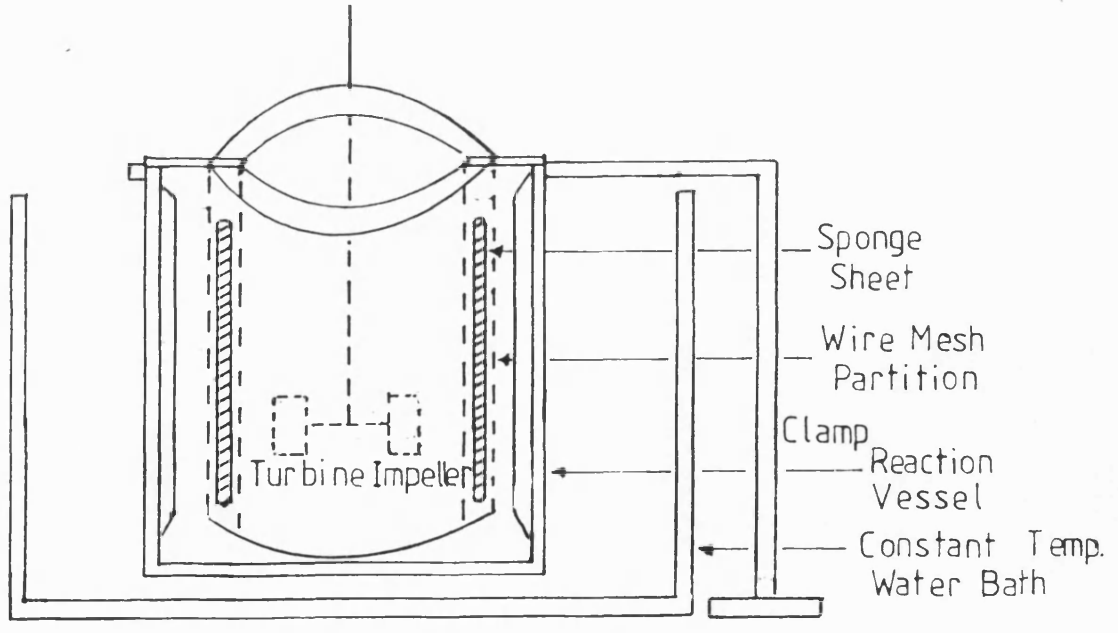

(b) Sponge Sheet

Fig 3.2 Experimental Set-up for Blue Sponge Derivatization

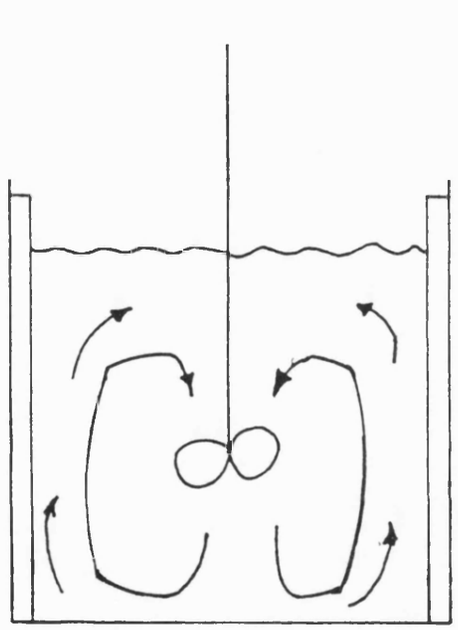

(a) Axial Flow with a Propeller Impeller

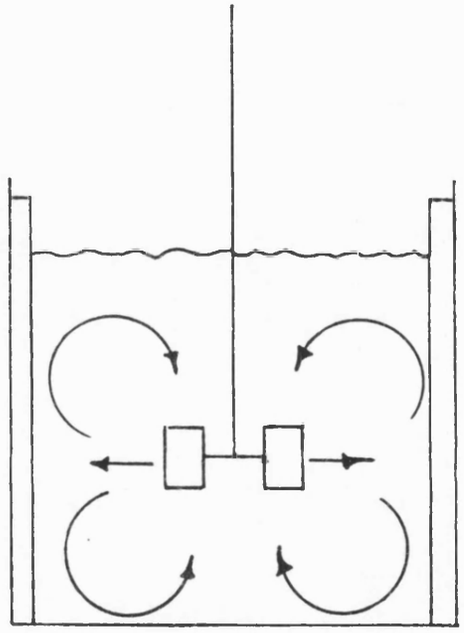

(b) Radial Flow With a Turbine Impeller

Fig 3.3 Typical Mixing Pattern(side view) in a Baffled Reactor With Impeller positioned at the Centre

wire mesh was cut to fit just inside the reaction vessel with a central space to pass the shaft of the impeller. The sponge was contained between the mesh discs and baffles were provided at the reactor walls as dents to fit the wire mesh separater. Mixing was by a marine-type propeller (0-600 r.p.m.) mounted centrally to provide axial mixing as shown in Fig. 3.3a. Heating was with a Citenco heater (0°-100° temperature range) mounted on a water bath in which the reactor vessel was immersed. Reaction mixture temperature was measured with a glass thermometer.

For derivatization of sponge sheets, the set up in Fig. 3.2b was used with a turbine impeller to provide a radial mixing pattern (Fig. 3.3b). The sponge sheet was sandwiched between two concentric steel wire cylinders surrounding it and coaxial with the impeller. All other conditions were the same as for the derivatization of the sponge discs.

Table 3.1 shows the typical steps and sets of conditions used in the derivatization of the blue sponge (a batch of sponge discs).

Usually, the reaction temperature chosen will depend on the stability of the matrix at that temperature. It was not known if the sponge (regenerated cellulose) would show any visible structural change. Therefore, four batches of the derivatized sponge were prepared at different temperatures, different reaction times and different timing of reagents addition. The sequence of operation is shown in Figs. 3.4a-d. The keys to the figures are: (a) Low-temperature; short time; (b) Low-temperature, long-time; (c) High-temperature, short time and (d) High-temperature, long time.

Table 3.1. Steps for Derivatization of Blue Sponge

STEP	OPERATION SEQUENCE	QUANTITY OF MATERIAL
(1)	CELLULOSE SPONGE, add: To CIBACRON BLUE 3GA SOLUTION (at 60°C) (After 30 mins) Add:	9 - 12 g 2.25 g in 650 ml of water
(2)	NaCl SOLUTION (i) Stir for 1 hr (ii) Then heat to 80°C	45 g in 50 ml of water
(3)	Add Na_2CO_3 SOLUTION (i) Stir for 2 hrs (ii) Leave to cool to room temperature	15 g in 50 ml of water
(4)	Wash copiously with (i) water; (ii) NaCl (1 M); (iii) 25% ethanol; (iv) water; (v) 1 M NaCl; (vi) water. Store product at 4°C in 0.1% azide solution	

The alterantive coupling method which involves the primary amino group of the anthraquinone moiety of the dye molecule (see Fig. 3.5) was not considered because it has been shown to be probably involved in an interaction with proteins; adsorbent prepared by this method, therefore, often exhibits poor protein binding (Leatherbarrow and Dean, 1980; Beissner and Rudolph, 1978; Bohme et al., 1972).

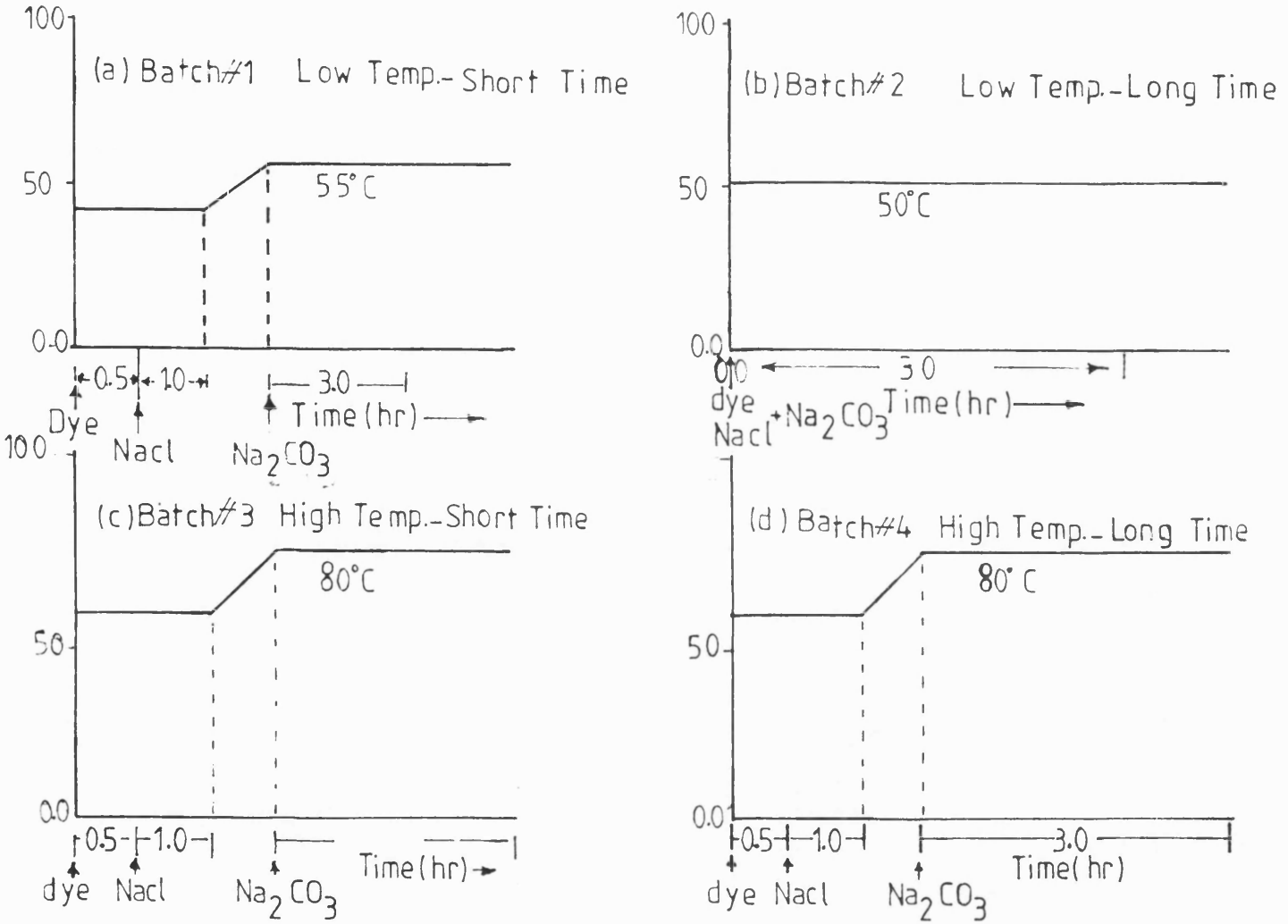

Fig 34 Temperature/Time Condition for the Preparation of Blue Sponge

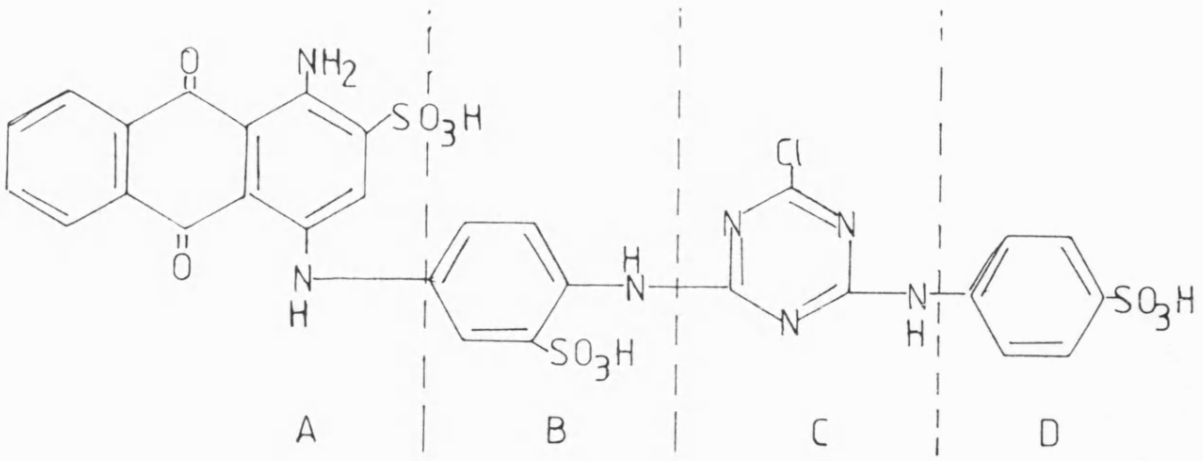

A = Anthraquinone group (contains reactive primary amino group)

B = Phenylendiamine sulphonic acid group.

C = Triazine ring (contains reactive chloride group)

D = Benzyl-sulphonic acid

Fig. 3.5. Chemical Structure of Cibacron Blue 3GA

Also the use of a spacer arm (short chain hydrocarbon) was not considered since a satisfactory capacity was obtained using the present method.

The activation of the sponge matrix prior to immobilization was also not considered since satisfactory protein capacity of the sponge derivatized by the method used here was obtained. This means also some savings in terms of time and cost in the whole process of the use of the sponge-dye matrix for affinity separations.

(b) SELECTION OF IMMOBILIZATION REACTION CONDITIONS

Three criteria were used to select the most suitable conditions (from Fig. 3.4) for the covalent coupling of the

Cibacron blue 3GA onto the sponge matrix. These are (i) capacity of the sponge for the human serum albumin; (ii) wash and elution volumes (process cycle time); (iii) the effect on the sponge texture at the reaction temperature.

Batches #1, #2 and #3 were used in the first set of the two adsorption experiments carried out. In the second experiment only Batches #3 and #4 were used.

The first experiment was aimed at determining, in general, whether the low temperature-short time, low temperature-long time or the high temperature-short time was the most suitable immobilization condition. Ten sponge discs (5.062 g dry wt.) were squashed to a thickness of about 1.65 cm in a 4.4 cm diameter Amicon Wright adjustable column. Twenty millilitre (20 cm^3) of human plasma diluted 10 times with 0.05 M Tris-HCl/0.05 M NaCl, pH 8.0 buffer was recirculated for thirty minutes with a 12 r.p.m. delta pump at a flow rate of 1 $cm^3 min^{-1}$. For the second experiment all the conditions were the same except that frontal analysis was used. The diluted plasma was passed through the sponge continuously - 50 mls being used in each experiment. All experiments were carried out at 4°C.

Unadsorbed protein was washed away with the same buffer used in adsorption at a flow rate of 1.0 $cm^3 min^{-1}$ until the absorbance at 280 nm (A_{280}) declined to less than 0.005.

Elution was effected with 0.5 M NaSCN/0.05 M Tris-HCl, pH 8.0 buffer at the same flow rate used in adsorption and washing.

The absorbency of protein was measured with a Pye Spectrophotometer model SP8-400. The protein concentration was calculated from a bovine serum albumin (BSA) standard curve.

The results of these experiments are shown in Table 3.2 below.

Table 3.2 Capacities of Blue Sponge (Batches 1, 2, 3 and 4) for HSA

(a) EXPERIMENT 1: Capacities of Batches 1, 2 and 3:

Recirculation of 20 mls of 1:10 diluted human blood plasma.

BATCH #	TOTAL PROTEIN (mg)	CAPACITY mg/g dry wt
1	12.31	2.432
	12.87	2.543
	10.99	2.171
	12.10	2.39
	11.68	2.307
2	16.51	3.260
	16.22	3.204
	15.9	3.141
	15.79	3.119
	16.1	3.181
3	35.2	6.954
	35.9	7.092
	36.4	7.191
	35.8	7.072
	34.9	6.895
	34.89	6.893

BATCH	AVERAGE CAPACITY mg/g dry wt
1	2.369
2	3.181
3	7.016

(b) EXPERIMENT 2: Capacities of Batches 3 and 4 using frontal analysis with 150 mls of 1:10 diluted human blood plasma.

BATCH #	TOTAL PROTEIN (MG)	CAPACITY mg/g dry wt	AVERAGE CAPACITY (mg/g)
3	65.21	12.88	
	64.68	12.78	
	64.99	12.84	12.77
	63.56	12.56	
	64.66	12.77	
4	85.28	16.85	
	84.69	16.73	
	84.14	16.62	16.73
	84.99	16.79	
	84.26	16.65	

During the experiments the average wash volumes were recorded and are shown in Table 3.3 below.

Table 3.3. Average Wash Volumes for Experiments 1 and 2.

(a) EXPERIMENT 1

BATCH #	AVERAGE WASH VOLUMES (cm^3)
1	151
2	175
3	182

(b) EXPERIMENT 2

BATCH #	AVERAGE WASH VOLUMES cm^3
3	250
4	325

Based on the results in Table 3.2 (a), the high temperature-short time was considered to be the best immobilization condition in terms of operational capacity.

From Tables 3.2(b) and 3.3(b) it can be seen that for the two high temperature-short time batches (#3 reaction time of 2 hrs at 80°C and #4 reaction time of 3 hrs at 80°C) the fourth batch has a higher average capacity but it needed some 30% more wash volumes than the third batch. Also it was observed that the sponge had a hardened texture. Based on criteria (ii) and (iii) the immobilization reaction condition for the third batch seemed better. However, a batch of intermediate reaction time, 2½ hrs at 80°C gave capacity (16.3 mg/g) comparable with the fourth batch and wash volume of only 5% more than the third batch. This intermediate condition was therefore adopted for further blue sponge preparations.

(c) DETERMINATION OF LIGAND (BLUE DYE) CONCENTRATION ON THE SPONGE MATRIX

The determination of the amount of Cibacron Blue 3GA covalently bound to the sponge was carried out according to the method of Chambers (1977).

(i) Standard Curve

A standard curve was constructed from standard solutions containing 0-200 µg/ml of Cibacron Blue 3GA. The standards were prepared by diluting a stock solution of a 2 mg/ml solution of Cibacron Blue 3GA in water to a final volume of 5 mls in 6 M HCl.

The solutions in test tubes were incubated in the water bath used for immobilization reaction at 40°C and were mixed every 15 mins. After 1 hr standards were removed and their absorbances at 515 nm recorded with a spectrophotometer. The calibration curve obtained using standard concentrations range of 0-200 μg/ml is shown in Fig. 3.6.

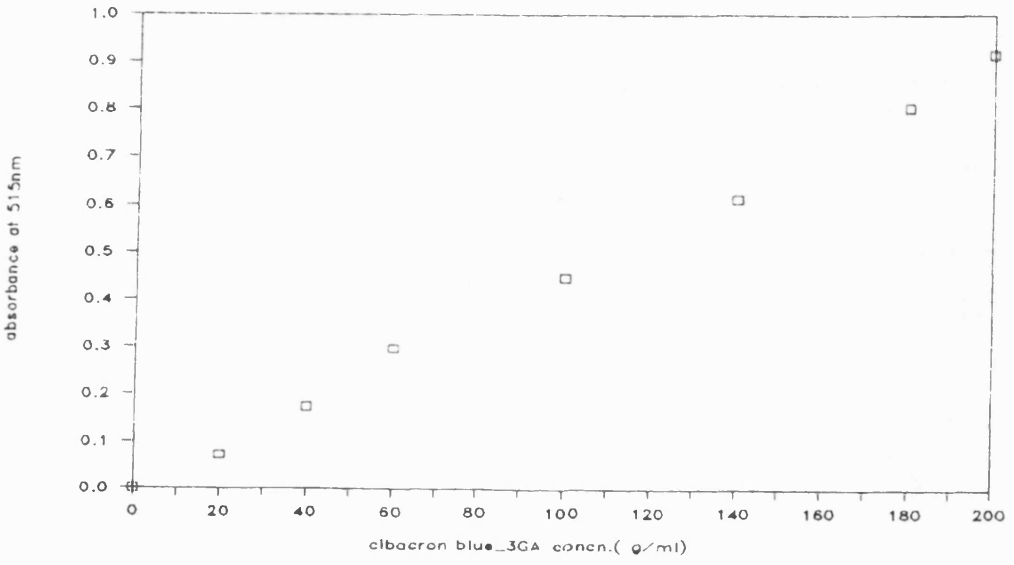

Fig. 3.6. Calibration curve for Cibacron Blue 36A solutions in 6 m HCl.

(ii) Determination of Dye Concentration in Sponge

Ten milligram samples of dry blue sponge were suspended in test tubes containing 5 mls of 6 M HCl. They were treated the same way as for the standards and were incubated at the same time as the standards. The concentrations obtained are shown in Table 3.4.

Table 3.4. Concentration of Bound Cibacron Blue 3GA Ligand in Sponge.

SAMPLE	TOTAL CONCENTRATION (µg)		CONCENTRATION (µg/g dry wt sponge)		AVERAGE CONCN. (µg/g dry wt)
	Tube 1	Tube 2	Tube 1	Tube 2	
1	451.82	451.96	45.182	45.196	45.189
2	453.11	452.07	45.311	45.207	45.259
3	456.2	452.18	45.620	45.218	45.419
			Overall Average Concentration = 45.289 µg/g		

(iii) Ligand Stability

The long term or commercial use of the blue sponge in affinity separation will depend on the stability of the covalently bound ligand. Apart from traces of blue dye eluted from freshly prepared blue sponge during the first few adsorptions, there were no apparent traces in eluting solution in subsequent usage.

The derivatized sponge discs were preserved at 4°C in 0.1% sodium azide solutions to avoid bacterial attack on the matrix.

3.2 SEPARATION PERFORMANCE OF THE BLUE MEMBRANE (BM) AND BLUE SPONGE

3.2.1 APPARATUS

Two types of columns, Amicon Wright Borosilicate glass, adjustable length column, model GA 44 x 90 (44 mm diameter) and Sartorius 200 ml stainless steel pressure holder, model SM 16249

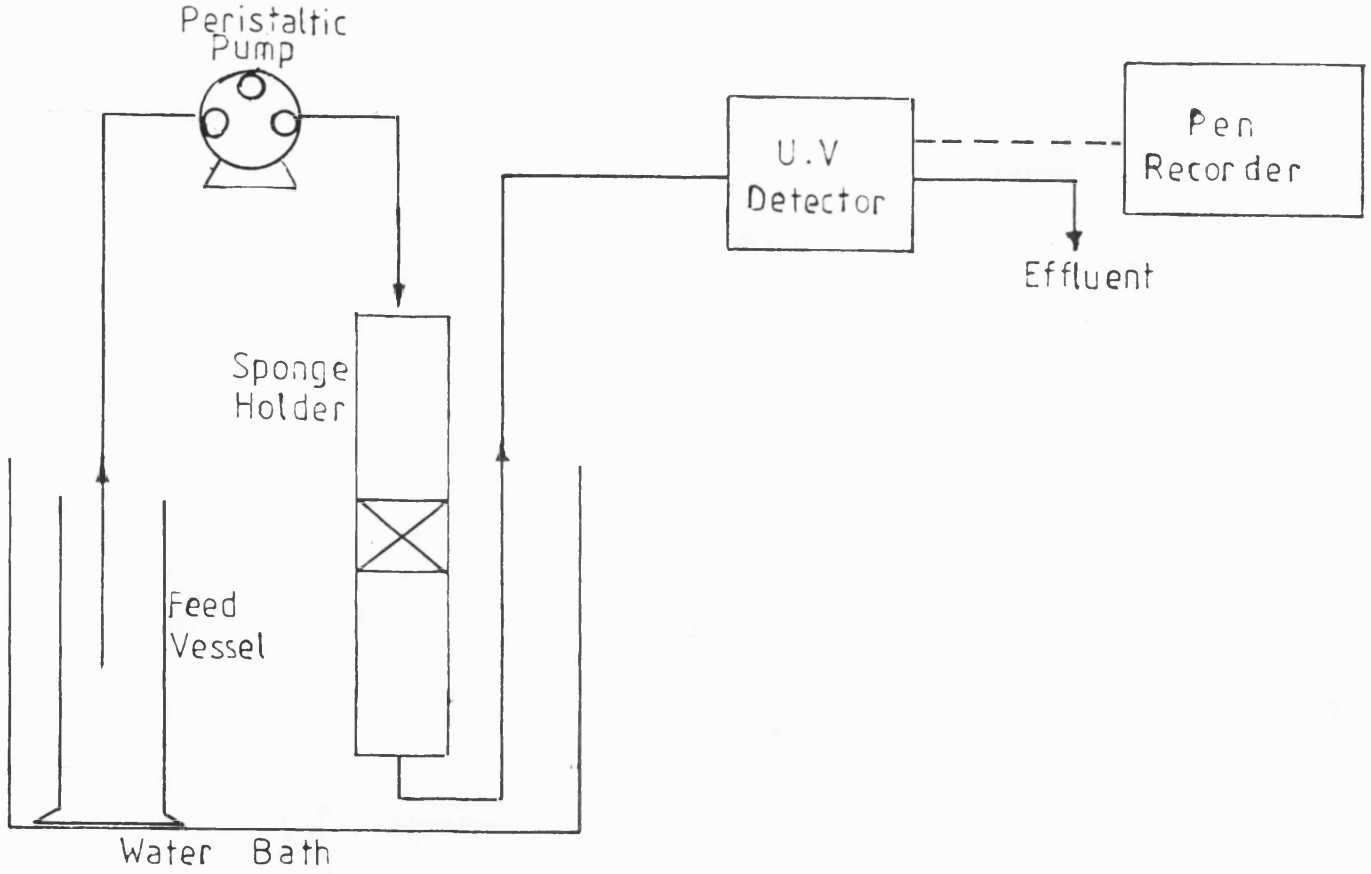

Fig 3.7a Flow Diagram of Experimental Set-up for Separation Studies with Blue Spong in Column Configuration

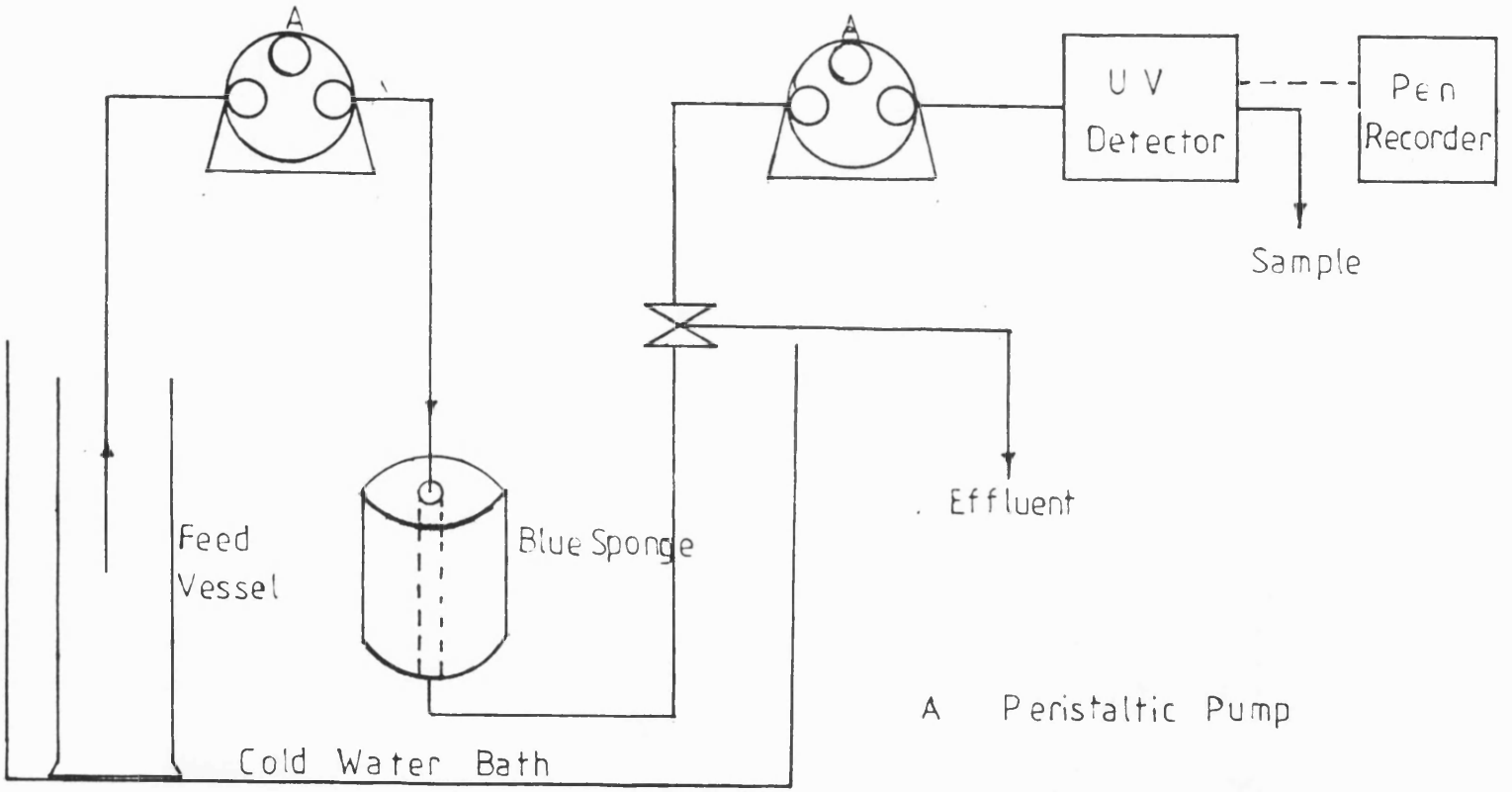

Fig 37b Flow Diagram of Experimental Set-up for Separation with Blue Sponge in Radial Flow Configuration

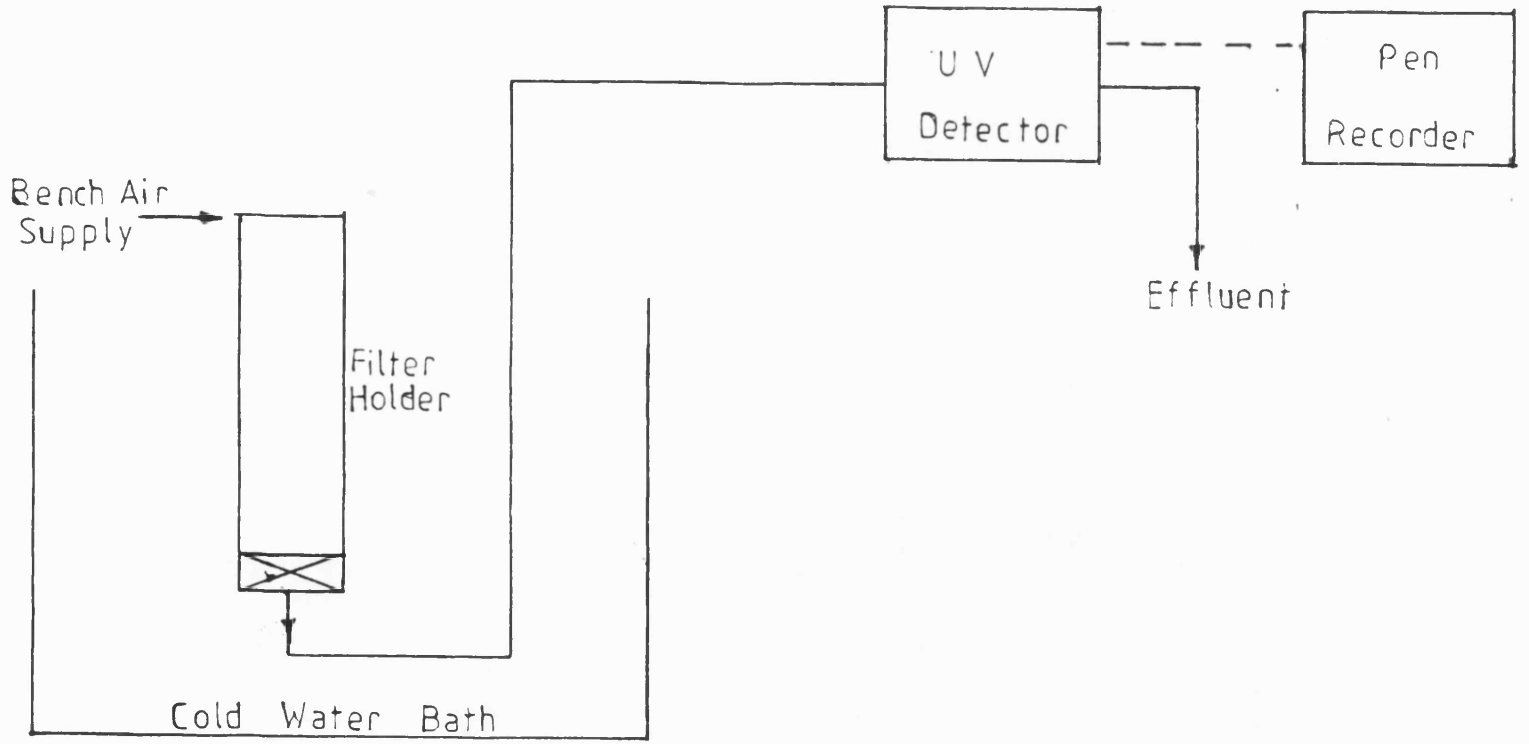

Fig 3.7c Flow Diagram for Experimental Set-up for Separation With Blue Membrane in Satorious Filter Holder

were used. The Sartorius filter holder was later modified to include an adjustable length plunger for use with the BS but was initially used, as received, for adsorption experiments with the blue membranes. Either one of the Watson-Marlow pumps (Model 101U or 501U) was used to pass protein solutions through the columns and the flow through the cell of the LKB Uvicord II detector at 280 nm. A micro column constructed from ¼" (0.464 mm in diameter and 50 mm length) stainless steel tubing with end fittings adaptable for use with Gilson HPLC was used for breakthrough studies.

A radial flow configuration was also used. With the radial flow system two pumps were used, one model 101U was used to direct a sufficiently small volume of effluent stream through the flow cell of the detector. The experimental set-up (flow diagrams) are shown in Figs. 3.7a-c.

(a) DESIGN OF RADIAL FLOW CONFIGURATION

The cross-section through the radial flow configuration is shown in Fig. 3.8a. The central porous polyethylene tube (19 mm O.D. x 3 mm wall thickness, 60 micron retention) was purchased from Plastok Filtration, 2 Inn Street, Birkenhead, U.K. The two end pieces (F) attached to the central tube were made from perspex blocks. H is the encasing nylon mesh with the sponge sheet wrapped round the central porous tube in place. D are perspex pieces (solid) used to connect the inner framework to the outer casing end pieces, B. E is the housing for the main adsorption system. The PVC end pieces, B (provided with O-rings, C) sits on the inner part of the perspex tubing to provide a small fluid space between

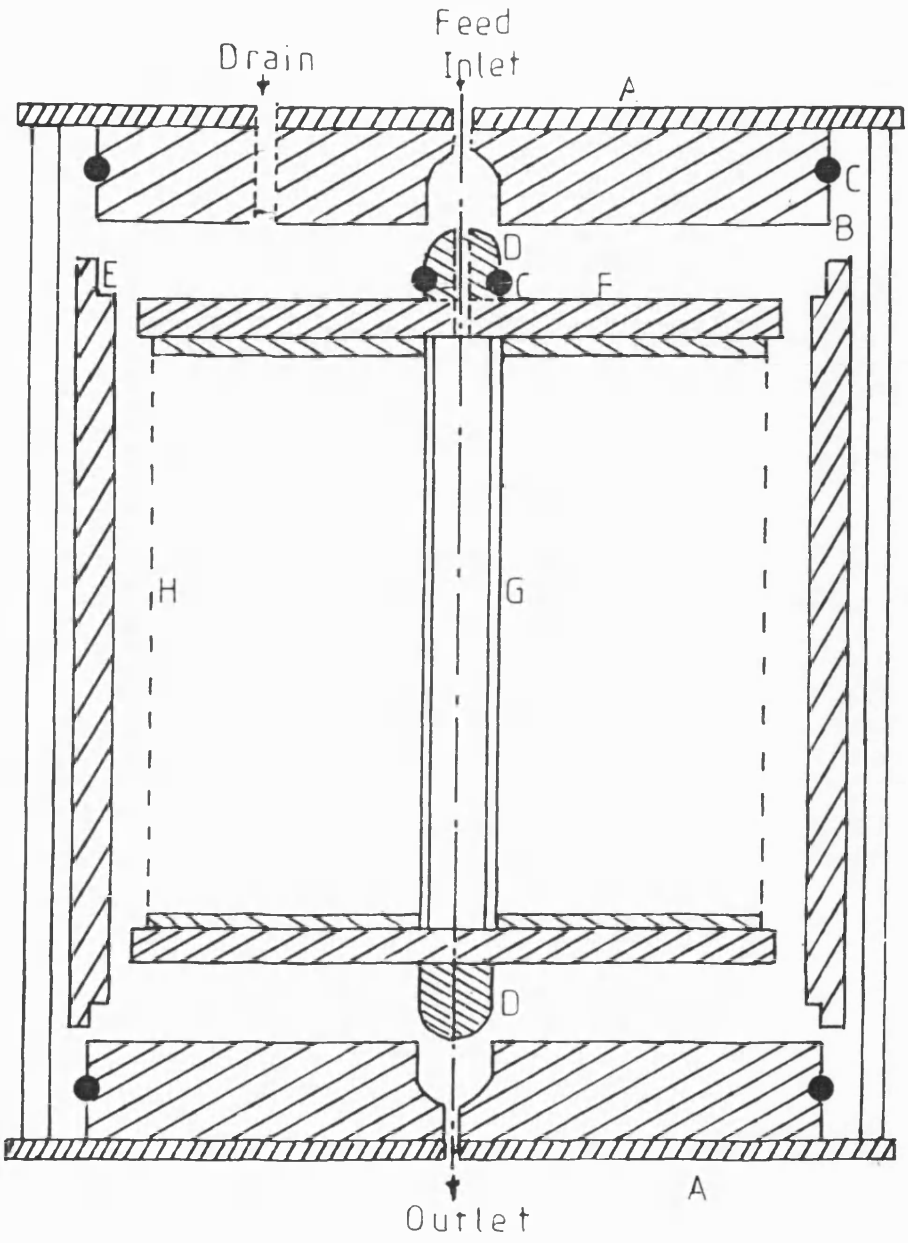

A	PVC End Plate Attached To Support Frame
B	Perspex End Pieces To Fit E
C	O Ring
D	Perspex Block
E	Perspex Tube
F	Perspex End Piece
G	Porous Polyethlene Tube[19mm O.D × 3mm Thickness 60 μ Retention]
H	Nylon Mesh

Fig 3.8a Cross-Section through the Radial Flow Configuration for Blue Sponge

the nylon mesh and the casing. The O-rings ensure a water-tight fluid space so that fluid flow is restricted to the inlet, the porous central tube and the outlet. The upper O-ring attached to the tip D stops backflow of fluid from the inner chamber. The PVC end pieces, A, and the stainless steel frame provide support for the whole system and provide a means for stand attachment. Drainage for the inner space or chamber is provided at both end plates but are plugged during normal use.

Fluid flows from the inlet through a hole running through the upper end piece, D, and then down the central hole of the porous tube. The fluid flows radially through the sponge and mesh into the mesh/casing fluid space and out through small slits between the lower end piece connector, D and the lower end piece, B. The flow pattern is shown in Fig. 3.8b below.

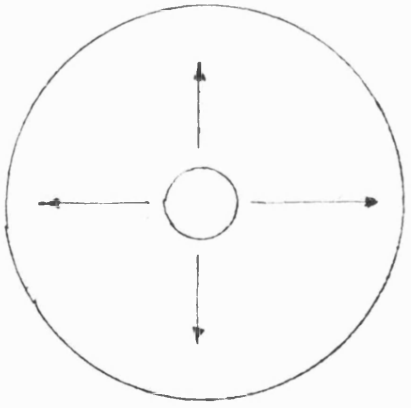

Fig. 3.8b. Flow pattern of the radial flow system.

(b) PUMPS

Watson Marlow variable speed peristaltic pumps models 101U and 501U were used for feed to the bed and the sample points to the U.V. detector.

(c) ULTRAVIOLET DETECTOR

An LKB U.V. detector model Unicord II was used for on-line monitoring of protein concentration at 280 nm. The protein solution flows through a continuous flow through cell of path dimensions 100 mm path length by 1 mm diameter.

(d) CHART RECORDER

As for Section 3.1.

3.2.2 MATERIALS

All chemicals were of Analar grade qualities and were purchased from Sigma Chemicals Ltd.

Other materials are the same as for Section 3.1.2.

3.2.3 EXPERIMENTAL METHODS

Two different types of cellulose based matrices to which Cibacron Blue 3GA has been covalently attached were used to adsorb human serum albumin (HSA) from human blood plasma. The first to be used was very thin blue membrane (BM) discs and then blue sponge.

(a) ADSORPTION WITH BLUE MEMBRANE

Batch adsorption of HSA from human blood plasma was carried out at 4°C and 2 bars by using 10 blue membranes per batch in a Sartorius stainless steel pressure filter holder with a membrane adsorption area of 13 cm^2. The membranes were equilibrated in the adsorption buffer and then placed on the lower part of the filter holder. An O-ring was placed on top of the holder part then screwed onto the upper cylindrical reservoir. The top cap was

opened and the required volume poured into the reservoir. The top was screwed back in and the protein solution (plasma) pushed through the membranes by means of air pressure. Washing and elution or desorption were carried out in the same way.

(i) Adsorption Step

Adsorption was effected with 10 mls of human blood plasma diluted 30 times with Tris-HCl buffer (50 mM Tris-HCl/50 mM NaCl, pH 8.0). Adsorption was monitored continuously with a continuous flow U.V. detector to measure the protein concentration at 280 nm (A_{280}). The output of the U.V. detector was connected to a chart recorder to give the time course of the adsorption. When required samples were collected at the sampling outlet in small volumes, usually 1 cm^3 for subsequent analysis of the protein concentration.

(ii) Wash

Washing was carried out with the same buffer for adsorption except for the exclusion of the adsorbate. Unadsorbed protein was washed off until the A_{280} declined to zero - this was indicated on the chart recorder output.

(iii) Elution or Desorption

The desorption of adsorbed HSA was effected with 10 to 20 mls of 500 mM NaSCN/50 mM Tris HCl buffer, pH 8.0. The eluate was collected and kept for subsequent determination of protein content. Because the eluate was very dilute, protein content was determined by the method of Lowry et al. (1951), with commercial HSA as standard.

(iv) Flux measurement

The flux through the membrane during adsorption was measured by sampling equal volumes - 0.5, 1 or 2 mls - and noting the time.

(v) Breakthrough Curve

The breakthrough behaviour of the membranes during passage of protein solution was studied by measuring effluent protein concentration at the same operating conditions as in the normal run. Commercial HSA was dissolved in 50 mM Tris-HCl/50 mM NaCl. Equal volumes (0.5, 1 or 2 mls) were sampled at recorded times and the protein concentration determined.

(b) HSA SEPARATION BY FRONTAL ANALYSIS METHOD WITH BLUE SPONGE (BS)

(i) Adsorption

The adsorption buffer was the same as that used for blue membrane and at 4°C. Figs. 3.7a-c show the flow diagrams of the experimental set-up. Protein solutions or plasma diluted with ten times the volume of adsorption buffer was passed continuously through a bed of squashed blue sponge (BS) until protein was detected in the effluent. The peristaltic pump was used to pass the adsorbate solution through the column and U.V. detector and out at the sampling point. Two different columns were used, the Sartorius (modified column) and the Amicon Wright adjustable length column.

Effluent protein solutions were collected with an LKB Redi-Rac fraction collector and the content analysed by measuring the A_{280} with the CE 588 spectrophotometer. The effluent protein content was also monitored by means of the chart recorder connected

to the U.V. detector.

(ii) Wash Step

Washing was done with the adsorption buffer (minus protein) as for the blue membrane but the buffer was passed continously through the column until the required level of washing was achieved, usually $A_{280} < 0.01$.

(iii) Elution Step

Elution was effected with 500 mM NaSCN/50 mM Tris-HCl buffer, pH 8.0 or with 1000 mM KCl/50 mM Tris-HCl, pH 8.0 for protein other than HSA. Eluate protein content was determined at absorbance of 280 nm using protein standard curves shown in Figs. 3.9 a-c.

(iv) Breakthrough Curve

The breakthrough behaviour of the adsorbate was studied by measuring the protein content of samples collected at the outlet of the column at given time intervals. The breakthrough curves of plasma, commercial HSA solution and lysozyme solutions were studied using the micro column, modified Sartorius column and the Amicon Wright adjustable length column. The parameters important in determining the breakthrough curve, like initial solute concentration, bed length and feed flow rates were varied one at a time whilst keeping the remaining conditions constant.

(c) BATCH ADSORPTION OF LYSOZYME WITH BLUE SPONGE

Because of the finding by Chase (1984a) that blue dye

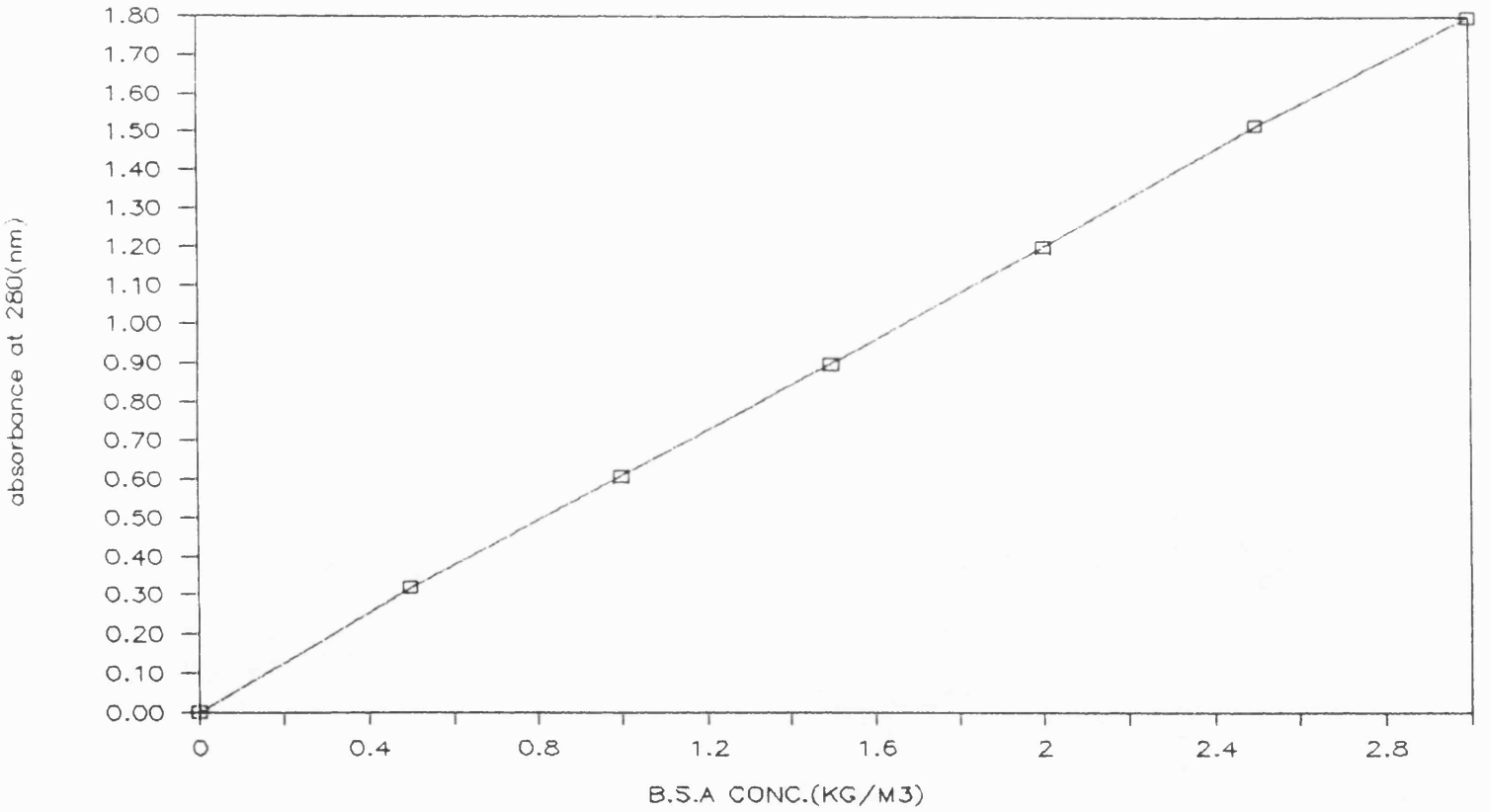

Fig. 3.9a. BSA calibration curve: Absorbance against protein concentration.

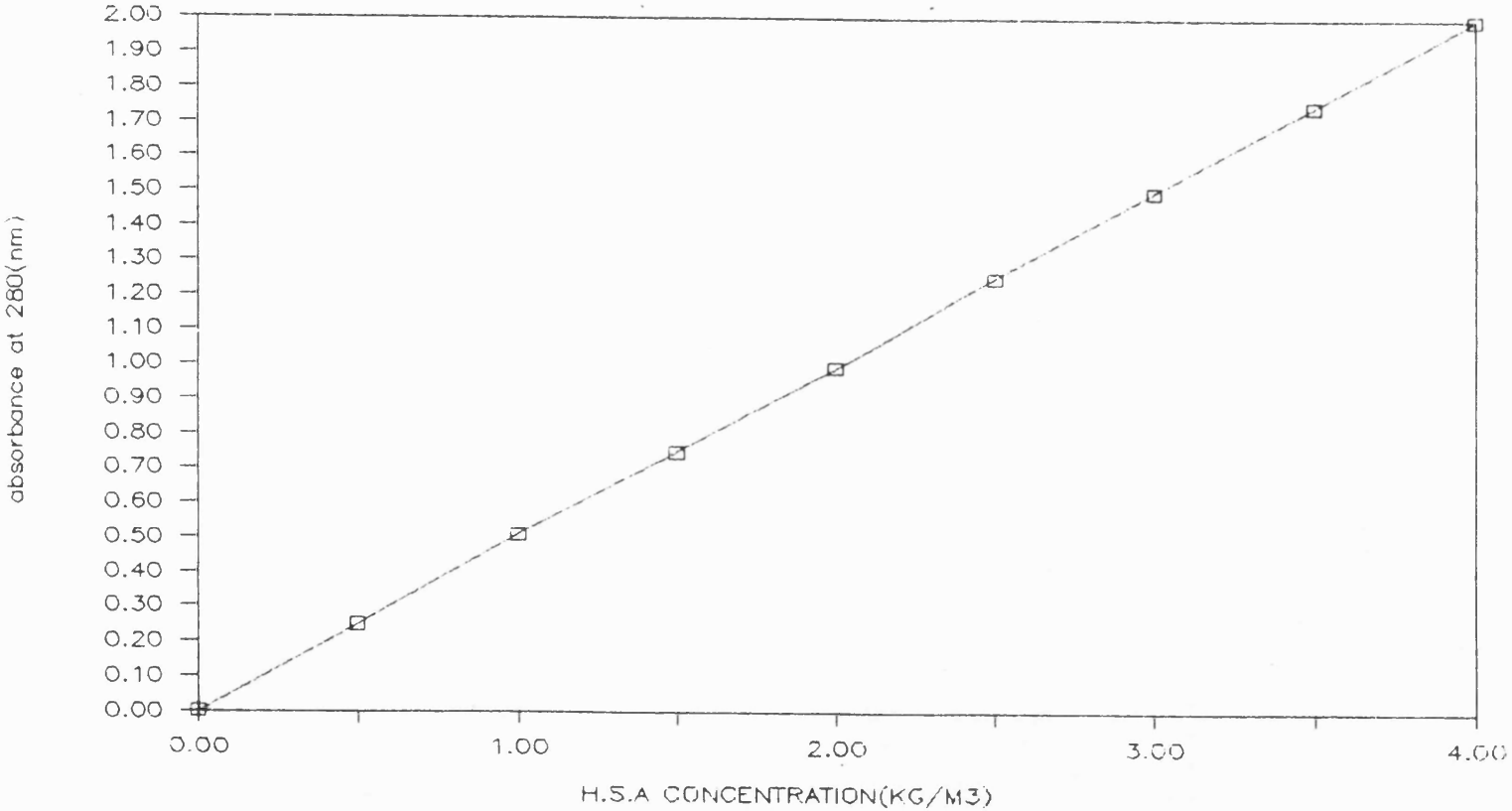

Fig. 3.9b. Human serum albumin calibration curve: Absorbance against protein concentration.

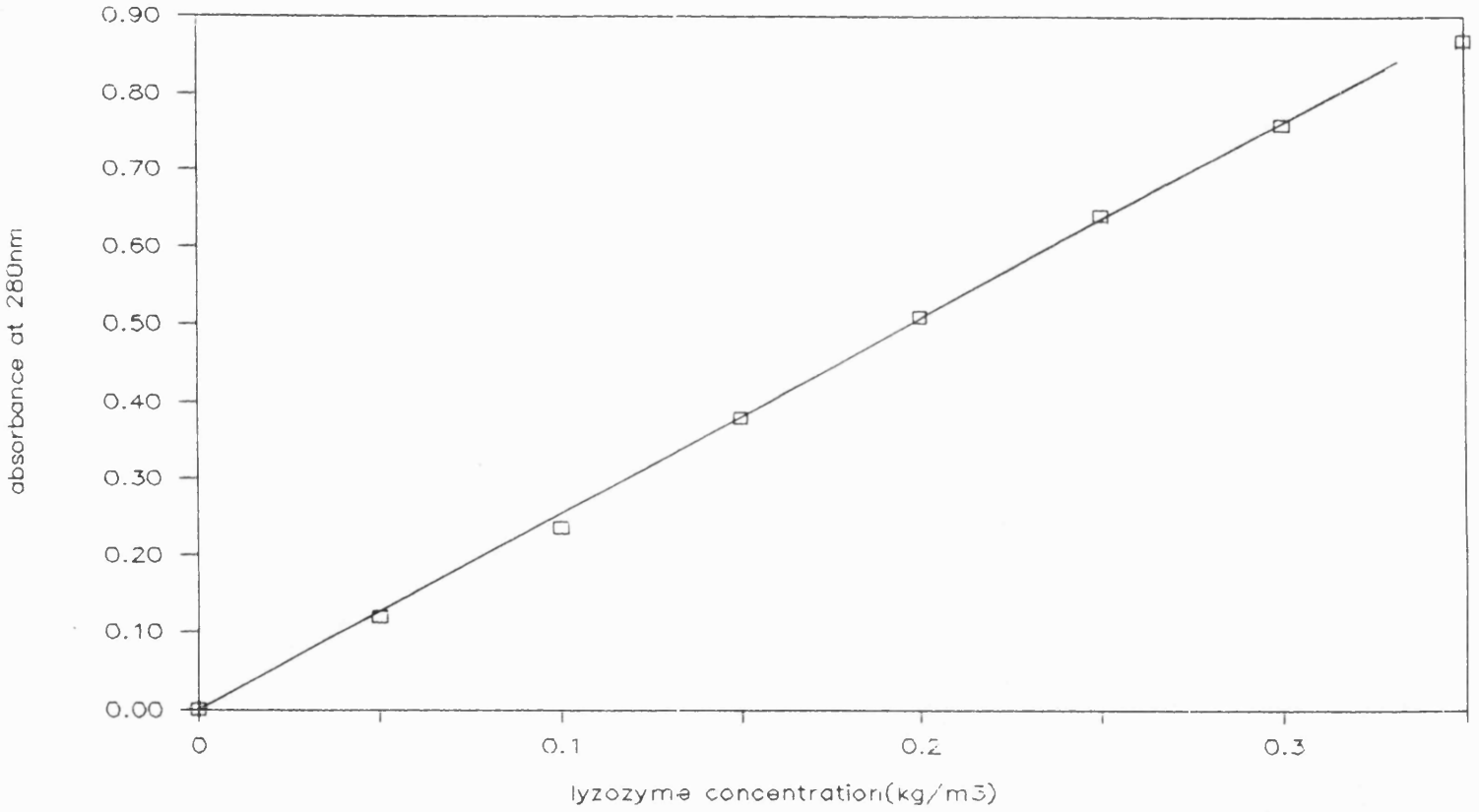

Fig. 3.9c. Lysozyme calibration curve: Absorbance against protein concentration.

adsorbents have good adsorption affinity for the lysozyme it was decided to carry out lysozyme adsorption by batch, although this work is not particularly concerned with lysozyme adsorption. A five-stage batch adsorption of lysozyme in 50 mM Tris-HCl/50 mM NaCl buffer, pH 8.0 was carried out. 5 mg/ml of lysozyme solution was incubated overnight with 2.531 g dry weight of blue sponge (5 discs) in a volumetric flask. Agitation was by shaking incubator in a cold room (constant temperature of 4°C).

After the first adsorption, the A_{280} was measured and the solution squeezed out of the blue sponge - wearing surgical gloves to avoid contact with the hands. The solution was then re-charged with fresh adsorbent of equal weight as for the first adsorption and the operation repeated.

(d) SEPARATION USING RADIAL FLOW SYSTEM

Adsorption, wash and elution conditions were as for the frontal analysis method except that two pumps were used. The smaller pump was used to pass sufficiently small volumes of the plasma through the flow through the U.V. detector.

(e) ESTIMATION OF PROTEIN CONCENTRATION BY THE LOWRY METHOD

(i) Principle

The protein is reacted with the Folin-Ciocalteau reagent to produce a coloured complex, the colour formed being due to the reaction of the protein with alkaline copper, the Biuret reaction of protein, and the reduction of the phosphomolybdic-phospho-tungstic reagents by tyrosine and tryptophan residues present in the protein. The intensity of the colour depends on the concentration of protein in the solution (Lowry et al., 1951).

(ii) Preparation of Reagents

1. Alkaline sodium carbonate solution (Reagent A)

20 g of sodium carbonate was dissolved in one litre of 0.1 molar sodium hydroxide to give 2% (w/v) Na_2CO_3 in 0.1 M NaOH.

2. Copper sulphate - sodium tartrate solution (Reagent B)

5 g of $CuSO_4.5H_2O$ was dissolved in one litre of distilled water containing 10 g of sodium potassium tartrate to give 0.5% (w/v) $CuSO_4.5H_2O$ in 1% (w/v) Na_2K tartrate.

3. Alkaline solution (Reagent C)

Prepared on the day of use by mixing 50 ml of Reagent A with 1 ml of Reagent B. This is discarded after one day.

4. Folin-Ciocalteau Reagent (Reagent E)

Prepared by mixing the commercially obtained reagents with an equal volume of distilled water to give a 1:1 (v/v) solution and to make the reagent 1 M in acid on the day of use. The commercial solution contains sodium tungstate and sodium molybdate in phosphoric and hydrolic acid.

5. Standard protein

10-100 µg of human serum albumin (HSA) in one ml distilled water.

6. Standard curve

Eleven standard samples of HSA were prepared in a range of

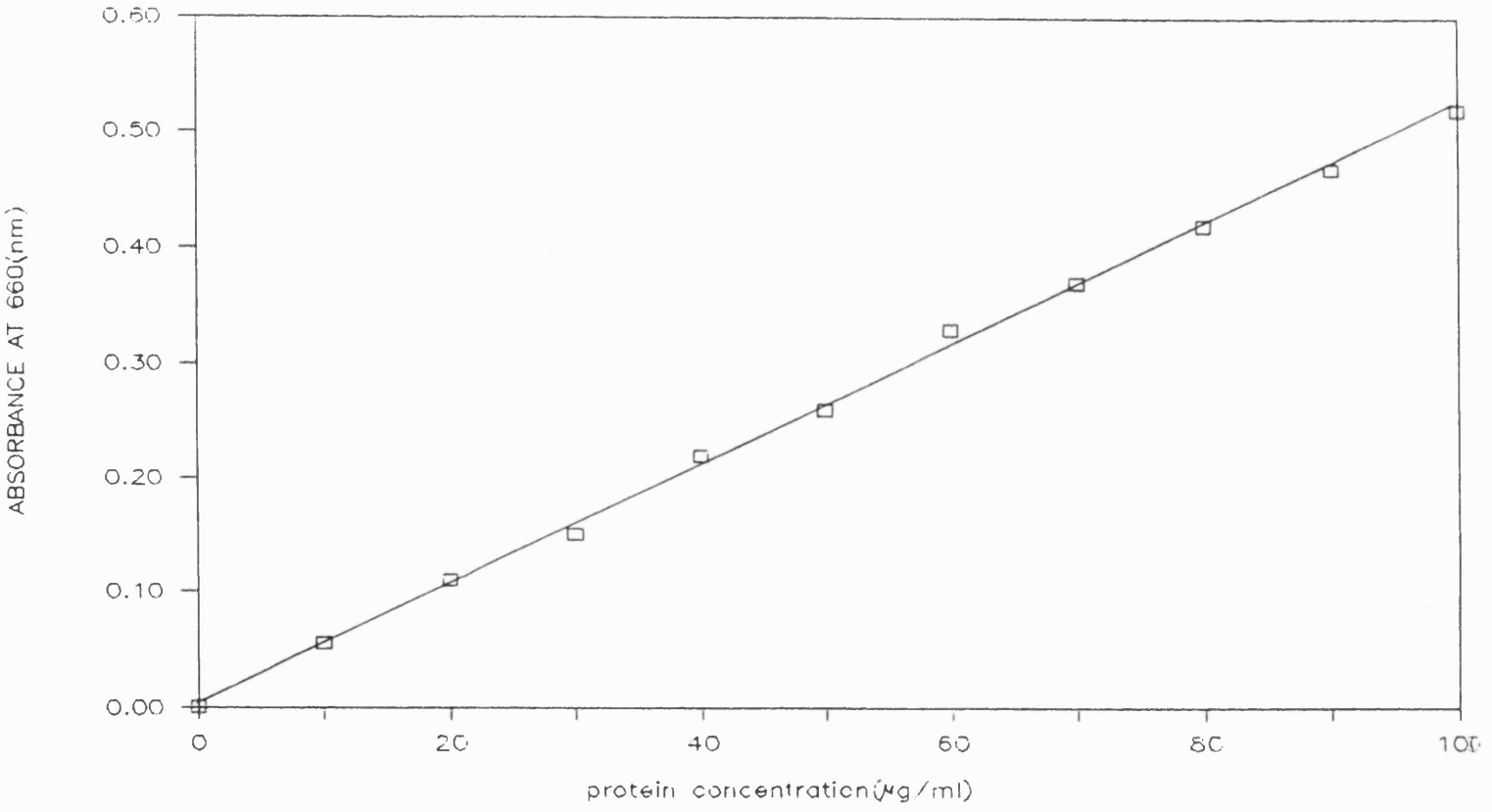

Fig. 3.10. Protein calibration curve (Absorbance against concentration) for the Lowry method.

concentrations from 0 to 100 µg/ml. These were each mixed with 5 ml of reagent A and allowed to stand at room temperature for at least ten minutes, then 0.5 ml of reagent E was added followed by thorough mixing for 1 minute using an automixer. The mixture was incubated for 30 minutes at room temperature then the absorbance measured at 660 nm in a spectrophotometer. A linear curve was obtained (Fig. 3.10) and used as a means of determining protein concentrations in unknowns.

7. Determination of proteins in eluates

This method was chosen for the protein determination for the eluates from the BM adsorption experiments, since it is more sensitive than the 280 nm absorbance and Biuret method. It is therefore very suitable for accurate determination of very dilute protein solutions, the level encountered in these experiments. However, the Tris-buffer used in desorption interferes with the colour development of this method, therefore, trichloroacetic acid (TCA) was added to all protein samples to a final concentration of 5% TCA. The resulting precipitate was washed twice with 5% TCA. The precipitate was recovered by centrifugation and later redissolved in alkaline Lowry reagent, then treated as described above for the standard solutions. Incubation (colour development) was performed in a dark cupboard, away from the sun.

3.2.4 PURITY OF ELUTED PRODUCT (HSA)

The polyacrylamide gel electrophoresis (P.A.G.E.) was used to assess the purity of the separated HSA from the blood plasma.

PRINCIPLE

The technique is based on the principle that substances migrate at different rates in an electric field due to differences in the number of charges they carry and their molecular weights. Details of this technique are shown in appendix 1.

3.2.5 RESULTS

(a) SEPARATION PERFORMANCE OF THE BM

(i) Thin Blue Membrane

(1) Membrane Capacity

The membrane capacity of the thin blue membrane (TBM) was calculated in terms of mg protein adsorbed per unit area of the membrane using the relation:

$$\text{Capacity} = \frac{c}{A \times N} \quad \text{mg/cm}^2$$

where c = total amount of eluted protein (mg)

A = membrane adsorption area (= 13 cm^2)

N = number of membranes used (=10)

The average weight of membrane = 0.05 g

The mean membrane capacity from 20 experiments (see Table 3.5 below) was 71.40 mg/m^2 . The standard deviation from the mean was 2.36.

Table 3.5. Total Adsorbed Protein and Membrane Capacity

EXPT. #	TOTAL PROTEIN ADSORBED (mg)	MEMBRANE CAPACITY (mg/m^2)	EXPT. #	TOTAL PROTEIN ADSORBED (mg)	MEMBRANE CAPACITY (mg/m^2)
1	8.867	68.21	11	8.780	67.53
2	8.962	68.94	12	9.478	72.91
3	8.978	69.06	13	9.326	71.74
4	9.481	72.93	14	9.359	71.99
5	9.664	74.34	15	9.460	72.77
6	9.187	70.67	16	9.681	74.47
7	9.485	72.96	17	9.050	69.62
8	9.648	74.22	18	9.457	72.75
9	9.730	74.85	19	9.30	68.69
10	8.811	67.78	20	9.460	72.77

(2) Membrane Flux

The measurement of the flux through the membrane was necessary in order to ascertain if the passage of the plasma leads to the blocking of the membrane pores and possibly fouling the membranes to the extent that reasonable flow is not obtained over an extended time. One can therefore decide if pre-treatment of the plasma would be necessary.

The results of the flux measurements are shown in Tables 3.6 a-c below. The plots of membrane flux against time are shown in Fig. 3.11.

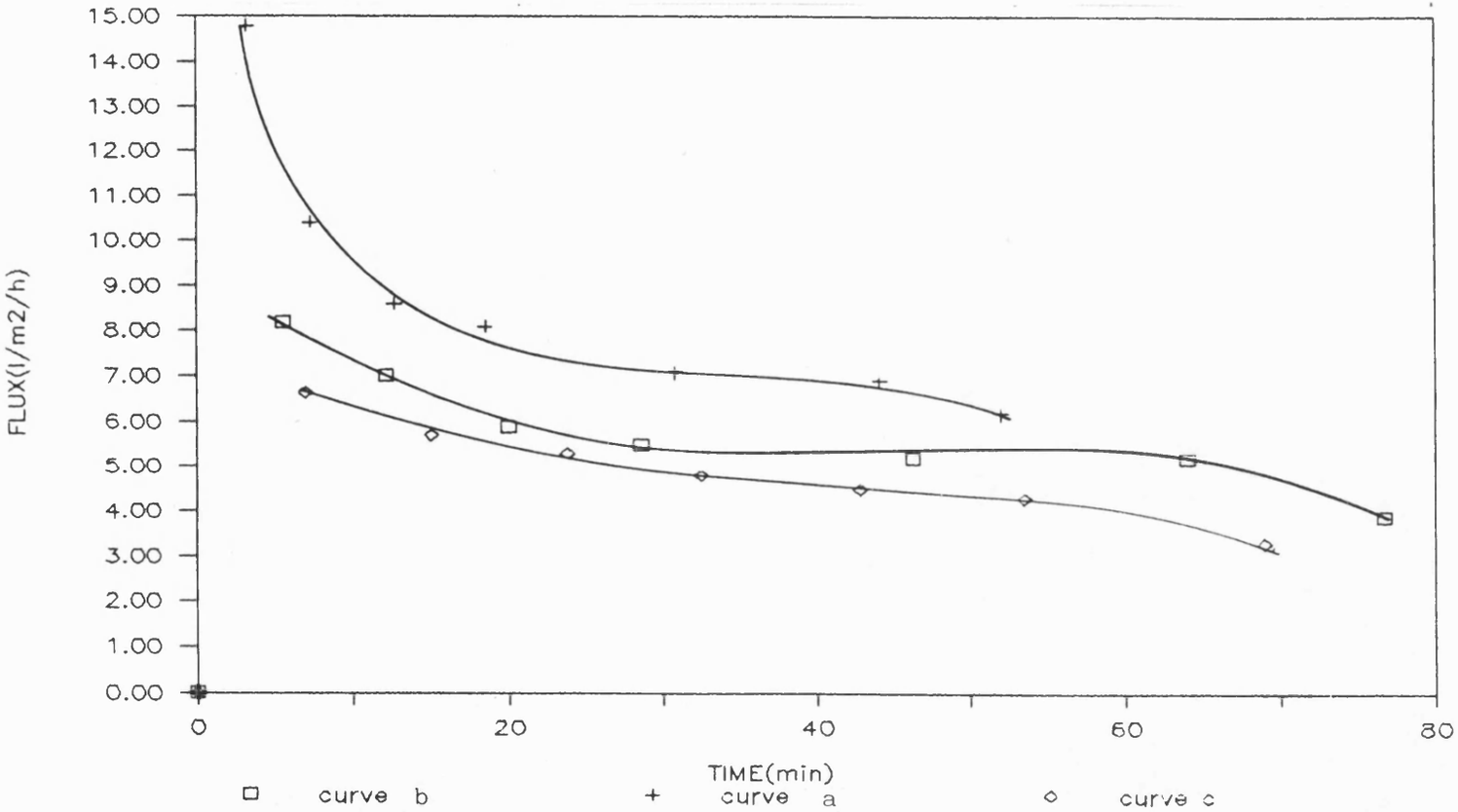

Fig. 3.11. Flux of 1:30 diluted plasma through Thin Blue membrane bed at different membrane conditions.

Table 3.6 a-c. Flux of 1:30 diluted plasma.

3.6a		3.6b		3.6c	
TIME (min)	MEMBRANE FLUX ($x10^{-1}$ ℓ/m² h)	TIME (min)	MEMBRANE FLUX ($x10^{-1}$ ℓ/m² h)	TIME (min)	MEMBRANE FLUX ($x10^{-1}$ ℓ/m² h)
5.6	0.82	3.31	1.48	7.0	0.636
12.18	0.70	7.33	1.04	15.08	0.57
20.00	0.59	12.71	0.86	23.83	0.53
28.62	0.55	18.51	0.81	32.50	0.48
46.27	0.52	30.83	0.71	42.83	0.45
64.03	0.52	44.15	0.69	53.50	0.43
76.77	0.39	52.00	0.62	69.00	0.33

The tables and curves have corresponding labelling, for example Table 3.6a for curve (a) in Fig. 3.11

Curve 3.11a corresponds with membrane condition #1, 3.11b for condition #2 and 3.11c for condition #3. The membrane conditions mentioned above are as follows:

Condition #1

Membranes kept over the weekend in 0.1% Na azide solution in 0.5 M NaSCN, with membranes completely separated with occasional stirring; membranes soaked in 0.01 M NaOH for 10 minutes after the first operation.

Condition #2

Membranes kept overnight in 0.1 g Na azide/100 mls of 0.5 M NaSCN with membranes left stacked together as at the time of removal from the membrane filter holder.

Condition #3

In-place re-use of membranes immediately after a previous separation run.

Condition #1 was assumed to be that of complete regeneration of the membranes, whilst conditions #2 and #3 were for membrane use under the normal operating conditions.

(4) Breakthrough Curve

The breakthrough curve measured with commercial HSA of 1.0 kg/m^3 is shown in Fig. 3.12.

(ii) Blue Sponge

(1) Capacity

The operational capacities of the blue sponge for HSA in 1:10 diluted human blood plasma in Tris-HCl, pH 8.0 using the frontal analysis method was measured in terms of weight of the protein adsorbed (eluted protein after wash) and the dry weight of the adsorbent used.

The capacity at different flow rates for membranes of different dry weights and different bed heights for near saturation of the bed (effluent concentration > 95%) are shown in Table 3.7 below for adsorption with the Amicon Wright column (diameter=4.4cm).

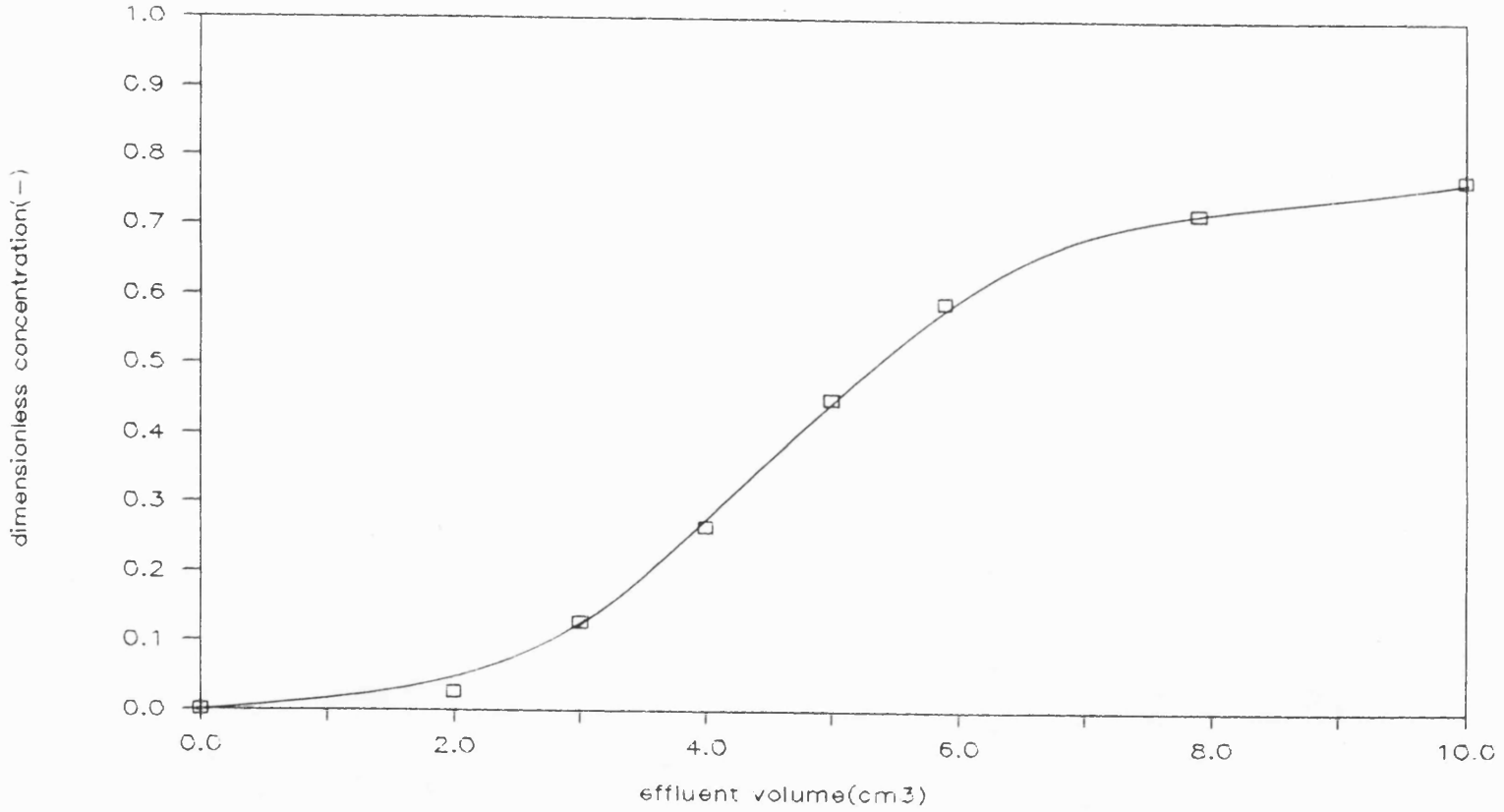

Fig. 3.12. Breakthrough curve for 10 stacked TBM using 1 mg/cm^3 HSA in Tris-buffer, pH 8.0.

Table 3.7 Near Saturation Operational Capacity of BS

(1 ml/min ≡ 1.01 x 10^{-5} m/s)

BED LENGTH = 1.65 cm ADSORBENT WT = 5.06 g		BED LENGTH = 3.61 cm ADSORBENT WT = 10.124 g	
FLOW RATE (cm^3/min)	CAPACITY (mg/g)	FLOW RATE (cm^3/min)	CAPACITY mg/g
1	17.12	1	16.883
2.5	16.56	5	16.65
5	16.55		

The operational capacity under the same adsorption conditions as above, but using the Sartorius column (modified) with diluted plasma (50 cm^3) is shown in Table 3.8.

Table 3.8 Operational Capacity of BS with 50 cm^3 1:10 diluted plasma (1 ml/min ≡ 1.2 x 10^{-5} m/s)

BED LENGTH = 1.88 cm ADSORBENT WT = 5.062 g DIAMETER = 4.2 cm	
FLOW RATE (cm^3/min)	CAPACITY (mg/g)
1	9.131
2	8.752
4	8.366
8	8.109

(2) Breakthrough Curves

The effect of the operating variables, namely initial concentration of adsorbate, CO, the feed flow rate, Q, and the bed length was investigated in order to assess the possible impact on the separation performance of the blue sponge.

(a) Effect of Adsorbate Initial Concentration

The effect of the adsorbate initial concentration on the breakthrough curve was investigated by the use of the micro-column using the Gilson HPLC at a constant flow of 0.3 cm^3/min (2.96 x 10^{-4} m/s). Adsorbate (HSA) concentrations of 0.25, 0.5 and 1.0 mg/ml were examined. The result is shown in Fig. 3.13.

(b) Effect of Length

The effect of length was examined using the Amicon Wright adjustable column with 1:10 diluted plasma in Tris-HCl at pH 8.0. Two lengths 1.65 cm and 3.61 cm were examined at volumetric flow rates of 1 cm^3/min and 5 cm^3/min. The result is shown in Figs. 3.14 a-b.

(c) Effect of Flow Rates

The effects of flow rates were investigated by the use of 50 cm^3 of 1:10 diluted plasma in Tris-HCl, pH 8.0 using the modified Sartorius column. The flow rates examined were 1, 2, 4, and 8 ml/min. The results are shown in Fig. 3.15. The feed flow rate effect with the Amicon Wright column at near column saturation is shown in Fig. 3.16.

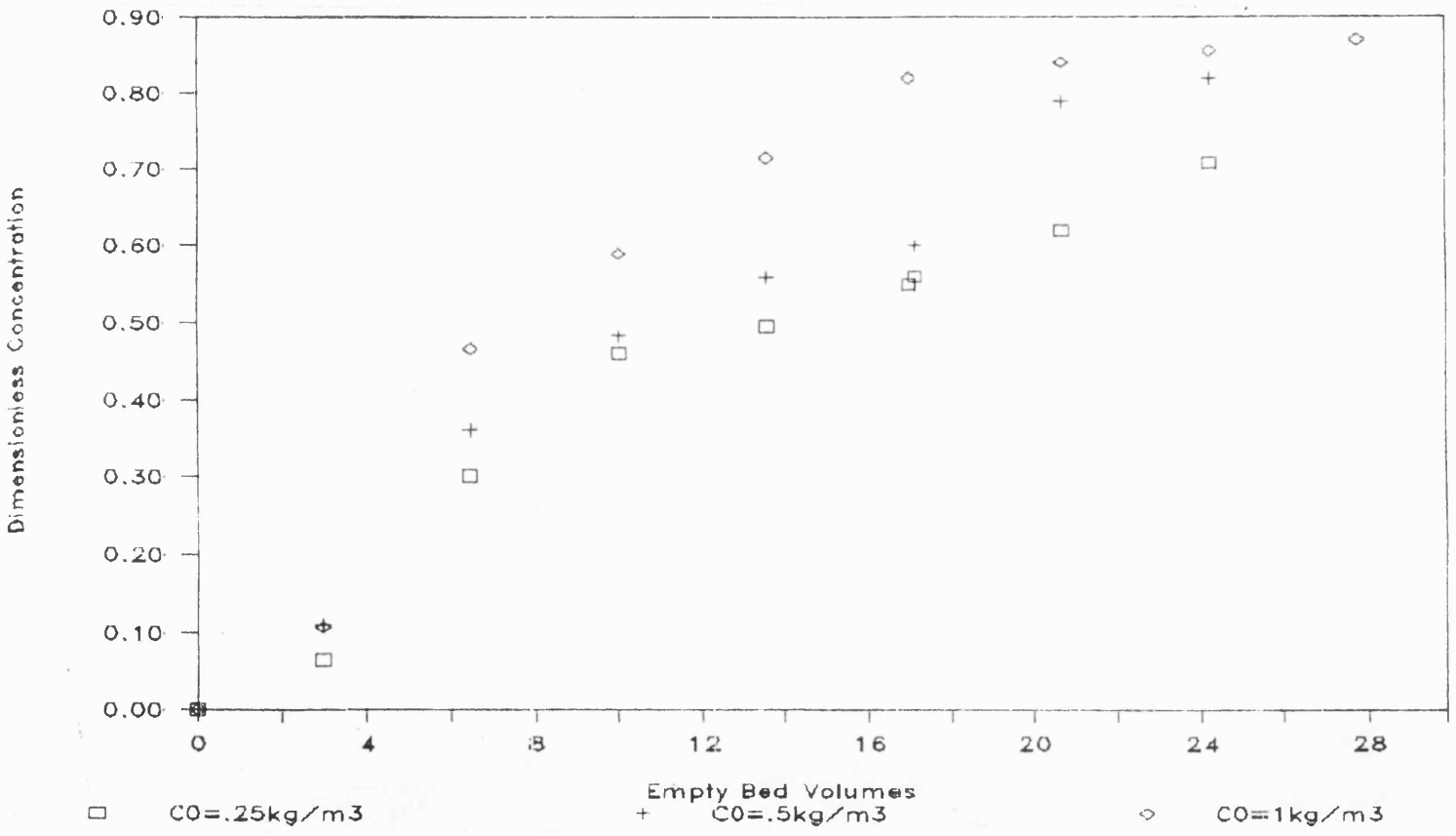

Fig. 3.13. Effect of initial concentration on the breakthrough curve of commercial HSA (with microcolumn on Gilson HPLC).

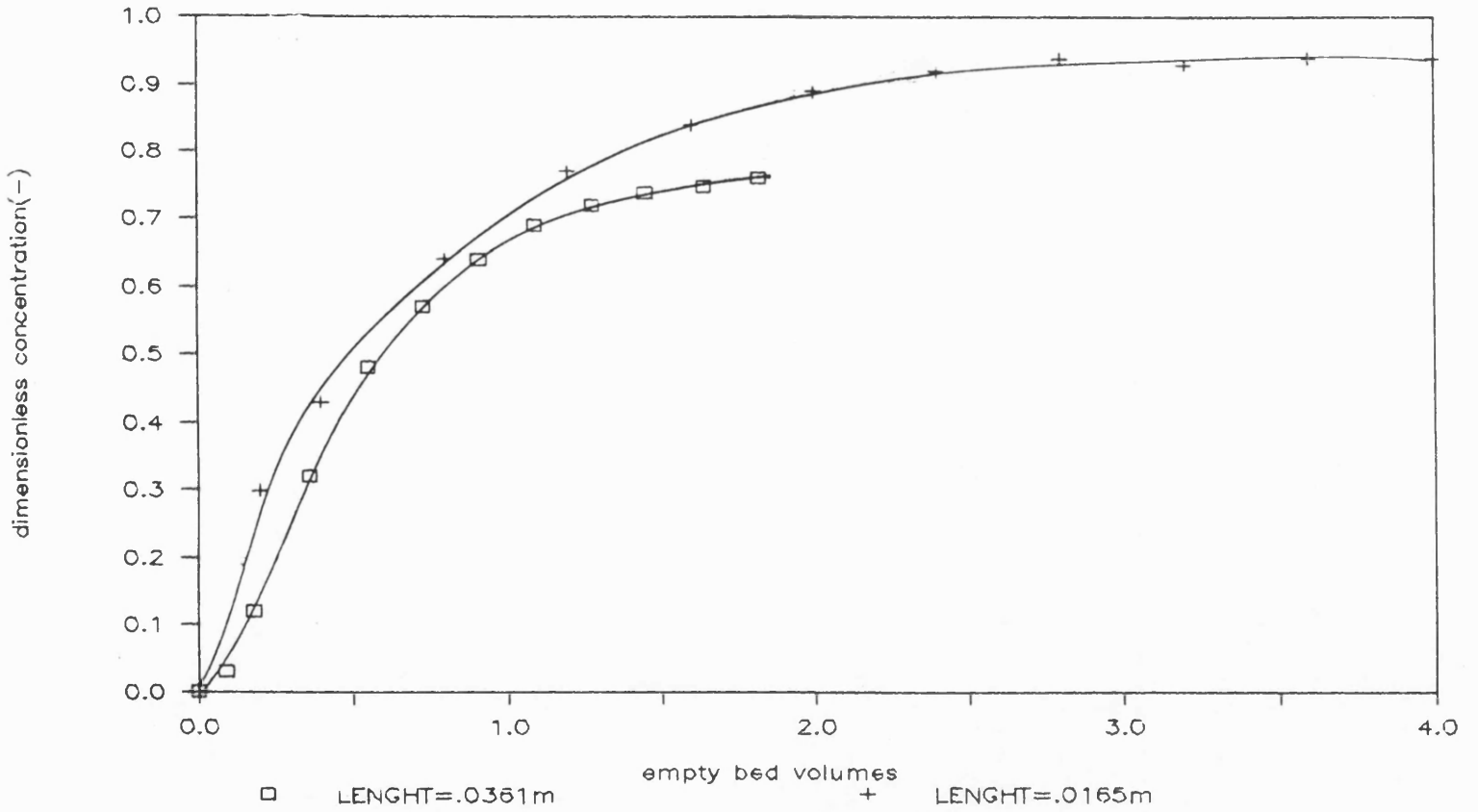

Fig. 3.14a. Effect of bed length on breakthrough curve of 1:10 diluted plasma (Amicon Wright Column) at a flow rate of 1 cm^3/min

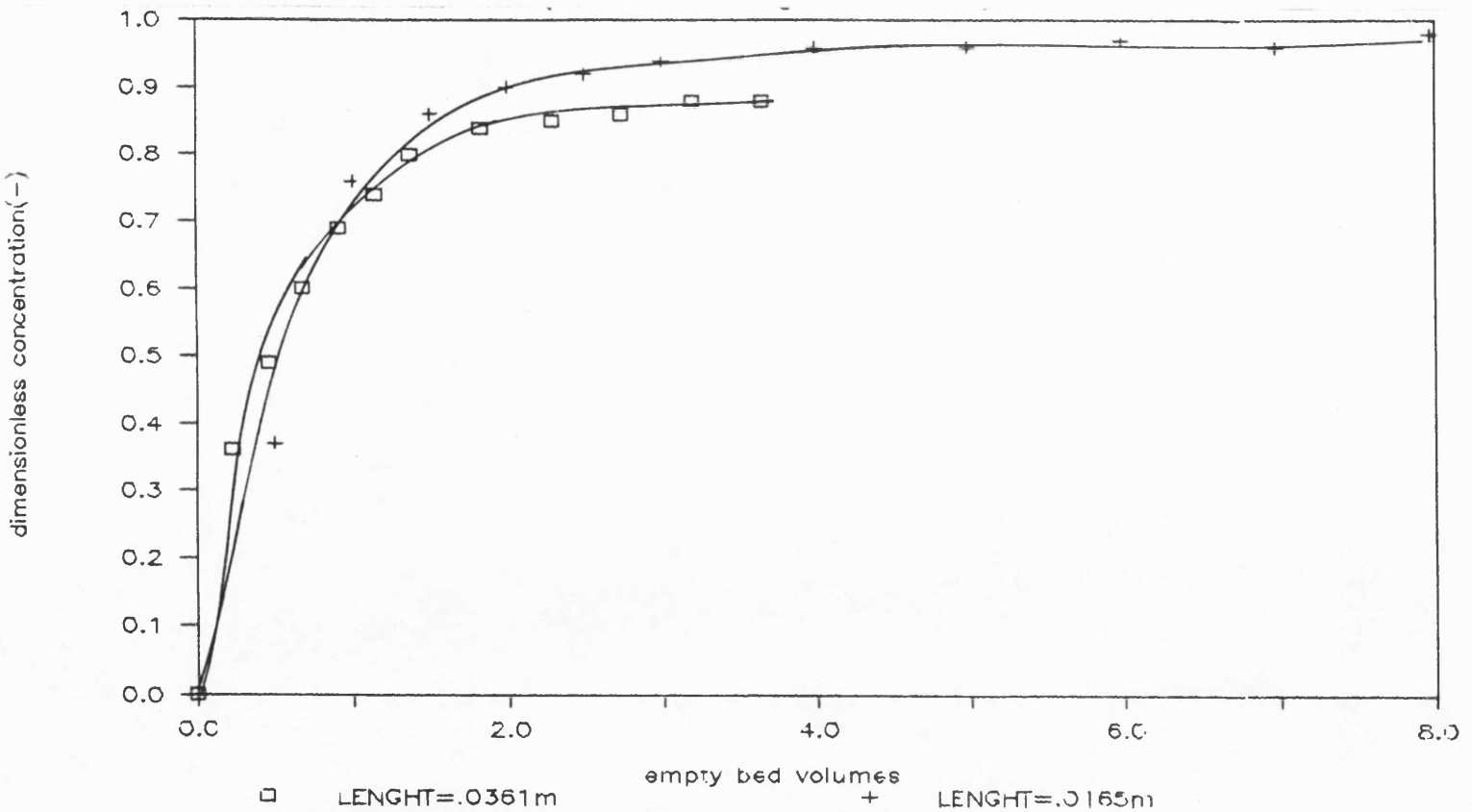

Fig. 3.14b. Effect of bed length on breakthrough curve of 1:10 diluted plasma (Amicon Wright column) at a flow rate of 5 cm^3/min (5.05×10^{-5} m/s).

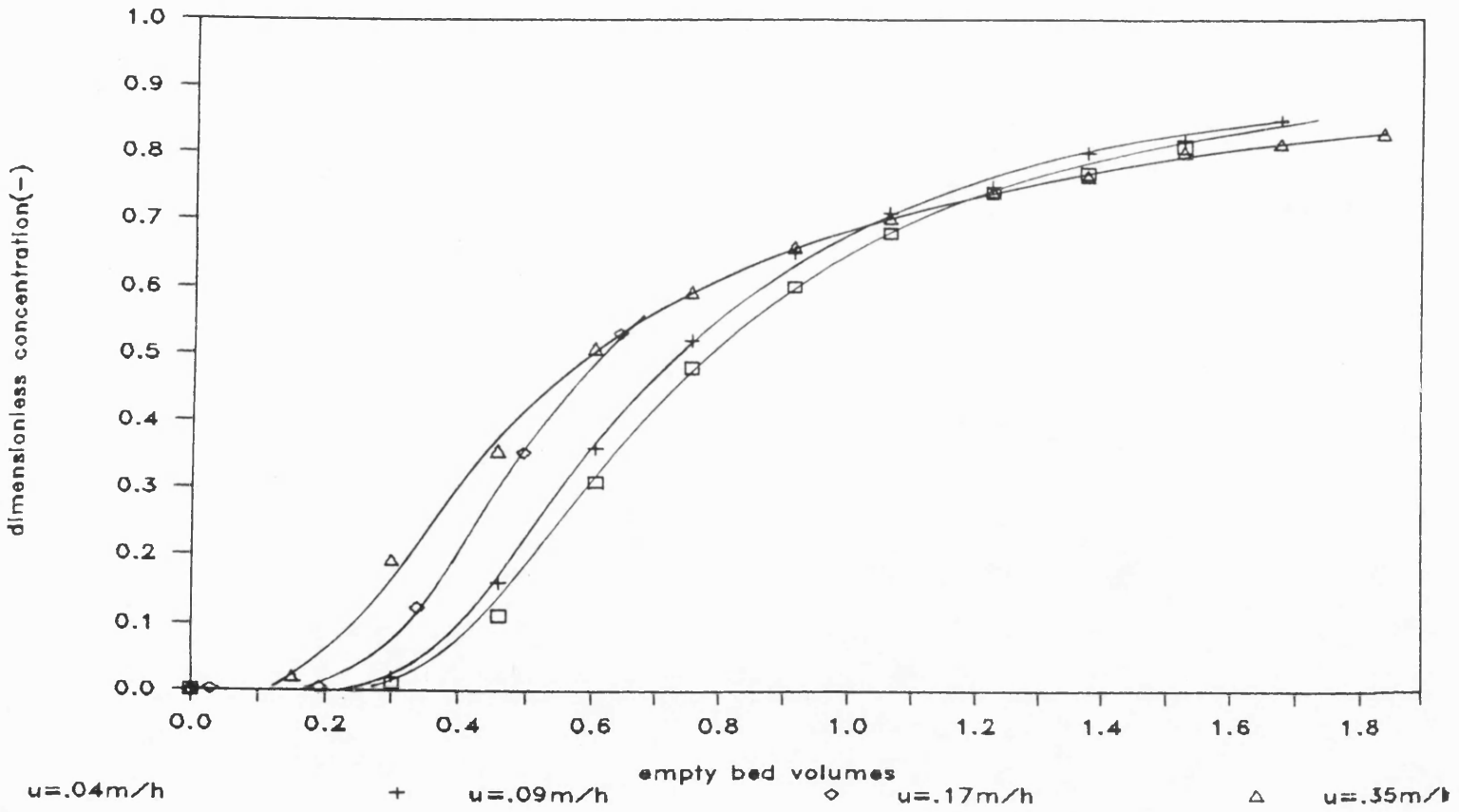

Fig. 3.15. Effect of flow rate on the breakthrough curve of 50 mls of 1:10 diluted plasma (with modified Sartorius filter holder).

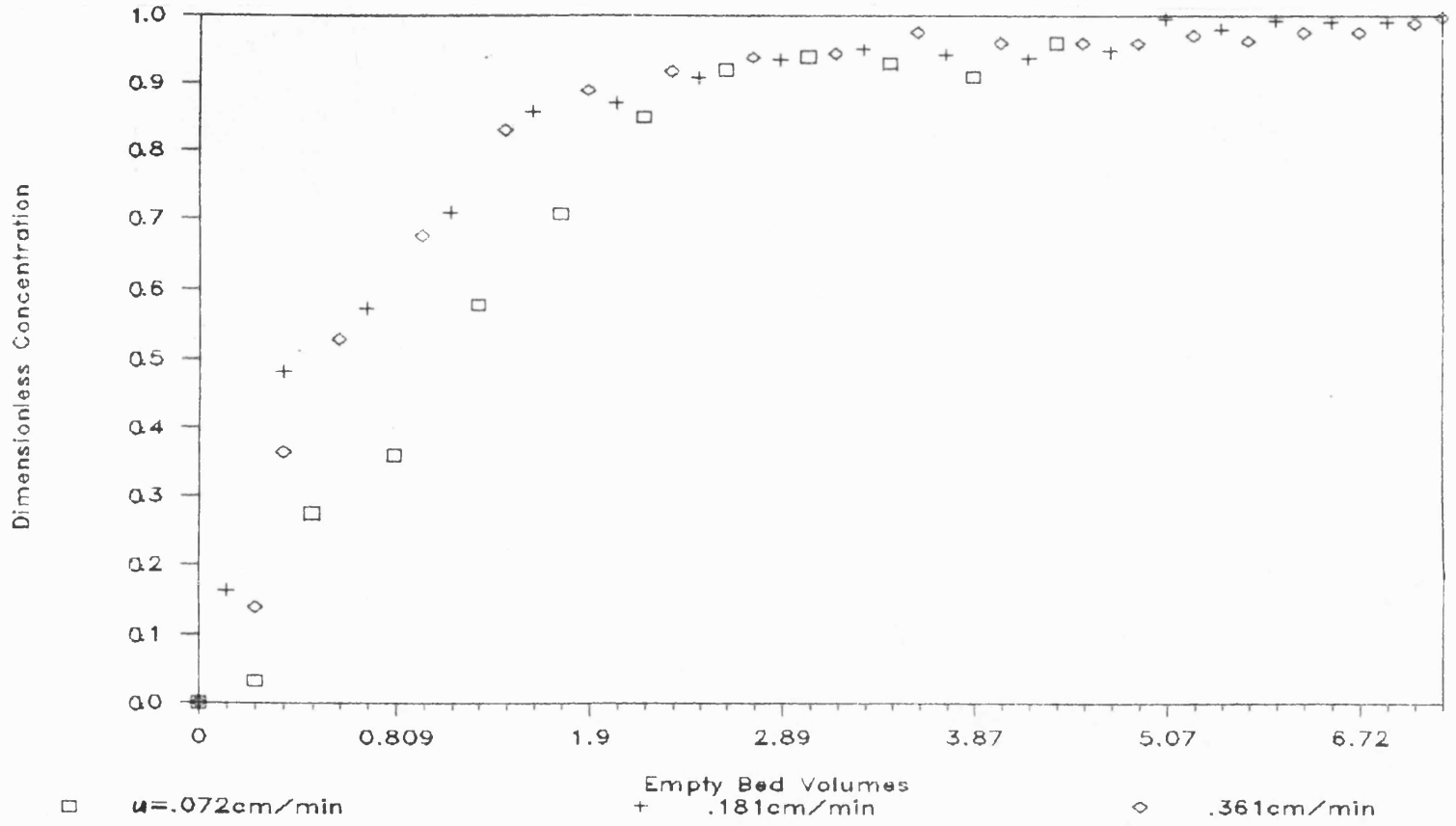

Fig. 3.16. Saturation breakthrough curve with 1:10 diluted plasma at different flow rates with Amicon Wright column).

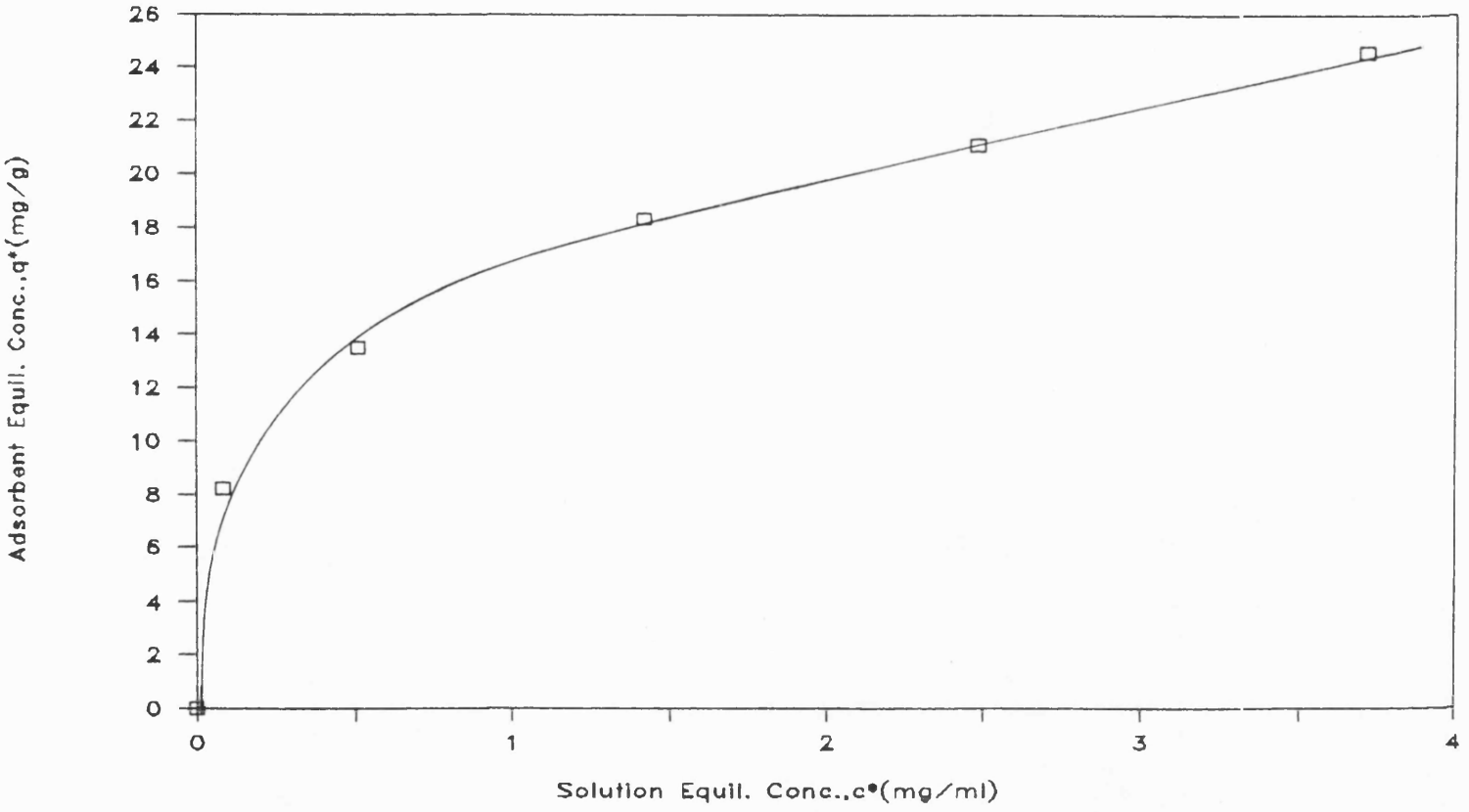

Fig. 3.17. Stage batch adsorption with 5 mg/ml initial concentratio of Lysozyme in Tris-HCl buffer, p. 8.0.

(3) Batch Adsorption of Lysozyme

The result for the five-stage batch adsorption of the lysozyme is shown in Fig. 3.17. It represents an isotherm plot which is non-linear and similar to the Langmuir type.

(4) Purity of Separated Product

The scan of the polyacrylamide gel after electrophoresis for samples of separated products and mixture of sample/commercial HSA and commercial HSA are shown in Figs. 3.18 a-c.

3.3 PREPARATION OF PROTEIN A - SPONGE AFFINITY MATRIX

3.3.1 APPARATUS

As for the previous sections.

3.3.2 MATERIALS

(a) Chemicals: All chemicals were Analar grades and were purchased from BDH.

(b) Protein A and Amino Acid: Protein A (from S. aureus) and bovine IgG were purchased from Sigma Chemicals Ltd. 1,6 diaminohexane and 6 hexanoic acid were purchased from BDH.

3.3.3 METHOD

(a) PRINCIPLE

When a polysaccharide support for an affinity separation is treated with 1,1' carbonyldiimidazole (CDI) in an organic solvent an intermediate matrix (an imidazoyl carbamate) is formed. This

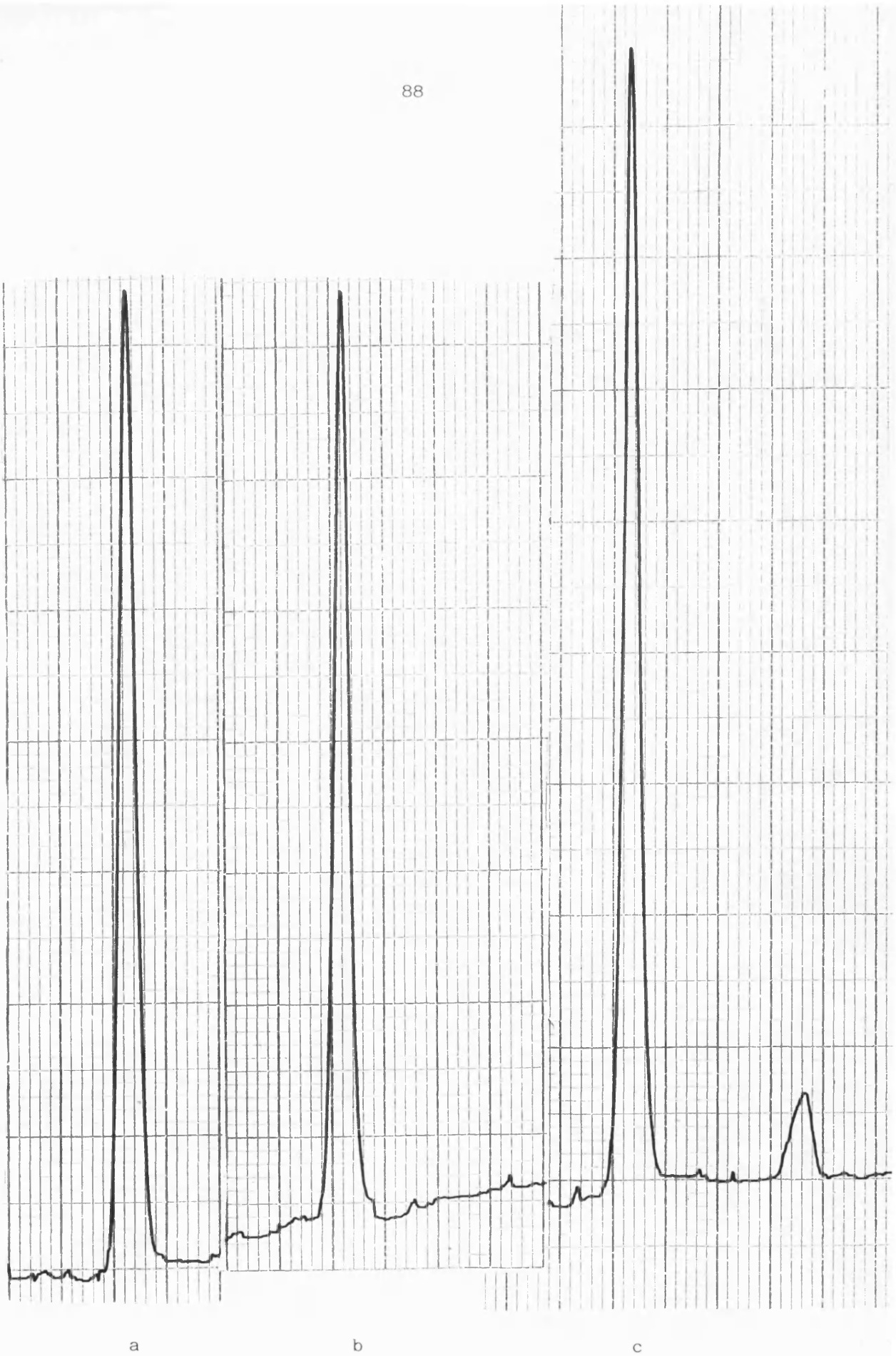

Fig. 3.18 a-c. Scan of electrophoresis gel.

couples smoothly with N-nucleophiles such as free amino groups present in protein ligands to give non basic urethane (N-alkyl carbamate) derivative. The covalent bond formed is stable under the conditions for affinity separation operations. The activation scheme is given by Bethell et al. (1979) and is shown in Fig. 3.19 below.

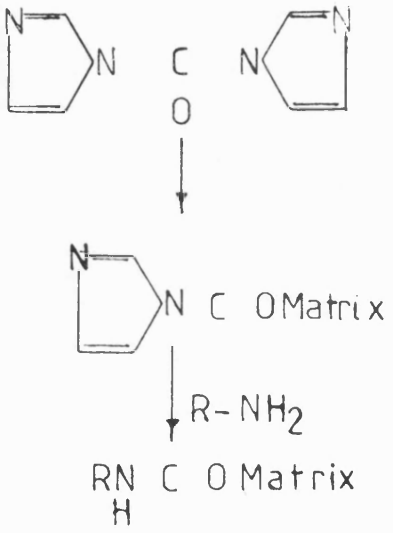

(a) I = Imidazolyl carbamate

(b) R = Alkyl group

(c) II = N-alkyl carbamate

Fig. 3.19. Activation of polysaccharide matrix using CDI and coupling of an amino group to the matrix through the intermediate of the activated matrix.

(b) ACTIVATION OF SPONGE WITH CDI

Two square pieces of sponge weighing 0.2 g dry weight was soaked in distilled water overnight and then further washed

sequentially with 3 : 7 dioxane:water (3 times, with 20 ml), 50 ml of 7:3 dioxane/water 3 times and then finally pure dioxane 3-5 times. in some experiments the dioxane was replaced with acetone.

The sponge was suspended in 6 ml of solvent (dioxane or acetone). A required amount of CDI (typically 1 mmol or 0.1622 g) was weighed very quickly (CDI is very sensitive to moisture, which hydrolyses it very easily) and added to the beaker in which the sponge pieces have been suspended and the suspension shaken gently at room temperature for 45 minutes or more. The product was washed thoroughly with dioxane or acetone (which ever has been used in the activation process). All the operations were carried out in the fume cupboard because of the toxicity of the solvent vapour, especially dioxane. The solvents were also dried with both $CaCO_3$ (anhydrous) and subsequently sodium metal in order to ensure that the readily hydrolysable CDI was not affect by traces of moisture usually found in the solvents used.

The activated sponge was always used immediately for the coupling operation.

(c) DETERMINATION OF THE AMOUNT OF CDI IN THE ACTIVATED SPONGE

Before use for coupling of a ligand, it was necessary to determine the degree of activation of the sponge in order to determine if the required activation level had been achieved.

The amount of CDI on the activated matrix was determined by hydrolysing the imidazolyl carbamate according to the scheme below:

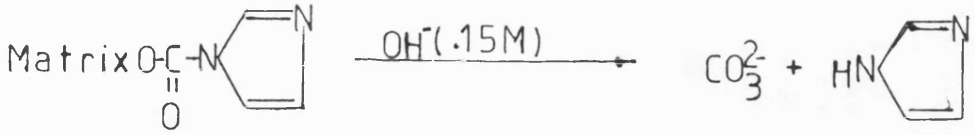

Usually 0.2 g activated sponge was added to 50 ml of 150 mM NaOH (flushed with N_2 to remove carbonates) in a 250 volumetric flask and then stoppered with a rubber bung. The flask was shaken (for 1 hr or more) periodically. A 25 ml portion of the hydrolysis product was titrated under a gentle stream of nitrogen between the limits of pH9 and 3 with 0.1 HCl for the total amount of carbon dioxide at pH 3.0 and a back titration using 0.1 M NaOH was carried out between pH 3 to 9. This gives the amount of imidazole present. The difference between the titration and the back titration between the used limits of titration gave the amount of the active groups present, that is based on the amount of carbon dioxide expelled. Another 20 ml portion of supernatant was titrated as for the 25 ml portion and the titre difference corrected for 25 ml.

(d) TEST FOR ACTIVATION

To confirm that the activated matrix contains imidazolyl carbamate (I in Fig. 3.20), the trinitrobenzene sulphonate (TNBS) test for amines was used as follows. 0.2 g (each) of activated matrix were used to couple 6-aminohexanoic acid and 1,6-diamino-hexane onto the sponge and another 0.2 g kept as a control.

(i) Coupling of Amino Acids

0.2 g of activated matrix was added to a volumetric flask containing 5.4 mmol of amine (6-aminohexanoic acid and 1,6 diaminohexane) in 8 ml of 1 M, $Na_2CO_3/NaHCO_3$ buffer, pH 10.0. The flask was shaken overnight in a shaker inside a cold room at a constant temperature of 4°C. After coupling, the amino-sponge matrix was washed sequentially with water, 1 M NaCl, 1 M KCl and then water. Thorough washing was required in order to avoid a false result.

(ii) Test for Free Amine

The sponge pieces, including the control, were divided into two parts (from each sample) and then dropped into test tubes containing 0.1 M sodium tetraborate, pH 9.3. The samples were treated with 25 µl of 0.03 M TNBS and then allowed to stand for 30 mins at room temperature. The 6-hexanoic acid treated CDI/matrix gave weak yellow (no reaction; no available free amine group for reaction with TNBS), the 1,6 diaminohexane showed an almost instant orange red colour (positive for free amino group) while the control activated matrix showed a very weak orange colour. The results of the tests corresponded with those obtained by Bethell et al. (1979).

(e) COUPLING OF PROTEIN A TO SPONGE

(i) Activation Procedure

Two circular sponge discs of total weight 0.982 g were activated by the procedure outlined earlier. A total of 0.796 g CDI

was used to give 1 mmol CDI/0.2 g dry weight of sponge) in 30 ml of dioxane.

(ii) Coupling Procedure

The activated sponge discs were added to a 250 ml volumetric flask containing 0.8 mg/ml of protein A in 20 ml of 1 M borate buffer, pH 8.5. The flask was agitated in a constant temperature cold room (4°C) by a shaker for two days. The resulting protein A sponge was washed sequentially with water, 1 M NaCl, 1 M KCl and then water. The protein A-sponge discs were stored in 0.01% sodium azide for subsequent use for the adsorption operation.

(f) DETERMINATION OF AMOUNT OF PROTEIN A COUPLED

The amount of protein A coupled onto the sponge matrix was determined by the difference between the absorbency (at 280 nm) before and after the coupling process. The measured absorbance before the coupling was 0.234 and 0.181 after the coupling.

(g) DETERMINATION OF ADSORPTION CAPACITY OF PROTEIN A-SPONGE FOR BOVINE IMMUNOGLOBULINE G (IgG)

The batch adsorption of bovine IgG was carried out at 4°C in a 0.01 M phosphate buffer, pH 7.5. 30 mg of IgG was dissolved in 30 ml of buffer to give a concentration of 1 mg/ml. The protein A-sponge discs were added onto the solution and agitated overnight in the cold room (Temperature 4°C). Unadsorbed protein was washed with the adsorption buffer until the A_{280} declined to zero.

Elution of the adsorbed IgG was effected with 0.1 M acetic acid.

As a control, 1 mg/ml BSA was equilibrated with the protein A-sponge under the same conditions as for the IgG solution but no adsorption of BSA was recorded.

3.3.4 RESULTS

(a) AMOUNT OF CDI ON THE SPONGE MATRIX

The amount of active groups present in 0.2 g dry weight of sponge for different amounts of CDI used in the activation procedure are shown in Table 3.9 below. Titration curves are shown on Fig. 3.20.

Table 3.9. Amount of CDI/0.2 g sponge

mmol CDI/0.2 g dry wt used	mmol CDI/0.2 g dry weight	SOLVENT USED
1	.641	
2	.88	Acetone
5	1.0	
1	.633	
2	.820	Dioxane
5	.96	

(b) AMOUNT OF PROTEIN A COUPLED INTO THE SPONGE

The amount of protein A coupled as determined by the difference between the concentration of protein A before and after coupling was 3.688 mg/g dry weight of sponge.

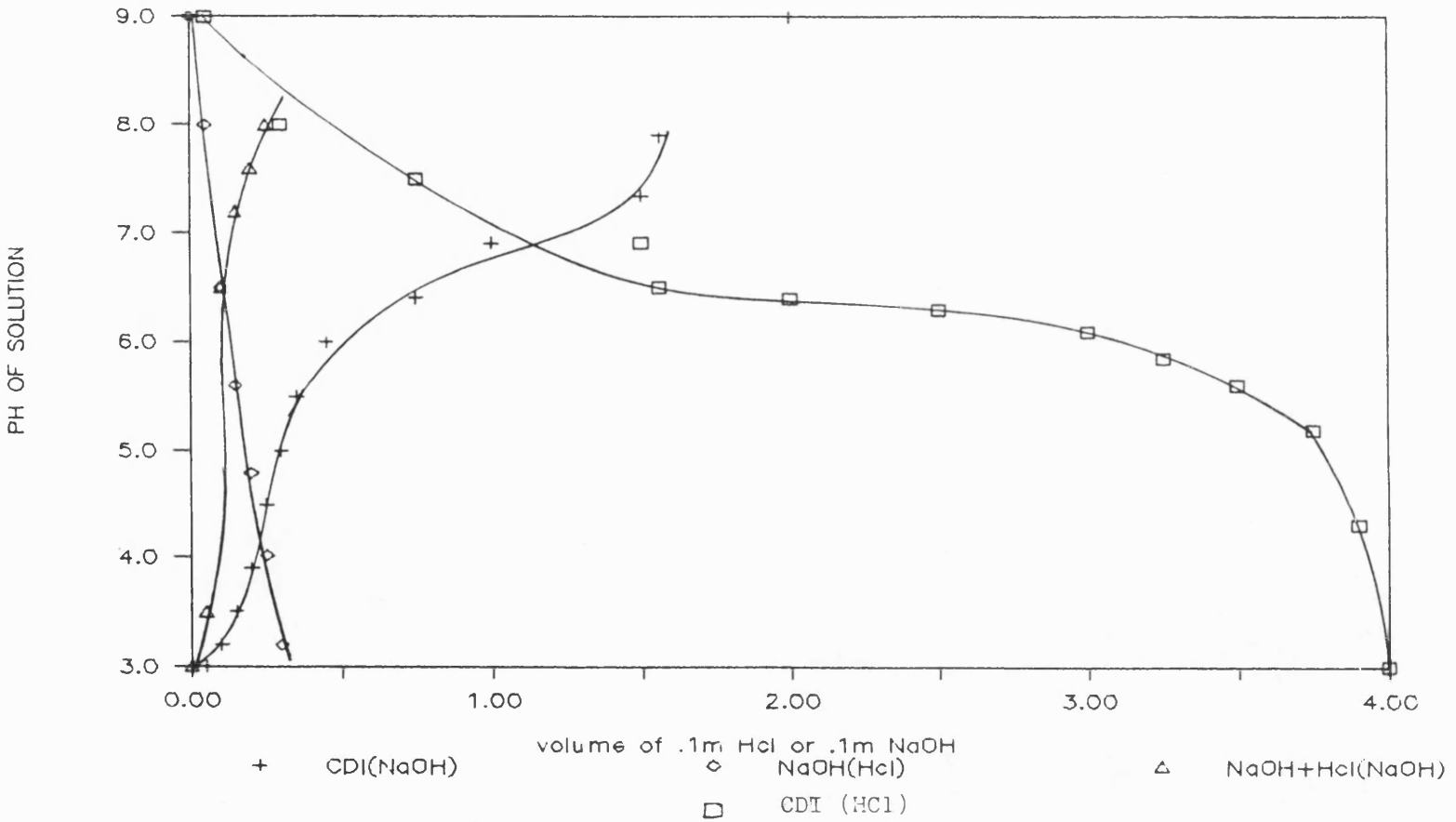

Fig. 3.20. Typical titration and back-titration curves for hydrolysate with 0.15 M NaOH of CDI activated sponge - pH vs volume of acid (0.1 M HCl) or base (0.1 M NaOH).

(c) ADSORPTION CAPACITY

The amount of bovine IgG adsorbed per gram of sponge is shown in Table 3.10 below.

Table 3.10. Adsorption capacity of Protein A - Sponge for bovine Immunoglobulin G (IgG).

Batch #	Capacity (mg/g)
1	15.7
2	16.2
3	15.83

3.4 DISCUSSION

3.4.1 ADSORBENT PREPARATIONS AND PERFORMANCE

(1) ADSORBENT PREPARATIONS

For the optimal use of adsorbents in protein recovery and purification, it is necessary to control the ligand concentration to balance the degree of purification obtained against efficient binding of adsorbates. Very low ligand density results in very low operational capacity or no binding of adsorbates. On the other hand, very high ligand density often increases the strength of binding, steric hindrance and non-specific binding. Sada et al. (1986) showed that a decrease in adsorption capacity/ligand concentration ratio with increase in ligand concentration in immunoaffinity interaction. Lowe et al. (1974) and Trayer et al. (1978) have found that elution volume increases with high ligand concentration. Trayer et al. (1978) applied the same amount of a preparation of glucokinase to a column of Sepharose covalently substituted with different amounts of ligand. At low ligand concentrations little or no binding was obtained. Increased ligand concentration necessitated increasing the concentration of glucose to effect elution. Very high ligand concentration required potassium chloride to release bound enzyme.

The increase in wash volume observed with increased Cibacron 3GA density on the sponge seems to suggest increased non-specific binding with higher ligand concentration. The low capacity of the protein A-sponge for bovine IgG is consistent with the low capacity

often associated with very low ligand density.

The degree of ligand substitution on a matrix obtained with Dye-Sponge adsorbent can be increased by increasing the dye concentration to about 4% without increase in reaction time at 80°C. In the light of evident lowering of the adsorbent efficiency with increased ligand concentration, the degree of substitution obtained with the sponge seems satisfactory. The necessary requirement should be satisfactory adsorbent capacity.

It is often necessary to use spacer arms in cases where the molecular weight of a ligand is low in order to improve the accessibility to macromolecular adsorbates. However, the use of spacer arms should normally be avoided except in systems where this is inevitable (Nishikawa et al., 1975). This is because of findings that leash structures may give rise to non-specific binding or even local steric hindrance (Yang and Tsao, 1982). Because a satisfactory binding capacity of the blue-sponge was obtained, it was therefore considered unnecessary to use a spacer arm.

The selected immobilization reaction conditions for the preparation of blue sponge can therefore be said to be somewhat near the optimum. The optimum conditions of an adsorbent preparation forms the basis for an efficient adsorbent. It has been assessed here on the basis of degree of substitution or capacity and also on the basis of the efficiency of the whole process of affinity separation. The criterion used here was, therefore, the degree of dye substitution which gave the highest capacity for minimum sponge damage and minimum non-specific adsorption.

(2) ADSORBENT RE-USE

One of the drawbacks of affinity technique that has made its use in commercial application uneconomic is the stability of the attached ligands. In preparations meant for clinical use, an unacceptable level of ligand in product due to leakage is not normally tolerated. Ligand leakage also means a progressive deterioration in adsorbent capacity, often to a point of near exhaustion.

The blue membranes did not show any marked decrease in capacity after some 50 repeated uses. Only about 0.1% loss of capacity (within experimental error) was observed. For the blue sponge the loss in capacity was somewhat more than for blue membrane after some 30 cycles. On the whole, the immobilized dyes were stable on both the membrane and sponge.

(3) ADSORPTION CAPACITY

The capacity of an affinity adsorbent actually depends on a number of factors which include ligand concentration per unit volume or weight of the matrix, adsorption conditions like adsorption buffer pH, and ionic strength, degree of mixing (in batch system) and flow rate (in frontal analysis) and physical nature of the matrix such as porosity, which determines the degree of accessibility of the adsorbate to the ligand.

These varied conditions that determine an adsorbent capacity make it difficult to make comparisons with other materials. However, one can attempt to compare capacity in order to give an idea of how that obtained with a new material compares with

existing materials for recovery of products by adsorption. The capacity for HSA in plasma obtained with the blue sponge and the blue membrane seem quite reasonable when compared with literature figures. Table 3.11 shows some capacity values from the literature and those of blue-membrane and sponge and the adsorption conditions.

Tables 3.7 and 3.8 seem to indicate that within a flow rate range of 6.585×10^{-4} to 3.61×10^{-3} m/s used in this experiment the flow rate does not affect the capacity of the blue sponge. This may be due to the good accessibility of the ligand to the protein molecules even at relatively high flow rates due to the very high porosity of the sponge. This view is supported even more by the capacity of 8.6 mg/g dry weight obtained with the radial flow configuration at a volumetric flow rate of 20 mls/min (using 140 ml of 1:10 diluted plasma).

It is necessary to point out that in large-scale preparative applications capacity though important, is usually sacrificed to a certain extent in order to achieve some set target production runs at the highest possible flow rate. This depends on how much raw material can be wasted without making the cost unacceptable. For example, from Tables 3.7 and 3.8 it can be seen that at a flow rate of 8 mls/min (3.61×10^{-3} m/s) half the saturation capacity of the blue sponge is achieved with only 50 cm^3 of plasma. In light of this it seems unnecessary to waste further two to three times plasma volume in order to achieve full operational capacity. Also, from Table 3.8 it would seem a waste of time and money to operate at a flow rate less than 3.61×10^{-3} m/s.

Table 3.11. Comparison of Adsorption Capacities of Membrane and Sponge Adsorbents with Literature Values

ADSORBENT	LIGAND CONCENTRATION	CAPACITY		ADSORPTION CONDITIONS	SOURCE
		mg/ml of gel	mg/g dry wt		
Blue Sepharose CL-6B	2 mol per swollen volume	5	17.98	Buffer. Sodium phosphate at at pH 7.0 at 20°C	Pharmacia Fine Chemicals Handbook (1983)
Blue Cellulose	3.2 g/ml	8	-	Buffer. Same as in this work	Angal and Dean, (1977)
Blue Sponge	4.58 mg/g dry wt	3.38 packing density = 0.202 g/ml	16.79	0.05 M Tris-HCl/ 0.05 M NaCl at 4°C (by frontal analysis)	this work
Blue membrane	-	-	17.1	0.05 M Tris-HCl/ 0.05 M NaCl at 4°C (batch adsorption)	this work

The capacity of Protein A/sponge (Table 3.10) was comparable with that obtained by Mandaro et al. (1987) using Protein A/cellulosic material for Bovine IgG (10.08 mg/g).

(4) MEMBRANE FLUX

There is no problem of flux with the sponge material. However, with the blue membrane, flux decline appears to be of critical consideration. The dilution of the plasma with adsorption buffer some 10 to 20 times resulted in flux decline due to pore blockage and fouling. It was only at a 1:30 plasma dilution that a reasonable flow rate was obtained throughout a run. From the flux measurements shown in Fig. 3.11, even with 1:30 plasma dilution a sharp flux decline occurred within the first 5-10 mins of an adsorption run. This was followed by a relatively constant flux and then by another sharp decline leading to almost complete stoppage.

These observations suggest that a prefiltration of the plasma should be carried out before adsorption. The flux measurements also suggest a need for complete regeneration of the membrane adsorbent after a few runs in order to avoid a build-up of protein in the membrane, leading to irreversible fouling.

It seems that the blue membrane will be more suitable for analytical applications rather than preparative applications. On the other hand, the sponge material will seem to be good for preparative or production scale applications on the basis of its fast flow property.

(5) PURITY OF THE SEPARATED PRODUCT

From the evidence shown on the scan of the polyacrylamide gel after the electrophoresis the HSA separated with blue sponge and blue membrane seems reasonably pure (see Fig. 3.19).

While the separated product showed a single band on the acrylamide gel, the Sigma commercial HSA showed a second (trailing band, probably globulin). This was reflected by a single peak for separated HSA using blue adsorbents and two peaks for the commercial HSA - a major and a minor peak. Given a purity criterion of a single peak, the blue adsorbents performance can be considered good.

(6) PROCESS CYCLE

The height of the sponge packing in the column and the radial flow configurations used in the experiments here approximate to a differential bed. This means that the sigmoid shape of the solute adsorption zone front is not fully developed in the bed before a 'breakthrough' of the solutes appears at the bed exit. This combined with a relatively high flow rate of the feed, fast kinetics of exchange of solutes between the passing feed (adsorbate) and the ligands attached to the adsorbent, and a reasonable adsorbent capacity for the adsorbate will greatly reduce the process time and make the system very suitable for the processing of large volumes of fluids in good time. This is one of the main objectives for the investigation of the use of the sponge material as an alternative to granular materials, which are not very suitable for the processing of a large volume of fluid due to

effects of bed compression and hence limitation of flow rate; thus low mass transfer rates (especially with macromolecules like protein).

The height of the sponge packings of 1.65 cm to 3.61 cm fall well within the definition of differential bed if the adsorption width is defined as the length of the bed which contains a fully developed breakthrough curve of the adsorbate

$$\text{Adsorption zone width} = \frac{Q \times t}{A}$$

where Q = volumetric flow rate (cm^3/min)

t = time difference between breakthrough point and saturation point of the breakthrough curve (mins)

A = Cross-sectional area of the bed (cm^2)

From the saturation breakthrough curves of Fig. 3.16, the calculated adsorption zone widths at 3 different flow rates with a sponge packing height of 1.65 cm are as follows

FLOW RATE (cm^3/min)	ADSORPTION ZONE WIDTH (cm)
1	6.49
2.5	9.536
5	11.246

The total process cycle time also includes the washing and elution times. The average volume for HSA adsorption from human plasma is about 3.7 bed volumes - at a flow rate of 2.5 cm^3/min - and 7.2 bed volumes - at 1 cm^3/min. The average elution volume at 1 ml/min is some 6 bed volumes - at flow rate of 1 cm^3/min - and 2.5-3 bed volumes - at 2 mls/min. The process cycle time therefore varies according to the adsorption, wash and elution flow rates. The typical cycle time used here was about 85 mins, 35 mins for adsorption at 5 ml/min, 25 mins for wash, 2.5 ml/min and 25 mins for elution - 2 ml/min.

CHAPTER 4

PARAMETER ESTIMATION

4.1 DETERMINATION OF EQUILIBRIUM PARAMETERS

4.1.1 INTRODUCTION

The contacting of a solution of adsorbate and the adsorbent for a long enough time allows an equilibrium distribution of the adsorbate between the solution and the solid phase to occur. This can provide the means of estimating some of the parameters needed in designing adsorption processes and modelling the performance of such processes. The equilibrium adsorbate distribution between the solid phase and the solution will depend on the initial concentration of the adsorbate. A plot of the solid phase equilibrium concentration against the solution equilibrium concentration of the adsorbate at different initial concentrations of the adsorbate and at constant temperature provides an adsorption isotherm from which the equilibrium parameters can be estimated.

Various models are in use for expressing the solid phase equilibrium concentration (measured in weight of adsorbate adsorbed per unit weight of the adsorbent), q^*, as a function of the concentration of adsorbate (weight per unit volume of solution), c^*. These models provide a means of estimating the equilibrium parameters from the experimental adsorption isotherms. These models must be considered empirical since some of their theoretical assumptions may not necessarily be met in some adsorption systems in which they are used. The type of model used depends on the shape of the adsorption isotherm and range of the initial adsorba te solution used in determining the experimental adsorption isotherm. For example in non-linear isotherms usually encountered in the

affinity interaction of biological molecules and a covalently attached molecule in a solid support can be described almost equally well by both the Langmuir isotherm (Chase, 1984a) and the Freundlich isotherm (Katoh et al., 1978; Sada et al., 1984). Sometimes, especially in gas adsorption the Braunauer, Emmett and Teller (BET, 1938) adsorption isotherm which is concerned with multi-layer adsorption can be used. The most commonly used in affinity interactions are the Freundlich and Langmuir models. The Freundlich equation, Freundlich (1924) is

$$q = K_F c^{1/\beta} \qquad (4.1)$$

where q = solid phase concentration (kg/kg)

c = liquid phase concentration (kg/m^3)

K_F = constant (m^3/kg)

β = constant (-)

The constant K_F is a relative indicator of adsorption capacity while the constant is indicative of energy or intensity of the reaction and normally more than unity for favourable types of isotherms (see general introduction) common with affinity interactions. Freundlich's model is consistent with an exponential distribution of site energies, characteristic of heterogeneous surfaces, and with immobile adsorption. It is an empirical model and mostly useful for dilute solutions over small concentration ranges. The Freundlich model did not give as good a fit as the Langmuir model to experimental isotherms obtained in this work and will therefore not be considered further.

The importance of adsorption isotherms, in general, in the packed bed adsorption system design lies in the fact that the

nature of the equilibrium isotherm is important in determining the shape of the breakthrough curve or the elution profile.

4.1.2 LANGMUIR ADSORPTION ISOTHERM MODEL

The model to describe equilibrium adsorption by Langmuir (1918) was derived originally for the adsorption of gases based on the assumptions of (i) single layer adsorption; (ii) immobile adsorption:- adsorbed molecules do not move freely on the surface; (iii) equal enthalpy of adsorption for all adsorbed molecules. These assumptions are essentially met by affinity interactions since specific sites of adsorption exist and multi-layer adsorption of protein molecules of the same charge (for specifically adsorbed proteins) is unlikely. The adsorption energy is not often high in affinity interactions and any difference in the adsorption energies would be quite insignificant.

Wankat (1974) was among the first, in his theory for enzyme-ligand interactions in affinity separation methods, to use the Langmuir model for quantitative description of the interaction between an adsorbate molecule and the immobilised binding site of the ligand. He described this interaction as a reversible equilibrium reaction such as

$$A + B \underset{k_2}{\overset{k_1}{\rightleftharpoons}} AB \qquad (4.2)$$

where A is one species of adsorbate and B is the immobilized binding site

AB is the amount of A bound specifically to B.

and k_1 and k_2 are the forward and backward rate constants.

The ratio (k_2/k_1) gives the dissociation constant k_d. The k_d is often used as one of the criteria for the selection of a potential ligand for specific adsorption of a target molecule from a heterogeneous solution (usually < 10^{-3} M, Young and Tsao, 1982). Wankat obtained a Langmuir type adsorption isotherm given by the equation

$$[AB] = \frac{B_O [A]}{k_{AB} + [A] \; A_A B_O} \qquad (4.2a)$$

where B_O is the original concentration of the ligand, $cm^2/\mu mole$

K_{AB} is the dissociation constant

A_A is the area covered by the AB complex, cm^2 / μ moles.

However, for practical purposes, it is better to consider the experimentally determined quantities since it is difficult to measure, for example, A_A in Wankat's formula. The empirical form of equation (4.2a) can be derived from conservation of mass balance on the adsorbate involved in the affinity interaction.

The form of conservation of mass in an adsorption is generally given at equilibrium as

adsorbate in = adsorbate out + (adsorbate removed by adsorption) - (adsorbate returned by desorption)

From equation (4.2) at equilibrium

Amount into the system = 0

Amount out of the system = 0

Amount removed by adsorption = $-k_1.c^*(q_m-q^*)$

Amount returned by desorption = $k_2 q$

$$- k_1\text{-}c^*.\ (q_m - q^*) = k_2 q$$

and

$$q^* = \frac{q_m \cdot c^*}{k_d + c^*} \qquad (4.3)$$

where q^* is the solid phase adsorbate concentration at equilibrium

c^* is the liquid phase concentration of adsorbate at equilibrium with q^*

q_m is the experimentally measured, highest equilibrium solid phase concentration

and k_d is the dissociation constant.

Equation (4.3) is a specific form of the Langmuir equation derived for gas adsorption of the original form, (Langmuir, 1918).

$$q^* = \frac{k_L\, q_m c^*}{1 + k_L c^*} \qquad (4.4)$$

equations (4.3) and (4.4) are equivalent since $k_L = 1/k_d$.

k_L is the Langmuir constant or equilibrium constant of the adsorption reaction of equation (4.2).

4.1.3 APPARATUS AND MATERIALS

The apparatus and materials were the same as given in Chapter 3.

4.1.4 EXPERIMENTAL METHODS

In the column experiments ten sponge pieces (dry weight, 5.062 g) were compressed between two end pieces of the adjustable Amicon Wright column to a thickness of 1.65 cm. In the experimental set up shown in Fig. 4.1, Pump A (Watson-Marlow peristaltic pump, model 101U) was used to pump cold water at 4°C from the main cold water bath into the subsidiary water bath in which was immersed the protein solution. Pump C was the same as A but pumped cold water back into the main cold water bath. A glass thermometer (mercury), E was used to make certain that a constant temperature was maintained. Pump B (Watson-Marlow peristaltic pump, model 501U) was used to recirculate a protein solution from the stirred vessel through the sponge stack in the column and the LKB UV detector (UVICORD II) with a flow through cell and 280 nm filter and then back to the feed vessel. The re-circulation pump was set to deliver 10 cm^3/min (about 1/5th bed volume). The output of the UV detector was connected to a pen recorder to monitor the protein level during the experiment. The magnetic stirrer was used to keep the protein solution well mixed by means of a magnetic bar inside the protein solution vessel. The temperature of the cold bath was at 3°C to give a protein solution temperature usually 3.5°C to 4°C.

Before each experiment, the protein solution was allowed to attain a constant temperature by keeping it inside the subsidiary cold water bath until a constant temperature was obtained as ascertained with a glass mercury thermometer. The column was first equilibrated with the adsorption buffer, at 4°C by recirculation with pump B. The buffer solution was then pumped out while the UV

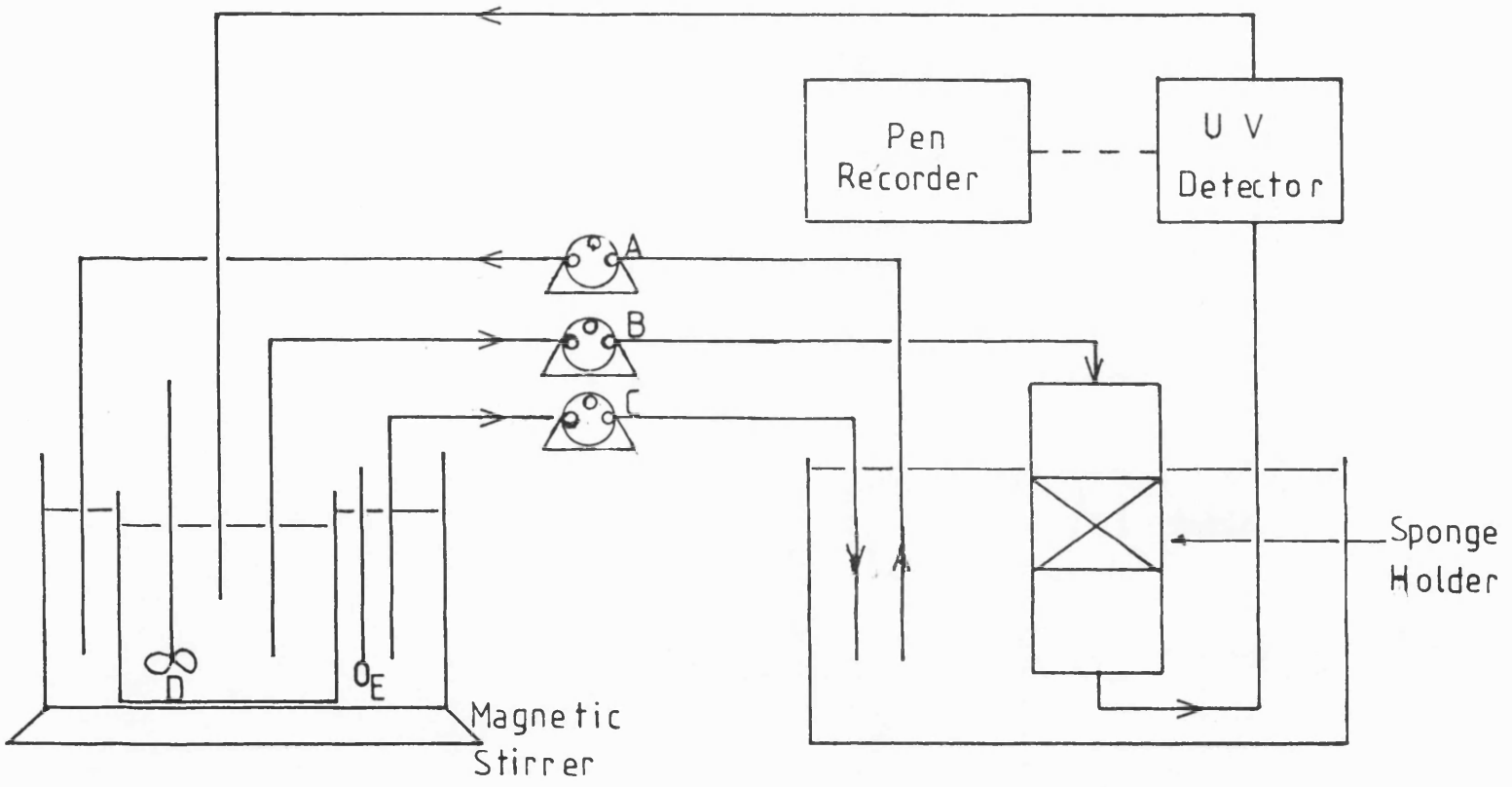

A,B,C Peristaltic Pumps

D Stirred Feed Tank

E Thermometer

Fig 4.1: Flow Diagram of the Experimental Set up For Isotherm Investigation

detector was switched off. The inlet and outlet tubes were then placed in the protein solution vessel and recirculated. The UV detector was switched back on to monitor the protein A_{280} level. Recirculation was continued until equilibrium was achieved as evidenced by lack of further reduction in the A_{280} of the protein solution as shown by the chart recorder output. The unadsorbed protein was washed off until the A_{280} declined to zero. The adsorbed protein was eluted with 2-2.5 bed volumes. The bed was then equilibrated again with adsorption buffer and the experiment repeated with different initial concentrations of protein. The adsorbed protein was taken as the difference between the starting amount and that at the end of the experiment.

Adsorption was generally effected with 0.05 M Tris-HCl/ 0.05 M NaCl buffer, pH 8.0 and elution was effected by 0.05 M Tris-HCl/0.5 M NaSCN buffer, pH 8.0.

In the second type of batch experiments, the blue sponge was cut into small square pieces or minced and pre-equilibrated in the adsorption buffer as used previously. The sponge pieces were then added to 250 ml volumetric flasks containing equal volumes of protein solution of different concentrations. Two samples (of the same wet weight) were kept and later dried at 150°C to obtain the dry weight. The incubator shaker was used to agitate the sponge suspension overnight in a cold room kept at a constant temperature of 4°C. The adsorbed protein was measured in the same way as for the column experiment.

4.1.5 RESULTS

The adsorption isotherms have been obtained at the pH and the ionic strength of the buffer usually used in the HSA separation from plasma. This therefore eliminates the effect these might have on the adsorption capacity or the isotherm shape.

Equation (4.3) can be linearized to give

$$\frac{c^*}{q^*} = \frac{c^*}{q_m} + \frac{k_d}{q_m} \qquad (4.5)$$

The slope of the straight line plots of C*/q* against C* provides a means of determining the dissociation constant, k_d, and the maximum solid phase equilibrium capacity. The intercept of the plot on the C* axis is at $-k_d$ while the gradient of the line is $1/q_m$.

The slope of the c*/q* Vs c* line was determined by linear regression analysis with regression coefficients of 0.99. Figs. 4.2a, 4.3a and 4.4a show the adsorption isotherm for HSA by column method), HSA (by batch method) and lysozyme (by batch method) respectively.

The plot of c*/q* Vs c* are shown in Figs. 4.2b, 4.3b and 4.4b (for HSA by column method), HSA (by batch method) and Lysozyme (by batch method) respectively.

The values of dissociation constants, k_d and maximum equilibrium solid concentrations are shown in Table 4.1.

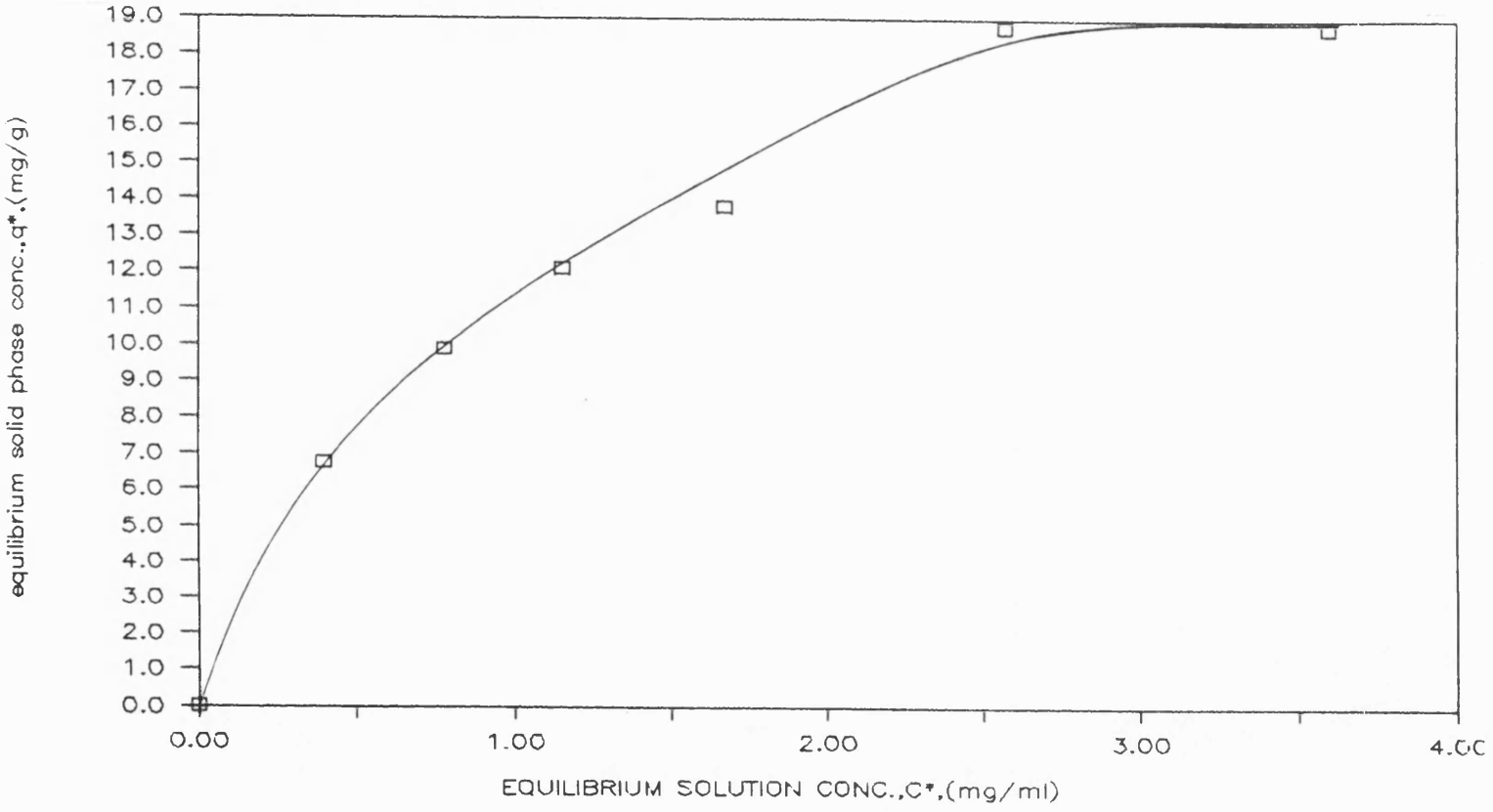

Fig.4.2a. Adsorption isotherm of HSA using column recirculation method (pH = 8.0).

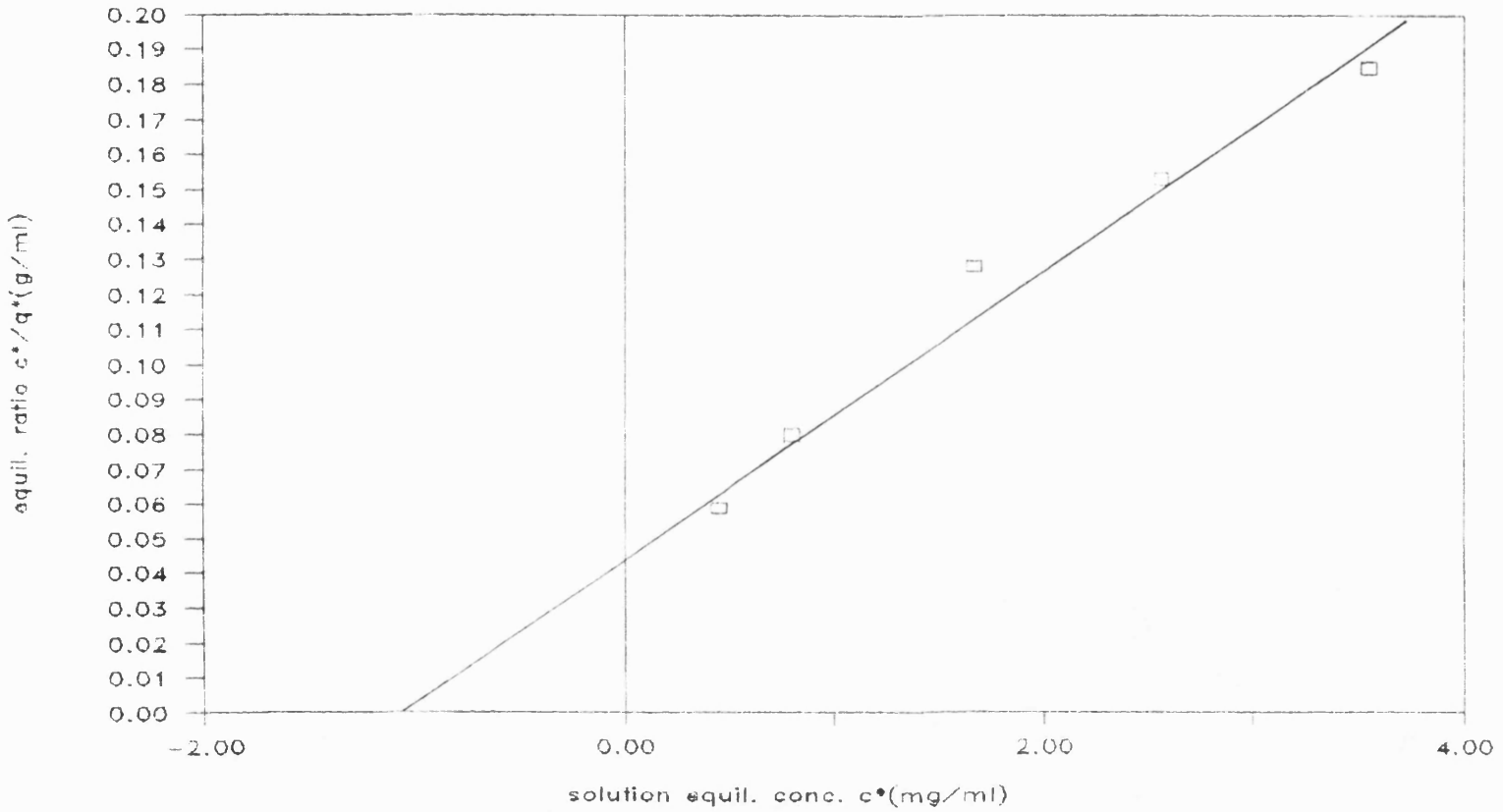

Fig. 4.2b. c*/q* against c* plot from HSA isotherm using Column Recirculation Method. (pH 8.0).

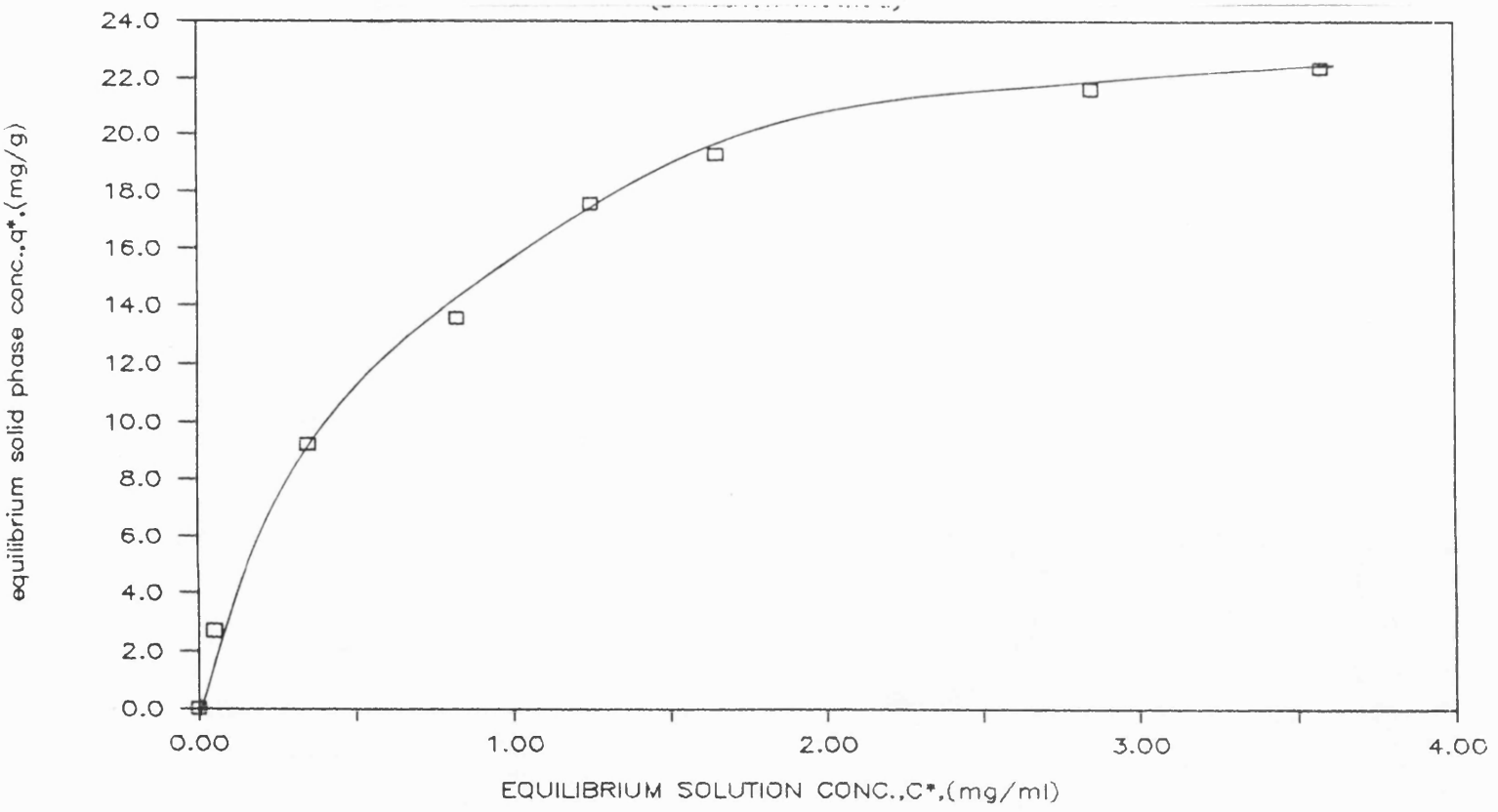

Fig. 4.3a. HSA adsorption isotherm by batch method at pH 8.0 using minced sponge (batch vol. = 10 mls, dry wt = 0.1769 g).

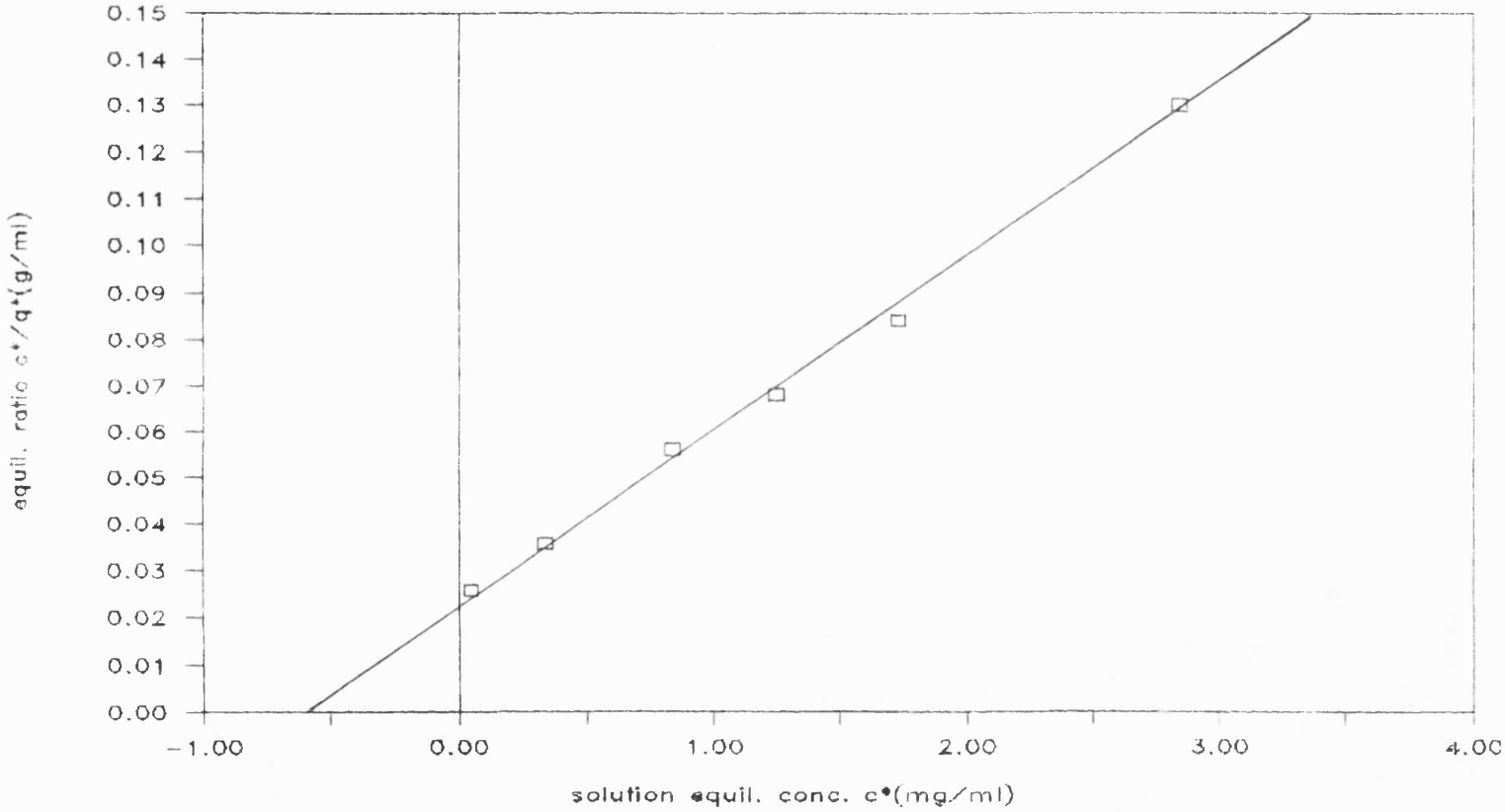

Fig. 4.3b. c*/q* against c* plot for HSA absorption isotherm by batch method (pH = 8.0)

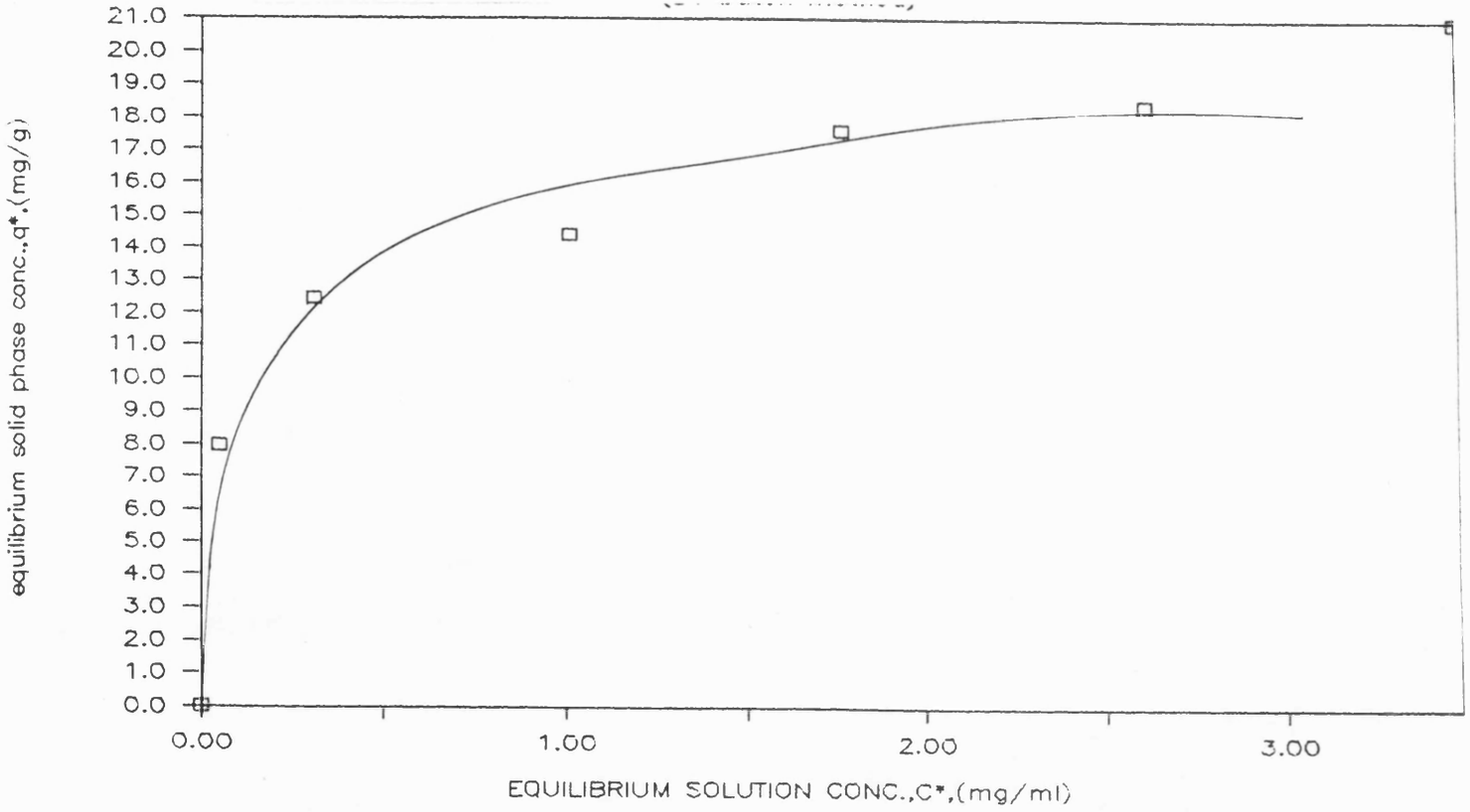

Fig. 4.4a. Lysozyme adsorption isotherm by batch method at pH 8.0 (batch vol. = 35 mls; sponge dry wt = 2 g).

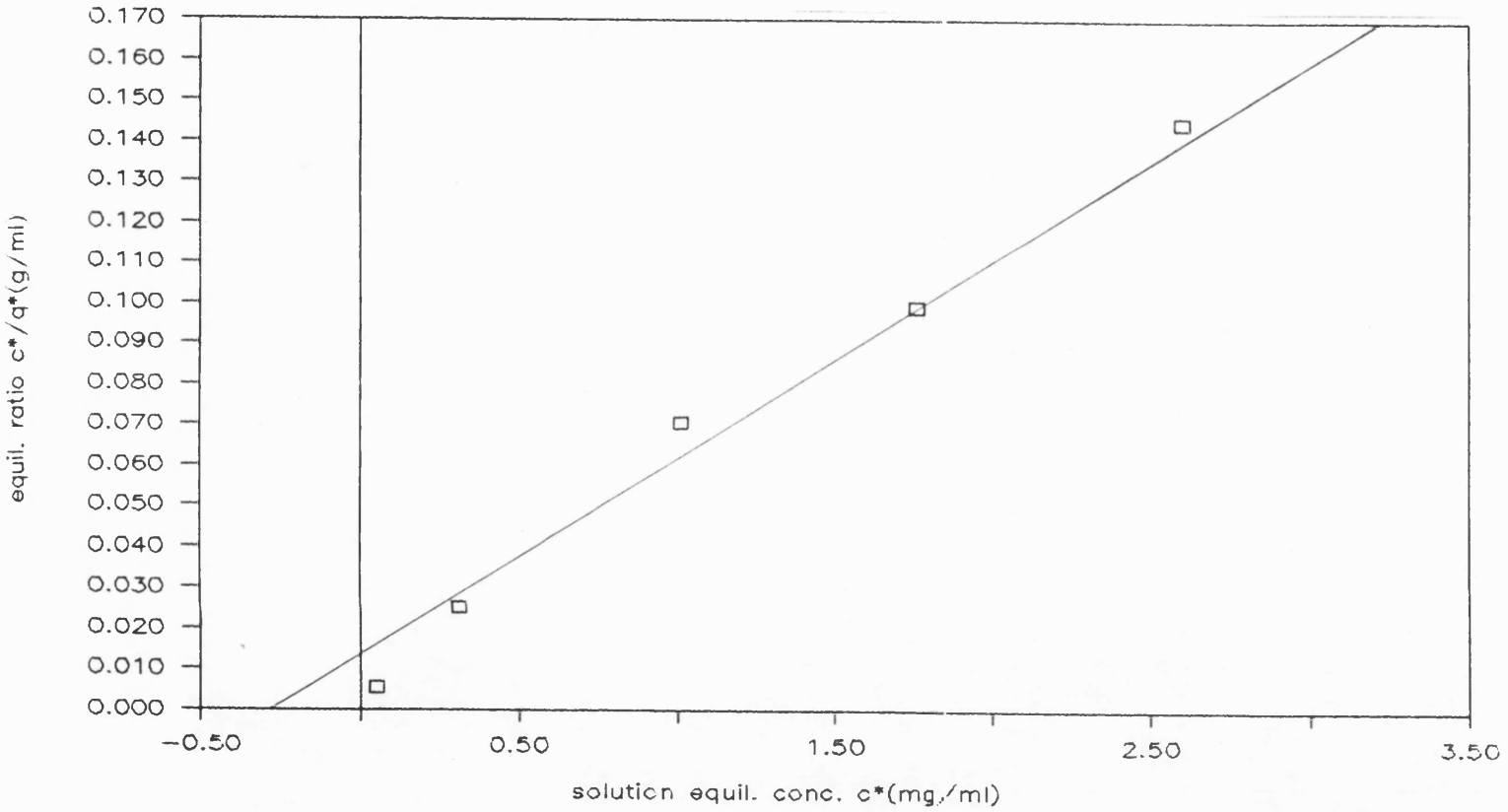

Fig. 4.4b. c*/q* against c* plot for Lysozyme Adsorption isotherm by batch method at pH 8.0.

Table 4.1. Equilibrium Parameters for HSA and Lysozyme

ADSORBATE	METHOD	MAX. SOLID CONCN, q_m (mg/g)	DISSOCIATION CONSTANT, k_d (mg/ml)
HSA	COLUMN RECIRCULATION	25.26	1.28
HSA	BATCH	28.17	0.55
LYSOZYME	BATCH	22.32	0.26

4.2 DETERMINATION OF ADSORPTION KINETICS PARAMETERS

4.2.1 INTRODUCTION

The design and the operation of an adsorption process requires not only the situation that obtains at infinite time or equilibrium but how fast that situation can be attained. The study of how fast an adsorption process proceeds is the basis of kinetics. The importance of the study of kinetics in the design calculations and the scaling-up of a process is evident. For example, if the kinetics of protein adsorption from a solution onto an adsorbent is fast enough and a favourable hydrodynamics of the system allows, a higher feed rate can be considered in order to speed up the processing of a large quantity of fluid within a given capacity range. This is especially important in the processing of biological fluids which are usually encountered in large dilute volumes. Also column length can be reduced and hence the operating

cost as a result in the reduction of the process cycle time without affecting productivity (in terms of product yield per production cycle, in fact, the overall productivity in terms of product yield per unit time will increase).

The mode of operation of the fixed-bed adsorption which has been used in this work - frontal analysis method - results essentially in a non-equilibrium situation. Two basic theories of chromatography have been used in the description of the interaction of proteins and a ligand in fixed beds. These are the plate theories and the rate theories. The plate theory is essentially an equilibrium-stage theory and was first introduced by Martin and Synge (1941) and later refined and modified by various workers. Wankat (1974) has used the plate theory to analyse the performance of an affinity system. However, the application of Wankat's analysis of affinity interaction is limited by the fact that these systems have highly non-linear equilibrium isotherms which are at variance with the linear equilibrium assumption which he made. Also the theory assumes that the column can be approximated by a number of equilibrium stages represented by theoretical plates which are constant in number. As pointed out by Yang and Tsao (1982) the most obvious shortcoming of the plate theory is its inability to predict the number of stages or effective plate height, and the failure to provide information as to how a change in operating conditions will affect the column performance. Obviously the assumptions of the plate theory is hardly practicable in the description of transient situations as obtain in frontal analysis.

For this reason the more sophisticated rate theory has been used most commonly in dealing with affinity interactions. The rate theories which are sets of equations derived from local material balances together with appropriate boundary and initial conditions make no assumptions regarding local equilibrium in the individual 'stages'. The analysis is based on the continuous flow of carrier fluid through the column, finite rates of mass transfer, and a certain equilibrium or sorption kinetics.

Various rate theory models have been applied to fixed bed adsorption processes and the diversity of these rate theory models is due to the variation in the rate equations for the transfer of materials from the liquid phase to the solid phase. When a solution of an adsorbate is contacted with an adsorbent, the adsorbate has to travel from the solution to the solid phase through the solution into the pores of the adsorbent before being adsorbed on the walls of the adsorbent. It therefore encounters various resistances which include:

(a) Bulk diffusion resistance - due to diffusion through the bulk solution.

(b) Film diffusion resistance - due to diffusion through the stagnant film surrounding the adsorbent.

(c) Pore diffusion resistance - due to diffusion through the pores of the adsorbent.

(d) Surface adsorption resistance - due to surface adsorption.

One or more of the mass transfer resistances usually contribute most to the overall resistance encountered by the adsorbate and is called the rate determining step. Steps (b) and (c) are the steps

most usually significant in the affinity interactions which utilize granular materials as adsorbent (Yang and Tsao, 1982). The surface adsorption resistance has been usually found to be insignificant. However, Arnold et al. (1985a)pointed out that this step can become rate controlling in systems where adsorption may be slow and for very small particles in which pore diffusion is very large and the film mass transfer resistance is low due, for example, to high feed rate. This is a situation which has been envisaged to exist with sponge material whose open structure suggests a fast transfer of protein through the film at high flow rates and small particles as suggested by the electron micrograph of its structure.

The mathematical analysis of column adsorption processes usually includes only the rate limiting steps in order to simplify the handling of the problem mathematically. A general mathematical treatment of fixed bed adsorbers was developed by Vermeulen (1958) and Vermeulen et al. (1963). Though originally developed for ion exchange adsorbers, this is also applicable to affinity interactions (Yang and Tsao, 1982).

In affinity separations the rate-determining steps of adsorption and elution using granular adsorbents have been found to be steps b and c (Katoh et al., 1978). However, the interaction of adsorbates and ligands in frontal analysis has been modelled successfully by Chase (1984a) using the general solution by Thomas (1944). This model presupposes that the surface adsorption is rate controlling. As has been mentioned earlier, under certain operating conditions and with certain systems this situation can prevail though the rate of surface adsorption is usually very fast compared

to that of the other mass transfer steps (Yang and Tsao, 1982; Katoh et al., 1978). The Thomas solution is not only a simplified model but also an empirical approach which assumes that the affinity interactions can be described by an experimentally determinable rate constant which can be used to test how well the experimental results would correlate with the theoretical model. This approach even if not very rigorous and accurate, provides a means of assessing newly developed adsorbents quickly. The kinetic-rate-expression (as it is called; Yang and Tsao, 1982) has therefore been chosen as the rate expression for initial assessment of the blue sponge adsorbent performance in affinity separations.

4.2.2 KINETIC-RATE-EXPRESSION

This type of rate equation belongs to what Yang and Tsao (1982) called simplified and empirical rate equations. The need to use these types of rate equations arises from the mathematical difficulties which have been encountered in solving rate theory models based on rigorous considerations. The simplification of the mathematical treatment by this group of rate equations arises from the fact that the solid matrix is assumed to be homogeneous not only in structure but also in concentration and hence disposes of the need to have partial differential equation (P.D.E.) in the rate expression. Instead the P.D.E. is replaced by an ordinary differential equation (O.D.E.) so that the rate equations become simple functions of time and position only, and no longer governed by the unsteady state P.D.E.; this simplifies the mathematical treatment.

The simplified and empirical rate equation used depends on which of the resistances to mass transfer is considered to be controlling. The Linear-Driving-Force (LDF) type are used in systems where either the film resistance, particle diffusion or pore diffusion is the controlling step. The LDF type generally assumes that the rate is proportional to the distance the system is from equilibrium. The driving force for adsorption is assumed to depend on the difference between either the equilibrium solid or liquid concentration and the average solid phase concentration or equilibrium liquid concentration respectively at any given time.

On the other hand the kinetic-rate-expression type treats sorption or adsorption processes as a chemical reaction, reversible or irreversible of some assumed order. The kinetic rate-type expression (KRE) is exact when surface adsorption rate is controlling.

Various types of KRE have been used in description of the local rate of removal of an adsorbate from solution in adsorption processes depending on the type of isotherm of the system under consideration.

Bohart and Adams (1920) have used the 2nd order form to study the adsorption of chlorine by charcoal, the rate equation presupposes an irreversible adsorption and is given by

$$R_v = k_1 c(q_m - q) \qquad (4.6)$$

where R_v is the rate of transfer of adsorbate from the solution into the adsorbent.

Thomas (1944, 1948) has used linear kinetics (corresponding to a linear isotherm) and reversible kinetics (corresponding to a

Langmuir isotherm) to study the rate of exchange of ions in ion exchange systems. Table 4.2 summarises the rate expression types and Fig. 4.5a-c shows corresponding isotherm types.

Table 4.2. Kinetic-Rate-Expression Models used in Adsorption Models

RATE EXPRESSION FOR R_v =	ISOTHERM TYPE	SYSTEM STUDIED	AUTHOR
(1) $k_1c - k_2q$	Linear	ion exchange	Thomas (1948)
(2) $k_1c(q_m-q)$	Irreversible (Rectangular)	chlorine/ charcoal	Bohart and Adams (1920)
(3) $k_1c(q_m-q)-k_2q$	Langmuir	(a) ion exchange	Thomas (1944)
		(b) affinity system	Chase (1984a)

In affinity interactions the linear isotherm (v. dilute solutions) and rectangular isotherm (very tight binding interactions, for example in some antigen-antibody affinity systems) are extreme cases, the most common being the Langmuir isotherm. This later model has therefore been used in the estimation of the kinetic parameters (see the adsorption isotherm plots of Figs. 4.2b, 4.3b and 4.4b).

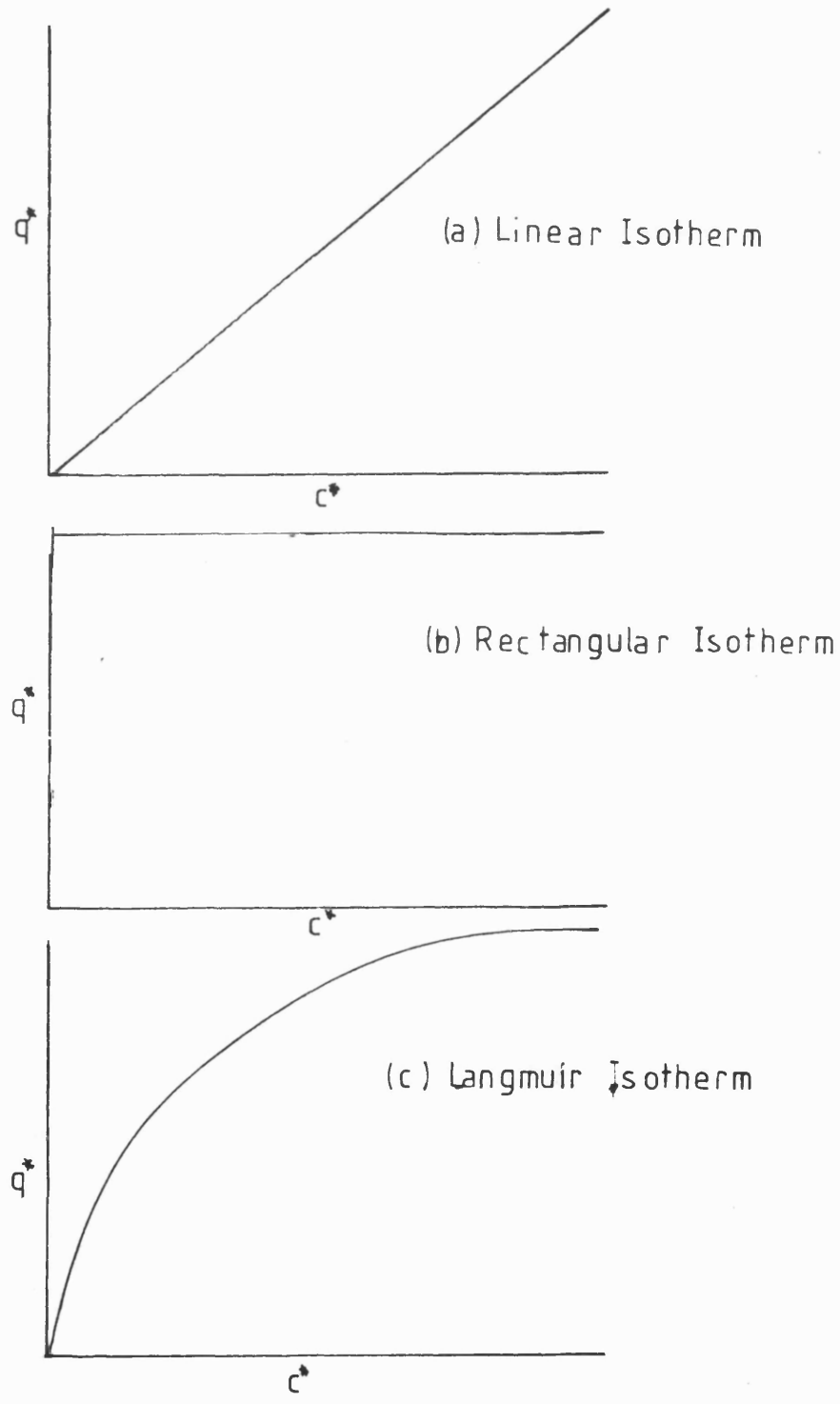

Fig 45 Isotherm Types Corresponding to (a) Linear (b) Irreversible (c) Langmuir Kinetics respectively for Kinetic Rate Expression Rate Models

4.2.3 DERIVATION OF THE RATE EQUATION

The rate equation based on the kinetic-rate-expression type and Langmuir adsorption isotherm can be derived directly from equation (4.2) which is restated:

$$A + B \underset{k_2}{\overset{k_1}{\rightleftharpoons}} AB \qquad (4.2)$$

From simple mass conservation, the rate of mass transfer to the immobilized phase in an interaction described by equation (4.2) is given by

rate of adsorbate adsorption − rate of adsorbate desorption = rate of accumulation of adsorbate on solid phase

that is, $k_1.c(q_m-q) - k_2q = dq/dt$

$$\therefore \frac{dq}{dt} = R = k_1.c.(q_m - q) - k_2q \qquad (4.6a)$$

where R is the rate per unit volume. If R is measured per unit mass equation (4.6a) becomes

$$\rho_s \frac{dq}{dt} = k_1.c.\ (q_m - q) - k_2q \qquad (4.6b)$$

Where ρ_s is adsorbent packing density (kg/m^3)

C is adsorbate concentration in solution (kg/m^3)

q is adsorbate concentration in solid (kg/kg)

q_m is maximum adsorption capacity (kg/kg)

It is necessary to clarify the units of the forward rate constant, k_1 and backward rate constant, k_2 plus those of q and q_m as used in equations (4.6a) and (4.6b) since this is subject to misinterpretation. Table 4.3 shows these units.

Table 4.3. Units of kinetics parameters

RATE EXPRESSION	UNIT k_1	UNIT k_2	q/q_m
(1) $dq/dt = k_1.c(q_m-q) - k_2q$	$m^3/kg\ sec$	s^{-1}	kg/m^3 bed
(2) $\rho_s dq/dt = k_1.(q_m-q) - k_2q$	s^{-1}	kg/m^3 sec	kg/kg dry wt of adsorbent

It should be noted that k_1 and k_2 do not simply represent the rates of adsorption and desorption of the adsorbate onto the immobilised binding site on the surface of the adsorbent but will also include significant contributions from resistances to mass transfer from the bulk of the mobile phase to the adsorption site that also occur in such systems. In this sense k_1 and k_2 should not be regarded as the usual rate constants of chemical systems but as some sort of lumped mass transfer parameter in the sense used for the volumetric mass transfer coefficient, k_f, in situations where film mass transfer is rate-controlling.

It should also be noted that the adsorption isotherm of the Langmuir type can be derived directly from equation (4.6b) where rate of accumulation on solid phase is zero, so that

$$dq^*/dt = k_1.c^*(q_m-q^*) - k_2q^* = 0$$

So that

$$q^* = \frac{q_m \cdot c^*}{(k_d + c^*)}$$

4.2.4 EXPERIMENTAL

The kinetic experiments were carried out in batch mode with blue sponge cut into small pieces (about 2 mm x 2 mm) or minced. Protein solutions in adsorption buffer, 0.05 M Tris-HCl, pH 8.0 were used.

The initial solution absorbance at 280 nm was measured and the blue sponge pieces were added in a solution of protein in a volumetric flask immersed in a water bath cooled by a refrigeration unit with its coil inside the incubator shaker (water bath) equipped with a thermostat to maintain a constant temperature of 4°C, the shaker agitation rate was normally set at 20 r.p.m. The solution samples were withdrawn quickly and the A_{280} measured and then returned to the flask at time intervals.

Control experiments were set up alongside with underivatised sponge pieces in place of the blue sponge. Sampling was done as for the blue sponge experiments.

Kinetics experiments were carried out with both commercial HSA and lysozyme. A similar method has been used by Chase (1984a) to determine the kinetic parameters used in modelling frontal analysis operation in Sepharose 4b-Cibacron blue 36A/BSA and lysozyme affinity interaction.

4.2.5 RESULTS

The kinetics experimental results are shown on Figs. 4.6-4.9.

The procedure was to correct for dilution at the time where the control curve A starts to flatten by subtracting the

concentration from the initial concentration and adding, the difference to that of the sample concentration at the same time as a first correction. Subsequent corrections, usually not very significant, were obtained by adding the concentration difference between given time intervals to that of the sample concentration between the same time intervals. This gives the corrected kinetics curve, C. The correction was necessary in order to eliminate dilution effect.

Fig. 4.6 shows how the experimental liquid phase lysozyme solution declined with time and the corrected kinetic curve used throughout from a given sample and corresponding control experiments.

Fig. 4.7 shows the kinetics curve of duplicated experiments using the same initial concentration of 0.5 mg/ml lysozyme and the same mass of blue sponge in order to check for reproducibility of the kinetics curves.

(a) Calculation of the kinetic parameters

The kinetic parameters k_1 and k_2 were calculated from the kinetics curves by using equations 4.7a-b given below:

$$\rho_s \frac{dq}{dt} = k_1.c(q_m - q) - k_2 q \qquad (4.7a)$$

and

$$c = c_o - (q_m \times M_s)/V \qquad (4.7b)$$

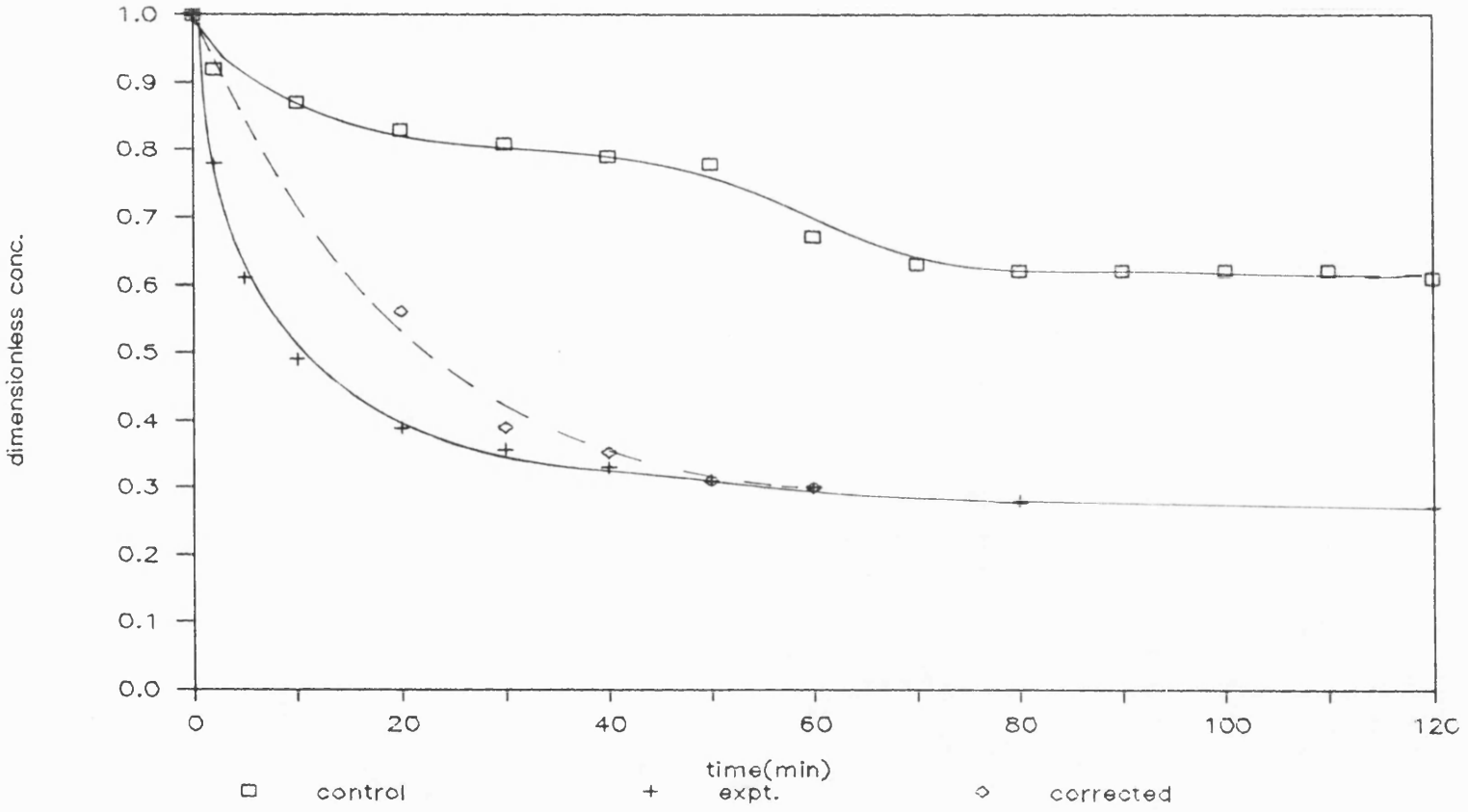

Fig. 4.6. Calculation of corrected kinetics curve: Example using 40 ml Lysozyme concentration of 0.5 mg/ml and blue sponge weight of 2 g (dry wt.).

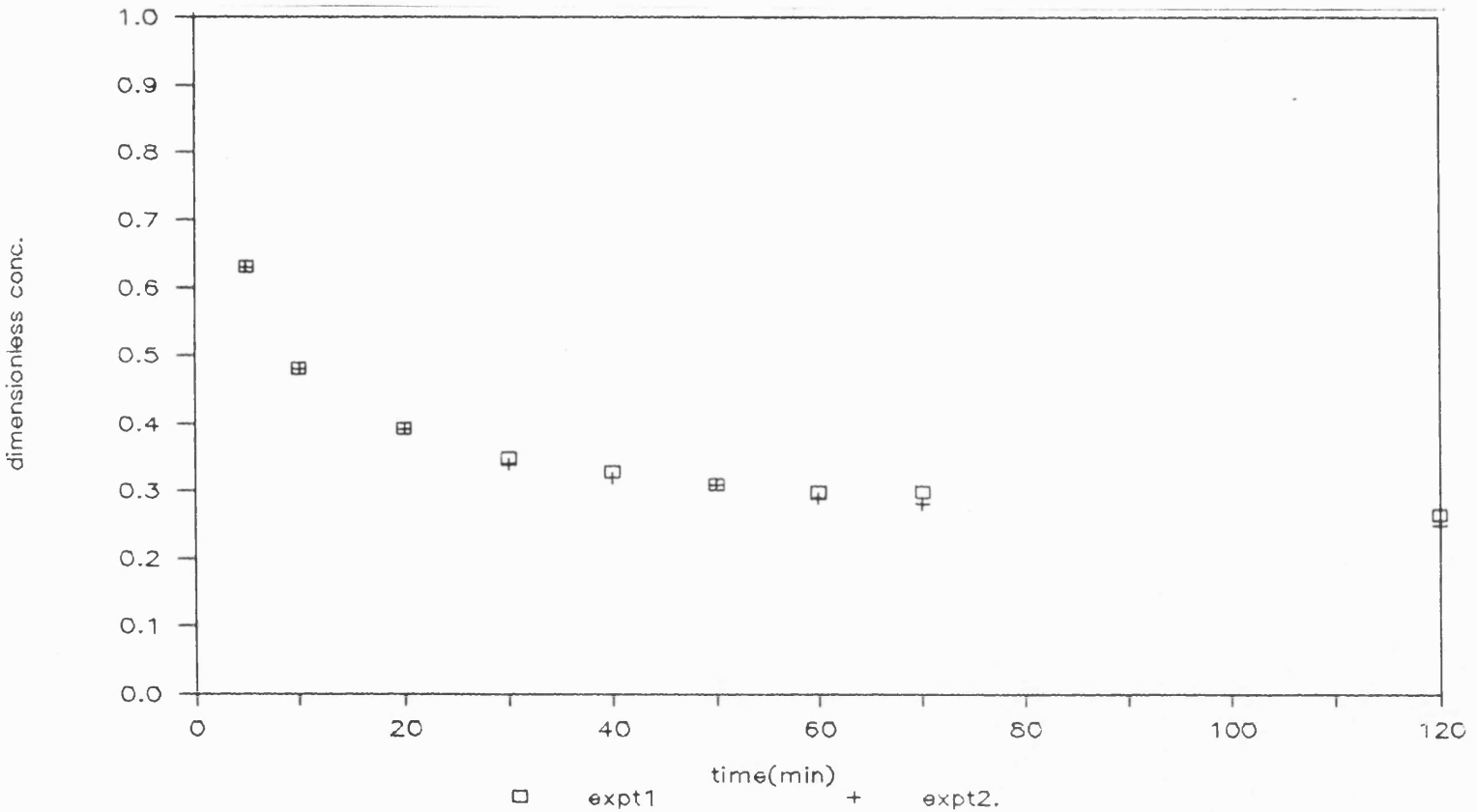

Fig. 4.7. Kinetics curves derived from the same initial Lysozyme concentration and the same mass of blue sponge to check for reproducibility.

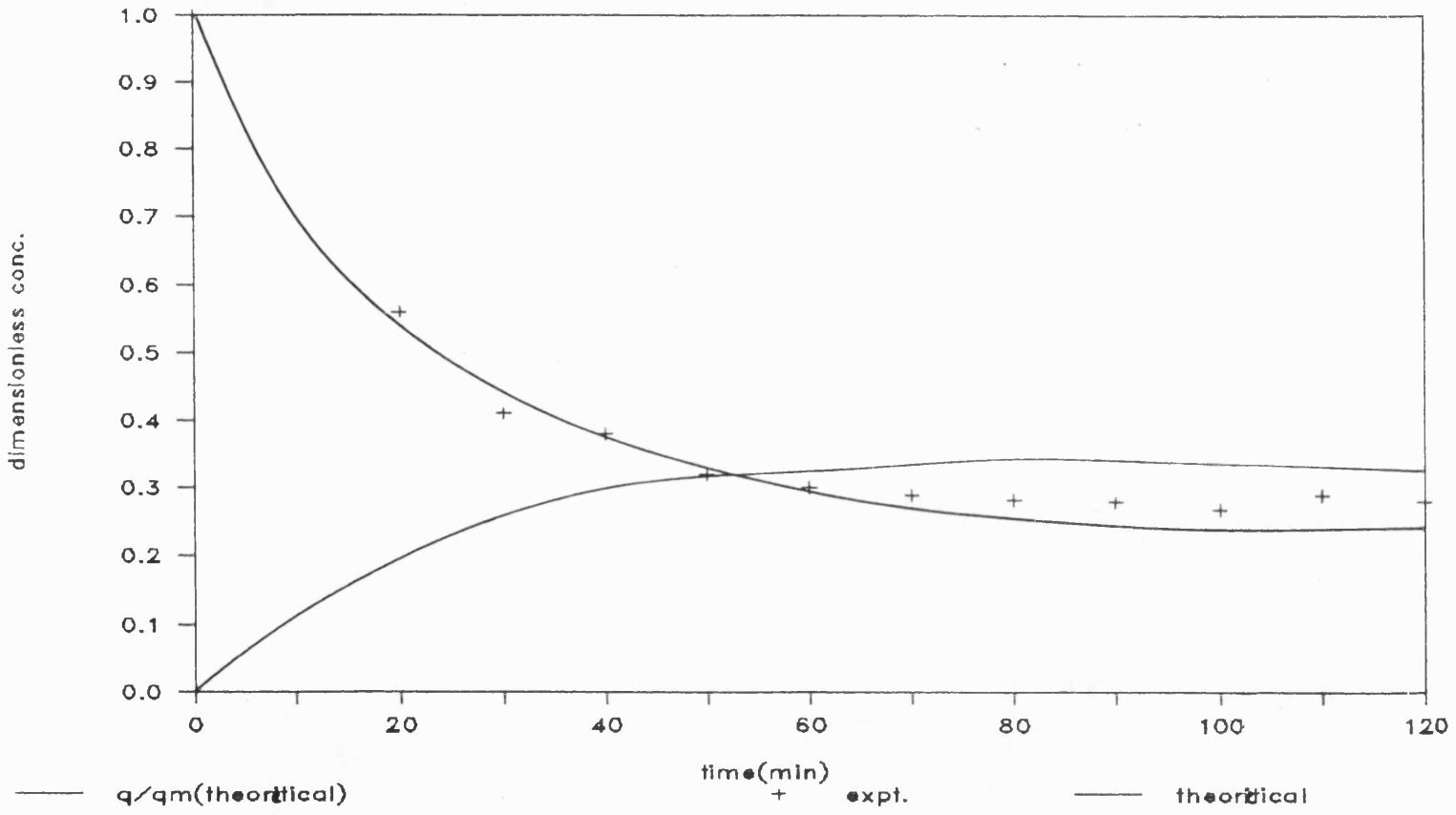

Fig. 4.18. Determination of adsorption rate constant k_1 using 40 ml 0.5 mg/ml lysozyme in Tris-HCl buffer, pH 8.0 and 2 g dry wt. blue sponge.

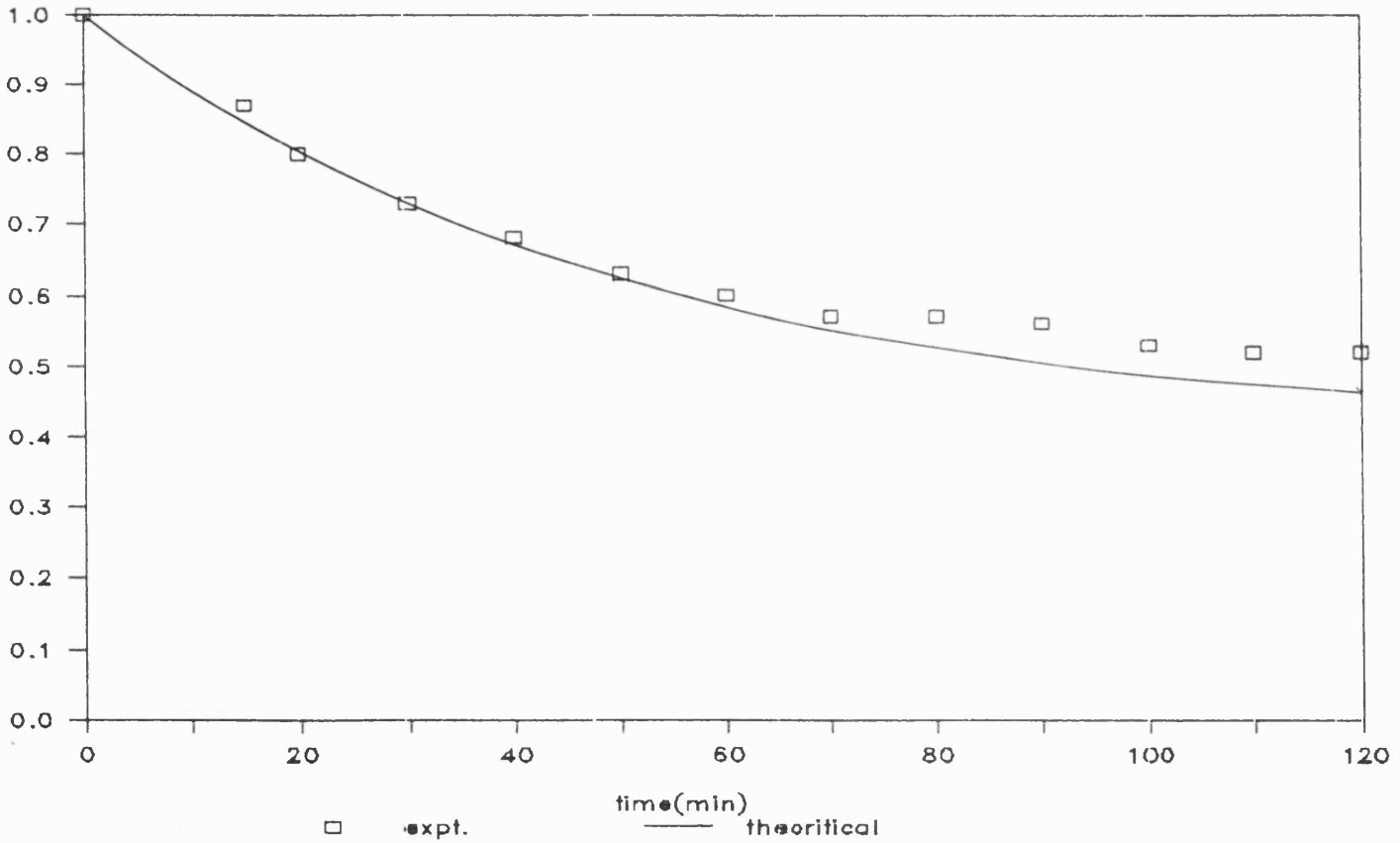

Fig. 4.9. Determination of adsorption rate constant k_1 using 50 mls of 0.5 mg/ml HSA in Tris-HCl, pH 8.0 and 2 g dry weight of blue sponge.

where V is solution volume and M is mass of adsorbent (dry wt)
The values of the maximum solid phase concentration, q_m, was that obtained from the isotherm experiments. The backward rate constant was replaced with $k_1.k_d$ and the value of the dissociation constant, k_d from the isotherm experiment was used. The procedure was to generate lines of kinetics curves using a range of values of k_1 by use of a computer. The theoretical curves generated by this means were compared with the experimental values and the value of k_1 that gave a matching curve was taken as that applicable to the system under consideration. The integration of the rate equation was carried out with the ISIM program using the fixed step Runge-Kutta method.

Fig. 4.8 shows the experimental curve for 40 mls of 0.5 mg/ml lysozyme with 2 g dry weight of blue sponge when compared with the theoretical curve generated by the above method. It also shows the curve for the solid phase concentration.

Fig. 4.9 is the plot of theoretical and experimental curve for HSA used in calculating k_1.

The value of required k_2 was calculated from the relation

$k_2 = k_1.k_d$

The values of k_1 and k_2 are shown in Table 4.4 below.

Table 4.4. Values for kinetic parameters

PROTEIN	k_1 (min^{-1})	k_2 ($kg/m^3/min$)
Lysozyme	1.91	0.4966
HSA	0.618	0.3399

4.3 ESTIMATION OF TRANSPORT PARAMETERS BY THE METHOD OF MOMENTS

4.3.1 THEORETICAL BACKGROUND

4.3.1.1 INTRODUCTION

The pulse response technique is a useful tool for measuring the transport parameters in packed beds. Such transport parameters include bed voidage, porosity, tortuosity, effective solid or pore diffusivity, axial diffusivity and adsorption rate constant. It has been used extensively in gas-phase packed columns (Schneider-Smith, 1968; Cerro-Smith, 1970; Suzuki-Smith, 1972 and Hashimoto-Smith, 1973), in gel permeation chromatography (Adachi et al., 1980) and in a few instances, in beds of immobilized enzyme (Marrazzo et al., 1975; Sirotti-Emergy, 1983).

Because the method is rapid and versatile, it is relatively easy to obtain the above parameters which are otherwise difficult to obtain by standard methods. The mathematical solutions (Kucera, 1965; Schneider-Smith, 1968) for the partial differential equations describing the concentration of the tracer component provide a clear interpretation in terms of the basic transport steps.

The technique involves the injection of a tracer pulse into the feed stream to a containing bed packing, and the analysis of the pattern of the tracer concentration as a function of time, and then, calculating parameters, characterising the resistances to transfer and capacities for the solute.

4.3.1.2 ALTERNATIVE EXPERIMENTAL METHODS

Apart from the pulse-input response of a tracer for the purpose of estimation of parameters useful for packed bed adsorber design, other input functions such as the sinusoidal and step inputs have been used. The choice of an experimental method depends on the experimental convenience, for example, it is only possible to use the step-input response in some circumstances, though it is less accurate than the pulse method. Although the pulse response can be derived from the step-response by the numerical differentiation of the curve, the inherent error in numerical differentiation makes this procedure less accurate than the direct pulse method.

The tracer pulse response and, to a lesser extent, the step response techniques have been chosen here becuase of experimental convenience and also because these methods have been found to be adequate for the design of packed bed reactors for liquid-solid systems of immobilized enzymes (Marrazzo et al., 1975; Adachi et al., 1980; Sirotti-Emery, 1983).

4.3.1.3 ALTERNATIVE METHODS FOR THE PULSE-RESPONSE ANALYSIS

Though the method of moments is the most commonly used technique of parameter estimation from the measurements of tracer input and response, (Schneider-Smith, 1968; Suzuki-Smith, 1971; Furusawa et al., 1976; Sirotti-Emery, 1983) its shortcomings, mainly that tailing and the frontal portions of the response curve are overly weighted in the evaluation of the moments, have prompted the use of modified methods in order to overcome this disadvantage.

The other methods which have been proposed for the estimation of parameters described by a dispersed plug flow model includes the weighted moment method and transfer function fitting by Ostergaard and Michielsen (1969); Fourier analysis by Gangwal et al. (1971); Curve fitting by Clements (1969) and others.

Despite the suggested better accuracy of some of these methods over the method of moments, in certain systems and conditions, the latter remains the most widely used because of its simplicity (Kamiyanagi and Furusaki, 1985). The popularity of the method may also be due to the inherent errors in the alternative methods, coupled with much more troublesome calculations. For example the transfer-function method while more accurate in the trailing region of the response curve, is subject to error in the rising region. In general, all the methods except fitting in real-time domain, deal with an output signal multiplied by a time function - a weighting factor which means that any weighting factor less than or more than unity is likely to introduce some errors under certain experimental conditions. Normally, model parameters have to be determined from measured signals, $c_{expt.}(t)$ (i) by evaluating the integral

$$\int_0^\infty c_{expt}(t)\, W(t)\, dt$$

where W(t) is the weighting function

$W(t) = t^n$ for momemt method

$= t^n e^{-pt}$ for weighted moment method

$= e^{-pt}$ for fitting in Laplace domain ($t.f^n$)

$= e^{-iwt}$ for fitting in frequency domain (Fourier)

or (ii) by fitting $C_{expt.}(t)$ to predicted signal in time domain.

It is therefore no wonder that the method of moments remains a good choice.

4.3.1.4 AXIALLY DISPERSED PLUG FLOW MODELS FOR PACKED BED MOMENT ANALYSIS

When a tracer pulse signal is imposed on a steadily flowing fluid in a packed bed of spherical particles of uniform size, one or more of the following proceses can affect the response - depending on whether the solid is porous or non-porous or if an adsorption takes place on the particles or not. These include axial mixing or dispersion in the flowing fluid, radial dispersion in flowing fluid, mass transport from the flowing fluid to the packing, mass transport in the interior of the packing and adsorption in the packing at an isothermal condition. The model chosen to describe the tracer response may or may not include all the transport steps depending on whether a non-adsorbing or adsorbing tracer is used, the complexity of the model required is justified in terms of computation time and accuracy. As the number of the parameters to be determined is increased, the effects of measurement error, effects of tails and the imperfection in the model chosen increases.

In the present investigation two models will be used based on a non-porous particle model and a porous particle model for the determination of the axial diffusion, D_L, external void fraction, ε, internal void fraction, ε_i, the effective pore diffusivity, D_e and tortuosity, τ.

4.3.1.5 NON-POROUS PARTICLE MODEL

When a tracer is imposed on a stream of fluid in a packed bed of non-porous particles, the differential mass balance over the system gives the fundamental equation according to the dispersed plug flow model as (see derivation in Appendix 2a)

$$D_L \frac{\partial^2 c}{\partial x^2} - u\frac{\partial c}{\partial x} - \frac{\partial c}{\partial t} - \left(\frac{1-\epsilon}{\epsilon}\right) \frac{\partial q}{\partial t} = 0 \qquad (4.7)$$

where

c = concentration of adsorbate in the liquid phase (kg/m^3)

ϵ = bed voidage (-)

u = fluid interstitial velocity (m/s)

D_L = axial dispersion coefficient (m^2/s)

q = concentration of adsorbate in the solid phase (kg/m^3)

The rate of adsorption is given by the relation:

$$\frac{dq}{dt} = ka_v (c - c^*) \qquad (4.8)$$

on the assumption of linear driving force for mass transfer of adsorbate from the fluid to the solid which is the difference between the fluid phase bulk concentration c and the equilibrium concentration corresponding to the adsorbate concentration in the packing, c*, and that adsorbent concentration q is uniform throughout the packing.

k = fluid phase film mass transfer coefficient (m/s)

a_v = the specific surface area of the packing (m^2/m^3)

ka_v = volumetric mass transfer coefficient (s^{-1})

Since the specific surface area of the packing is rather difficult to determine with the sponge equation (4.8) can be rewritten as

$$\frac{dq}{dt} = k' (c - c^*) \tag{4.9}$$

where k ' = volumetric mass transfer coefficient measured in units of (s^{-1}).

Assuming that the adsorption process is governed by a linear isotherm relationship (implicit in the method of moment) that is

$$q = k_m c^* \tag{4.10}$$

where m is the equilibrium constant

$$\frac{dq}{dt} = k'(c - q/k_m) \tag{4.11}$$

Boundary Conditions

For a bed of finite length (the system in use approximates to a short bed) the Danckwerts boundary condition (Danckwerts, 1953) is often used, namely,

at x = 0

$$uc - D_L \frac{dc}{dx} = f(t) \tag{4.12}$$

and at x = ℓ

$$\frac{dc}{dx} = 0$$

where f(t) = δ(t) the impulse function for an ideal application of tracer. The dimensionless form of equations (4.7), (4.11), (4.12) and (4.13) are respectively:

$$\frac{1}{Pe} \frac{\partial^2 c'}{\partial z^2} - \frac{\partial \bar{c}}{\partial z} - \frac{\partial \bar{c}}{\partial \vartheta} - \frac{(1-\epsilon)}{\epsilon} \frac{\partial \bar{q}}{\partial \vartheta} = 0 \tag{4.14}$$

$$\beta \frac{d\bar{q}}{d\theta} = k_f (\bar{c} - \beta \bar{q}/k_m) \tag{4.15}$$

at z = 0

$$\bar{c} - \frac{1}{Pe} \frac{d\bar{c}}{dz} = \delta(\theta) \tag{4.16}$$

at z = 1

$$\frac{d\bar{c}}{dz} = 0 \tag{4.17}$$

where the dimensionless variables are defined as:

$$\bar{c} = \frac{c}{c_0} ; \quad \bar{q} = \frac{q}{q_m} ; \quad z = \frac{x}{\ell} ; \quad \theta = \frac{ut}{\ell} = \frac{t}{\bar{t}}$$

$$Pe = \frac{u\ell}{D_L} ; \quad \beta = \frac{q_m}{c_0} \quad \text{and} \quad K_f = k'\bar{t}$$

c_0 = initial (or reference) concentration of adsorbate in solution.

q_m = maximum (or reference) solid phase concentration of adsorbate

$\bar{t}$ = bed residence time

and

ℓ = bed total (or reference)length

The solution of equations (4.14) - (4.17) is obtained by the application of the Laplace transform. It is not usually necessary to invert the transform since the statistical moments of the pulse response is given by Van der Laan, 1957 as

$$\text{1st absolute moment } \mu_1 = -\lim_{p \to 0} \frac{\partial c}{\partial p}$$

$$\text{2nd central moment } \mu'_2 = \lim_{p \to 0} \frac{\partial^2 c}{\partial^2 p^2} - \mu_1^2$$

where p is the Laplace transform parameter.

4.3.1.6 COMPUTATION OF MOMENTS FROM EXPERIMENTAL DATA

The equation for the nth moment of the pulse response peak for a bed is defined by the integral (Seinfield and Lapidus, 1974) as

$$I_n = \int_0^\infty t^n \, c \, dt \qquad n = 0, 1, 2..... \tag{4.18}$$

The normalized mean and variance, i.e. 1st and 2nd moments become respectively

1st absolute moment,

$$\mu_{1expt} = \frac{1}{t} \frac{I_1}{I_0} \tag{4.19}$$

and 2nd central moment becomes

$$\mu_2' \text{ expt} = \frac{1}{\bar{t}^2} \left[\frac{I_2}{I_0} - \left(\frac{I_1}{I_0}\right)^2 \right] \qquad (4.20)$$

The experimental values of the moments are calculated from the observed pulse peaks using equations (4.19) and (4.20). The integrals in these equations are evaluated by numerical integration using for example, Simpson's rule which was used in this work.

The experimental moments are then expressed in terms of the system parameters using the solution from the theoretical model. For the present model

$$\mu_1 = 1 \qquad (4.21)$$

and

$$\mu_2' = \frac{2}{Pe} - \frac{2}{Pe^2} (1-\exp(-Pe)) \qquad (4.22)$$

(see appendix 3 and Levenspiel, 1972).

4.3.1.7 POROUS PARTICLE MODEL

Relaxing the assumption of the non-porous particles and treating the sponge as being made up of spherical particles (sphericity factors can be used for the non-sphericity of particles to give an equivalent spherical radius) of average uniform pore size. The continuity equations for adsorbate in the external fluid and pore fluids are as follows (see Appendix 2b).

(i) External fluid mass balance

$$\varepsilon \frac{\partial c}{\partial t} = D_L \frac{\partial^2 c}{\partial x^2} - u \frac{\partial c}{\partial x} - \frac{3(1-\varepsilon)}{R} D_e \frac{\partial c_i}{\partial r}\Big|_{r=R} \qquad (4.23)$$

(ii) Particle material balance

$$\epsilon_i \frac{\partial c_i}{\partial t} = \frac{1}{r^2} \frac{\partial}{\partial r} \left(D_e r^2 \frac{\partial c_i}{\partial r} \right) - \frac{\partial q_i}{\partial t} \qquad (4.24)$$

where c = external fluid phase concentration

ϵ_i = internal porosity

c_i = pore fluid phase concentration

D_e = effective pore diffusivity

q_i = solid phase concentration

R = particle radius

r = radial co-ordinate in the particle

Other symbols have the same meanings as for the non-porous particle models - see previous section.

Equations (4.23) and (4.24) are coupled using c_i and c which can be related by the rate of mass transfer of mass through the fluid film, namely,

$$k(c - c_i|_{r=R}) = D_e \frac{\partial c_i}{\partial r}\Big|_{r=R} \quad \text{at } r = R \qquad (4.25)$$

Assuming that tracer adsorption is descrbed by first order kinetics, then

$$\frac{dq_i}{dt} = k_a(c_i - q/k_m) \qquad (4.26)$$

where k_a is adsorption rate constant

and k_m is adsorption equilibrium constant.

Equations (4.23) - (4.26) together with the following boundary and initial conditions

$$\frac{\partial c_i}{\partial r} = 0 \qquad \text{at } r = 0 \qquad \text{for } t > 0 \qquad (4.27)$$

$$c = 0 \qquad \text{at } x > 0 \qquad \text{for } t = 0$$

$$c_i = 0 \qquad \text{at } r > 0 \qquad \text{for } t = 0$$

$$c = C_0 \qquad \text{at } x = 0 \qquad 0 < t < t_0$$

may be transformed to the Laplace domain and solved for $\bar{c}(p,x)/\bar{c}_o$ where p is the Laplace parameter.

Furusawa et al. (1976) and others including Kucera (1965) have solved for $\bar{c}(p, x)$ using equations (4.23) - (4.27) to obtain a general solution. Instead of inverting the solution in terms of the Laplace Transform parameter (p) to obtain a solution in terms of time parameter, t, Vaan dar Laan's relation is used, as in the case of the non-porous model, to obtain the solution in terms of moments.

The Vaan der Laan relation for nth moment I_n, is

$$I_n = (-1)^{n-1} \lim_{p \to 0} \frac{\partial^n \bar{c}}{\partial p^n}(p,\ell) = \int_0^\infty c(t)t^n dt \qquad (4.28)$$

and the equation for the nth absolute moment of a peak is defined as

$$\mu_n = \frac{\int_0^\infty c(t)\, t^n\, dt}{\int_0^\infty c(t)\, dt} = \frac{I_n}{I_0} \qquad (4.29)$$

and the nth central moment is:

$$\mu_n' = \frac{\int_0^\infty c(t)(t-\mu_1)^n\, dt}{\int_0^\infty c(t)\, dt} = \frac{I}{I_0} \int_0^\infty (t-\mu_1)^n c(t)dt \qquad (4.30)$$

For the case of the non-adsorbing tracer the moments expression in terms of the rate parameters using solution of equations (4.23) - (4.27) in Laplace domain and Vaan der Laan's relation (equation

4.28) as obtained by Furusawa et al. (1976) and used by Sirotti and Emery (1983) for mass transfer analysis in an immobilized enzyme reactor are

$$\mu_1 = \frac{\ell}{u_0}(\varepsilon + (1-\varepsilon)\,\varepsilon_i) \tag{4.31}$$

$$\frac{\mu_2'}{2\ell/u_0} = \delta_D + \delta_f + D_L \frac{1}{u_0^2}(\varepsilon + (1-\varepsilon)\varepsilon_i)^2 \tag{4.32}$$

where

$$\delta_D = \frac{\varepsilon_i^2 R^2 (1-\varepsilon)}{15 D_e} \qquad \text{and} \qquad \delta_f = \frac{\varepsilon_i^2 R (1-\varepsilon)}{3k}$$

4.3.1.8 MATERIALS AND APPARATUS

The chemicals used as for Chapter 3. Blue dextran (molecular weight 2×10^6) was purchased from Sigma Chemicals Ltd.

The Gilson HPLC system (Model 702) was supplied by Anachem Ltd., 20 Charles Street, Luton, Beds. The Cecil spectrophotometer (model CE588) was used for absorbance measurement for step response.

4.3.2 EXPERIMENTAL METHOD

For the step response experiments the experimental set up was the same as that for the adsorption experiment (Fig. 3.7) and that for the pulse is shown in Fig. 4.10. The experiments were carried out with ten circular discs compressed between a plunger and end piece of a column or between two plungers in the case of the adjustable column. The columns and materials used were the same as those for the kinetics and adsorption isotherm experiments.

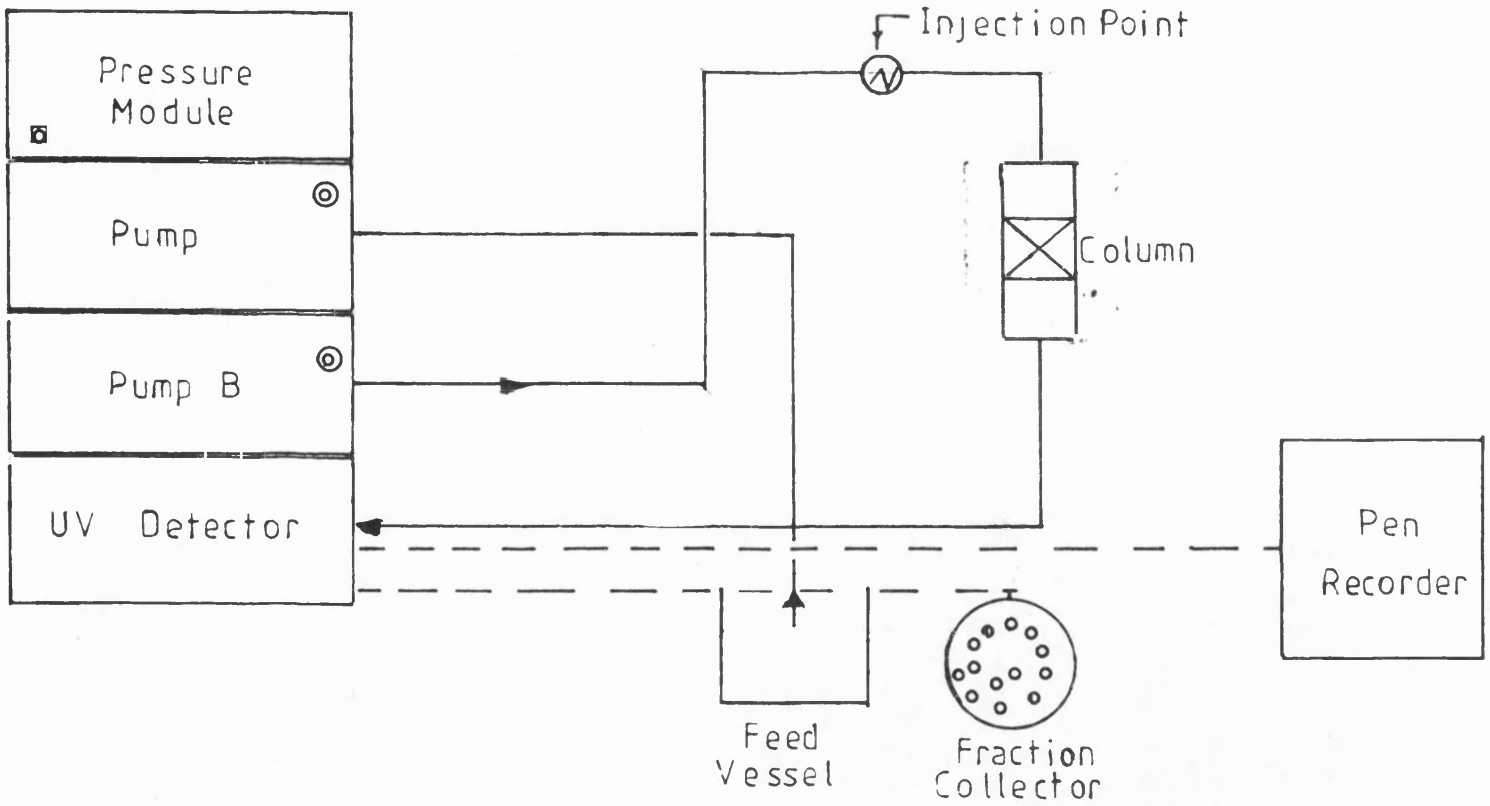

Fig. 4.10 Experimental Set-up for Pulse Response Analysis With Gilson HPLC System

The first set of the step response experiments was carried out with the arrangement of equipment and connections as shown in Fig. 3.7a (no further use of this set up was made). The connecting tubes were made as short as possible in order to minimize the dead volume (about 2.5 ml) in the system and then subsequently tested for leakage by passing 0.01% blue dextran through the system (without the column) and observing any possible leakage visually. Samples were collected with an LKB 2112 RediRac fraction collector in volumes, typically, 5 cm^3. The effluent sample concentrations were then determined at the appropriate absorbancy with the CECIL (Model CE588) spectrophotometer.

(a) Pulse Response Experiments

For pulse response experiments the columns were fitted to the Gilson HPLC System (Fig. 4.10). The 'dead' volumes between pulse injection and bed entrance and between bed exit and detector were minimized by use of shortest possible, narrow (1/16") tubings. This ensures the reduction of the corrections necessary to obtain moments of the bed from the observed moments. An rhodyne injection system was used to introduce the pulse of solute solution, typically 20 μl or 100 μl in volume. Injection time was about 3 seconds. The column effluent was monitored by a UV detector and recorded on a chart. Responses were all measured at room temperature.

The system response was measured with no column present using 0.2% blue dextran. The response proved to be very small compared with the responses when the column was in place. Responses were measured at several flow rates.

The experiments were carried out under conditions that effectively suppress the affinity binding since only hydrodynamic effects were desired. Protein solutions were therefore made with 0.5 M NaSCN 50 mM Tris-Buffer, pH 8.0, a protein concentration of 25 kg/m^3 or 50 kg/m^3. Blue dextran (M. Wt. 2,000,000) - purchased from Sigma Chemicals Limited (Poole, Dorset) - was dissolved in phosphate buffer solution, pH 7.06. A concentration of 0.2% was used in all experiments. An alternative experimental condition would have been to use underivatized sponge but this was not done because of the possibility of having altered the sponge texture during the manufacture of the affinity sponge.

The solutes used were lysozyme (M. Wt. 14,000), BSA (M. Wt. 67,000) and blue dextran (M. Wt 2 x 10^6). BSA was chosen because it should exhibit diffusional properties similar to the model protein, HSA (M. Wt 66,300) since they have similar molecular weight. BSA is also much cheaper than HSA and is much less likely to be adsorbed under the eluting conditions used in the experiments. Since it has much less affinity for the adsorbent than the HSA, blue dextran was used since it would be excluded, hopefully, from all the small pores of the sponge which should normally be accessible to molecules like lysozyme, BSA or HSA because of its size and shape, but would occupy the spaces in the larger pores of the sponge.

STEP RESPONSE EXPERIMENTS

The step response curves were numerically differentiated using central difference formula to yield pulse response curves. The first and second moments were calculated from equations (4.35) and (4.36). In the case of pulse response curves, numerical integration was carried out according to equations (4.18) to (4.20)

to give the first and second moments. The moments were then analysed as in equations (4.31) and (4.32) to yield the parameters of interest.

4.3.4 ANALYSIS AND RESULTS

4.3.4.1 STEP RESPONSE EXPERIMENTS (WITH AMICON WRIGHT COLUMN)

The data collection was by mixing cup readings at given time intervals such as is shown in Table 4.5 below

Table 4.5. Mixing-cup calculation procedure

TIME INTERVAL t_i	AVERAGE TIME IN INTERVAL t_i	AVERAGE CONCENTRATION IN MIXING CUP c_i
0-5	2.5	0.0
5-10	5.0	0.3
10-15	7.5	0.4
90-100	95.0	1.0

The pulse-mean and the pulse-variance were then calculated by the method suggested by Levenspiel (1979) for step response data collected by mixing cup methods, namely

mean response time,

$$\bar{t} = \frac{\int_0^\infty (c_{max}-c)dt}{\Delta c_{max}} \qquad (4.33)$$

and the variance,

$$\sigma^2 = \frac{2\int_0^\infty t(c_{max}-c)dt}{\Delta c_{max}} - \bar{t}^2 \qquad (4.34)$$

The Δc_{max} was calculated from the step response curve as the difference between the maximum and the minimum concentration. For example, Δc_{max} for Table 4.5 is 1.0 - 0 = 1.0.

The approximation of equations (4.33) and (4.34) for discrete data is

$$\bar{t} = \frac{\sum_{i=1}^{n} (c_{max}-c_i)\ \Delta t_i}{\Delta c_{max}} \qquad (4.35)$$

$$\sigma^2 = \frac{2\sum_{i=1}^{n} t_i(c_{max}-c_i)\ \Delta t_i}{\Delta c_{max}} - \bar{t}^2 \qquad (4.36)$$

Equations (4.35) and (4.36) were converted to computer code and used to generate the mean and the variances from the experimental results. The step response curves for BSA in Tris/SCN^- is shown in Figs. 4.11 and 4.12. The pulse response curves derived from the step curves by numerical differentiation are shown in Fig. 4.13.

The reduced mean time, μ_1 was obtained by division with the bed residence time (ℓ/u) and the reduced variance, μ_2 obtained by division by the square of the mean time, namely

$$\mu_1 = \frac{\bar{t}}{\bar{t}_b} = \frac{\bar{t}}{(\ell/u)} = \frac{1}{\bar{t}_b} \cdot \frac{\sum_{i=1}^{n} (c_{max}-c_i)\ \Delta t_i}{\Delta c_{max}} \qquad (4.37)$$

$$\mu_2' = \frac{\sigma^2}{\bar{t}_b^{\,2}} = \frac{1}{\bar{t}_b^{\,2}} \left(\frac{2\sum_{i=1}^{n} t_i(c_{max}-c_i)\ \Delta t_1}{\Delta c_{max}} - \bar{t}^2 \right) \qquad (4.38)$$

CALCULATION OF BED VOIDAGE, ε AND PECLET NUMBER, Pe

The bed external void fraction, ε, was calculated from equation (4.39), from the retention time of blue dextran, t_{BD}:

$$\varepsilon = \frac{V_0}{V_t} = \frac{\bar{t}_{BD}}{(\ell/u)} = \mu_{1\ BD} \qquad (4.39)$$

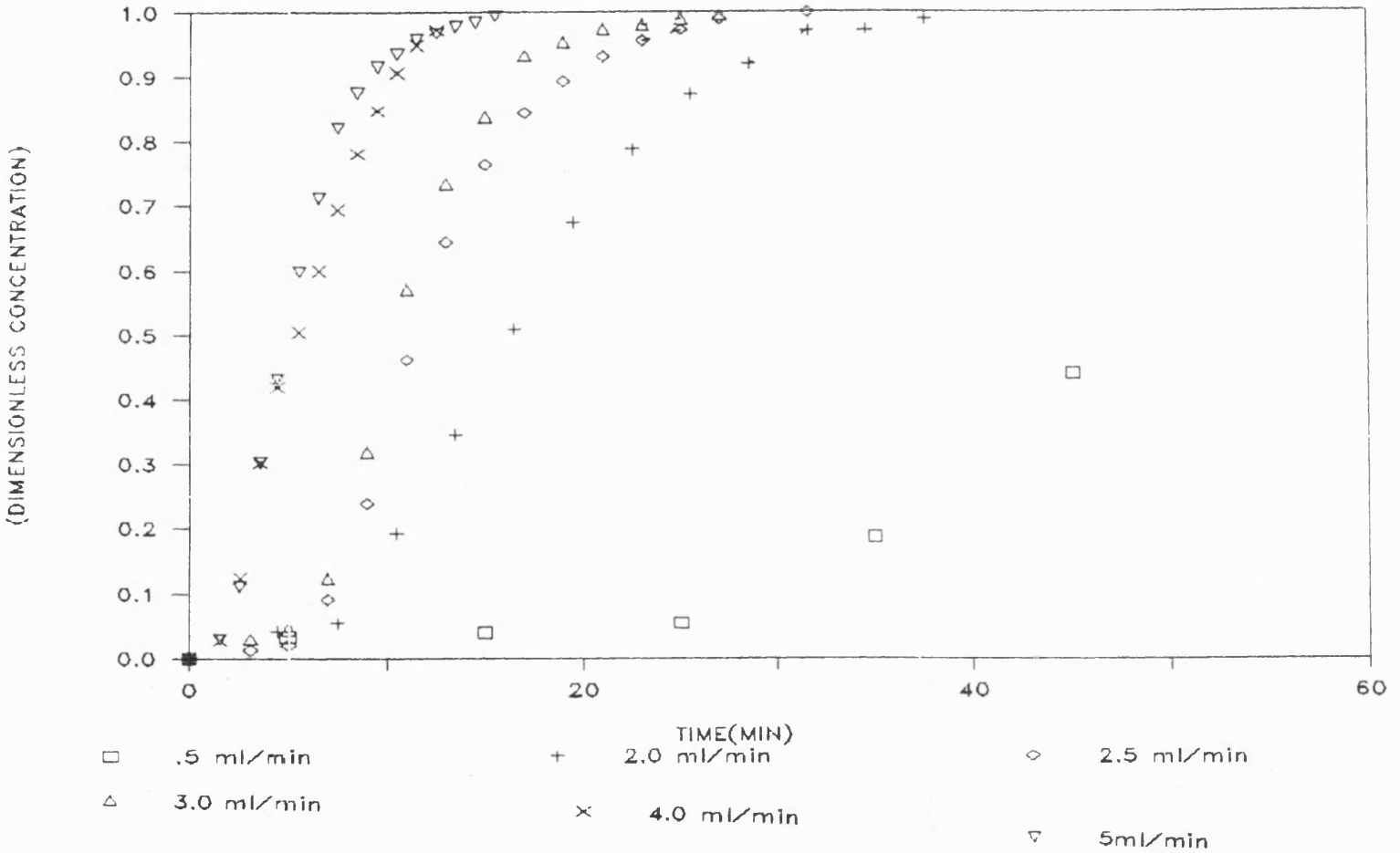

Fig. 4.11. Step response curve for BSA in Tris-SCN^- (flow rate range, 0-5 ml /min).

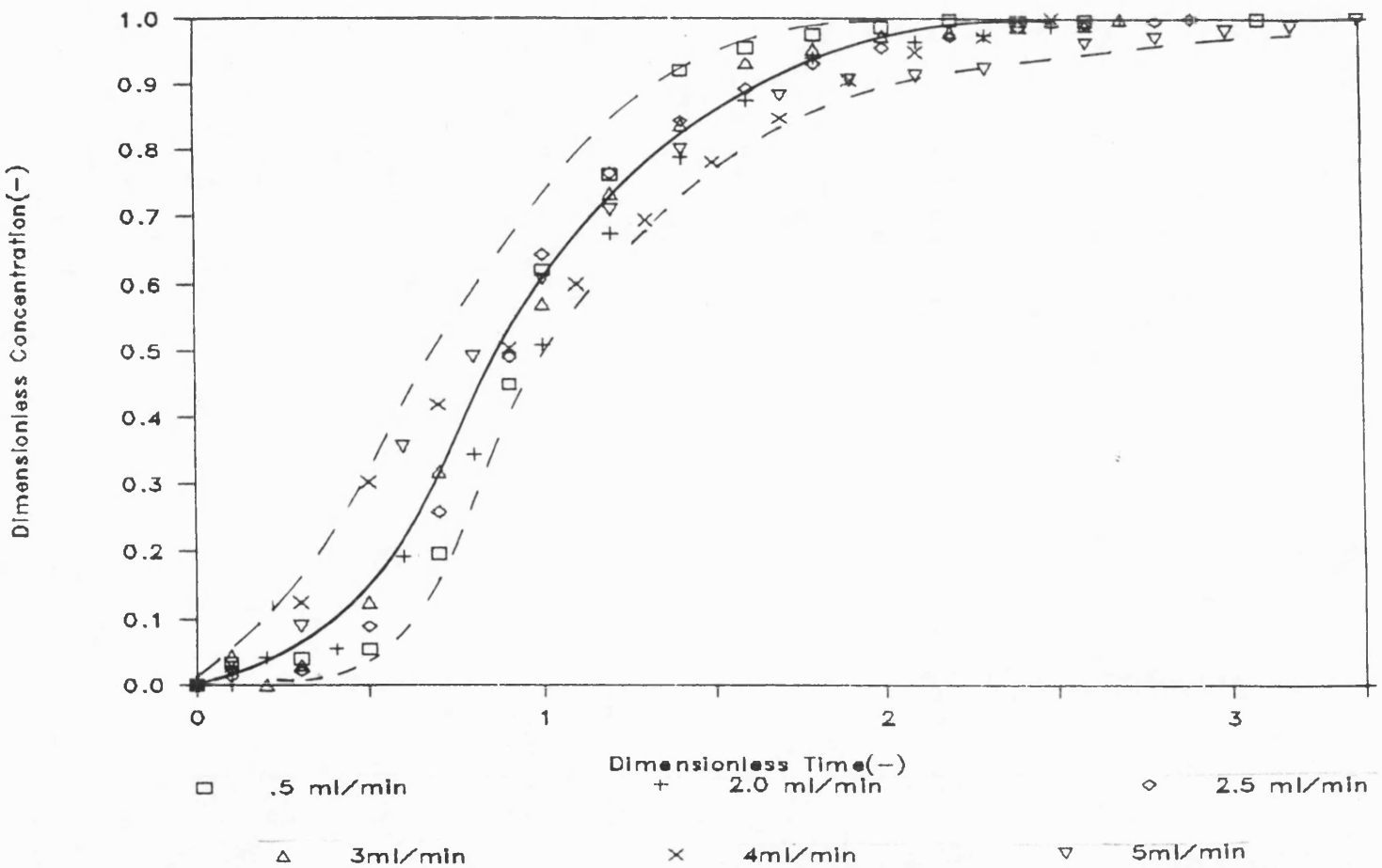

Fig. 4.12. Normalised F vs curve for step response of BSA in Tris-SCN^-.

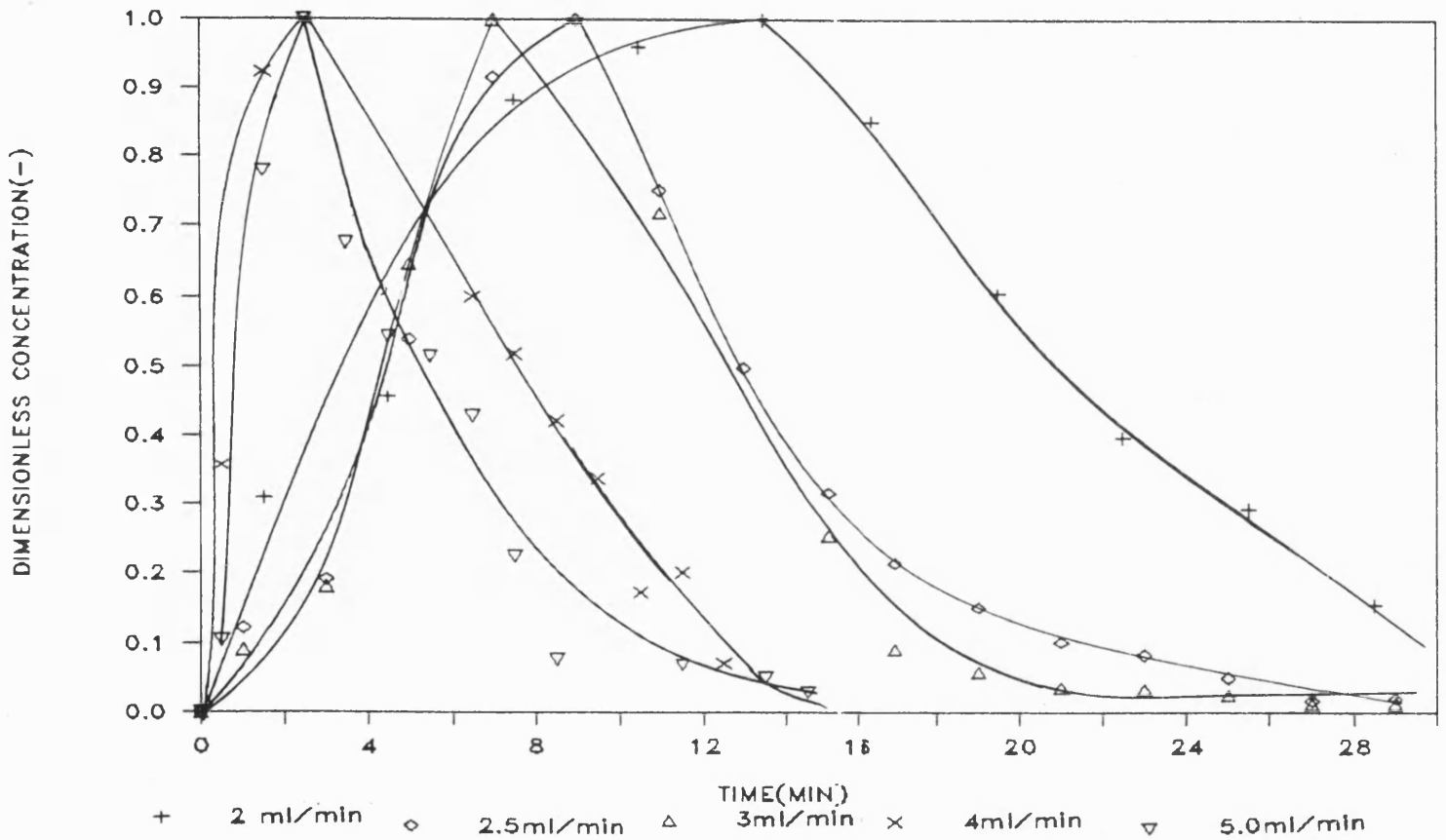

Fig. 4.13. Pulse response curves of BSA in Tris-SCN^-, pH 8.0 derived from step response curves of Figs. 4.11 and 4.12 by numerical differentiation.

Similarly, the intraparticle void, ε_i, for BSA, $\bar{t}_{BSA}$ was calculated by equation (4.40)

$$\varepsilon + \varepsilon_i = \frac{V_0+V_i}{V_t} = \frac{\bar{t}_{BSA}}{(\ell/u)} = \mu_{1\ BSA} \qquad (4.40)$$

where V_0 = void volume of bed

V_i = void volume available to BSA

V_t = total bed volume

(a) Calculation of the Peclet Number

According to equations (4.21) and (4.22):

$$\mu_{1\ BSA} = 1 \qquad (4.21)$$

and

$$\mu_2'_{\ BSA} = \frac{2}{Pe} - \frac{2}{Pe^2}(1 - \exp(-Pe)) \qquad (4.22)$$

The peclet number was calculated from the second central moment since the experimentally observed first absolute moment ($\mu_{1\ BSA}$) was close to unity - average of 0.942, standard deviation 0.082.

The results for the estimated voidage and axial diffusion coefficient/peclet number are shown in Table 4.6 below.

DATA FOR CALCULATION (Column dimensions and density of packing)

Length ℓ = 1.71 cm; Bed volume, V = 26.242 cm^3

Diameter d = 4.4 cm; X-sec. area, A = 15.904 cm^2

Packing density ρ_S = 0.193 g/cm^3

Table 4.6. Experimental Values of External Void and Peclet Number from Step Response Analysis.

(a) BSA

AXIAL VELOCITY u (cm/min)	1st ABSOLUTE MOMENT μ_1 (min)	2nd CENTRAL MOMENT μ_2' (min^2)	BED RESIDENCE TIME $\bar{t}$ (ℓ/u)	$\frac{\mu_1}{\bar{t}}$ (-)	$\frac{\mu_{2'}}{\bar{t}^2}$ (-)	Pe (-)
0.031	53.958	457	54.459	0.991	0.154	12.903
0.157	10.62	24.733	10.892	0.975	0.208	8.511
0.189	9.312	16.558	9.048	1.02	0.202	8.772
0.252	6.013	9.204	6.786	0.886	0.1999	8.929
0.314	4.516	7.940	5.446	0.829	0.268	6.299

(b) BLUE DEXTRAN

AXIAL VELOCITY u (cm/min)	1st ABSOLUTE MOMENT, μ_1 (min)	RESIDENCE TIME OF BED $\bar{t}$ (ℓ/u) (min)	$\frac{\mu_1}{\bar{t}}$ (-)
0.63	25.212	27.196	0.927
0.063	24.91	27.196	0.9159
AVERAGE	25.01	27.196	0.921

4.3.3.2 PULSE RESPONSE (WITH SARTORIUS COLUMN AND MICRO-COLUMN)

Experimental data for pulse response of lysozyme, BSA and blue dextran tracers which were carried out with the modified Sartorius column and a micro-column was analysed with the equations of the non-porous model (equations 4.31 and 4.32).

According to the model, the first absolute moment, μ_1, is given by

$$\mu_1 = \frac{\int_0^\infty c(t)\, t\, dt}{\int_0^\infty c(t)\, dt} = \frac{\ell}{u}\left(\varepsilon + (1-\varepsilon)\varepsilon_i\right) \qquad (4.31)$$

and the second central moment, μ_2' is given by

$$\mu_2' = \frac{\int_0^\infty c(t)\,(t-\ _1)dt}{\int_0^\infty c(t)\, dt} = \frac{2\ell}{u}\left[\delta_D+\delta_f+\ \frac{D_L}{u^2}\left(\varepsilon+(1-\varepsilon)\varepsilon_i\right)^2\ \right] \qquad (4.32)$$

where

$$\delta_D = \frac{\varepsilon_i^2 R^2 (1-\varepsilon)}{15 D_e}$$

and

$$\delta_f = \frac{\varepsilon_i^{\ 2}\ R(1-\varepsilon)}{3k}$$

ε_i = internal porosity of the sponge material(-)

ε = external bed voidage (-)

D_L = axial dispersion coefficient (m^2/s)

D_e = effective pore diffusivity (m^2/s)

R = particle radius (m)

k = external film mass transfer coefficient (m/s

Equation (4.31) indicates that a plot of μ_1 vs ℓ/u should be linear, with a slope $\varepsilon + (1-\varepsilon)\varepsilon_i$, which is the total void fraction of the bed. Equation (4.32) indicates that a plot of $\mu_2/(2\ \ell/u)$ vs ℓ/u will give a linear line. The value of $D_{L/u}$ can be calculated from the slope of such a plot, while the intercept will give the value of $\delta_D = \delta_f$. The μ_1 vs ℓ/u plots for BSA and lysozyme using

the micro-column or the modified Sartorius column are shown in Figs. 4.14a, 4.15a and 4.16a. The corresponding $\mu_2'/(2\ell/u)$ vs ℓ/u plots are shown in Figs. 4.14b, 4.15b and 4.16b. The estimated external voidage for micro and Sartorius column packings using the retention time of Blue dextran from the pulse response experiments are shown in Table 4.10.

Subject to the estimation of δ_f values, the value of δ_D can be estimated from the intercept value of the $\mu_2'/(2x\ell/u)$ vs ℓ/u plot. From the δ_D value, the effective pore diffusivity D_e, can be estimated.

(a) ESTIMATION OF THE EXTERNAL FILM MASS TRANSFER COEFFICIENT

Very little information is available from the literature on the fluid film mass transfer coefficient correlations for proteins (Schmidt number > 8000) in packed beds. However, Rovito and Kittrel (1973), Sirotti and Emery, (1983) and Marrazzo et al. (1975) have shown that the few available packed bed correlations did correlate well for the external film mass transfer in immobilised enzyme systems.

The correlation by Wilson and Geankoplis (1966) was obtained from data in a packed bed with properties similar to those used in the present experiments: particle Reynold number (Re_p) between 0.0016 and 55, Schmidt number (Sc) between 165 and 70,600. The calculation of the Re_p was based on the particle radius of 50 μm which is the average size of the particle suggested by the electron micrograph of the sponge.

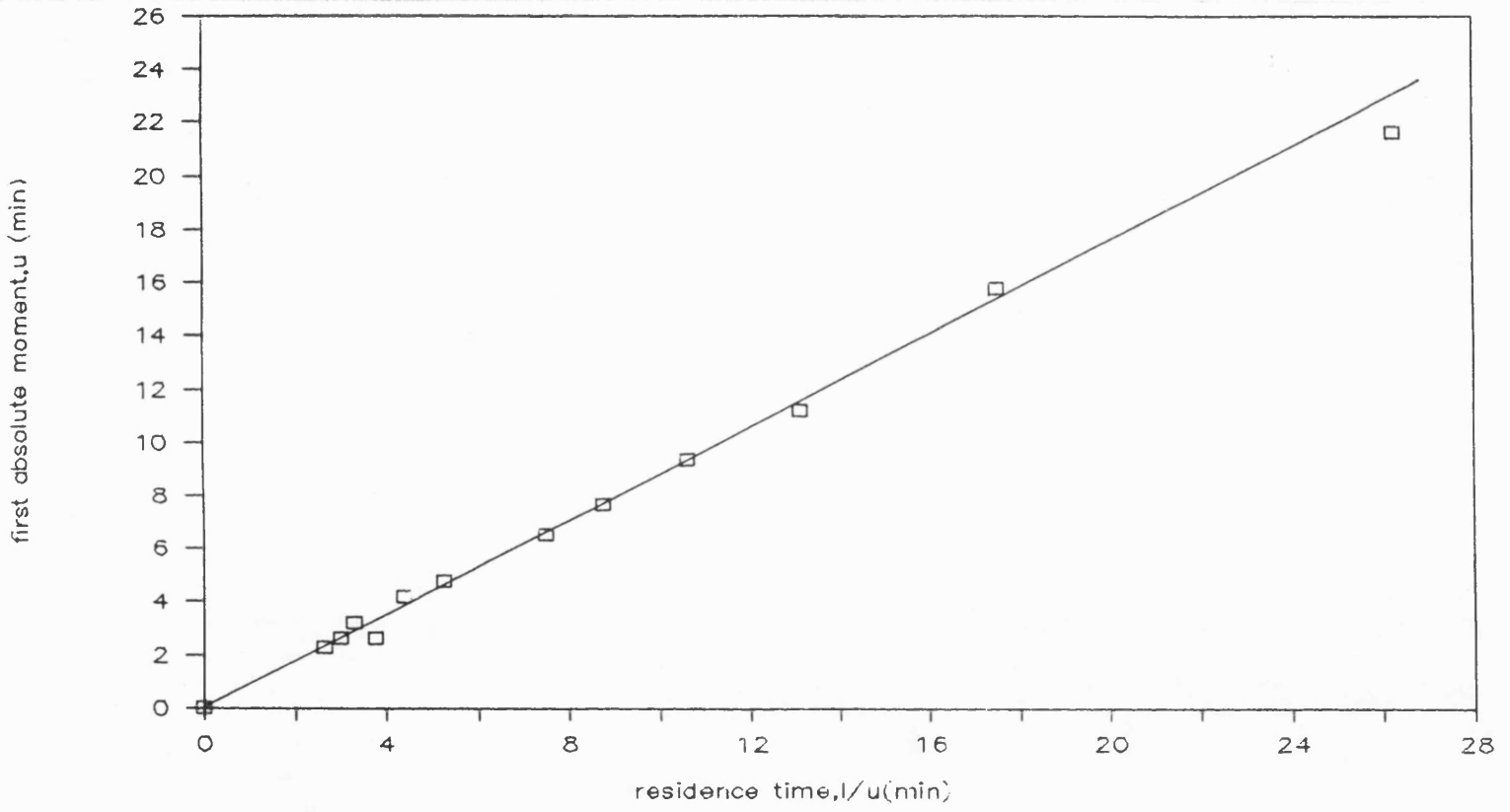

Fig. 4.14a.First absolute moment vs superficial residence time for the pulse response of BSA in Tris-SCN^-, pH 8.0 using the Satorious column.

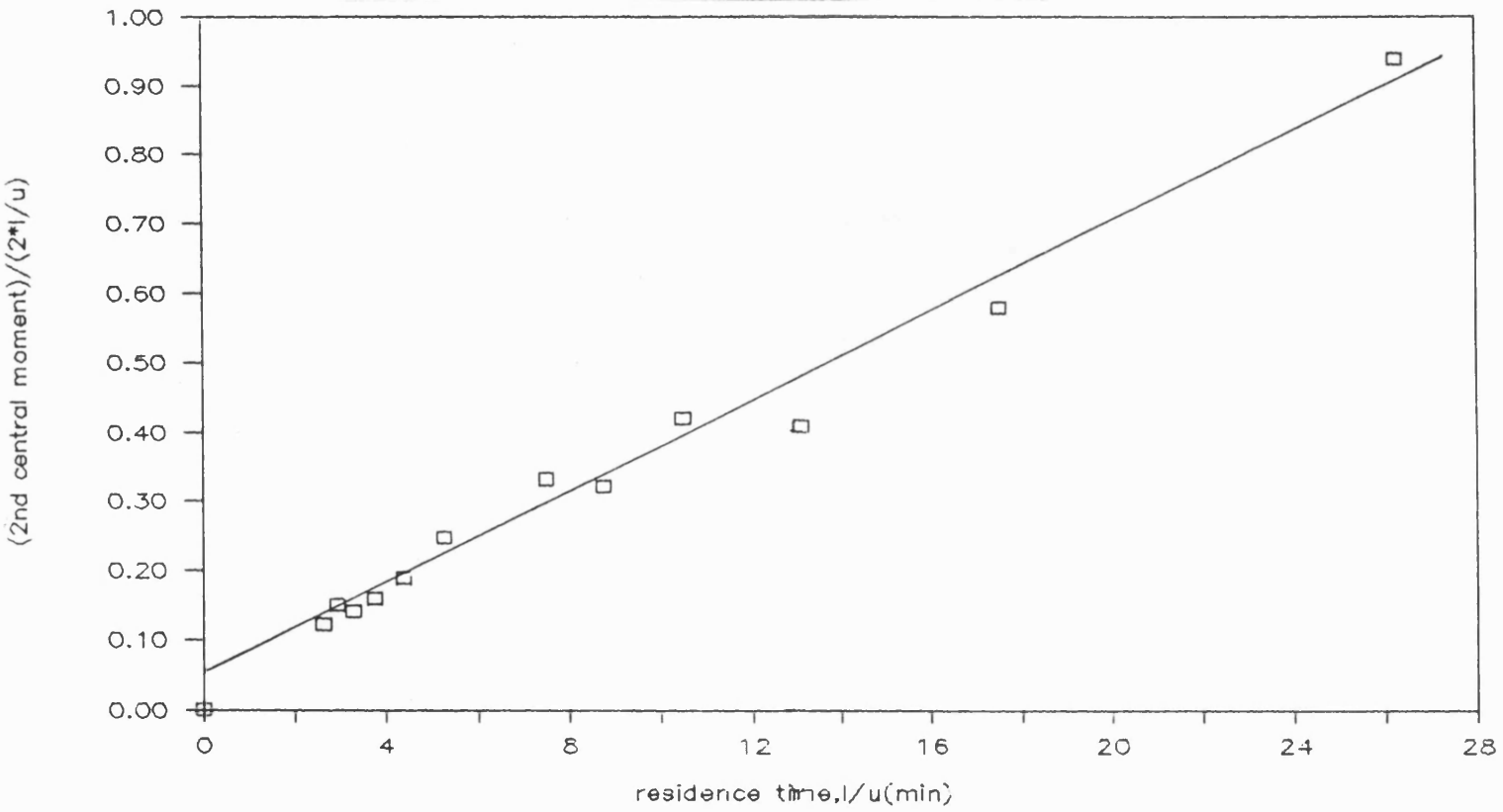

Fig. 4.14b. Ratio of second central moment to residence time vs. superficial residence time for pulse response of bSA in Tris-SCN, pH 8.0 using modified Satorious column.

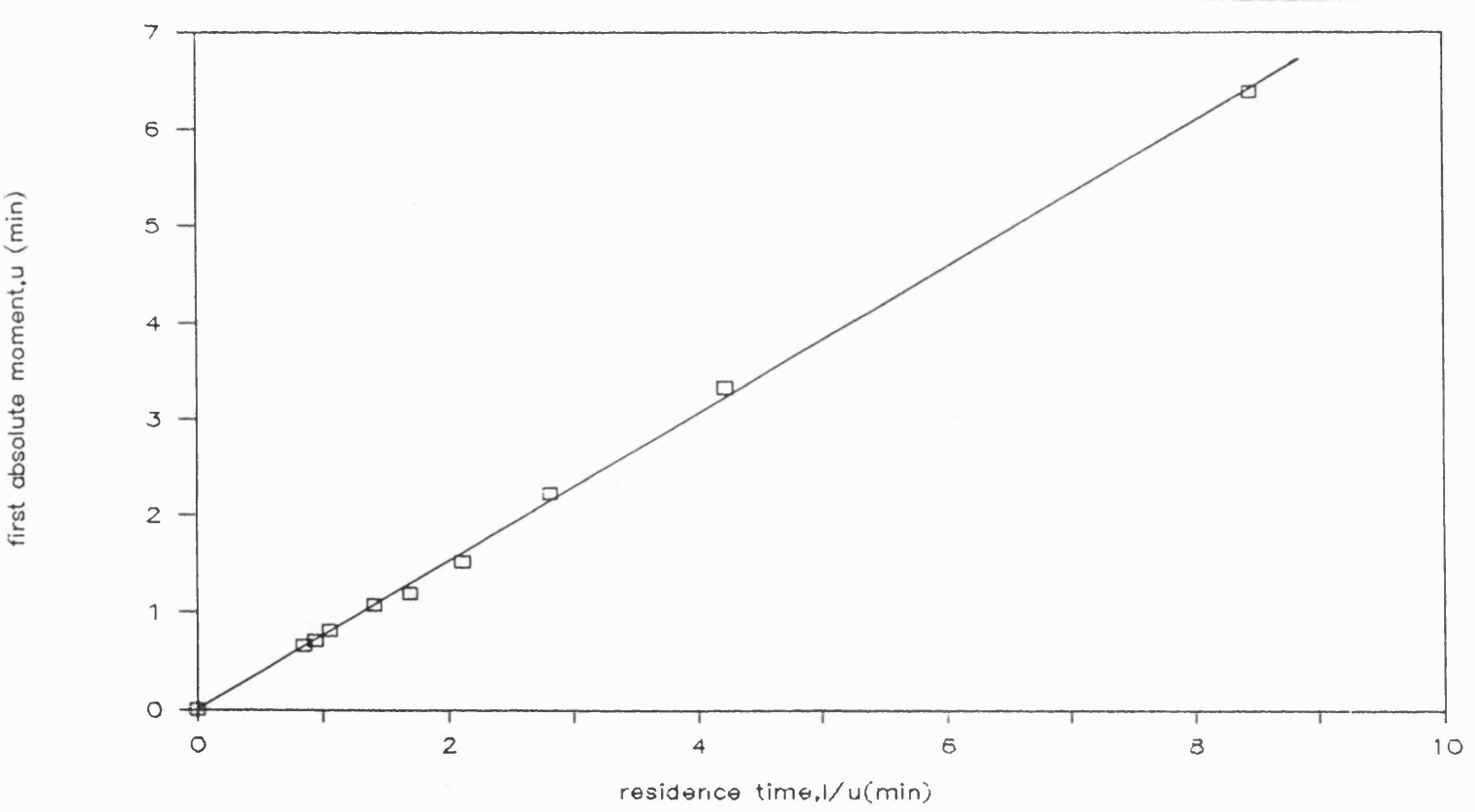

Fig. 4.15a.First absolute moment vs. superficial residence time for the pulse response of Lysozyme in Tris-SCN, pH 8.0 using modified Sartorious column.

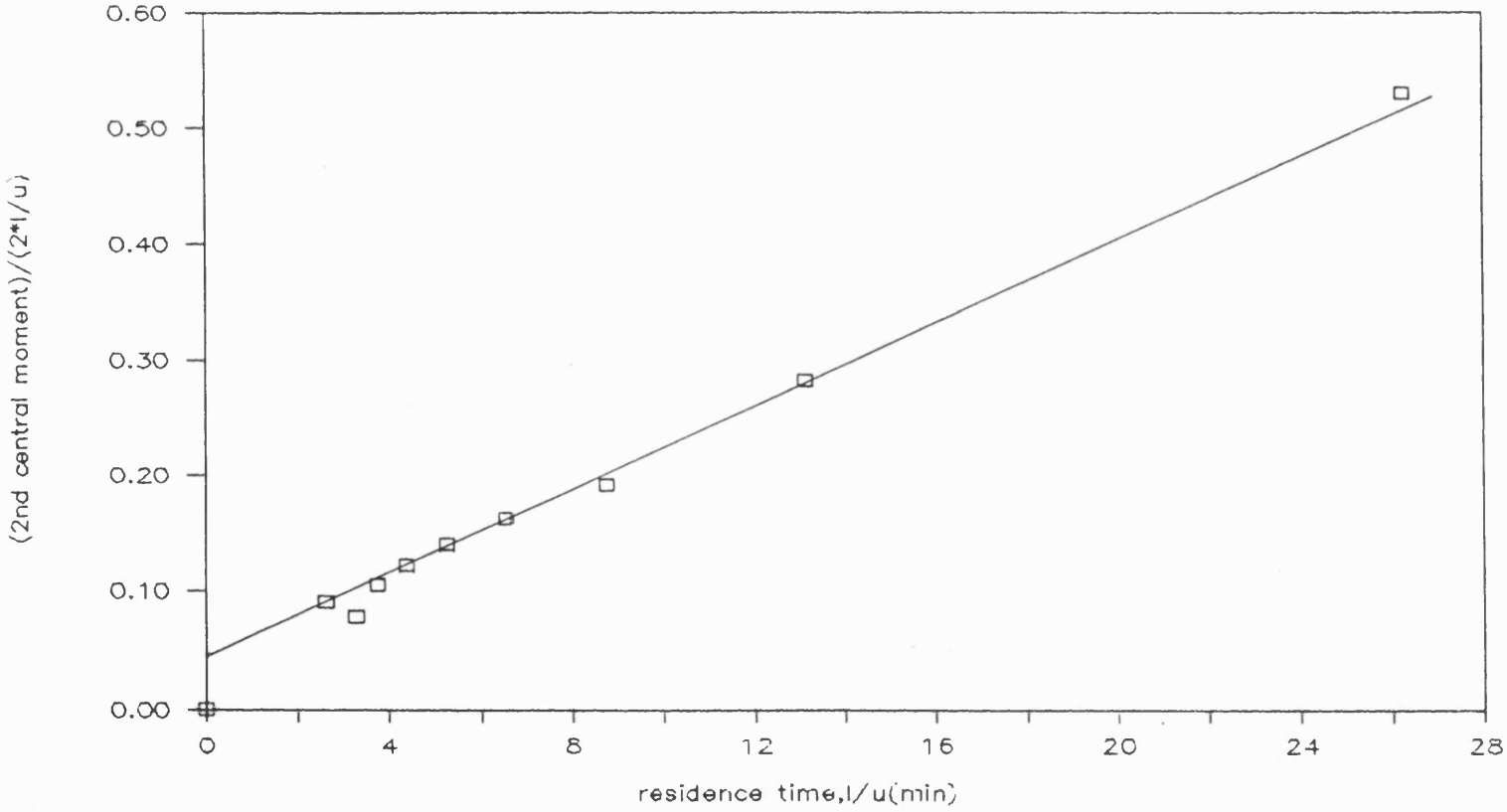

Fig. 4.15b. Ratio of second central moment to residence time vs. superficial residence time for pulse response of Lysozyme in Tris-SCN, pH 8.0 using modified Satorious column.

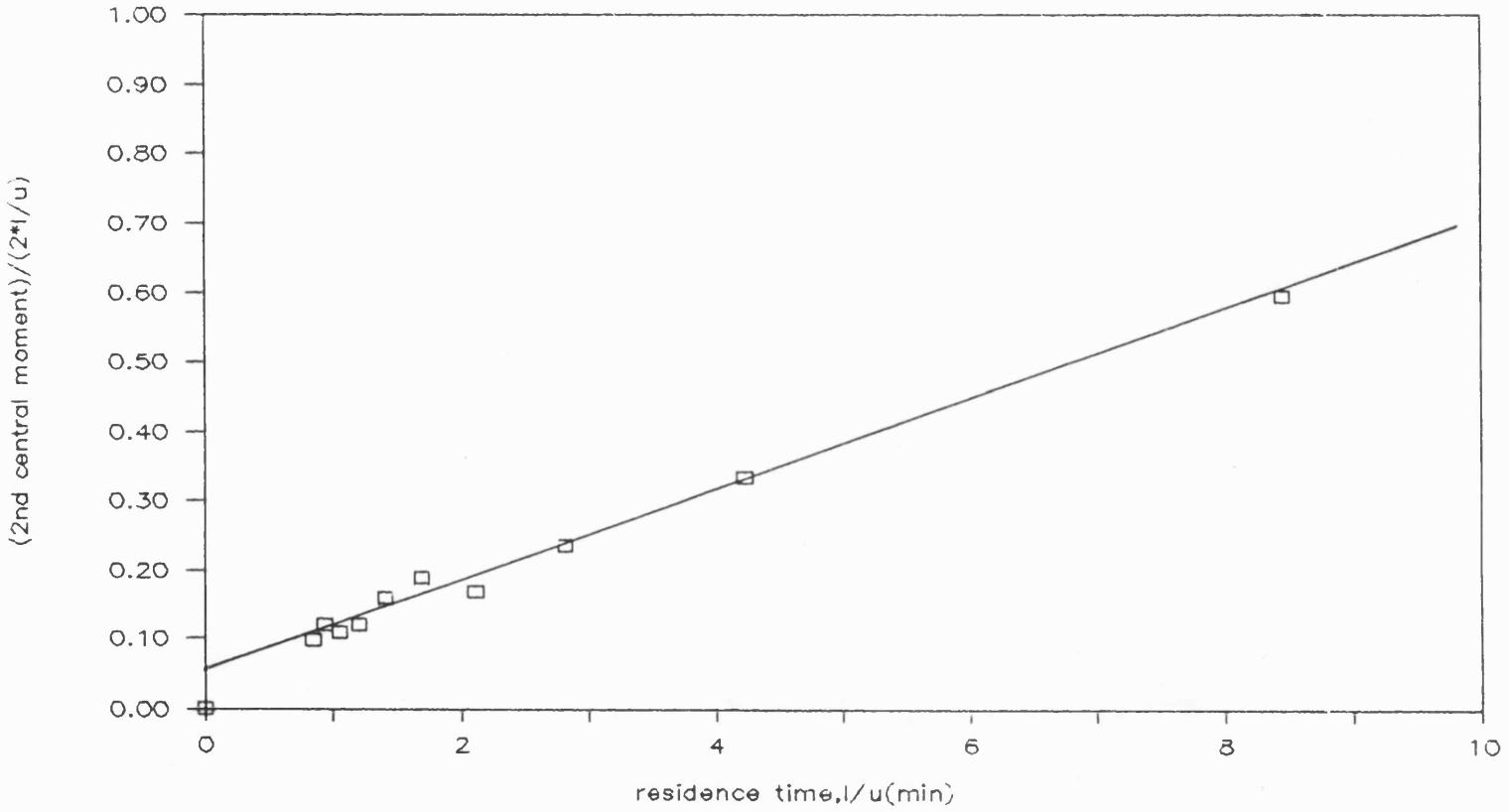

Fig. 4.16b. Ratio of 2nd central moment to residence time vs superficial residence time for the pulse response of BSA in Tris-SCN, pH 8.0 using micro-column.

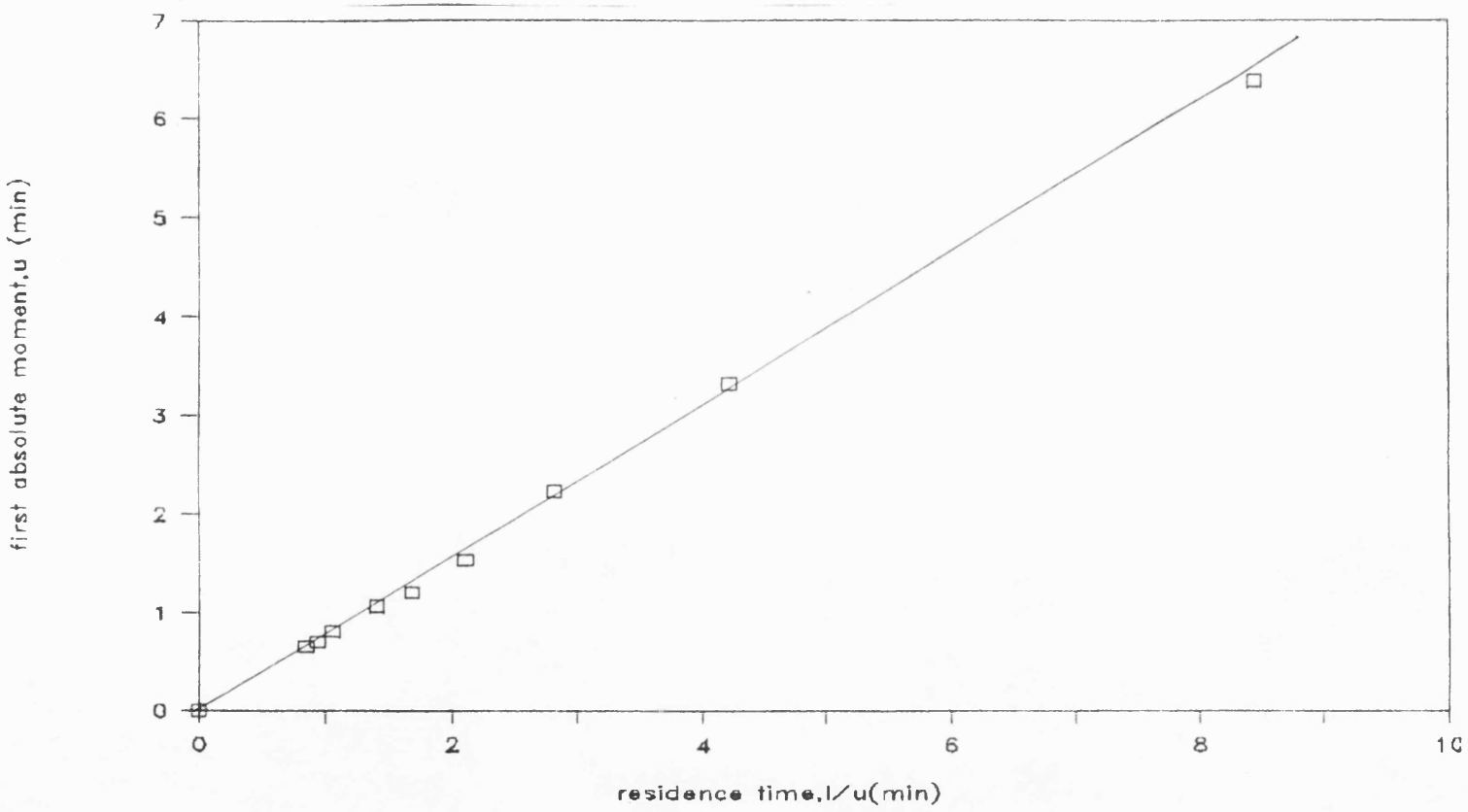

Fig. 4.16a. First absolute moment vs. superficial residence time for the pulse response of BSA in Tris-SCN, pH 8.0 using micro-column.

The Wilson-Geankoplis correlation is given by the equation

$$\varepsilon j_D = \frac{1.09}{Re_p}$$

or

$$\frac{2k\ R_h}{D_m} = 1.09\ Re_p^{1/3} Sc^{1/3}\ \varepsilon^{-1} = 1.09\ \left(\frac{2\rho_u R_h}{\mu}\right)^{1/3} \left(\frac{\mu}{\rho D_m}\right)^{1/3}\ \varepsilon^{-1} \qquad (4.41)$$

where ε = external bed voidage (-)

D_m = free solution solute diffusive coefficient (m^2/s)

j_D = Colburn and Chilton factor

R_h = hydraulic radius of the particle

ρ = fluid density

The sponge used in this experiment has irregular particle structures which are rather non-spherical. However, Haughey and Beveridge (1969) have pointed out that many granular materials used in packed beds deviate radically from the spherical shape. Thus non spherical particles tend to have regions rather than point contacts. This is even more so with relatively soft granular materials normally used in affinity chromatography which do compress to some extent under slight pressure. Since these systems have been modelled successfully by assuming spherical shape, it seems reasonable therefore that the same assumption with the sponge, with correction factor for non-sphericity may not be far fetched.

The shape factor is normally used to correct for non-sphericity. Here, the effective particle diameter or the hydraulic

diameter will be used too for the non-sphericity of the sponge particles.

The effective particle radius or hydraulic radius, R_h has been defined by Marrazzo *et al.* (1975) as

$$R_h = \frac{R\, d_t\, \epsilon}{3d_t(1-\epsilon) + 4R} \qquad (4.42)$$

for a column of diameter d_t packed with spherical particles of radius, R.

The estimation of the free solution diffusivity, D_m,is by the correlation due to Young *et al.* (1980) for the estimation of diffusion coefficients of proteins in free solution. The correlation is

$$D_m = 8.34 \times 10^{-15} \frac{T}{\mu M.Wt.^{1/3}} \ m^2/s \qquad (4.43)$$

where T = absolute temperature (K)

μ = solution viscosity (0.001 kg/ms)

M.Wt. = molecular weight of protein.

For BSA, HSA and lysozyme solutions, assuming that viscosity of dilute protein solutions is the same as that of water at the same temperature. The estimated free solution diffusion coefficients for BSA and lysozyme using equation (4.43) at 4°C and 20°C are shown in Table 4.7 below.

Table 4.7. Free Solution Diffusivity of HSA, BSA and lysozyme

TEMP (K)	PROTEIN	MOLECULAR WEIGHT	VISCOSITY μ (Kg/ms)	DIFFUSION COEFFICIENT D_m ($\times 10^{11} m^2/s$)
	Lysozyme	14,000		5.758
277	HSA	66,300	0.00167	3.433
	BSA	67,000		3.419
	Lysozyme	14,000		10.18
293	HSA	66,300	0.001	6.064
	BSA	67,000		6.039

(a) SARTORIUS COLUMN

From equation (4.42) the hydraulic radius, R_h is 3.538 x 10^{-5} m. Therefore the hydraulic diameter is 70.76 μm

At the temperature of 20°C (293K) the following values of k_f were estimated for BSA and lysozyme.

Table 4.8. External film mass transfer coefficient values

Sc = 16,559 TEMP = 293 K		PROTEIN: BSA a_v = specific particle surface area = $\frac{3(1-\varepsilon)}{R_h}$ $k' = ka_v$	
AXIAL VELOCITY, u, (m/s x 10^{-5})	PARTICLE REYNOLDS NUMBER Re_p(-)	MASS TRANSFER COEFFICIENT k($x10^{-6}$m/s)	MASS TRANSFER COEFFICIENT k'(s^{-1})
2.408	0.0017	3.489	0.055
3.612	0.0026	4.019	0.0637
4.816	0.0034	4.395	0.0697
6.020	0.0043	4.572	0.0754
7.224	0.0051	5.030	0.0798
8.428	0.0060	5.310	0.084
9.632	0.0068	5.536	0.088
10.836	0.0077	5.770	0.0915
12.04	0.0085	5.963	0.0946

Sc = 9823.18 TEMP. = 293K		PROTEIN: LYSOZYME $a_v = \frac{3(1-\varepsilon)}{R_h} = 1.5856 \times 10^4\ m^{-1}$	
AXIAL VELOCITY, u, (m/s x 10^{-5})	PARTICLE REYNOLDS NUMBER Re_p (-)	MASS TRANSFER COEFFICIENT k($x10^{-6}$m/s)	MASS TRANSFER COEFFICIENT k'(s^{-1})
2.408	0.0017	4.947	0.078
3.612	0.0026	5.700	0.090
4.816	0.0034	6.231	0.098
6.020	0.0043	6.738	0.107
7.224	0.0051	7.132	0.113
8.428	0.0060	7.528	0.119
9.632	0.0068	7.849	0.125
10.836	0.0077	8.181	0.130
12.040	0.0085	8.454	0.134

(b) MICRO COLUMN

For the micro column, at the temperature of 293 K the following estimated values of k were obtained. The calculated hydraulic radius was 2.089×10^{-5} m.

SC = 16,559
TEMP = 293K

PROTEIN: BSA

AXIAL VELOCITY, u, ($m/s \times 10^{-5}$)	PARTICLE REYNOLDS NUMBER Re_p (-)	MASS TRANSFER COEFFICIENT $k(\times 10^{-6} m/s)$
9.858	0.0021	7.135
19.716	0.0042	8.987
29.574	0.0063	10.286
39.432	0.0084	11.320
49.290	0.0105	12.194
59.148	0.0126	12.957
69.006	0.0147	13.639
78.864	0.0168	14.259
88.722	0.0189	14.830
98.580	0.021	13.359

SC = 9,823
TEMP = 293K

PROTEIN: LYSOZYME

AXIAL VELOCITY, u, ($m/s \times 10^{-5}$)	PARTICLE REYNOLDS NUMBER Re_p (-)	MASS TRANSFER COEFFICIENT $k(\times 10^{-6} m/s)$
9.859	0.0021	10.114
19.716	0.0042	12.740
29.574	0.0063	14.581
39.432	0.0084	16.047
49.290	0.0105	17.285
59.148	0.0126	18.335
69.006	0.0147	19.335
78.864	0.0168	20.214
88.722	0.0189	21.022
98.580	0.021	21.773

Table 4.9. Summary of Average Values of External Film Mass Transfer Coefficient

COLUMN	ADSORBATE	AVERAGE MASS TRANSFER COEFFICIENT k_{av}. ($\times 10^6$ m/s)
SARTORIUS	LYSOZYME	6.973
	BSA	4.918
MICRO-COLUMN	LYSOZYME	17.148
	BSA	12.097

(b) ESTIMATION OF THE INTERNAL POROSITY

The internal porosity or the internal voidage of the bed which was estimated from the slope of the first absolute moment, μ_1 vs ℓ/u (the superficial residence time) is shown in Table 4.10 below. The calculation was with the formula:

$$\text{Slope} = \epsilon + (1-\epsilon)\,\epsilon_i$$

where ϵ is the external voidage as calculated from the regression of the blue dextran points and ϵ_i = internal porosity.

Table 4.10. Sponge Bed Internal Porosity, ϵ_i

COLUMN	ADSORBATE	EXTERNAL VOIDAGE ϵ (-)	INTERNAL POROSITY ϵ_i (-)
SARTORIUS	BSA	0.813	0.326
	LYSOZYME		0.441
MICRO-COLUMN	BSA	0.721	0.346

(c) CALCULATION OF THE EFFECTIVE DIFFUSIVITY, De

Using the intercept of the graph of $\mu_2'/(2\frac{\ell}{u})$ vs ℓ/u the effective diffusion coefficient, De, was calculated from the relation

$$\text{Intercept} = \delta_f + \delta_D \quad .....$$

where δ_f and δ_D were as defined earlier. The value of δ_f was estimated using the correlated average value of mass transfer coefficient and the hydraulic radius. The subtraction of the δ_f value from the intercept, therefore yielded δ_D.

The De values were calculated from the relation

$$\delta_D = \frac{\varepsilon_i^2 \; R_h^2 \; (1-\varepsilon)}{15 D_e}$$

The results are shown in Table 4.11 below.

Table 4.11. Estimated Effective Diffusivity, De

COLUMN	ADSORBATE	INTERCEPT $\delta_f + \delta_D$ (sec)	δ_f (sec)	EFFECTIVE DIFFUSION COEFFICIENT De (m^2/s)
SARTORIUS	BSA	2.826	0.0095	2.117×10^{-13}
	LYSOZYME	2.0394	0.123	3.017×10^{-13}
MICRO	BSA	2.964	0.0019	2.9342×10^{-13}

(d) ESTIMATION OF AXIAL DISPERSION COEFFICIENT, D_L

The slope of the $\mu_2'/(2t)$ vs ℓ/u plot was used to calculate the axial dispersion coefficient, D_L from the relation:

$$\text{Slope} = \frac{D_L}{u} \left[(\varepsilon + (1-\varepsilon)\, \varepsilon_i)^2 \right] \times \frac{1}{\ell}$$

The slopes were determined by linear regression of the curves with linear regression coefficients of 0.99 using Figs. 4.14b, 4.15b and 4.20, and are shown in Table 4.12a below. The axial dispersion values and the peclet numbers at various axial velocities are shown in Table 4.12b.

Table 4.12a. Slopes from $\mu_2'/(2\ \ell/u)$ vs ℓ/u lines

COLUMN	PROTEIN	SLOPE
Sartorius	BSA	0.033
	LYSOZYME	0.035
MICRO	BSA	0.065

Table 4.12b. Estimated Values of Axial Diffusivity and Peclet Number.

(i) BSA

SARTORIUS COLUMN

SUPERFICIAL VELOCITY, u , ($\times 10^{-5}$ m/s)	AXIAL DIFFUSIVITY D_L ($\times 10^{9}$ m^2/s)
1.193	9.687
1.79	14.536
2.387	19.383
2.983	24.22
3.580	29.07
4.175	33.903
5.965	41.844
7.158	55.731
8.352	67.82
9.543	77.093
10.737	87.189
11.930	96.877

Peclet number = 23

(ii) LYSOZYME

SUPERFICIAL VELOCITY, u, ($\times 10^{-5}$ m/s)	AXIAL DIFFUSIVITY D_L ($\times 10^{9}$ m^2/s)
1.193	10.068
2.387	20.144
3.58	30.211
4.772	40.270
5.965	50.338
7.158	60.407
8.352	70.549
9.545	80.549
11.930	100.674

Peclet number, Pe = 22.3

(iii) BSA WITH MICRO-COLUMN

SUPERFICIAL VELOCITY, u, ($\times 10^{-5}$ m/s)	AXIAL DIFFUSIVITY D_L ($\times 10^{7}$ m^2/s)
9.859	4.794
19.716	9.587
29.574	14.38
39.432	19 .173
49.290	23.967
59.148	28.760
69.006	33.553
78.864	38.346
88.722	43.140
98.580	47.933

Peclet number, Pe = 10.28

4.4 DISCUSSION

(1) EQUILIBRIUM PARAMETERS

Favourable adsorption isotherms were obtained for the binding of lysozyme and human albumin in 0.05 M Tris-HCl/0.05 M NaCl buffer, pH 8.0 - to blue sponge. A good fit was obtained in the plots of the linearized adsorption isotherm equation - the resulting straight line from a c*/q* vs c* plot fitted by the method of linear regression gave regression coefficients of .99. This confirms that the adsorption equilibrium isotherm for the adsorption of lysozyme and human albumin can be described well by the Langmuir type adsorption isotherm.

The values of maximum equilibrium capacity of lysozyme differs from that of HSA (see Table 4.1). The average q_m value for HSA was higher than that of lysozyme. However, when measured on a molar basis this situation is reversed due to the smaller molecular weight of lysozyme. The values are 1.594×10^{-6} moles/g for lysozyme (M.Wt. = 14,000) and 4.03×10^{-7} moles/g for HSA (M.Wt. = 66,300).

The dissociation constant, k_d value for lysozyme was lower than that of HSA (Table 1). On a molar basis the values of 1.38×10^{-5} M for HSA and 1.857×10^{-5} for lysozyme are much closer than the values of 2 to 3 times suggested by the k_d values based on the basis of mg/ml.

Human albumin is known to bind very strongly to blue dye adsorbents and was thought to involve the bilirubin binding site of albumin (Leatherbarrow and Dean, 1980), rabbit, chicken and cattle albumins were found to bind much less strongly especially at pH 8.0

and above. The values of k_d obtained for the binding of lysozyme on blue-sponge seems therefore to suggest a strong binding strength.

The binding capacity of immobilized Cibacron blue 3FG-A and its binding strength depend on the nature of the matrix, ligand concentration and pH of buffer used for adsorption (Yang and Tsao, 1982). Binding capacity and the k_d values would vary therefore depending on the conditions of adsorption. At the adsorption conditions used in this study, Angal and Dean (1977) obtained k_d values ranging from 1.10×10^3 M^{-1} (or K_L=9.1×10^{-4} M) for cellulose-ligand concentration 3.2 μg dye/ml of packed gel - to 16.8×10^3 M^{-1} (or K_L = 2.136×10^{-5} M) for Cibacron Blue F3G-A sepharose CL 4B-ligand concentration (4 μg dye/ml of packed gel). The average k_L value for human albumin obtained in this study is 1.38×10^{-5} M. This is just below this range.

For lysozyme, the k_d value obtained was 1.86×10^{-6} M. This is somewhat higher than the value of 1.7×10^{-6} M obtained by Chase (1984a) with Cibacron Blue 3GA-Sepharose CL-6B. The difference may be due to differences in matrix and adsorption conditions used in the two studies. In this study the adsorption buffer pH was 8.0 while that used by Chase was 7.2, the same buffer, Tris, was used in both cases. The ligand concentrations for Chase's study is not known.

(2) KINETICS PARAMETERS

Figs. 4.8 and 4.9 show the kinetics curves obtained both experimentally and theoretically for the adsorption of lysozyme and

HSA on the blue sponge. A comparison of the theoretical and experimental curves shows a fairly good agreement initially, but a consistent difference at later times. Taking the deviation of the predicted curve from the actual (experimental) curve as given by the relation (actual - theoretical)/actual. Deviations of up to 13-15% were shown for HSA and Lysozyme theoretically predicted kinetics curves. This suggests, therefore, that the rate equation used to describe the transfer of materials from the solution into the blue sponge does not describe accurately the present system under study. The deviation for HSA was over a longer period of time than that for lysozyme.

The reason for the observed deviation of the experimental curves from the theoretical curve may be due to other kinetic mechanisms operating at later periods of adsorption. These mechanisms may include film mass transfer resistance or pore diffusion resistance. Either one or both of the above mechanisms may be in competition with the adsorption mechanism as the rate limiting step. It is, in fact, possible that the adsorption mechanism is not at all one of the rate-limiting steps. However, Chase (1984a) and Arnold et al. (1986) findings suggest that the adsorption step is the rate limiting step for the adsorption of BSA on Cibacron Blue-Sepharose-CLB and Reactive Blue Sepharose CL-4B/6B respectively. The former also obtained the same result for lysozyme adsorption on Sepharose CL6B and adsorption of β-galactosidase-silica adsorbents. The latter found that the k_1 measured for

BSA interacting with immobilized blue dye was three orders of magnitude smaller than rate constants of diffusion-controlled biological binding reactions in solution. The source of this slow binding of the protein to the immobilized ligand is not clear (Arnold et al., 1986).

The difference between this study and the work of the above authors may be due to matrix effect or possibly to the adsorption conditions. Chase carried out the adsorption with Tris-HCl buffer, pH 7.2 at 20°C; the adsorption buffer or pH was not stated by Arnold and co-workers.

However, the values for the rate constants, k_1 and k_2 for the forward and backward steps of the adsorptions of lysozyme and HSA onto the sponge obtained in this study will be useful in the initial simplified modelling of the affinity system under consideration.

The k_1 value for lysozyme was higher than that of HSA which is consistent with the lower molecular weight of the lysozyme molecules. However, the k_2 value for HSA was lower than that for lysozyme. This suggests a tighter binding of HSA to the immobilized dye though the k_d values suggested the opposite. Though the binding of HSA to immobilized Cibacron Blue may involve specific sites as mentioned earlier, the binding mechanism of lysozyme and other proteins such as interferons and blood coagulation factors is not known.

(3) BED AND TRANSPORT PARAMETERS

The normalised concentration profile of the step response shown in Figure 4.12 for different flow rates suggests an error estimate of some 10% at half the normalized concentration and somewhat higher and lower percentage at other concentrations of the stated value for all runs. For gas flow through packed beds, Urban and Gomezplata (1969) suggested that for all runs, a reasonable error estimate is 25% of the stated value of the dispersion coefficient. They used the non-porous axial dispersed plug flow model for their evaluation of the dispersion coefficients and pulse technique for the evaluation of the system moments.

Levenspiel (1979) used the criterion based on the dispersion number (1/Peclet number) for deviation of flow patterns from plug flow in chemical reactors. He showed that for small deviation from plug flow the dispersion number, $N_D(\frac{D_L}{u\ell})$ should be less than .01 but values of N_D higher than 0.01 indicate higher dispersion. Based on this, the dispersion obtained with sponge is rather high (N_D = 0.04 - 0.11).

The Peclet numbers obtained with the microcolumn show a significant difference from that for the Sartorius column (see Table 8 a,b) using BSA as the solute. This is consistent with observations by Langer et al. (1978) that dispersion in large diameter columns (or production scale columns) is smaller than those for smaller diameters (or laboratory scale columns). In addition, approximately 8-fold higher flow rates were used for the microcolumn (9.9 - 98.6 x 10^{-5} m/s) than for the Sartorious column (1.19 - 11.9 x 10^{-5} m/s), Fig. 4.17 shows that within the flow

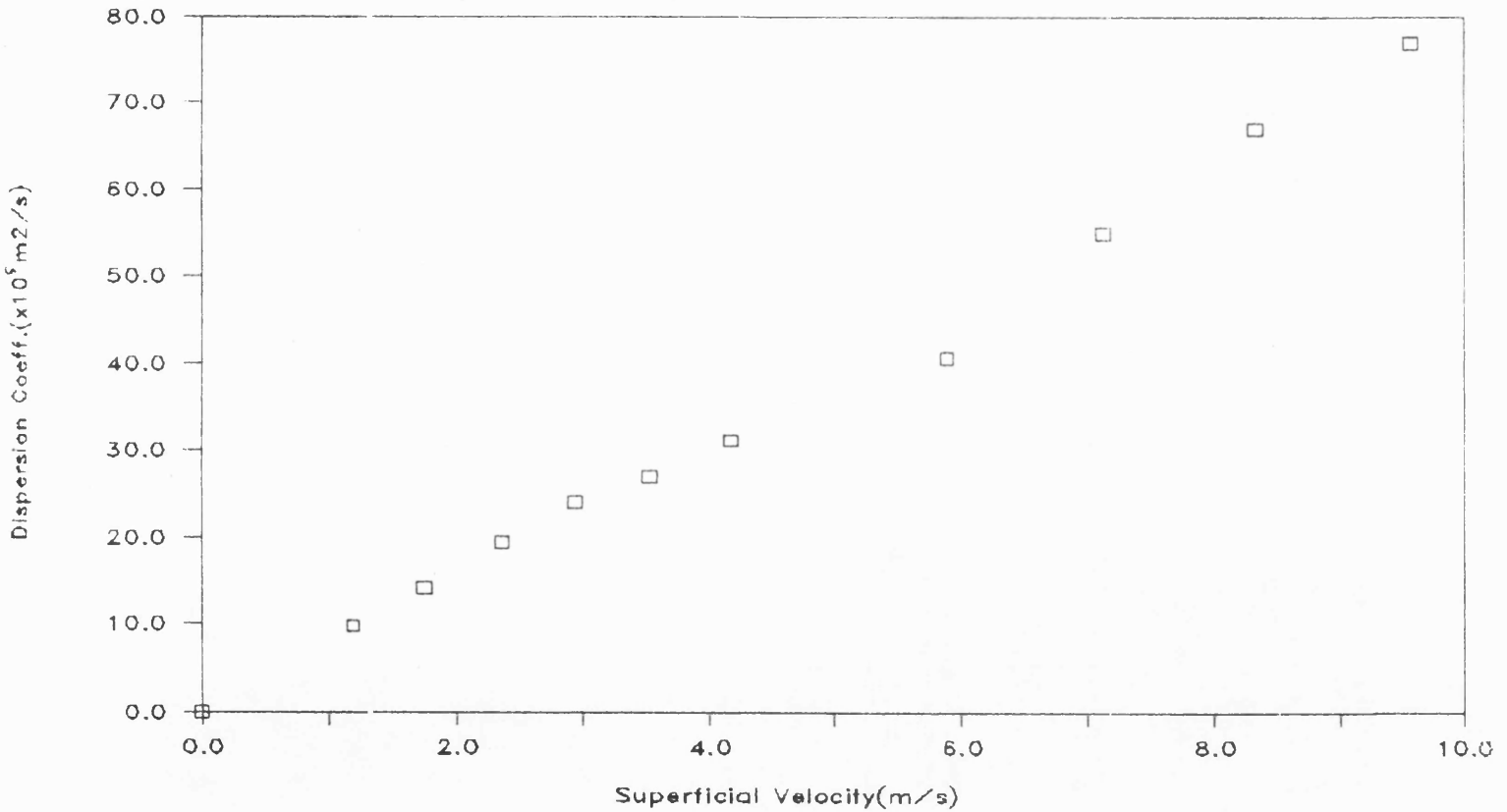

Fig. 4.17. Effect of flow rate on dispersion coefficient for BSA using Satorious Column.

rates considered, dispersion increased steadily with flow rates.

The effect of dispersion cannot therefore be discounted for the use of the sponge as a support matrix for affinity separation. The large dispersion may be due to the open and rather randomized structure of the sponge which results in fluid back mixing within the sponge voids. This is reflected in the tortuosity value as will be seen later.

Table 4.10 indicates that the external voidage of the sponge could be decreased by increasing the density of the sponge packing, ρ_s. For BSA, an increase of packing density (from x 0.191 in Sartorious column to 0.393 g dry wt/cm^3 in microcolumn) resulted in some 11% decrease in the external voidage. However, this may have been partly responsible for the increase in dispersion as shown in Tables 4.12b. The density of the sponge is quite low; 0.051 g dry wt/swollen volume (see appendix 1) but can be increased up to 0.25 g dry weight without substantial increase in hydraulic pressure drops. The decrease of voidage of the sponge with reasonble bed packing density is a way of increasing the productivity using a sponge column in terms of volume of bed. However, overcompression of the sponge may lead to increased pressure drop and possibly reduced capacity. For the same flow rate, the pressure difference beween the Sartorious column (ρ_s = 0.191) and the microcolumn (ρ_s = 0.393) was more than 2 bars. In addition. Tsou and Graham (1985) have found evidence which suggested that under column operations, reduced capacity could result if a bed has been highly compressed due to a restriction and loss of some of the protein exchange site. The adsorption system

they studied was ion exchange adsorption and desorption of BSA on DEAE-Sephadex-50.

In general, the solute penetration of the sponge structures, as evident in their average retention times, is in decreasing order of their molecular weights. The internal voidage values shown in Table 4.10 indicates that a greater fraction of the sponge structure is available to lysozyme than the higher molecular weight BSA. However, the difference between the fraction available to lysozyme and that for BSA is not as much as in Sepharose CL-4B, for example. Arnold et al. (1985) obtained internal voidage of 0.52 for BSA and 0.80 for myoglobin (M.Wt. = 17,500) on a column packed with Sepharose CL-4B as against 0.333 (average) for BSA and 0.441 for lysozyme obtained with the sponge. The reason may be due to the presence of larger fractions of large pores, that can be penetrated by both proteins in the sponge than in Sepharose CL-4B (bed voidage = 0.39).

Tortuosity of the sponge can be estimated by relation given by Marrazzo et al. (1975) namely

$$D_e = \frac{\varepsilon_i D_m}{\tau}$$

where τ = tortuosity of the sponge

ε = internal voidage

D_m = free solution diffusivity

and D_e = effective pore diffusivity.

The higher the tortuosity, the more difficult it is for the particles to diffuse through the pores due to uneven path or the

size of the diffusing molecule/pore size. Using the above equation and the diffusivities estimated using Young's correlation, Table 4.7, and the effective diffusivity value of Table 4.11 gives the following tortuosity values for lysozyme and BSA. For the Sartorious columns: Lysozyme (148.8) and BSA (93). For the microcolumn the tortuosity of the sponge using only BSA is 71.023. While there are no literature values for comparable systems with sponge, the tortuosity value is quite high. This is inconsistent with the large pores of sponge as indicated by Blue dextran penetration but shows that the sponge structure is unordered with random network. The latter is suported by the electron micrograph of the sponge.

If tortuosity is dependent only on the pore size, lysozyme would be expected to have a lower value than BSA. However, this is not the case as shown above, an indication of significant effect of the random network of the sponge on the tortuosity.

The sponge has been assumed to be made up of spherical particles but that may be an oversimplification. Cylindrical co-ordinates may describe better the solid dimensions of the sponge particles. In that case, some errors are inherent in the assumption of sphericity.

CHAPTER 5

MATHEMATICAL MODELLING

5. MATHEMATICAL MODELLING

5.1 THEORETICAL BACKGROUND

5.1.1 INTRODUCTION

It is important to develop a mathematical model which is useful in predicting the performance of the affinity systems based on the sponge matrix. Such a predictive model is necessary for the optimal design and scale-up of a successful laboratory operation. A successful theoretical model will usually be used to predict the performance or describe the adsorption behaviour of a given affinity system under varying sets of operating conditions.

As has been pointed out earlier, most affinity adsorption operations are carried out in fixed beds. The advantages of fixed bed operations include relative ease of scale-up from the bench scale operation and automation, fixed bed adsorption processes can be operated in elution development or frontal analysis mode (Yang and Tsao, 1982). The latter is usually used for preparative purposes and will be considered here. Models for design and operation of fixed bed adsorbers have been reviewed and investigated extensively by Vermeulen and Le Van (1984), Weber and Chakravorti (1974), Hiester and Vermeulen (1952), Vermeulen (1958) and several others. The theories of fixed-bed affinity adsorption is not as well developed as those treated by these workers.

Yang and Tsao (1982) have reviewed the fixed bed adsorption theories and their applications to affinity chromatography. They noted that the non-linear isotherm often resulting from affinity interactions make it difficult to apply these theories which are usually based on the assumption of a linear isotherm (often common

in adsorption systems involving gases) to affinity adsorption.

Developing a mathematical model for the description or prediction of adsorption dynamics in a column generally involves three main steps, namely,

(a) representation of the rate uptake associated with adsorption;

(b) differential mass balance on the adsorbate at a point in the column;

(c) description of the equilibrium behaviour for a particular adsorbate/adsorbent system.

These steps provide a model in the form of differential equations, often partial differential equations; they form the basis of the rate theories of chromatography. The usable form of the model requires integration of the differential equations comprising the model and appropriate boundary and initial conditions. A method for performing the required integration is also required.

The above general principles for developing a mathematical model for fixed bed affinity adsorption systems are illustrated in this work. The previous chapter provides steps (a) and (c) while appendices 2 tackle step (b). Section 5.1.3 will link all the steps together in a usable form which is integrated using the mathematical method described in the next section.

Ideally, the mathematical model obtained from the above steps for the description of an affinity adsorption process includes all the transport and adsorption resistances encountered

by a protein molecule during transfer from the fluid phase to the solid phase. These resistances are due to (i) bulk transport with axial dispersion, (ii) external film diffusion, (iii) pore diffusion, (iv) surface diffusion and (v) surface adsorption. The ideal model accounting for all these resistances is too complex for mathematical manipulations. In practice, therefore, some simplifying assumptions are made in order to reduce the mathematical complexity of a given model.

Simplified models are derived from two basic principles, namely,

(1) Conceptual depiction of adsorbent particles packed inside a bed.

(2) Assumption that the rate limiting step of the adsorption process is due to one or more of the above transfer resistances ((i) - (v)).

The simplest depiction of the adsorbent particles is that of non-porosity. This means that the adsorbate concentration is uniform throughout the packing. In a more complex depiction, the assumption of non-porosity is relaxed to account for the pores of the adsorbent particles; the adsorbent is now composed of macropores or/and micropores.

The general continuity equation for the adsorbate in a mobile phase for the non-porous model (see appendix 2) is

$$\frac{\partial c}{\partial t} = D_L \frac{\partial^2 c}{\partial x^2} - u \frac{\partial c}{\partial x} - \frac{R_a(c)}{\varepsilon} \qquad (5.I.1)$$

The variables in equation (5.I.1) have the meanings assigned to them in appendix 2 and $R_a(c)$ is the rate of uptake of adsorbate. $R_a(c)$ depends on whether (ii), (iv) or (v) is the rate limiting step. Expressions for $R_a(c)$ in a given limiting situation are given below.

Rate expression, $R_a(c)$	Rate controlling step
$k\, a_v(c - c_i)$	External film diffusion (ii)
$k_1\, c\, (q_m - q) - k_2 q$	Surface adsorption (v)
$- a\, D_e \left.\frac{\partial q}{\partial r}\right\|_{r=R}$	Surface diffusion (iv)

where c_i is concentration of adsorbate inside the particle. Other variables have their usual meanings.

Equation (5.I.1) and expression for $R_a(c)$ together with initial and boundary conditions and equilibrium relation form a mathematical model of the rate theory; further simplification of this model is possible usually by assumptions of:

(a) absence of axial dispersion;

(b) constant pattern behaviour of concentration distribution;

(c) simplified and empirical rate equations.

Assumption (a) is often valid for long particulate beds but are sometimes unsatisfactory for short bed packings. Also with an adsorbent based on a material such as the sponge with irregular internal structure and high voidage, the failure to take axial

dispersion into account may result in serious errors in the model. Assumption (b) presupposes that the shape of the concentration wave front becomes essentially time-independent after a certain distance from the entrance of the bed; this constant pattern assumption is mostly applicable to relatively long beds. Assumption (c) has been discussed in the last chapter; essentially, it presupposes that the solid matrix is homogeneous in both structure and concentration of adsorbate, which is usually represented by the average concentration within the particle. This model and all the simplifications possible plus the mathematical solutions of the models can be found in Yang and Tsao (1982). Some of the models belonging to this category used in affinity system and their simplifying assumptions and method of mathematical solutions are shown in Table 5.1.

In the porous particle model, adsorbent particles contain "macropores" or/and "micropores" and are surrounded by a boundary layer of film. The macropores are essentially large enough that diffusion in them is unhindered by the pore walls, while the micropores have radii comparable to the size of diffusing adsorbate so that diffusion is hindered by the pore walls. This conceptual view translates into the series resistance rate model shown schematically below

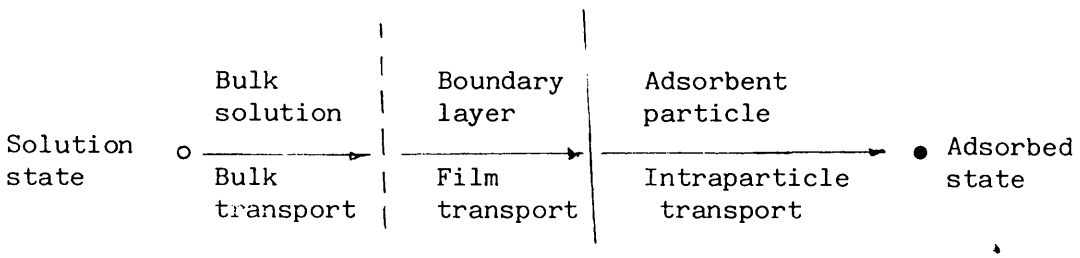

Table 5.1.

Model Equation: $\frac{\partial c}{\partial t} = D_L \frac{\partial^2 c}{\partial x^2} - u \frac{\partial c}{\partial x} - \frac{R_a(c)}{\varepsilon}$

Rate expression $R_a(c)$	Simplifying assumptions	System studied	Solution method	Reference
$k_{a_v}(c-c^*)$	(a) Constant pattern (b) Linear driving force (c) Neglect axial dispersion	Sepharose 4B-trypsin/ trypsin inhibitor	Finite difference (numerical)	Katoh et al. (1978)
$k_1 c(q_m-q) - k_2 q$	(a) Kinetic rate	(a) Sepharose 4B-anti-galactosidase	analytical	Chase (1984a)
	(b) Neglect axial dispersion	(b) Blue Sepharose 4B/ Lysozyme or BSA		
$k_{a_v}(c-c^*)$ and $k_1 c(q_m-q) - k_2 q$	(a) Linear driving (b) Kinetic rate expression		Orthogonal collocation (numerical)	This work

For a porous particle composed of uniform pore sizes, the particle material balance is usually of the general form (see appendix 2):

$$\frac{\partial q_a}{\partial t} = D_a \nabla^2 c_a - \frac{\partial c_a}{\partial t} \qquad (5.I.2)$$

rate expression $R_a(c)$ becomes:

$$R_a(c) = -a\, \varepsilon_a D_a \left.\frac{\partial c_a}{\partial r_a}\right|_{r_a=R} = k\, a\, (c-c^*) \qquad (5.I.3)$$

These equations combined with equation (5.I.1) with the appropriate boundary and initial conditions and appropriate equilibrium relation forms the mathematical model of rate theories. This is the film/particle or pore diffusion model.

For an adsorbent composed of micro- and macro-pores, in addition to equations (5.I.1) to (5.I.3) a microporous material balance gives:

$$\frac{\partial q_i}{\partial t} = D_i \frac{1}{r^2_i} \frac{\partial}{\partial r_i} \left(r^2_i \frac{\partial q_i}{\partial r_i}\right) \qquad (5.I.4)$$

This is an extremely complex model and is unusual in affinity adsorbents. However, it may represent the situation occurring in the sponge.

In general, it is better to use simplified models rather than the more complex models whenever possible. Simplified models do not only save computation time but also the experimentation time

needed to determine the extra parameters needed for complex models. They are often very good initial models for new adsorbent solid matrix.

With the blue sponge, there is some evidence that the adsorption step may be rate limiting in small particle systems (Sportsman et al., 1983). Also studies by Chase (1984a) and Arnold et al. (1986) have suggested that the adsorption step may be rate-limiting in the interaction of dye ligand adsorbents with certain proteins. Since the sponge structure is made up of the equivalent of very small particles, it seems reasonable to use the kinetic rate- expression type rate expression with the simplified non-porous model for blue sponge modelling as an initial step.

For an affinity separation separation process, the design of the adsorption stage will appear to be the most critical aspect of the overall design of the process (Chase, 1984b). The adsorption stage will therefore be considered here.

The solution method of orthogonal collocation (O.C.) which has been hardly tried for protein adsorption models will be used to integrate the model equations.

The next section deals with the fundamentals of the O.C. and its applications follow in the subsequent sections.

5.1.2 ORTHOGONAL COLLOCATION METHOD (O.C.M.)

The orthogonal collocation method is a solution method applicable to initial and boundary value differential equations (D.E.). It is a special form of the collocation method which is one of the several methods of weighted residuals (M.W.R.).

In the M.W.R., the unknown solution to a D.E. is expanded in a series. The approximating function is chosen by requiring the D.E. and boundary conditions to be satisfied in some specified approximate sense (Finlayson, 1969). The trial solution is substituted into the differential equation to define a residual. The constants of the approximating polynomial are chosen in such a way that the residual is forced to zero in some weighted-average sense. The weighted integrals of the residual are set equal to zero. The weighting functions can be chosen in several ways and each corresponds to a different criterion in M.W.Rs; for example, the method of moments, the least squares method and the collocation method (Finlayson, 1969). Finlayson (1969) has treated the applications of M.W.R. to boundary and initial value problems but the collocation method, especially orthogonal collocation, is of special interest here and illustrates the general principles of M.W.R.

In the orthogonal collocation method (O.C.M.) residuals are set equal to zero at the collocation points - the roots of the approximating polynomial. Since the introduction of O.CM. by Villadsen and Stewart (1967) and further refined by Villadsen (1970) and Finlayson (1972), it has proved to be superior to a number of alternative solution methods for differential equations. For example, for a given accuracy of solution, it has often been found to require less computation time than standard finite difference (F.D.) method. Ferguson and Finlayson (1970) found the O.C.M. to be more accurate than F.D. solutions which use 3 to 12 times as many spatial grid points. O.C.M. has been applied to

fixed-bed reactors (for example, Karanth and Hughes, 1974; Hanson, 1971) and to simulation of an adsorption column (Liapis and Rippin, 1978; Liapis and Litchfield, 1980; and Raghavan and Ruthven, 1983); Ramachandran (1974) has applied O.C.M. to solution of a model for the performance of a packed bed encapsulated enzyme reactor). However, O.C.M. is yet to become widely adopted as a standard technique. Its use in solution to model equations for fixed-bed adsorption of proteins is virtually non-existent. The method will therefore be treated in some detail here.

The orthogonal collocation method (O.C.M.) is an enhancement of the original collocation method (C.M.). The historic development of the collocation method has been reviewed by Villadsen and Stewart (1967). According to them, the principles of collocation method have been used for more than fifty years. The principles of C.M. for application to differential equations are briefly as follows:

Let Y(X) be an unknown function which satisfies a linear or non linear differential equation

$$F\ Y(X) = 0 \text{ in } V \tag{5.1}$$

and the linear or non-linear boundary condition

$$G\ Y(X) = 0 \text{ in } S \tag{5.2}$$

where X is the position vector and S is the boundary adjoining the domain V; F and G are the linear and non-linear differential operators, respectively.

Let the unknown Y(X) be approximated by a series expansion

$$Y_N = \sum_{i=1}^{N} a_i\ Y_i(x) \tag{5.3}$$

containing N undetermined coefficients; the coefficients are determined by applying equation (5.1) or equation (5.2) at each of the N selected points or collocation points. The trial function Y_N (or linear approximating operator) with N undetermined coefficients is the proposed approximation to Y. The approximating operator, Y_N, can be, for example, Taylor Series, Jacobi Series, Fourier Series or an interpolation procedure such as Lagrange interpolation. The coefficients a_i, are then determined so that Y_N satisfies equations (5.1) and (5.2) at each of the N selected points. Once the trial function Y_N is proposed, the error of approximation is indicated by the interior residual $F\ Y_N$ and the boundary residual $B\ Y_N$ which can be calculated by substitution of Y_N into equations (5.1) and (5.2) respectively. By making these residuals vanish at a set of well-chosen points, the error due to the approximation solution can be minimized.

There are three general classes of collocation methods, namely, interior, boundary and mixed (Villadsen and Stewart, 1967). The interior collocation requires that the trial function Y_N satisfies equation (5.2) identically, that is $G\ Y = 0$ on S; Y_N is then adjusted to satisfy equation (5.1) at N points in V. Conversely, the boundary collocation requires that the trial function Y_N satisfy equation (5.1) identically, that is $F\ Y_N = 0$ in V; Y_N is then adjusted to satisfy equation (5.2) at N points on S. The mixed collocation is employed if the trial function Y_N satisfies neither equation (5.1) nor equation (5.2) rigorously, that is, $F\ Y_N = 0$ and $B\ Y_N = 0$; Y_N is adjusted to satisfy equation (5.1) and (5.2) by selecting N points from both V and S (Fan et al., 1971).

The modifications of the original collocation method by Villadsen and Stewart (1967) and Villadsen (1970) for boundary value problems include; the choice of the trial functions from sets of orthogonal polynomials that satisfy the boundary conditions, with the roots to a higher order polynomial being selected as the collocation points. Thus the choice of collocation points is no longer arbitrary and the solutions can be derived not in terms of the coefficients in the trial function but in terms of the value of the solution at the collocation points.

The general procedure for the formulation of the orthogonal collocation method is as follows:

Define a polynomial, $P_N(x)$ of Nth order as,

$$P_N(x) = \sum_{i=0}^{N} a_i x^i \qquad (5.4)$$

whose coefficients, a_i are determined by the requirement that P_N is orthogonal on the interval domain $a < x < b$ to all polynomials of order less than N, relative to the weighting function $w(x) > 0$,

$$\int_a^b w(x)\, P_N(x)\, P_M(x)\, dx = 0 \qquad M = 0, 1, \ldots N-1 \qquad (5.5)$$

Equation (5.5) specifies each polynomial up to a multiplicative constant. The values assigned to that constant are usually determined by some requirement such as $P_N(1) = 1$. Commonly used orthogonal polynomials include Chebyshev, Legendre and Jacobi. Each polynomial of order $N > 0$ has N roots.

Additional properties for the trial function may be suggested by the problem under investigation. These are illustrated

by the continuity equation obtained by transient material balance for the adsorption of an adsorbate on spherical particles in a packed bed.

For the bulk liquid protein concentration, the continuity equation is in general,

$$\epsilon \frac{\partial c}{\partial t} = D_L \frac{\partial^2 c}{\partial x^2} - u_o \frac{\partial c}{\partial x} - R(c) \qquad (5.6)$$

where ϵ = bed void volume

c = adsorbate concentration

u_o = fluid velocity

D_L = axial dispersion coefficient

x = axial coordinate

$R(C)$ = rate term.

Equation (5.6) has no special symmetric properties; therefore, polynomials are needed that are orthogonal on (0,1) interval and which possess both even and odd powers of x. In this case the typical trial function is (Finlayson, 1980):

$$c(x,t) = a(t) + b(t)x + x(1-x) \sum_{i=1}^{N} a_i(t) P_{i-1}(x) \qquad (5.7)$$

The orthogonal polynomials of equation (5.7) are constructed using the orthogonality condition

$$\int_0^1 w(x) P_N(x) P_M(x)\, dx = C_{(N)}\ \delta_{NM} \quad M = 1, \ldots N-1$$

Where δ_{NM} is Kronecker delta;

$$\left.\begin{aligned}\delta_{NM} &= 0\\ &= 1\end{aligned}\right\}\begin{aligned}N &\neq M\\ N &= M\end{aligned}$$

$C_{(N)}$ is a constant.

The polynomials satisfying equation (5.5) with w(x) = 1 are shifted Legendre polynomials.

For the particle protein concentration, the continuity equation is of the general form:

$$D_e \nabla^2 c_p - R_p(c_p) = \epsilon_i \frac{\partial c_p}{\partial t} \qquad (5.8)$$

which is symmetric about the centre of the particles in which solution is sought on the domain $0 < r < 1$.

where De = effective particle diffusivity

c_p = pore adsorbate concentration

$R_p(c_p)$ = rate expression for particle/bulk liquid transfer

ϵ_i = internal voidage

∇ = differential operator

t = time

r = radial co-ordinate

Because of central symmetry, the solution is a function of only even powers of x and excludes all the odd powers. In this case, orthogonal polynomials are constructed which are functions of x^2 only. One choice is (Finlayson, 1980):

$$c(x^2) = c(1) + (1-x^2) \sum_{i=1}^{N} a_i(t)\, P_{i-1}(x^2) \qquad (5.9)$$

the orthogonal polynomials of equation (5.9) are constructed using the general orthogonal condition;

$$\int_0^1 w(x^2)P_N(x^2)P_M(x^2)x^{z-1}dx = C_{(N)}\,\delta_{NM} \qquad M = 1, \ldots N-1 \tag{5.10a}$$

where z = 1, 2, 3 for planar, cylindrical or spherical geometry respectively. $w(x^2) = (1-x^2)$, 1 or $(1-x^2)^{-\frac{1}{2}}$ depending on whether the required approximating polynomial is Jacobi, Legendre or Chebycheff polynomials respectively.

For spherical particles with Jacobi approximating polynomials, equation (5.10a) becomes

$$\int_0^1 (1-x^2)P_N(x^2)P_M(x^2)x^2 = C_{(N)}\delta_{NM}, \; M = 1,\ldots. N-1 \tag{5.10}$$

The first coefficient of each polynomial is usually taken as one, so that the choice of the weighting function completely determines the polynomial, and hence the trial function and collocation points (Finlayson, 1980).

The substitution of the trial functions into the differential equation to form the residual, which is set to zero at the N collocation points, x_j is the next step. These are roots to the Nth order polynomial ($P_N(x)$ or $P_N(x^2) = 0$ at x_j. This provides N equations to solve for the N coefficients a_i. However, it is simpler for computer coding if the resulting equations are written in terms of the solution at the ordinate $y(x_j)$ rather than a_i (This

is one of the refinements of C.M. by Villadsen and Stewart, 1967).

(i) Non Symmetric Equation

For equation (5.6) whose solution can be approximated by the trial function of equation (5.7); since $p_{i-1}(x)$ is a polynomial of degree N-1 in x, the trial function is a polynomial of degree N in x. Equation (5.7) can be reformulated in terms of the ordinates as:

$$c(x,t) = \sum_{i=1}^{N+2} d_i(t)\, x^{i-1} \tag{5.11a}$$

and when evaluated at collocation points, x_j, is

$$c(x_j,t) = \sum_{i=1}^{N+2} d_i(t)\, x_j^{i-1} \tag{5.11b}$$

For substitution into equation (5.6) which is a second order partial differential equation, the first and second derivatives of (5.11b) are required and are:

$$\frac{\partial c}{\partial t}(x,t)\Big|_{x_j} = \frac{dc_j}{dt} \tag{5.12}$$

$$\frac{\partial c}{\partial x}(x,t)\Big|_{x_j} = \sum_{i=1}^{N+2} d_i(t)(i-1)x_j^{i-2} \tag{5.13}$$

$$\nabla^2 c(x,t)\Big|_{x_j} = \sum_{i=1}^{N+2} d_i(t)(i-1)(i-2)x_j^{i-3} \tag{5.14}$$

The roots of the polynomials are between 0 and 1. The collocation points are then $x_1 = 0.0$, x_2 ....., x_{N+1} are the interior roots, and $x_{N+2} = 1.0$ as shown in Fig. 5.1

Fig. 5.1. Location of collocation points for N=3 in Non-Symmetric systems.

In Fig. 5.1 the two boundary conditions at x = 0 and x = 1 provide two additional collocation points giving a total of N + 2 collocation points. This is the mixed collocation method (Villadsen and Stewart, 1967).

Equations (5.11b), (5.13) and (5.14) can be written in matrix notation as

$$\bar{c} = \bar{Q}\,\bar{d} \; ; \quad \frac{\bar{dc}}{dx} = \bar{C}\,\bar{d} \; ; \quad \frac{\overline{d^2 c}}{dx^2} = \bar{D}\,\bar{d} \qquad (5.15)$$

where

$$Q_{ji} = x_j^{i-1}; \quad C_{ji} = (i-1)x_j^{i-2} \; ; \; D_{ji} = (i-1)(i-2)x_j^{i-3} \qquad (5.16)$$

and $\bar{Q}$, $\bar{C}$ and $\bar{D}$ are N+2 x N+2 matrices. Solving for $\bar{d}$, the first derivatives and Laplacian can be re-written as

$$\frac{\bar{dc}}{dx} = \bar{C}\,\bar{Q}^{-1}\bar{c} \equiv \bar{A}\bar{c} \; ; \quad \overline{\nabla^2 c} = \bar{D}\,\bar{Q}^{-1} \equiv \bar{B}\,\bar{c} \qquad (5.17)$$

Thus the derivatives at any collocation point are expressed in terms of the values of the function at all collocation points. The orthogonal collocation method applied to the dimensionless form of equation (5.6), (see appendix 4) gives

$$\frac{dc_j}{d\theta} = \frac{1}{Pe} \sum_{i=1}^{N+2} B_{ji} c_i - \sum_{i=1}^{N+2} A_{ji} c_j - R(c_j) \qquad (5.18)$$

Thus the orthogonal collocation reduces the parabolic P.D.E. to a system of O.D.E.'s.

(ii) Symmetrical Equation

The derivation of the collocation matrices A and B for the symmetric system is similar to that of the non-symmetric system. Briefly, the trial function, equation (5.9) is re-written in terms of the ordinates at collocation points as

$$c(x_j^2) = \sum_{i=1}^{N+1} x_j^{2i-2} d_i(t) \qquad (5.19)$$

The first derivative and the Laplacian are respectively:

$$\frac{dc}{dx}(x_j^2) = \sum_{i=1}^{N+1} x_j^{2i-3} (2i-2) d_i(t) \qquad (5.20)$$

$$\nabla^2 c(x_j^2) = \sum_{i=1}^{N+1} \nabla^2 (x^{2i-2}) \Big|_{x_j} d(t) \qquad (5.21)$$

and in matrix notation are ($\bar{Q}$, $\bar{C}$, $\bar{D}$ are N+1 x N+1 matrices):

$$\bar{c} = \bar{Q}\,\bar{d}\ ; \quad \overline{\frac{dc}{dx}} = \bar{C}\,\bar{d}\ ; \qquad \overline{\nabla^2 c} = \bar{D}\,\bar{d} \tag{5.22}$$

$$Q_{ji} = x_j^{2i-2}\ ;\ C_{ji} = (2i-2)x_j^{2i-3};\ D_{ji} = \nabla^2(x^{2i-2})x_j \tag{5.23}$$

Solving for d gives

$$\overline{\frac{dc}{dx}} = \bar{C}\,\bar{Q}^{-1}c \equiv \bar{A}\,\bar{c}\ ;\ \overline{\nabla^2}\,c = \bar{D}\,Q^{-1}\bar{c} \equiv \bar{B}\,\bar{c} \tag{5.24}$$

The roots of the polynomials are between zero and 1. The collocation points are then x_1....., x_N are interior roots, and $x_{N+1} = 1.0$ as shown in Fig. 5.2.

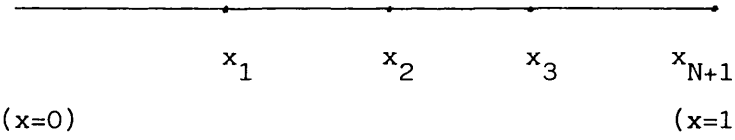

Fig. 5.2. Location of collocation points for N = 3 in Symmetric problems.

This is the interior collocation method (Villadsen and Stewart, 1967). The orthogonal collocation applied to equation (5.8) gives:

$$\varepsilon_i \frac{dc_{pj}}{dt} = D_e \sum_{i=1}^{N+1} \bar{B}_{ji} - R_p(c_{pj}) \tag{5.25}$$

Like in the non-symmetrical system the P.D.E. is reduced to a system of O.D.E.'s

The system of O.D.E.'s in equations (5.18) and (5.25) are then solved with standard numerical integration methods for O.D.E.'s such as Runge-Kutta or Euler methods with appropriate initial conditions.

To use the collocation method, some constants such as A and B and the roots of chosen approximating polynomials are needed. The details of the computation of these constants are shown in appendix 5 but are discussed in brief below.

5.1.2.1 COMPUTATIONAL SCHEME FOR COLLOCATION CONSTANTS

Most of the applications of the orthogonal collocation methods (O.C.M.) to solutions of initial value and boundary value differential equations use collocation at the zeros of Jacobi-polynomials (Michelsen and Villadsen, 1972).

In general, the following procedure is adopted for computing collocation constants.

(1) Explicit expression for orthogonal polynomials

$$P_N^{(\alpha,\beta)}(x) = P_N(x)$$

which can be represented as power series:

$$P_N^{(\alpha,\beta)}(x) = \sum_{i=0}^{N} (-1)^{N-i} a_i x^i$$

where $\alpha = \beta = 0$ for Legendre polynomial.

$\alpha = 1$; $\beta = 0$ for Jacobi polynomial

$a_0 = 1$ and the remaining N coefficients can be found directly from the orthogonality property

$$\int_0^1 x^{\beta} (1-x)^{\alpha} \; P_M(x) \; P_N(x) \; dx = 0 \qquad M = 0, 1 \ldots., N-1$$

$w(x)$

(2) zeros x of $P_N(x)$

(3) Discretization matrices A and B for the first derivatize and Laplacian at the collocation points x.

The coefficients of an orthogonal polynomial $P_N(x)$, which is normalized such that the coefficient of x^0 is $(-1)^n$, are most conveniently found by simple recurrence formula (Villadsen, 1980):

For the polynomial

$$P_N(x) = a_N x^N - a_{N-1} x^{N-1} + a_{N-2} x^{N-2} - \ldots + (-1)^N \tag{5.26}$$

$$a_i = \frac{N-i+1}{i} \qquad \frac{N+i+\alpha+\beta}{i+\beta} \qquad a_{i-1} \tag{5.27}$$

with $a_0 \equiv 1$ and i = 1, 2, ...N and α and β are both greater than -1.0.

However, the constants of primary interest are the zeros $\bar{x}$, and the collocation matrics, $\bar{A}$ and $\bar{B}$.

The algorithm for the construction of A and B matrices for symmetric systems has been given by Villadsen and Stewart (1967). The algorithm for the construction of A and B matrices for non-symmetrical systems are discussed in appendix 5 with a computer program written in Fortran and in double precision. The

calculated constants were compared with those given by Finlayson (1972) for their validity. The general procedure was to form matrices A and B from the inverted matrix of Q (Q^{-1}) according to equations (5.15) to (5.17). The matrix Q^{-1} is premultiplied by matrices containing first or second derivatives of the monomials x^K at x_i in the ith row to give A and B.

Michelsen and Villadsen (1972) have discussed an alternative method for calculating the A and B matrices. This method is based on Lagrange interpolation polynomials and involves neither the matrix inversion nor the explicit expression of the power series representation of the polynomials.

This method is discussed fully in appendix 5 but is discussed briefly here.

For the non-symmetrical problem the Lagrange interpolation polynomial is given by the expression

$$P_{N+2}(x) = (x-x_0)(x-x_1) \ldots\ldots (x-x_N)(x-x_{N+1})$$

$$= \prod_{0}^{N+1} (x-x_i) = (x-x_0)(x-x_{N+1})P_N(x) \qquad (5.28)$$

where x_i are the interpolation points which in this case will be the same as the collocation points.

The Lagrange interpolation formula for the function Y can be expressed in terms of the ordinates y_i at the selected interpolation points x_i as:

$$Y(x) = \sum_{i=0}^{N+1} \ell_i(x) y_i \qquad (5.29)$$

where

$$\ell_i(x) = \frac{1}{x-x_i} \frac{P_{N+2}(x)}{P^{(1)}_{N+2}(x_i)}$$

$P_{N+2}(x)$ is called the node polynomial while $\ell_i(x)$ are the Lagrange polynomials.

The first and second derivatives at the interpolation points, $x = x_j$ are:

$$Y^{(1)}(x_j) = \left(\frac{dy}{dz}\right)\Big|_{x=x_j} = \sum_{i=0}^{N+1} \ell_i^{(1)}(x_j) y_i = \sum_{i=0}^{N+1} A_{ji} y_i \qquad (5.30)$$

$$Y^{(2)}(x_j) = \sum_{i=0}^{N+1} \ell_i^{(2)}(x_j) y_i = \sum_{i=0}^{N+1} B_{ji} y_i \qquad (5.31)$$

Superscripts (1) and (2) denote first and second derivatives respectively.

Hence the A and B matrices are obtained by differentiation of the Lagrange polynomials $\ell_i(x)$. Appendix 5 shows the procedure for computing collocation constants using this method. As before, the validity of this method was ascertained using published data.

5.1.3 FORMULATION OF THE NON-POROUS PARTICLE MODEL

The non-porous particle model is based on the following assumptions:

(i) Axial dispersion of fluid is significant.

(ii) Radial dispersion of fluid is negligible.

(iii) Adsorbent concentration of adsorbate is uniform in the packing, that is, the diffusivity of adsorbate within the particle is very large.

(iv) The adsorption step is rate-limiting or at least, competes with other mechanisms of mass transfer as the rate-limiting step.

(v) The linear fluid flow rate is constant.

(vi) Isothermal adsorption

(vii) Average constant axial dispersion coefficient.

The model is developed for the adsorption reaction represented by the 2nd order/1st order reversible reaction equation.

$$A + B \underset{k_2}{\overset{k_1}{\rightleftharpoons}} AB \qquad (5.32)$$

where A = absorbate concentration left in solution

B = ligand binding site

AB = amount of affinity complex of ligand and adsorbate

k_1 = forward rate constant

k_2 = backward rate constant

$k_2/k_1 = k_d$ = dissociation constants

It has been shown in the last chapter that the rate of mass transfer of the adsorbate from the solution to the solid phase based on the interaction described by equation (5.32) is given by

$$\frac{\rho_s}{\epsilon} \frac{dq_w}{dt} = k_1.c.(q_m - q) - k_2 q \qquad (5.33a)$$

or

$$\frac{dq_b}{dt} = k_1 \cdot c \cdot (q_m - q) - k_2 q \qquad (5.33b)$$

where ρ_s is adsorbent packing density (kg/m^3)

q_w is solid phase concentration (kg/kg)

q_b is solid phase concentration (kg/m^3 of bed)

q_m is maximum solid phase concentration of adsorbate

c is liquid phase concentration of adsorbate.

With the assumptions stated earlier, the transient material balance equations for the packed bed of sponge are as follows (see appendices 2 and 4)

$$\frac{\partial c}{\partial t} = D_L \frac{\partial^2 c}{\partial x^2} - u \frac{\partial c}{\partial x} - \frac{1}{\epsilon} \frac{\partial q}{\partial t} \qquad (5.34a)$$

$$\frac{dq}{dt} = k_1 \cdot c \cdot (q_m - q) - k_2 q \qquad (5.35b)$$

with (a) boundary conditions

$$D_L \frac{dc}{dx} = u (c_0^+ - c_0^-) \quad \text{at } x = 0 \qquad (5.36a)$$

$$\frac{d\theta}{dx} = 0 \quad \text{at } x = \ell \qquad (5.37a)$$

and (b) initial conditions

$$q = 0; \quad c = 0 \quad \text{at } t = 0 \qquad (5.38a)$$

The boundary conditions (see derivation in appendix 4) are the Danckwerts (1953) type.

It is usually more convenient to re-write equations (5.34a) to (5.38a) in dimensionless forms as shown below (see appendix 4). We define the dimensionless variables:

$$\bar{c} = \frac{c}{c_o} \; ; \quad \bar{q} = q/q_m \; ; \quad z = x/\ell \; ; \quad \theta = \frac{ut}{\ell} \; ; \quad P_e = u\ell/D_L ;$$

$$k_A = k_1 . c_o . \ell/u ; \quad k_B = k_2 . \ell/u \; , \quad \beta = q_m/c_o$$

where ℓ is the total length of the bed

c_o is the initial adsorbate concentration

The dimensionless form of equations (5.34a) to (5.38a) are as follows:

$$\frac{\partial \bar{c}}{\partial \theta} = \frac{1}{Pe} \frac{\partial^2 \bar{c}}{\partial z^2} - \frac{\partial \bar{c}}{\partial z} - \frac{\beta}{\epsilon} \left[k_A \bar{c} (1-\bar{q}) - k_B \bar{q} \right] \qquad (5.34)$$

$$\frac{d\bar{q}}{d\theta} = k_A \bar{c} (1-\bar{q}) - k_B \bar{q} \qquad (5.35)$$

$$\frac{d\bar{c}}{dz} = Pe (\bar{c} - 1) \qquad \text{at } z = 0 \qquad (5.36)$$

$$\frac{d\bar{c}}{dz} = 0 \qquad \text{at } z = 1 \qquad (5.37)$$

$$\bar{q} = 0; \quad \bar{c} = 0 \qquad \text{at } \theta = 0 \qquad (5.38)$$

It should be noted that the rate expression in this non-porous model is a lumped parameter one. The rate constants k_1 and k_2 represent not only the effect of adsorption but also those of other mass transfer resistances (Chase, 1984a).

The solution of equations (5.34) to (5.38) give the complete description of the adsorption process in the affinity blue sponge.

Equations (5.34) to (5.38) expressed in orthogonal collocation formulation (see appendix 4) at collocation points z_j are:

$$\frac{dc_j}{d\theta} = \frac{1}{Pe} \sum_{i=1}^{m} B_{ji} c_i - \sum_{i=1}^{m} A_{ji} c_i - \beta/\varepsilon \left[k_A c_j (1-\bar{q}_j) - k_B q_j \right] \qquad (5.39)$$

$$\frac{dq_j}{d\theta} = k_A c_j (1-q_j) - k_B q_j \qquad (5.40)$$

at $z = 0$

$$\sum_{i=1}^{m} A_{1i} c_i = Pe\,(c_1 - 1) \qquad (5.41)$$

at $z = z_m = 1$

$$\sum_{i=1}^{m} A_{mi} c_i = 0 \qquad (5.42)$$

where N = number of interior collocation points

$m = N + 2$

The expansion of equation (5.39) and the simplification of equations (5.41) and (5.42) results in the following equations

$$\frac{dc_j}{d\theta} = \sum_{i=2}^{m-1} (M1B_{ji}-A_{ji})c_i + (M1B_{ji}-A_{j1})c_1 + (M1B_{jm}-A_{jm})c_m$$

$$- BT\,[K_A c_j(1-q_j) - K_B q_j] \qquad (5.43)$$

$$\frac{dq_j}{d\theta} = K_A c_j(1-q_j) - K_B q_j; \qquad (5.44)$$

$$c_1 = - Pe - \sum_{i=2}^{M-1} \left(A_{1j} - \frac{A_{mi}A_{1m}}{A_{mm}}\right)c_i \qquad (5.45)$$

$$c_m = - \sum_{i=1}^{m-1} \frac{A_{mi}}{A_{mm}} c_i \qquad (5.46)$$

where $BT = \beta/\varepsilon$; $M1 = 1/Pe$.

The simulation of the breakthrough curve was based on the $(m-1) \times (m-1)$ or $N \times N$ simultaneous O.D.E.'s using the 4th order fixed step Runge-Kutta.

5.2 PREDICTION OF BREAKTHROUGH CURVE (B.T.C.) USING COMPUTER SIMULATION

The prediction of B.T.C. based on the non-porous model of equations (5.43) to (5.46) by computer simulation is discussed in detail in appendix 6. The computer simulation was carried out with a dynamic simulation package for ordinary differential equations (O.D.E.) - ISIM. The ISIM has its own built-in numerical

integration system. The ISIM integration routine is based on 2nd order, 4th order fixed step Runge-Kutta (R-K) method, and 5th order, variable step (Sarafyan method) R-K. The 4th order fixed step R-K was used for the simulations reported here. The details of use of the ISIM interactive simulator is available in the ISIM manual (School Chem. Eng., University of Bath).

The general flow sheet for the simulations based on equations (5.43) to (5.46) is shown in Fig. 5.3. The constants of the model equation are initialised in ISIM constant statements. After the calculation of model variables and dimensionless parameters, the fluid phase and solid phase adsorbate concentrations are set to their initial values determined by the initial conditions, equation (5.38). Computation is started at the top of the column (boundary condition, $z = 0$) which is the first collocation point. First, the boundary fluid phase concentration, c_1 is calculated using equation (5.45). Subsequently, at each collocation point (from 2nd to N+1th collocation points), the liquid phase concentration followed by the solid phase concentration using the initial values of adsorbate concentration at the given collocation point and other points are computed. This is achieved by computing the right hand side (R.H.S) of equation (5.43) followed by integration and then the computation of the R.H.S. of equation (5.44) followed by integration. Finally, at the bed outlet, the adsorbate concentration in liquid phase, c_m is computed according to equation (5.46). The time is increased by the chosen integration step and further computation is started at the top of the bed (boundary condition, $z = 0$) and a repeat of previous

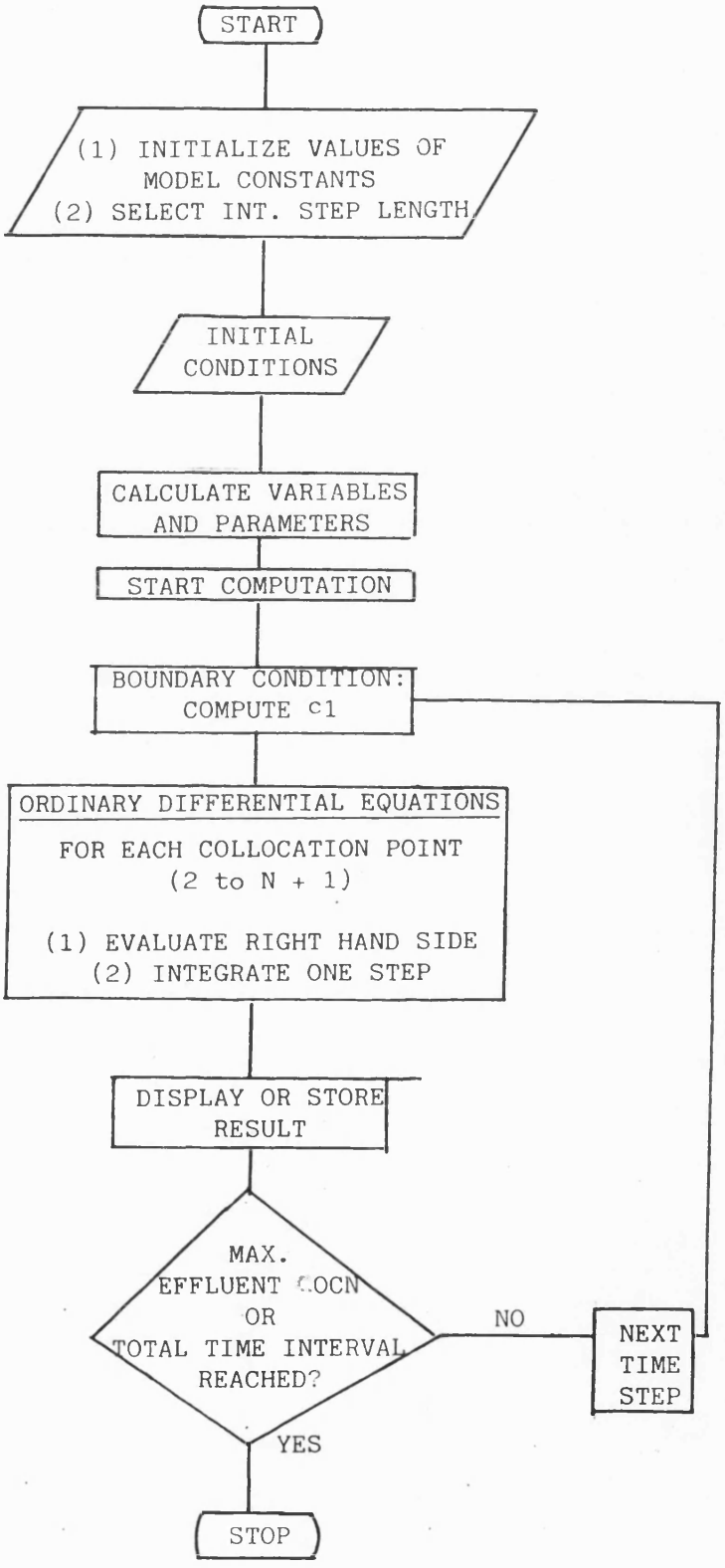

Fig. 5.3. General Flowsheet for Computer Simulation of Breakthrough Curve using ISIM.

processes is carried out. Each repeat process utilizes the previously computed values of the liquid and solid phase concentrations of the adsorbate. When the required total time interval or effluent concentration of the adsorbate has been reached, the simulation is terminated. The computed concentrations at given times can be output on a screen or stored in a file. Graphic display or printout of the simulation is also possible.

5.2.1 COMPARISON OF EXPERIMENTAL AND PREDICTED B.T.C. USING KINETIC RATE EXPRESSION

Figs. 5.4 a-b and 5.4c show the comparison of the predicted B.T.C. with that determined experimentally for the adsorption of HSA and lysozyme respectively.

For HSA adsorption, curves (i) - (iii) show the comparison using a single forward rate constant value. It is clear from these that a single rate value is not capable of predicting the initial break point and the entire breakthrough curve. The theoretical B.T.C. generated by using low k_1 value (curve (i)) gave a fairly good prediction of the later part of B.T.C. up to 20 bed volumes but does not predict the break point; intermediate k_1 value (curve (ii)) neither predicted the breakpoint nor the entire B.T.C.; finally high k_1 value (curve (iii)) predicted the breakpoint but failed to predict other parts of the B.T.C. However, division of the B.T.C. into three parts and using different values of k_1 (high and low values from curves (iii) and (i) produced curve (iv) which gave a fairly good prediction of the B.T.C. up to 20 bed volumes (first two parts of the B.T.C.) of effluent (and some 0.8

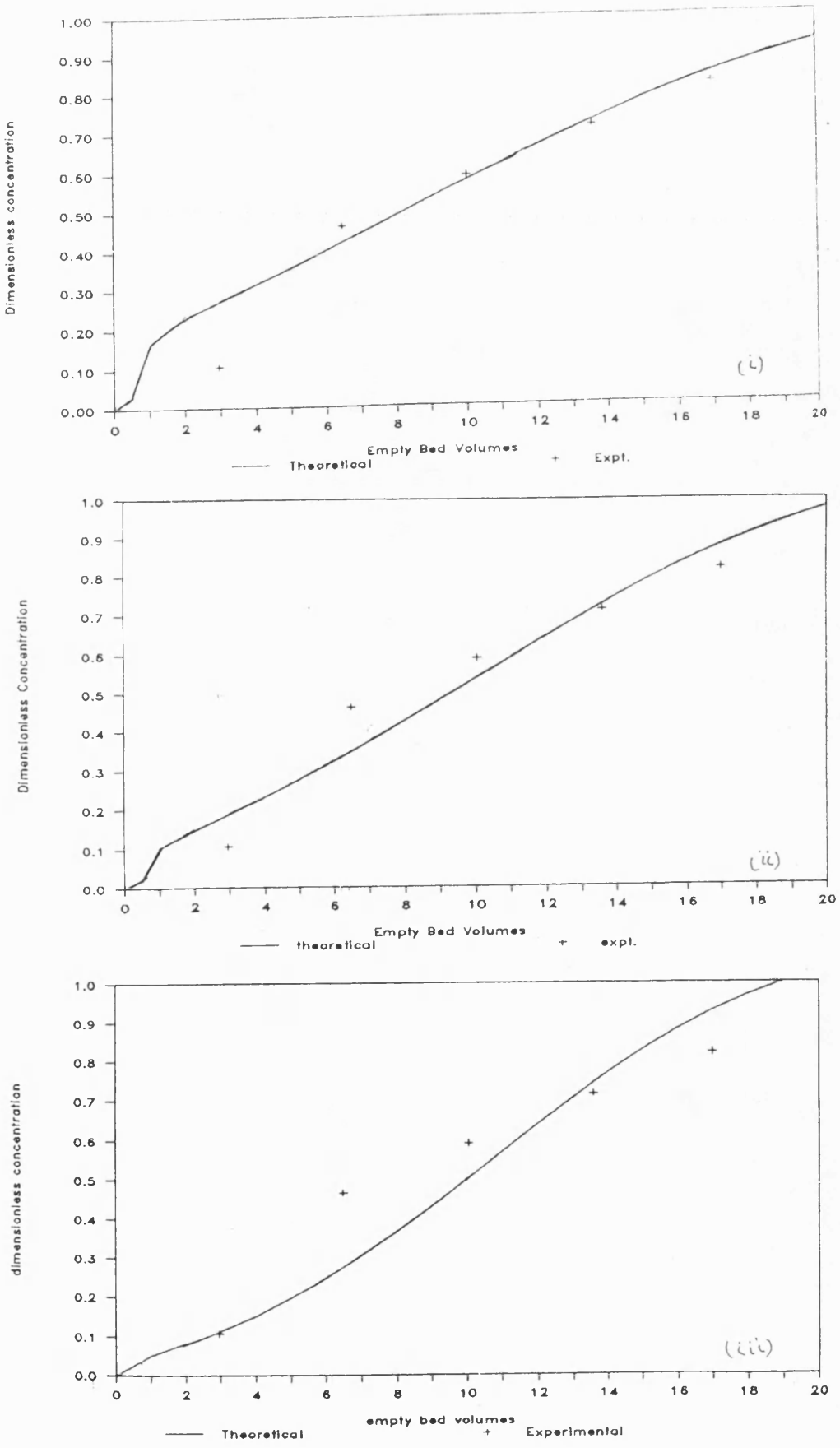

Fig. 5.4a. (i-iii) Single forward rate constant simulation: comparison of simulated and experimental B.T.C. for adsorption of HSA on blue sponge. Parameters used are: ℓ = 0.05 m, u = 1.478 m/h; Pe = 10, c_o = 1.0 kg/m^3 ; k_d = 0.56 kg/m^3 ; q_m = 11.2 kg/m^3 . Curve (i) k_1 = 3.6 m^3/kg-h; Curve (ii) k_1 = 5.0 m^3/kg-h. Curve (iii) k_1 = 7.5 m^3/kg-h.

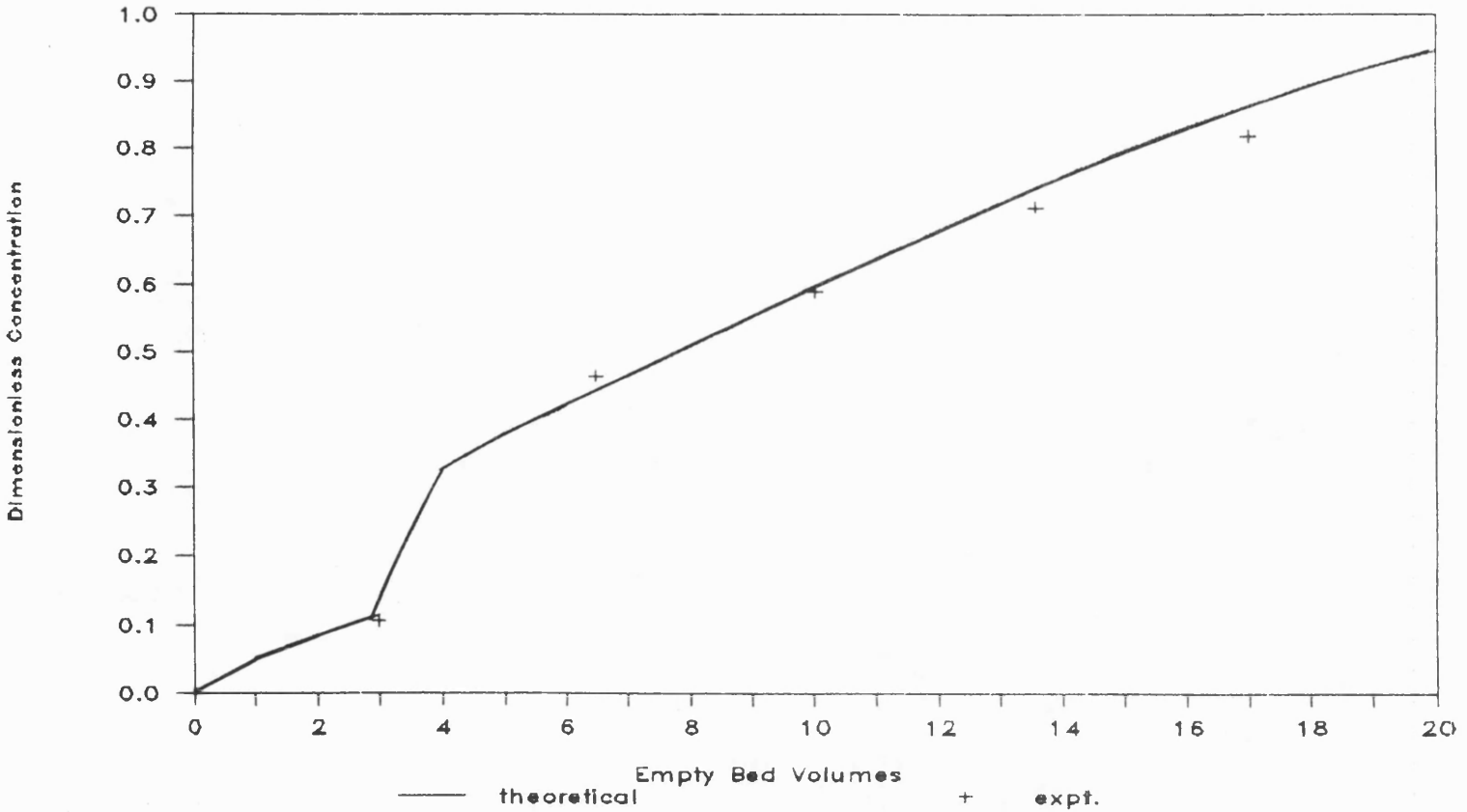

Fig. 5.4a. (iv): Dual forward rate constant simulation. Comparison of simulated and experimental B.T.C. for adsorption of HSA on blue sponge. Parameters used: as for Fig. 5.4a (i-iii). For k_1; empty bed volume = 3, k_1 = 7.5 m^3/kg-h and empty bed volume $\geq$ 3, k_1 = 3.5 m^3/kg-h.

dimensionless effluent concentration).

It seemes therefore, that the adsorption process is controlled by more than one mass transfer mechanism. This is consistent with the observation made by Graham and Fook (1982) in the adsorption/desorption rate studies for the adsorption of bovine serum albumin (B.S.A.)on a cellulose based ion-exchange resin. They observed that during the initial period of adsorption, the rate was controlled by film diffusion, after which it was controlled by an intraparticle diffisuion. Eveleigh and Levy (1977) have also observed a similar behaviour for the binding of antigens to immunosorbents prepared from Sepharose 4B and polyclonal antibodies. They obtained a pseudo-first-order rate constant for the earlier portion of the reaction of $2.4 \times 10^{-3} sec^{-1}$ (85%) but the last 15% of the reaction was much slower, with a constant of $6.3 \times 10^{-4} sec^{-1}$. The later workers interpreted the slower rate to represent the diffusion of antigen within the pores of the support; about 80% of the reactive antibody population was considered readily accessible.

Fig. 5.4b shows the prediction of B.T.C. generated by a lower feed concentration using the concept of dual k_1 values as for Fig. 5.4a in order to check the applicability, under different operating conditions.

Prediction of lysozyme adsorption using a single k_1 value is shown in Fig. 5.4c. A fairly good prediction was obtained.

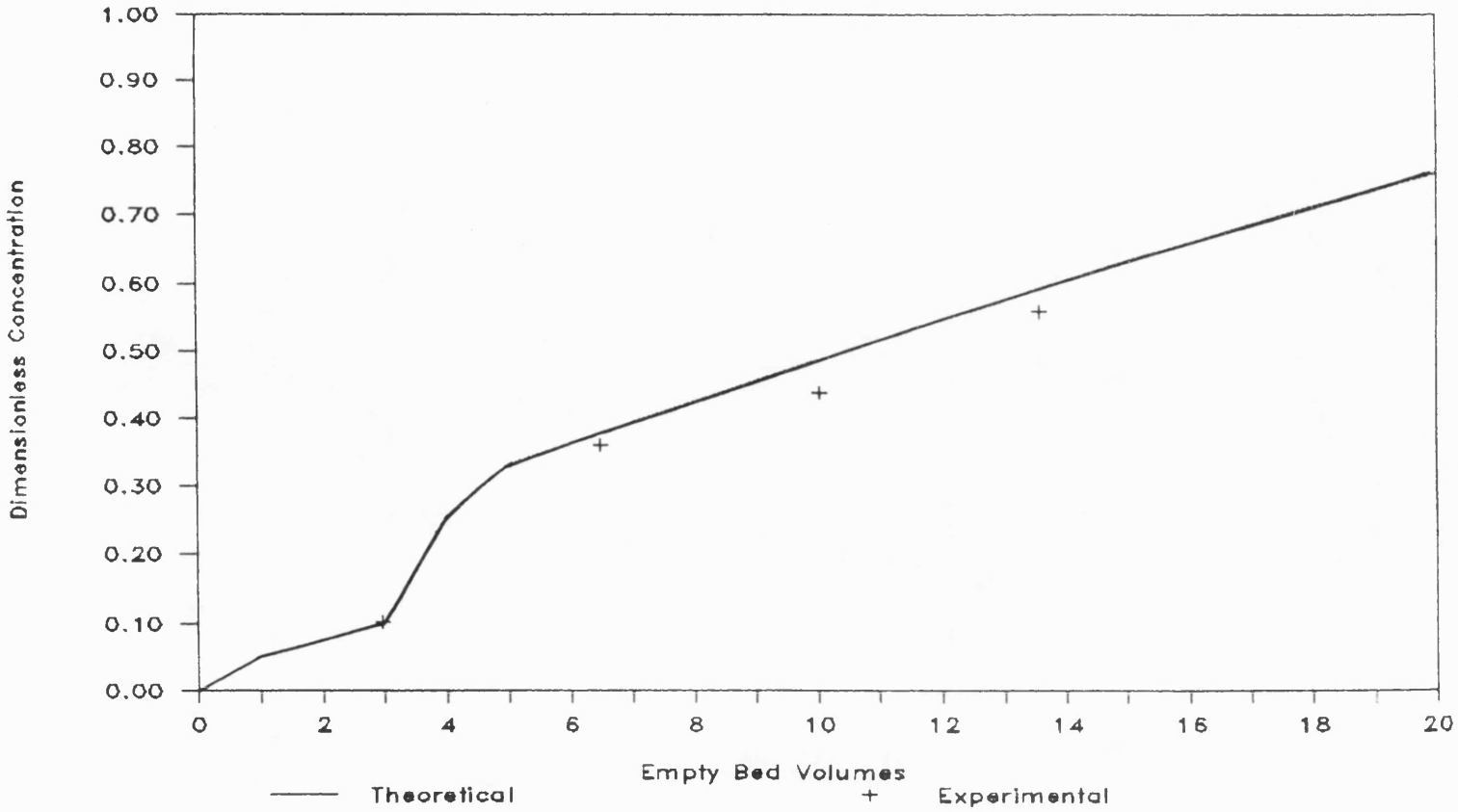

Fig. 5.4b. Dual forward rate constant simulations: Comparison of simulated and experimental B.T.C. for adsorption of HSA on blue sponge. Parameters used are as for Fig. 5.4a(iv) except that $C_0 = 0.5$.

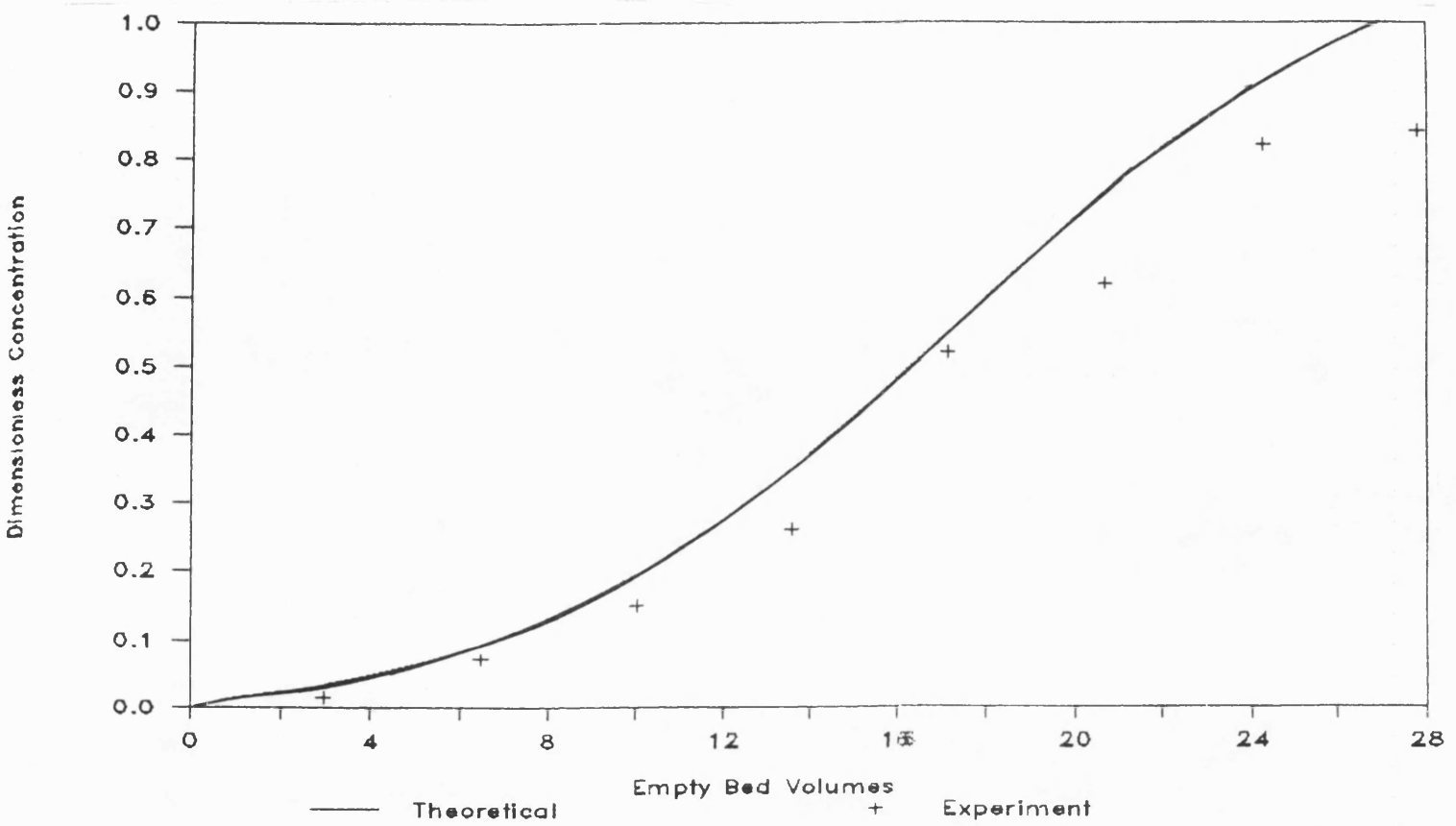

Fig. 5.4c. Single forward rate constant stimulation: Comparison of simulated and experimental B.T.C. for adsorption of Lysozyme on blue sponge. Parameters used: q_m = 8.8 kg/m^3, k_d = 0.26 kg/m^3; k_1 = 15.1 m^3/kg-h, Pe = 10, C_o = 0.5; u = 1.478 m/h.

5.2.2 SIMULATION OF BREAKTHROUGH CURVES USING KINETIC-RATE-EXPRESSION RATE MODEL: EFFECT OF MODEL PARAMETERS AND OPERATING VARIABLES.

The effects of the model equation parameters and the operating variables on the adsorption breakthrough curve were investigated using the model equations (5.34) to (5.38). The general response of the adsorption system to parameter and operating variable changes were consistent with what would be expected from the literature. These simulated B.T.C.s are shown in Figs. 5.5 to 5.14; the values of dimensionless parameters (Pe, k_A and k_B) and operating variables (U, ℓ, A , k_1, k_d, c_o, q_m) used in the simulation studies are shown in Table 5.2. Generally, one variable or dimensionless parameter was varied at a time while the values of others were kept constant.

The theoretical curves have been drawn with both symbols and solid lines in order to provide necessary legends.

The parameters k_A ($k_1 . c_o . \ell/u$) and k_B ($k_2 . \ell/u$ or $k_1 k_d . \ell/u$) are the dimensionless forward rate constant and backward rate constant respectively. Their values are determined by the combination of the operating variables shown in brackets. The operating variables appear in the dimensionless parameters in equations (5.34) to (5.38) and changes in them will have effects on the B.T.C. through the changes in the dimensionless parameters of the model equations as was adapted to transmit these effects or suppress them.

The B.T.C.s have been plotted in terms of dimensionless concentration and empty bed volumes (normalised breakthrough

Table 5.2. Parameter and operating variable values used in simulation of breakthrough curve.

FIG	MODEL PARAMETERS AND OPERATING VARIABLES									
	PECLET #	DIMENSION-LESS k_1,	DIMENSION-LESS k_d	INTERSTITIAL VELOCITY	BED LENGTH	CROSS-SEC. AREA	FORWARD RATE CONSTANT	DISSOCIATION CONST.	FEED CONCEN-TRATION	MAX. SOLID CONCENTRATION
	Pe	k_A	k_B	u	ℓ	A	k_1	k_d	c_o	q_m
	(-)	(-)	(-)	(m/h)	(m)	($x10^4$ m)	(m^3/kg.h)	(kg/m^3)	(kg/m^3)	(kg/m^3)
5.5	10 30 50	-	-	.764	.014	.785	72	.025	.1	14
5.6	10	0.1 0.2 0.3	-	.764	.014	.785	72	.025	.1	14
5.7	10	-	0.025 0.05 0.075	.764	.014	.785	72	.025	.1	14
5.8a,b	10	-	-	0.75 1.0 1.25	.014	.785	72	.025	.1	14
5.9a,b	10	-	-	.764	0.015 0.030 0.045	.785	72	.025	.1	14

Table 5.2.(continued).

FIG	MODEL PARAMETERS AND OPERATING VARIABLES									
	PECLET #	DIMENSION-LESS k_1,	DIMENSION-LESS k_d	INTERSTITIAL VELOCITY	BED LENGTH	CROSS-SEC. AREA	FORWARD RATE CONSTANT	DISSOCIATION CONST.	FEED CONCEN-TRATION	MAX. SOLID CONCENTRATION
	Pe	k_A	k_B	u	ℓ	A	k_1	k_d	c_o	q_m
	(-)	(-)	(-)	(m/h)	(m)	($x10^4$ m)	(m^3/kg.h)	(kg/m^3)	(kg/m^3)	(kg/m^3)
5.10	10	-	-	.764	.014	0.50 3.0 6.0	72	.025	.1	14
5.11	10	-	-	.764	.014	.785	20 60 100	.025	.1	14
5.12	10	-	-	.764	.014	.785	72	.025 .050 .075	.1	14
5.13	10	-	-	.764	.014	.785	72	.025	0.5 1.0 1.5	14
5.14	10	-	-	.764	.014	.785	72	.025	.1	5.0 10.0 15.0

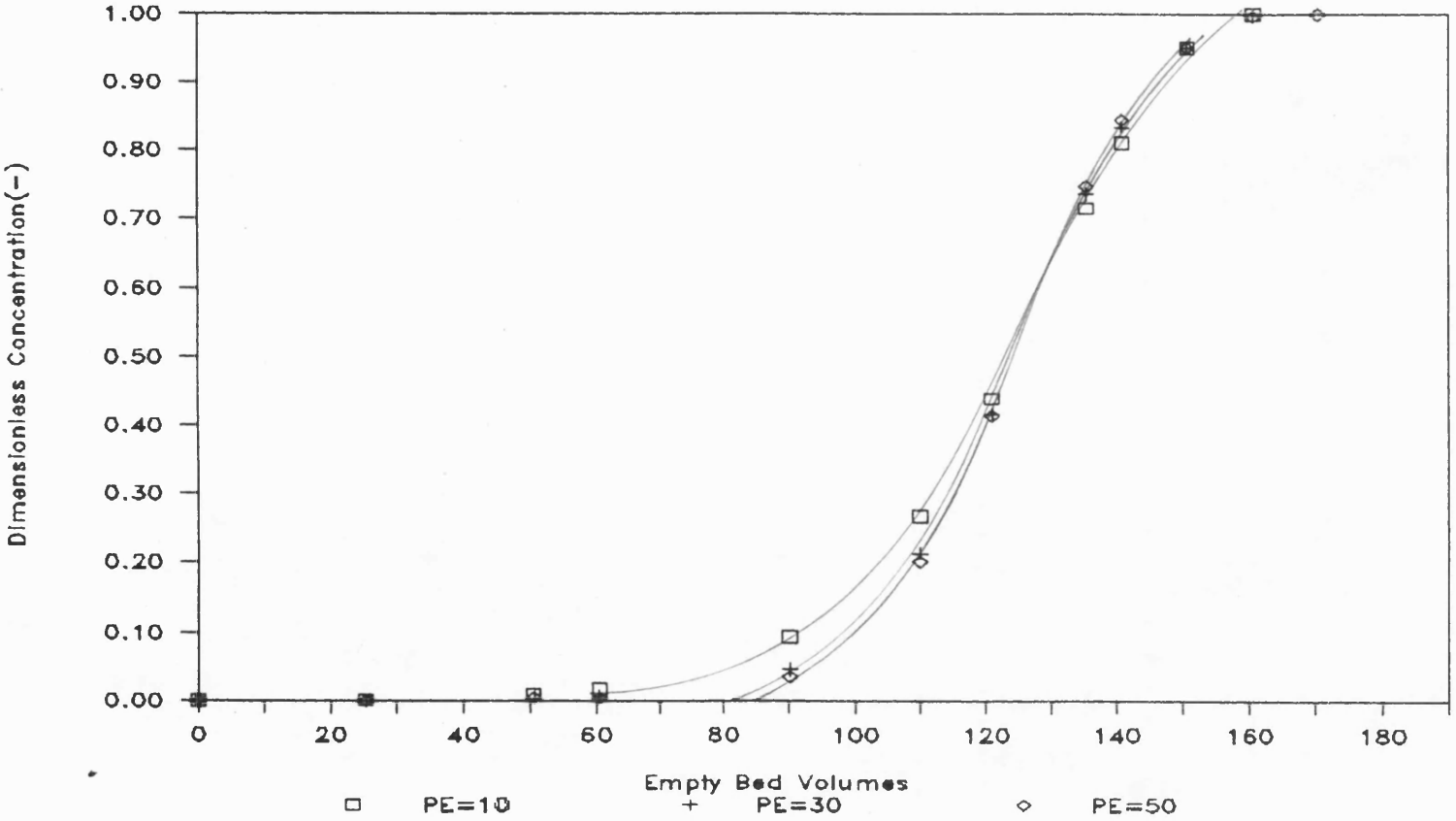

Fig. 5.5. Effect of Peclet Number, Pe.

curve). However, concentration vs. time plot was used in addition, in cases where the effect of the variables on B.T.C. was different in both plots. The values of operating parameters used in the kinetic rate expression were essentially those obtained from the literature.

Fig. 5.5 shows that the effect of Peclet number, Pe (or axial dispersion) on the B.T.C. is to increase the adsorption zone width or the widening of the adsorption width of the B.T.C. as dispersion increases (Pe decreases). It is evident that for axial Pe above, say 50, the effect of this parameter is minimal. This seems to justify the use of the plug-flow assumption in most practical adsorber design models. In very short beds, however, axial dispersion may be important due to entry effects. With bed packings similar to the sponge, as has been shown earlier, it may be inadvisable to ignore dispersion effects. The simulation result here is consistent with that obtained by Raghavan and Ruthven (1983) in their numerical simulation studies of a fixed-bed adsorption column by the method of orthogonal collocation. They observed that for axial Peclet number of less than about 40, the breaktime falls rapidly with decreasing Pe; if the Pe is greater than 40, the effect of this parameter is minimal.

The effect of the dimensionless forward rate constant (k_A) and backward rate constant (k_B) as shown in Figs. 5.6 and 5.7 shows that these two parameters have opposite effects on the B.T.C. While the increase in k_A results in delayed breakthrough time and sharper B.T.C., increasing k_B results in earlier breakthrough time. This is expected since k_A is influenced predominantly by the forward rate

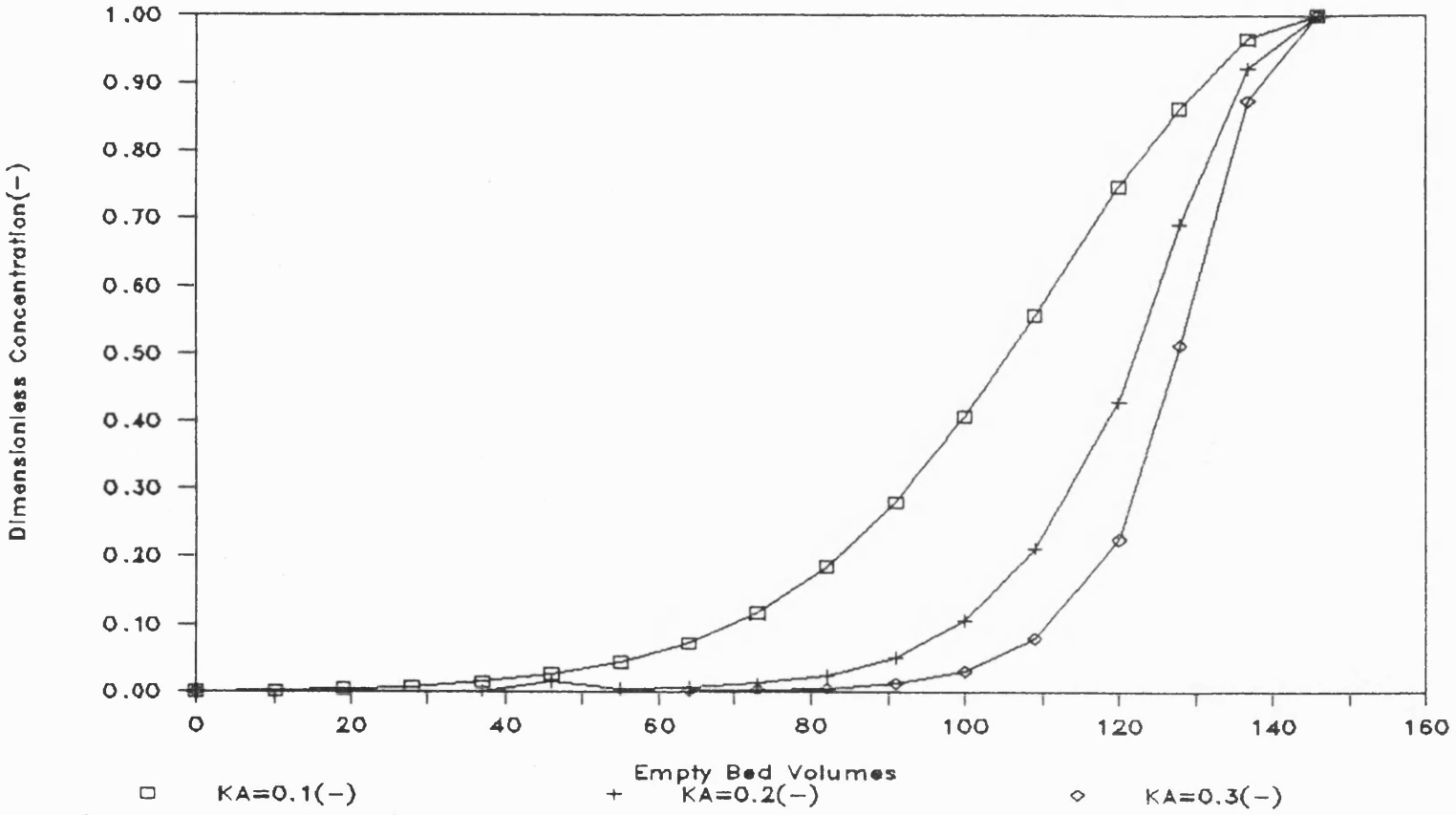

Fig. 5.6. Effect of dimensionless forward rate constant, k_A.

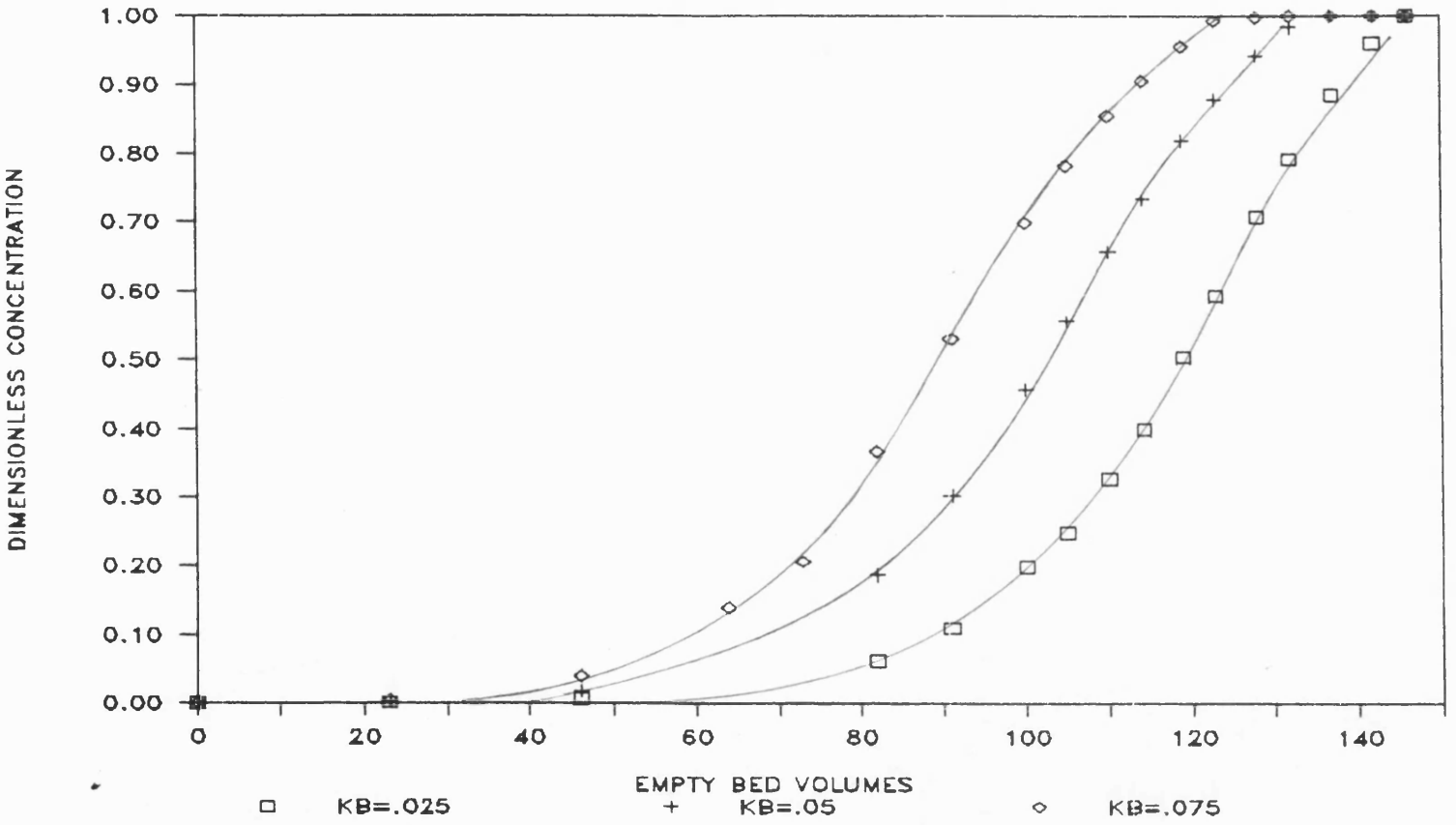

Fig. 5.7. Effect of dimensionless backward rate constant, k_B.

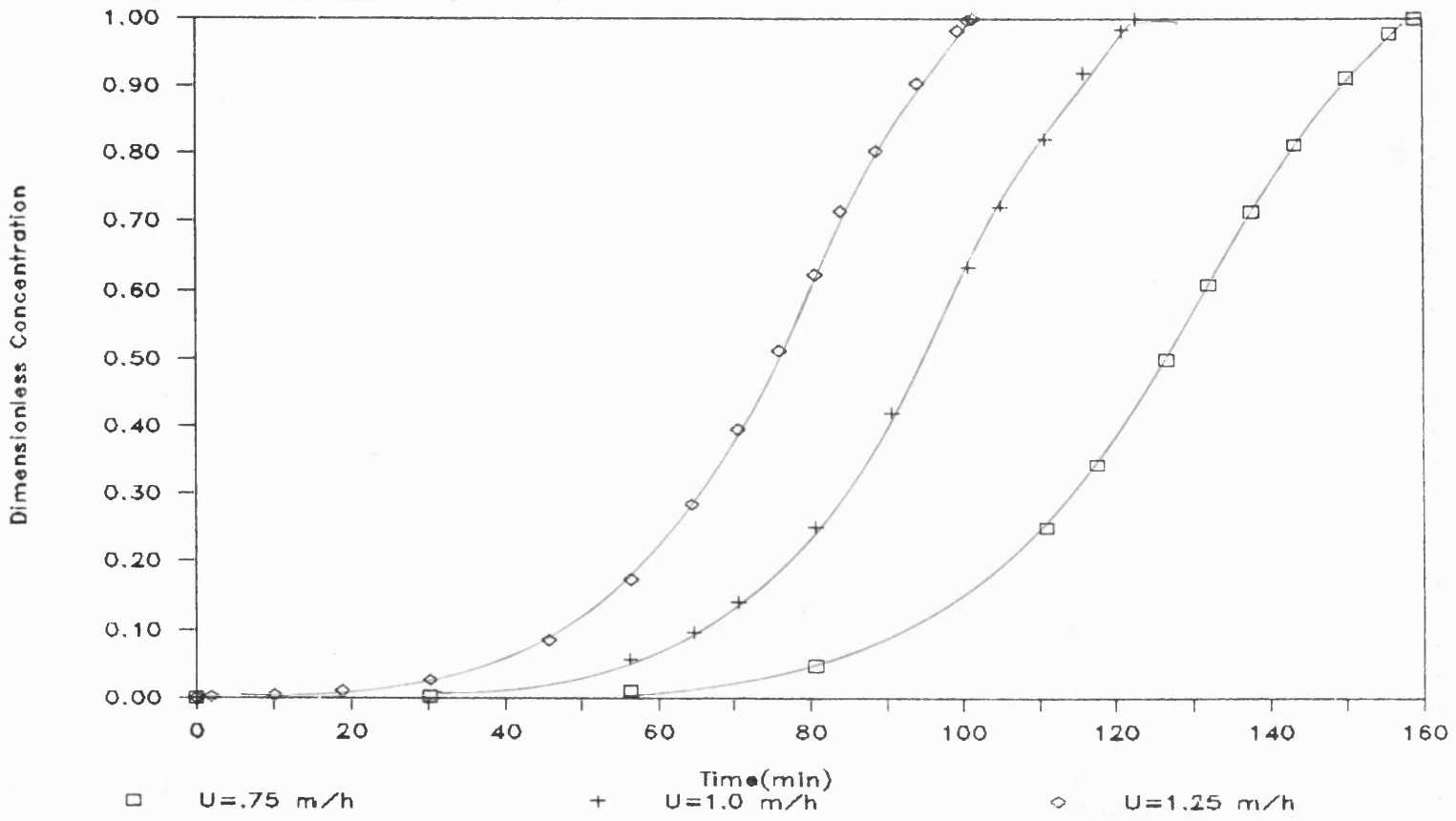

Fig. 5.8a. Effect of axial velocity, u.

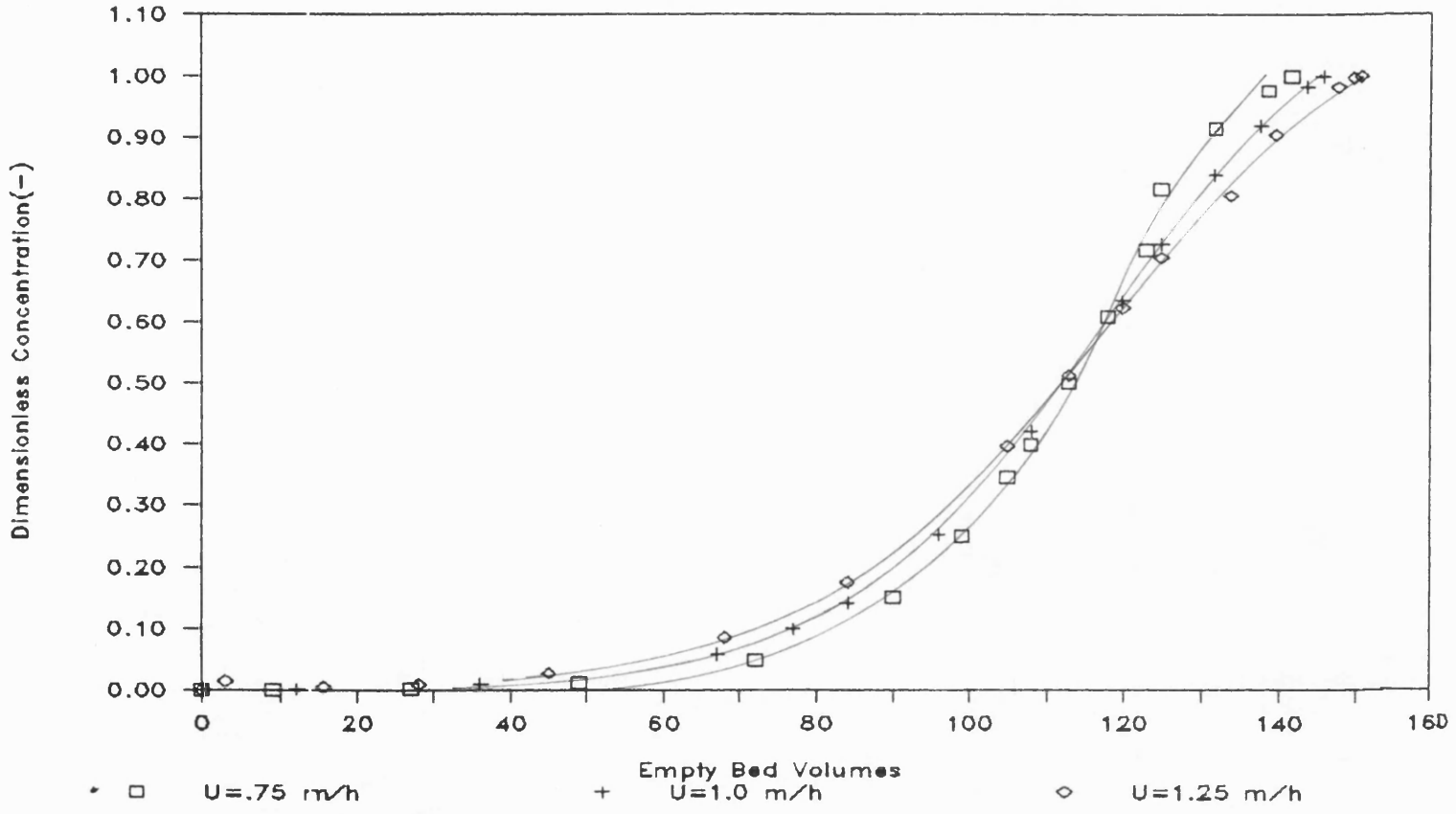

Fig. 5.8b. Effect of axial velocity, u.

constant, while k_B is influenced mainly by the backward rate constant k_2 or dissociation constant, k_d. The influence of k_1 and k_2 on k_A and k_B are proportional. From the adsorption rate equation (equation (5.35b)) it is clear that higher k_1 values and lower k_2 values favour adsorption.

Fig. 5.8a suggests that, at least within the flow rate range used in the simulation, the effect of the axial velocity is not linear. A change of 0.25 m/h in velocity does not give a proportional change in the breakthrough point of the B.T.C. The shape and the sharpness of the B.T.C., however, does not seem to be affected to any great extent in this range of flow rates. The dimensionless B.T.C. of Fig. 5.8b shows an improved performance at lower flow rates. This is indicated by the sharpening of the B.T.C. at lower flow rates.

The effect of the bed length is shown in Figs. 5.9a and 5.9b in terms of exit concentration vs time and exit concentration vs empty bed volume respectively. In general, the breakthrough points are delayed as the bed length is increased. For the termination of adsorption at a given dimensionless concentration in the effluent, more adsorption should be expected for longer columns. This is because increased column length leads to a closer approach to equilibrium because a lower percentage of the total column is affected by axial dispersion effects. The concentration vs bed volumes plot shows more clearly this effect. The bed volume plot shows increased sharpness of the curves as the column length increased which is indicative of the higher resolution known to occur with longer chromatography columns.

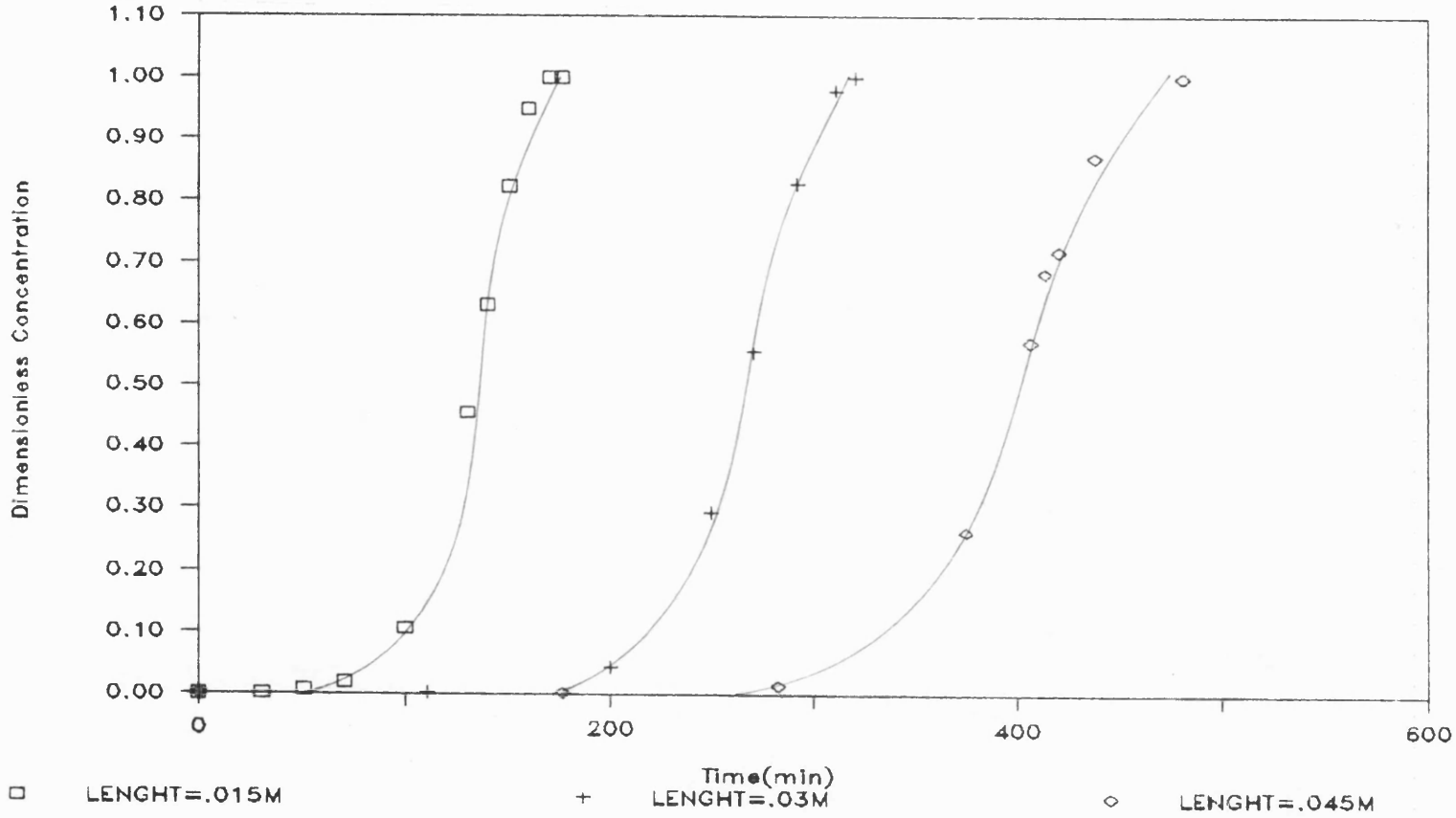

Fig. 5.9a. Effect of length, LC.

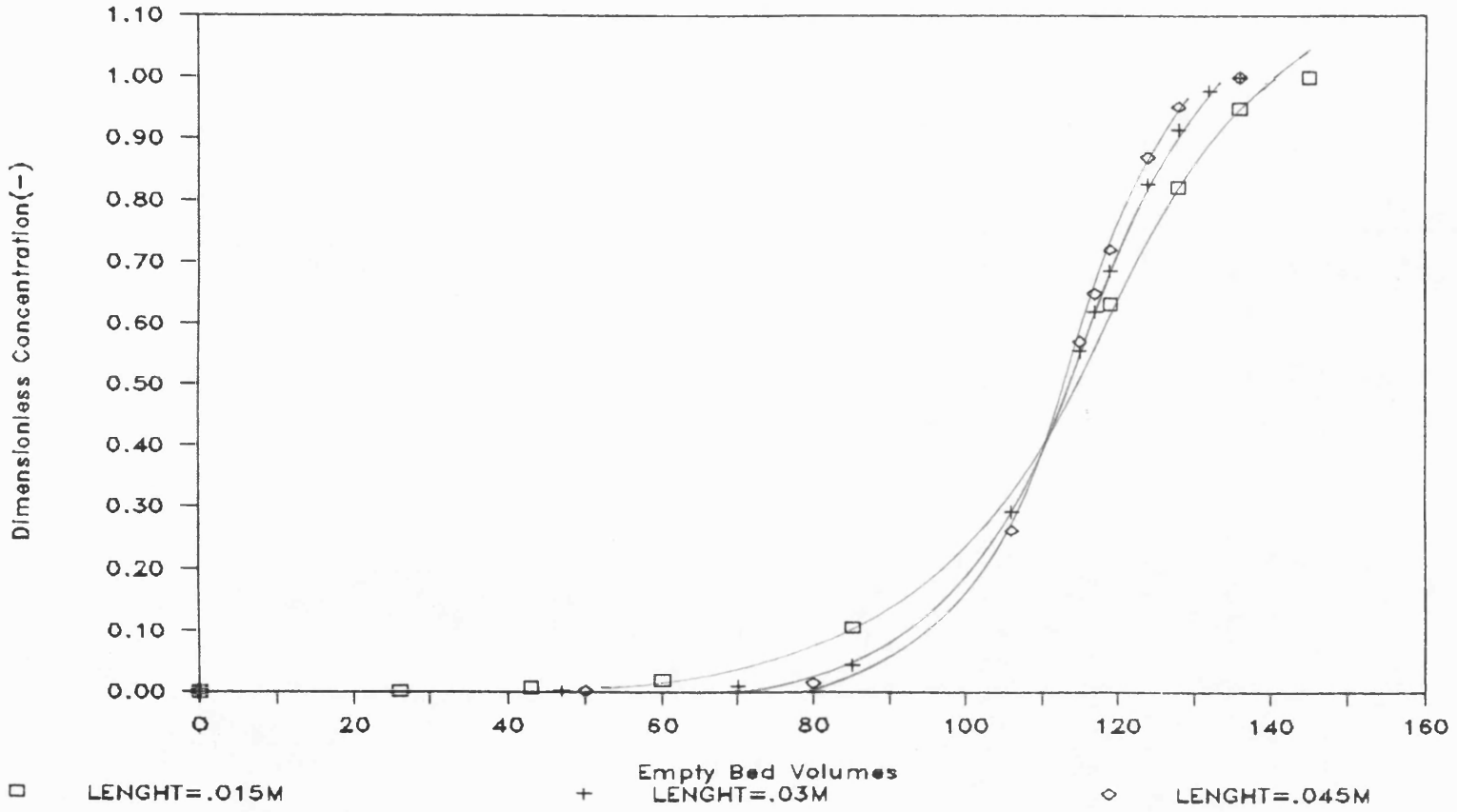

Fig. 5.9b. Effect of bed length, LC.

Increase in the bed cross-sectional area - as shown in Fig. 5.10 - does not make any difference in the breakthrough curve. This result is significant in the scale-up of affinity absorption process in a packed bed. It has been mentioned in the general introduction that scaling-up at fixed velocity and fixed length simply involves increase in the bed diameter. The only limitation to the bed diameter that can be used is that of the feed distribution at the bed entrance and subsequently inside the bed. The effect of such maldistribution has not been modelled.

Fig. 5.11 shows that a lower forward rate constant, k_1 results in the broadening of the adsorption wave length, poor utilization of adsorbent capacity and earlier breakthrough point. This is consistent with the effect of the mass transfer rates on the fixed bed adsorption processes in general. Large values of k_1 mean that local equilibrium is attained or approached more quickly within the column. This means that adsorption can be stopped at a lower effluent concentration of the adsorbate with substantial utilization of the adsorbent capacity and hence, shorter process cycle and better net yield of product. Short process cycle as has been pointed out earlier, is very important in the large-scale processes.

Fig. 5.12 shows that higher values of the dissociation constant, k_d, result in early breakthrough of the adsorbate but does not seem to alter the basic shape of the B.T.C. High values of k_d as should be expected result in unfavourable adsorption. One of the criteria for adsorbent selection for a given affinity separation is a low enough k_d to allow strong binding between the

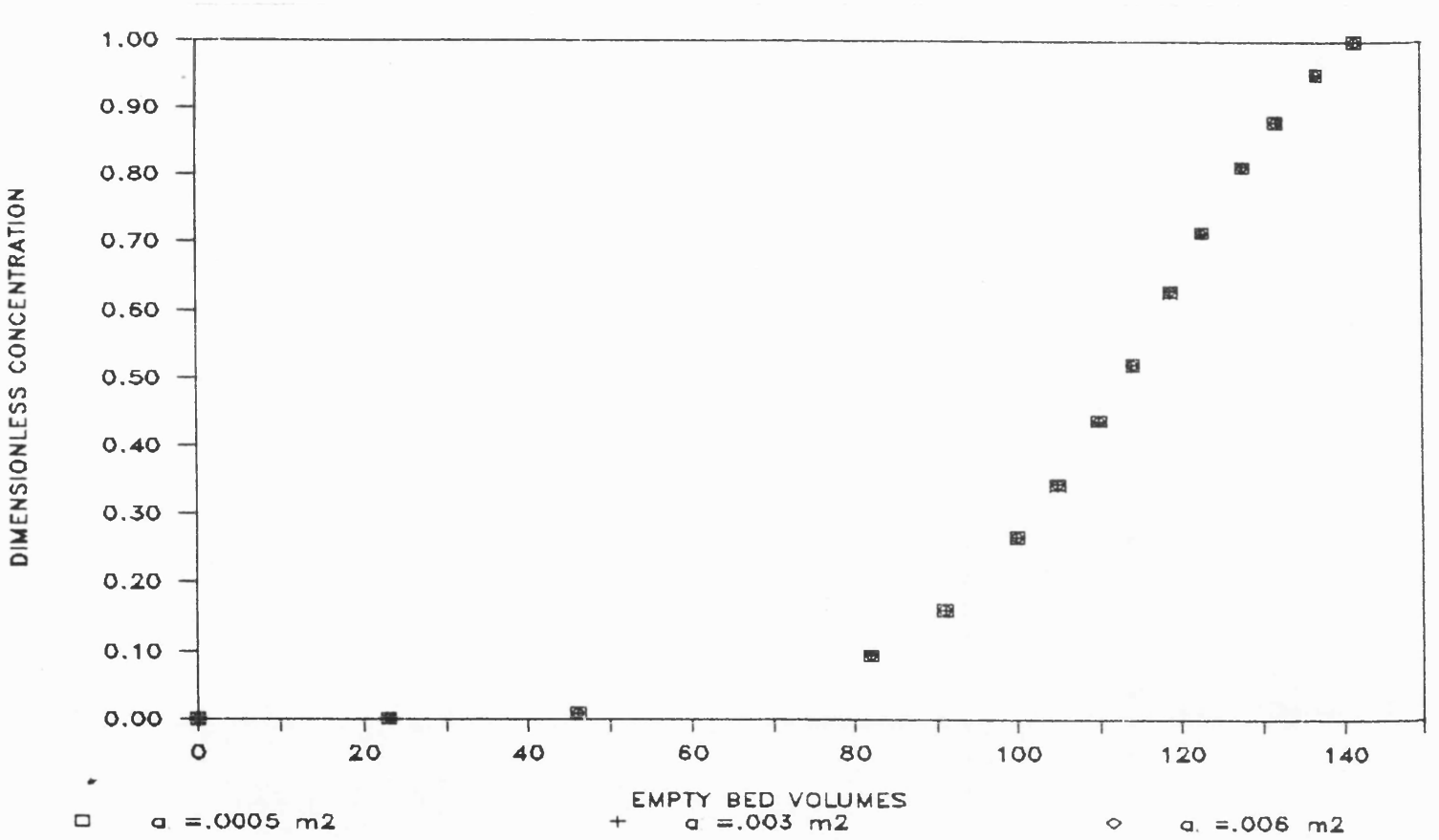

Fig. 5.10. Effect of cross sectional area, A .

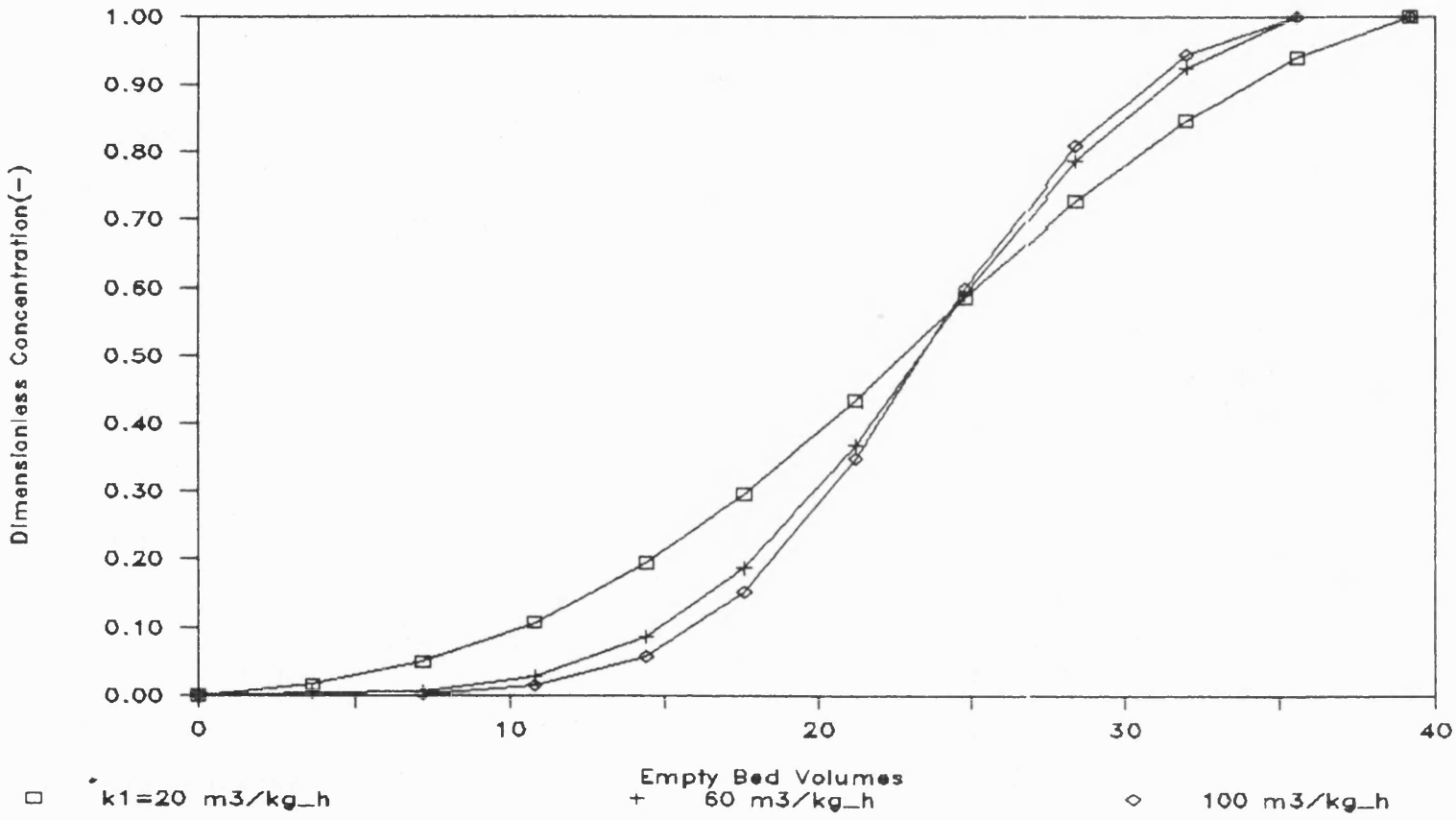

Fig. 5.11. Effect of foward rate constant, k_1.

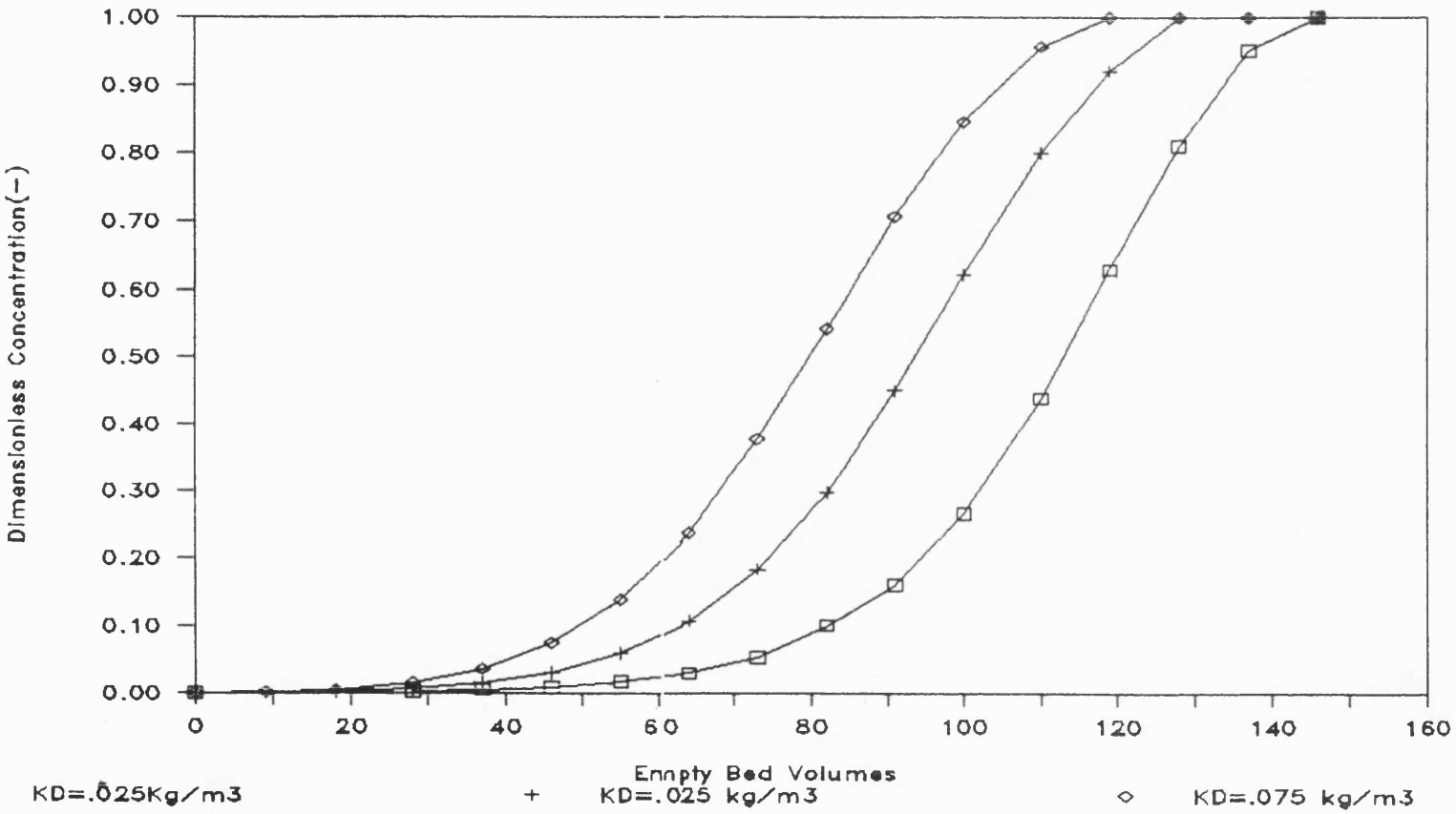

Fig. 5.12. Effect of dissociation constant, k_d.

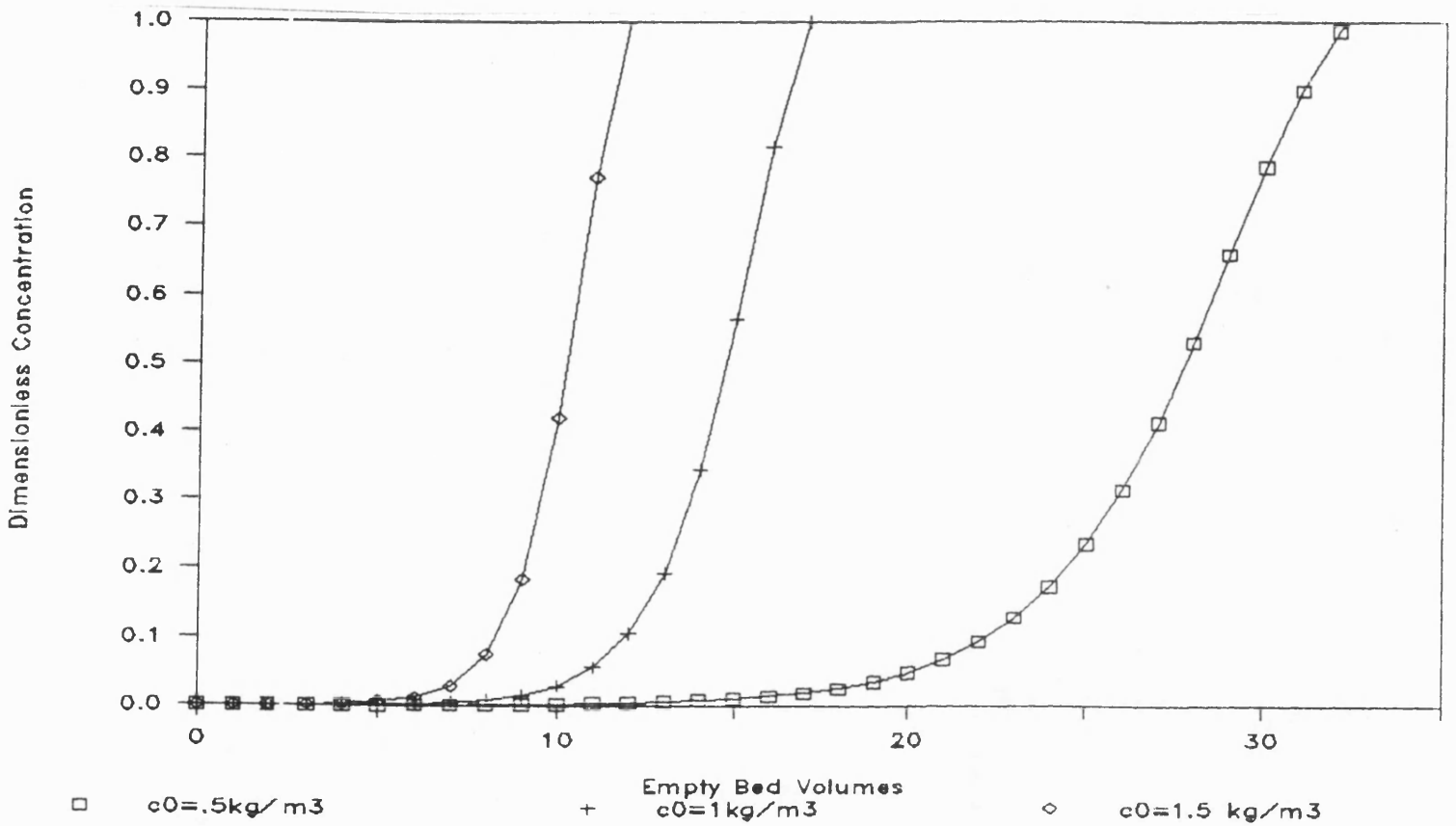

Fig. 5.13. Effect of initial Adsorbate Concentration.

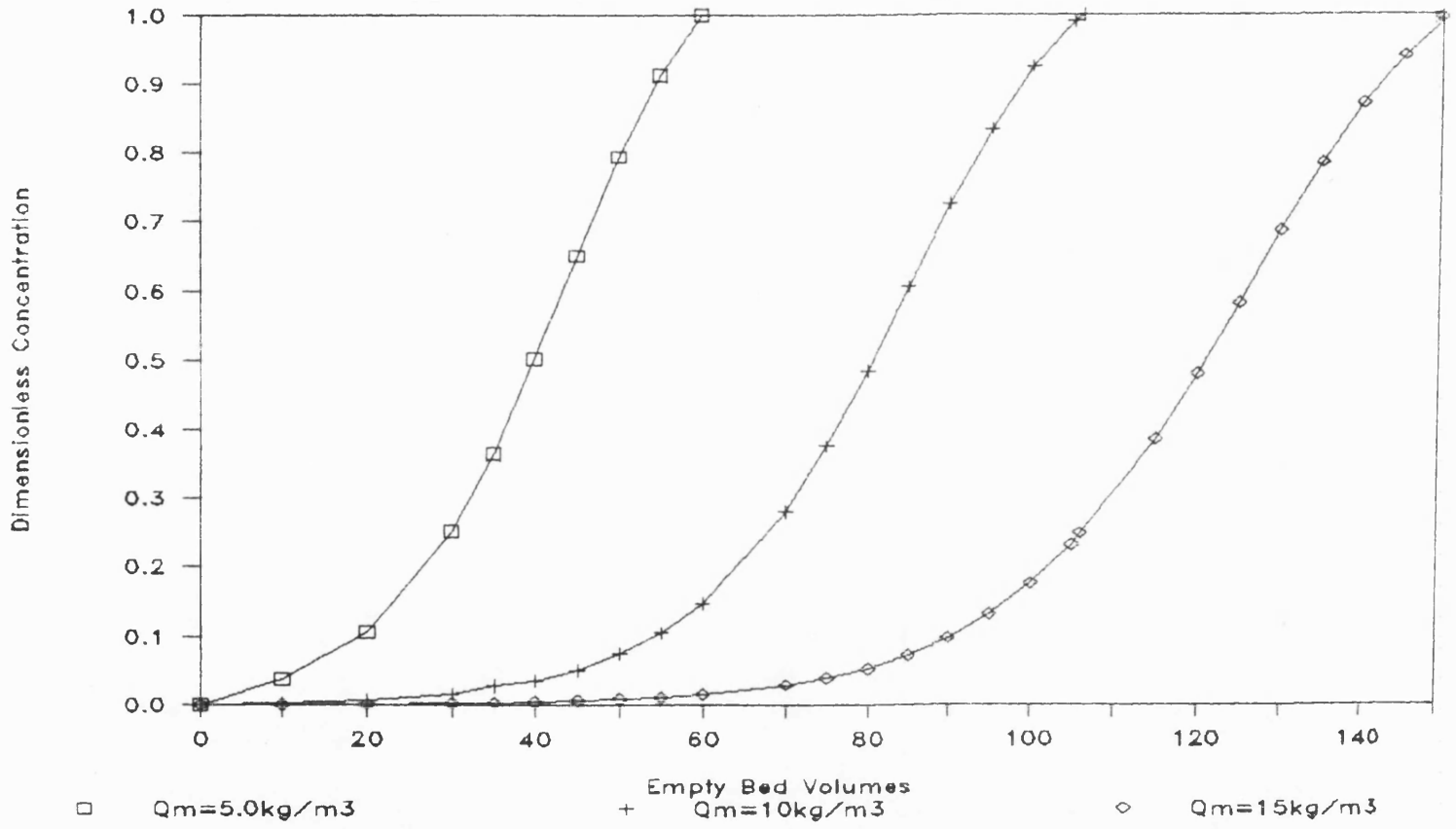

Fig. 5.14. Effect of maximum adsorbent capacity.

attached ligand and the target molecule.

As should be expected, lower initial feed concentration (c_o) and higher maximum solid phase capacity (q_m) result in delayed breakthrough, as shown in Figs. 5.13 and 5.14 respectively. The effect of solid capacity is proportional but that of the adsorbate initial concentration is not, owing to the non-linearity of the adsorption isotherm.

5.2.3 SIMULATION OF B.T.C. USING THE LINEAR-DRIVING-FORCE TYPE RATE EXPRESSION

Since the previous model based on the kinetic-rate-expression rate model did not predict accurately the last 15-18% of the breakthrough curve it was decided to use the rate expression model which assumes that the adsorption process is controlled by film mass transfer. This also demonstrates the beauty of the orthogonal collocation method (O.C.M.) in handling the present model being used in this work. The flexibility in the O.C.M. lies in the ability to change the rate expression in the model without major structural changes in the algorithm used in the computer simulation code. With a method like the finite difference this is hardly as easy.

In the formulation of solution scheme shown in appendix 4, the general form of equation (1) is

$$\frac{\partial c}{\partial t} = D_L \frac{\partial^2 c}{\partial x^2} - u \frac{\partial c}{\partial x} - \frac{R}{\epsilon}(c) \qquad (5.47a)$$

where R is the appropriate rate expression

On assumption of film mass transfer controlling the adsorption process

$$R(t) = \frac{\partial q}{\partial t} = k\, a_v\, (c - c^*) \qquad (5.48a)$$

where k = mass transfer coefficient (m/s)

c^* = equilibrium concn. on the surface particle (kg/m^3)

a_v = specific surface area of paticle (m^2/m^3 of bed)

and $k'a_v$ = k = volumetric mass transfer coeficient (s^{-1})

defining the dimensionless parameters as before, in addition $k_F = K.\ \ell/u$; using the same manipulation previously used:

The dimensionless form of equations (5.47a) and (5.48a) are respectively:

$$\frac{\partial \bar{c}}{\partial \theta} = \frac{1}{Pe}\ \frac{\partial^2 \bar{c}}{\partial z} - \frac{1}{\epsilon}\, k_f\, (\bar{c} - \bar{c}^*) \qquad (5.47)$$

$$\frac{\partial \bar{q}}{\partial \theta} = \frac{1}{\beta}\, k_f\, (\bar{c} - \bar{c}^*) \qquad (5.48)$$

from the equilibrium relation $c^* = \dfrac{\bar{q} k_E}{(1-\bar{q})}$ (5.49)

where $k_E = k_d/c_o$.

All assumptions and the boundary conditions are the same as for model equation used previously, therefore boundary conditions as given in equations (5.36) to (5.38) are:

$$\frac{dc}{dz} = Pe\ (c-1) \qquad \text{at } z = 0 \qquad (5.50)$$

$$\frac{dC}{dz} = 0 \qquad \text{at } z = 1 \tag{5.51}$$

$$\text{and } \bar{q} = 0; \quad c = 0 \quad \text{at} \quad \theta = 0 \tag{5.52}$$

The orthogonal collocation formulation is basically the same as in equations (5.43) to (5.46) and is given below.

$$\frac{dc_j}{d\theta} = \sum_{i=2}^{m-1} (M1B_{ji} - A_{ji})c_i + (M1B_{j1} - A_{j1})c_1 + (M_1B_{jm} - A_{jm})c_m - \frac{k_f}{\epsilon}\left[c_j - \left(\frac{\bar{q}_j k_E}{1-\bar{q}_j}\right) \right] \tag{5.53}$$

$$\frac{dq_j}{d\theta} = \frac{k_f}{\beta}\left(c_j - \frac{\bar{q}_j k_E}{1-\bar{q}_j}\right) \tag{5.54}$$

$$c_1 = - Pe - \sum_{i=2}^{m-1} \left(A_{1i} - \frac{A_{mi}A_{1m}}{A_{mm}}\right)c_i \tag{5.55}$$

$$c_m = - \sum_{i=1}^{m-1} \frac{A_{mi}}{A_{mm}} c_i \tag{5.56}$$

In appendix 6, the simulation scheme gives equation (5.53) in general form as

$$\frac{dc_j}{d\theta} = X_j - [\text{Rate expression}] \tag{5.57}$$

The only change required in program SIM is that of the second term on the R.H.S. of equation (5.57) and the substitution of equation (5.54) for (5.44). The dimensionless parameters are the same except for k_A, k_B and k_E which are specific to rate expressions.

The result of the comparison between experimental and

predicted adsorption of HSA on blue sponge is shown in Fig. 5.15. The k_f value used was 1.2.

The adsorption conditions are the same as those shown in Fig. 5.4b. Fig. 5.15 shows a similar fit as that obtained with the model based on the kinetic rate expression. This confirms the earlier observation that different mass transfer mechanisms operate during the later part of B.T.C. after the first 75-85% of initial adsorption. This is probably due to an internal diffusion mechanism acting alone or in combination with, say, the external film mass transfer limiting process.

5.2.4 SIMULATION OF EFFECT OF MODEL PARAMETERS ON THE B.T.C. USING LINEAR-DRIVING-FORCE TYPE RATE MODEL

The effect of the other parameters apart from k_F and k_E on B.T.C. have already been shown. Fig. 5.16 shows the effect of the dimensionless mass transfer coefficient on the B.T.C. The sharpening of the B.T.C. results from an increase in the k_F values; also later breakthrough point results. The effect of the dimensionless dissociation constant, k_E is shown on Fig. 5.17; this is similar to that shown by k_d in Fig. 5.12. This is not surprising since ($k_E = k_d/c_o$) the k_E value increases as k_d increases. For affinity systems with low k_d values lower feed concentration of the adsorbate will be required to achieve a given particular column performance. The reverse is also true.

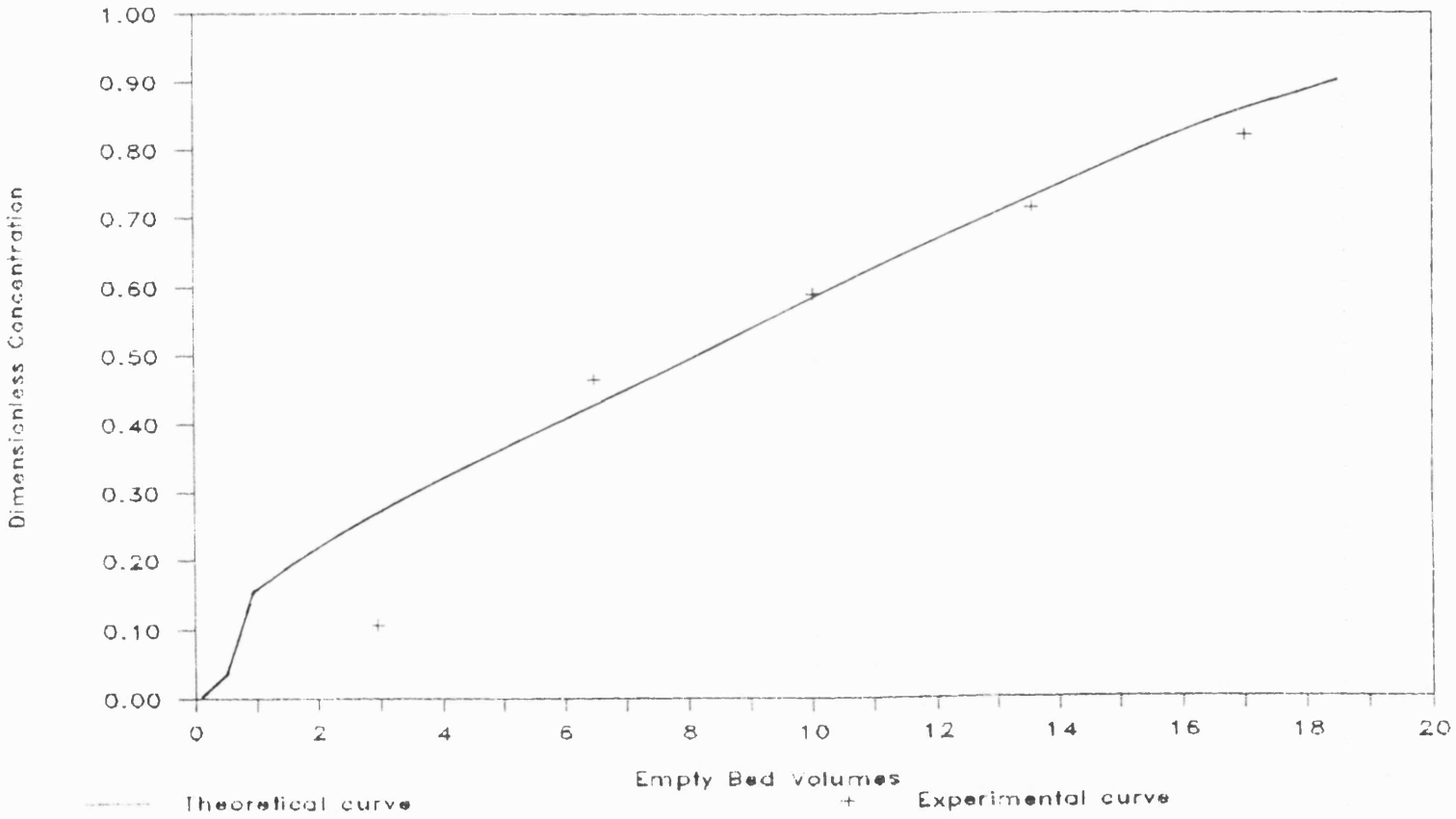

Fig 5.15 Comparison of Experimental and Simulated B.T.C for Adsorption of HSA on blue Sponge using linear_driving_force rate model Parameters used are:kf=1.2,co=.5,others as for kinetic_rate_ expression model

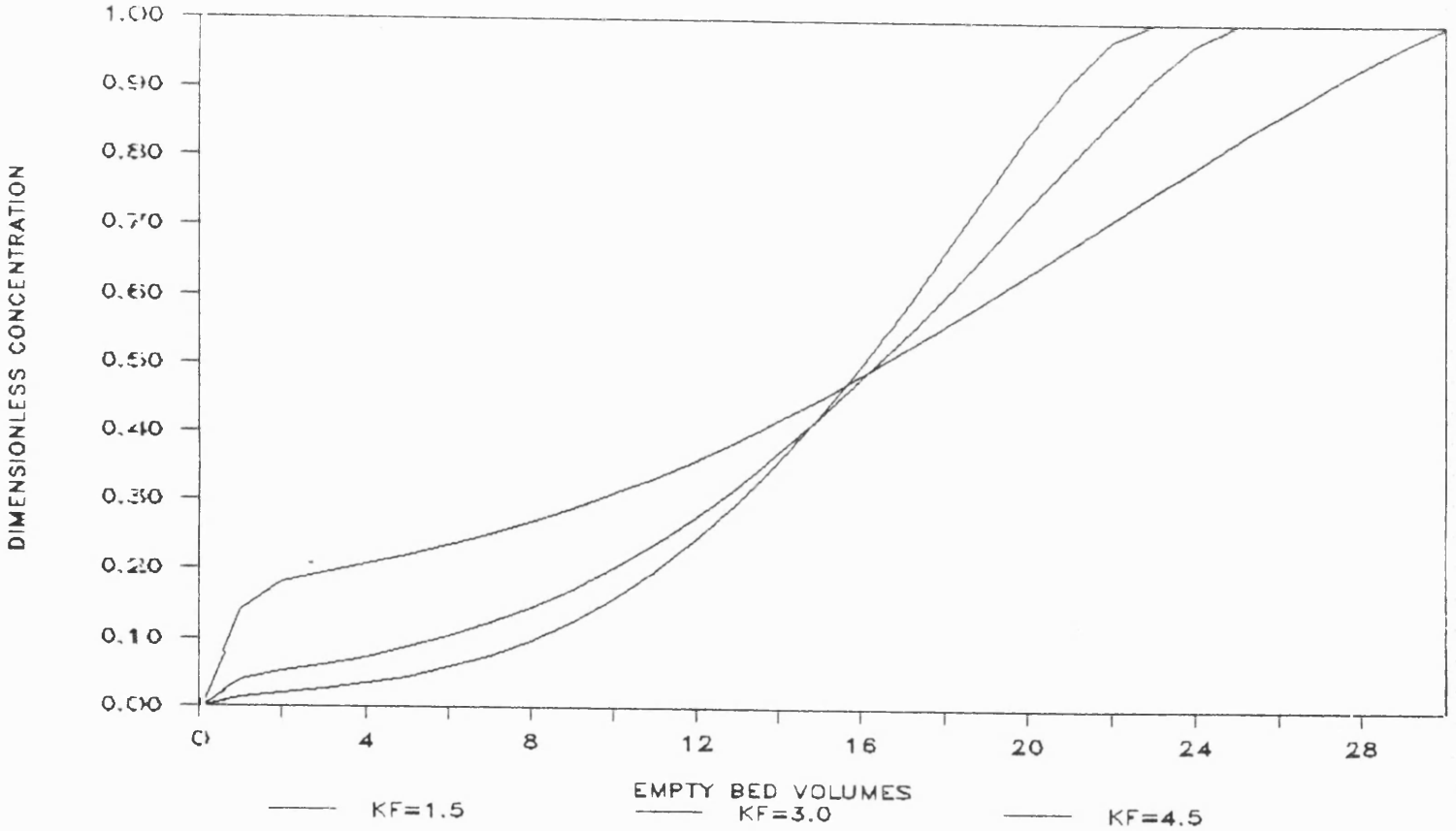

Fig. 5.16. Effect of k_f.

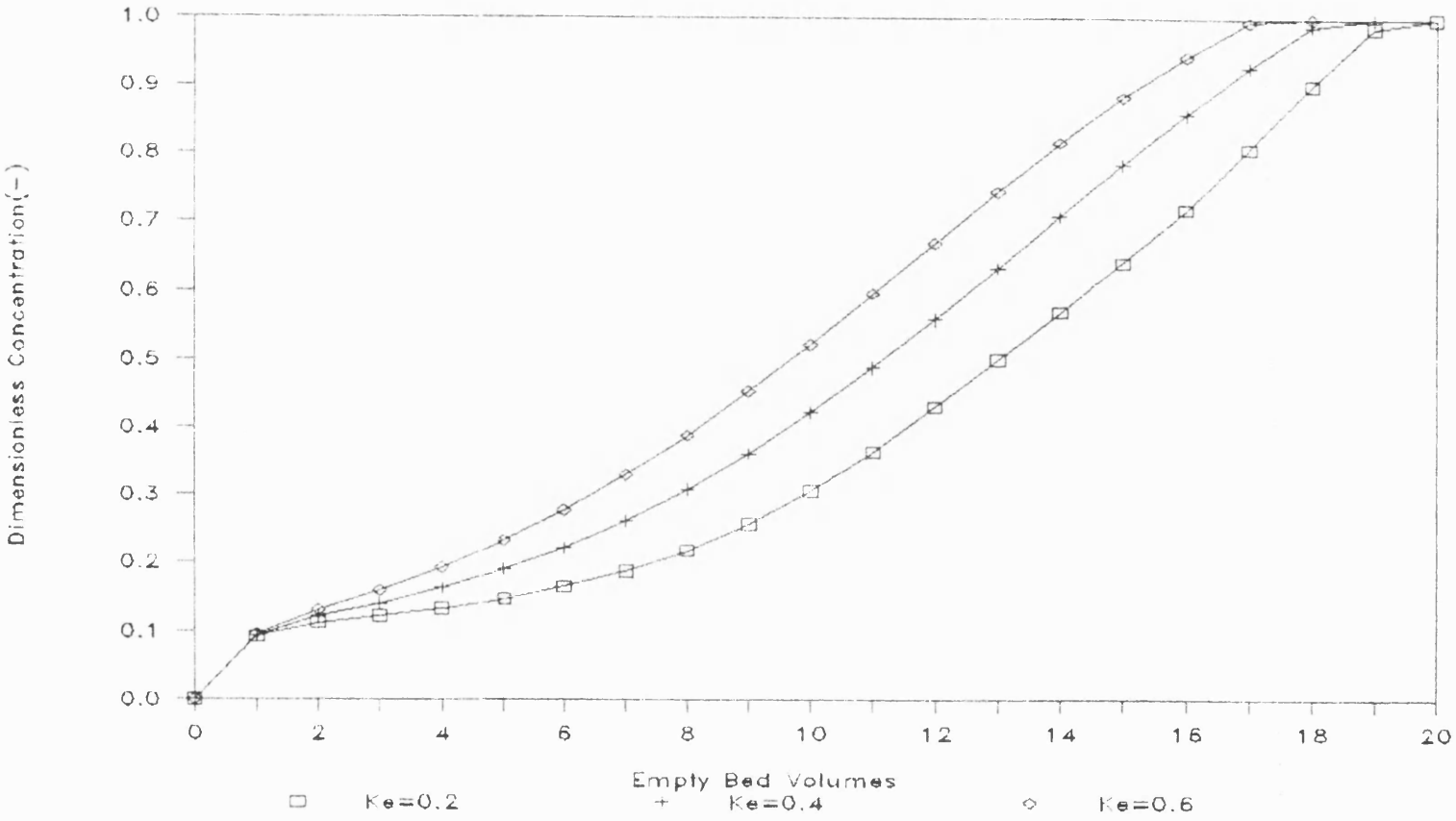

Fig. 5.17. Effect of k_E.

6. CONCLUSIONS AND RECOMMENDATIONS

A novel support matrix based on regenerated cellulose (in form of membrane and sponge) has been investigated for use in affinity separation. The following areas were considered:

(i) Adsorbent preparation and separation performance.

(ii) Experimental investigation of some factors affecting adsorption.

(iii) Estimation of transport and physical parameters of the sponge, adsorption kinetics and equilibrium parameters.

(iv) Mathematical modelling of the adsorption stage and simulation of factors affecting adsorption.

Below are the main conclusions and recommendations for further work.

6.1 SEPARATION PERFORMANCE

In the development of the affinity adsorbents based on the sponge or membrane support matrix it has been envisaged that some superiority over the existing particulate adsorbents will have to be demonstrated. Superiority may be in terms of, for example,

(1) Capacity.

(2) Throughput.

Although the present investigation could be regarded as preliminary, it has been shown that blue sponge and blue membrane have capacities (w/w) which are comparable with those of existing

blue adsorbents (Chapter 3; Discussion) for the adsorption of human serum albumin (HSA) from human blood plasma.

Protein A sponge has a capacity comparable with that obtained by Mandaro et al. (1987) using a composite matrix of vinyl monomer grafted to a cellulose support. Mandaro's values were 10.08 mg/g (for bovine IgG) and 17.6 mg/g (for human IgG).

In terms of throughput, the sponge has an advantage over the existing particulate support matrix most commonly used in affinity separations. The open structure of the sponge makes it possible to pass fluid at high flow rates without appreciable drop in pressure at moderate packing density of the sponge. The blue membrane does have good flow for water and very dilute plasma but as been shown experimentally, flux decline occurs at moderate plasma dilution. On the basis of flow properties, it can therefore be concluded that while the sponge is a good candidate for further assessment for large-scale use, the membrane discs will be more useful for analytical purposes. In fact, the blue membranes (included in a range of other dye/membrane adsorbents) are now being marketed by Domnick Hunters Ltd. for analytical uses. The performance evaluation reported here is part of the initial development/ performance evaluation of blue membrane by the above company.

One way of further improvement of blue sponge performance will be to use a spacer arm to attach the dye ligand to the sponge. This will improve accessibility of the protein (adsorbate) molecules to the ligand.

With the blue sponge, it appears that there is slow binding (perhaps due to internal pore diffusion limitation) after the

initial period of relatively fast adsorption. This suggests that a short sponge packing (as used for the adsorption of HSA from blood plasma here) combined with relatively high flow rate is a good way of utilizing the fast flow property of the sponge. Further, mass transfer limitations can be reduced by the use of moderate ligand density, by sparsely attaching ligands, most of the ligands will be attached to bigger pore walls that are readily available to the adsorbate.

It has been shown by the step and pulse response analysis that in column packing, relatively high dispersion occurs with the sponge. Either a differential bed packing or a micro column (narrow) was used in the experiments reported here. Possibly, the use of wider and longer columns may reduce the entry and exit effects of the differential bed and the relatively high dispersion often associated with very narrow columns. However, use of very long columns may not be desirable because of the observation of the last paragraph. Also, the tortuosity value indicates a rather high randomness in the sponge internal structure; this causes backmixing of the fluid within the pores which is responsible for dispersion. It is therefore difficult to envisage a substantial reduction of dispersion in the sponge. The question that is very important in this situation is whether the high dispersion level in the sponge can be tolerated. From the adsorption performance evidence and the simulation studies (effect of Peclet number) of Chapter 5, dispersion in the sponge although high, is tolerable.

It is also necessary to consider the best configuration for the adsorption/desorption operations with sponge based adsorbents.

Mainly column configurations have been considered in this project although a radial flow configuration has also been used. Batch adsorption has not been considered although it has been used in the adsorption kinetics studies. Each of the three possible methods of adsorption has its advantages and disadvantages. The column operation offers a means of high rate of transfer of adsorbate and hence operation cycle but dispersion is relatively high. With the batch operation, dispersion effect may not be as high as in the column operation but mass transfer rate is inherently lower than that in column separations. Conceivably, the sponge sheets can be wrapped around a porous support in a concentric manner with multiple turbine impeller mounted centrally to provide radial mixing. In this way mass transfer rate can be improved but protein in dilute solutoins may not withstand the shear due to mixing. The radial flow configuration seems to be a good compromise between the column and batch operating modes. With it, a higher throughput can be obtained for equivalent average velocity. It is recommended therefore that the radial flow system be studied in more detail for large scale operation.

6.1.1 SUMMARY OF CONCLUSIONS AND RECOMMENDATIONS

(a) CONCLUSIONS

(1) The cellulosic blue membrane and blue sponge have capacity (average 16.78 mg/g) comparable with that of agarose based blue Sepharose, (17.98 mg/g).

(2) The sponge matrix has throughput superiority over the particulate support matrices commonly used in affinity

separations.

(3) Protein A sponge capacity (15.7 mg/g) has comparable capacity to other cellulosic matrix-protein A adsorbents for bovine IgG (10.08 mg/g).

(4) The membrane discs are suitable for analytical applications. On the other hand, the sponge is more suitable than the membrane for large scale application.

(5) The kinetic parameters, with the sponge, are better evaluated in the column configuration than in batch.

(6) The sponge has relatively high voidage and tortuosity.

(7) Axial dispersion in sponge packed in a column is fairly high but tolerable.

(8) Radial flow configuration appears to be a good alternative to column configuration.

(b) RECOMMENDATIONS

(1) To improve adsorption capacity of the blue sponge, possibly by use of spacer arm to attach the blue dye to the sponge.

(2) Further investigation of the radial flow configuration is recommended for possible scale-up. Scale-up will, for example, involve the use of an inert support (say nylon) with the sponge forming the inner layer.

(3) The pore distribution of the sponge should be investigated. This could throw some light on the reason for the inability to model the adsorption stage with blue sponge using a single rate mechanism.

(4) Use of short depths of sponge packing is recommended.

6.2 MATHEMATICAL MODELLING

The mathematical model of the adsorption step has provided a means of assessing the effect of important parameters on the adsorption process in a systematic way. This will aid in the scaling up of the process. It was shown by means of the mathematical model developed here that:

(1) More than one mass transfer mechanism operates in the adsorption of HSA with blue sponge.

(2) Film/pore diffusion resistance may be important.

However, the modelling can be improved as follows:

(1) Optimization of the model parameters is required.

(2) Use of additional collocation points for both axial and radial coordinates.

(3) Study and inclusion of multicomponent adsorption parameters because they may differ from those of the pure (single) component used here.

(4) Only the non-porous particle model has been considered in this work. It will be desirable to use a porous particle model which may describe the adsorption process better than what was obtained here.

There appeares to be some assymmetry in the theoretical B.T.C. when the c/c_0 is exactly one. A symmetric curve is obtained only when the maximum value of c/c_0 is some 1.01 (an error of about 1%). More collocation points should therefore be investigated. Also there appeared to be some numerical instability at higher number of

collocation points than those used here. This may also be responsible for the 1% error mentioned above. One possibility is the use of a microcomputer which probably is extending the limits of its numerical accuracy. This problem requires some investigation using the main frame computer.

For the design and operation of the large-scale adsorber with the sponge as the adsorbent, wash and elution models will be necessary. These stages have not been investigated here. Investigation of these are therefore required.

REFERENCES

ADACHI, S., HASHIMOTO, K., MATSUNO, R., NAKANISHI, K. and KAMIKUBO, T. (1980). "Pulse Response in an Immobilized Enzyme Column: Theoretical Method for Predicting Elution Curves" Biotech. Bioeng. XXII, pp. 779-797.

ANDERSEN, A.S. and WHITE, E.T. (1971). "Parameter Estimation by the Moments Method" Chem. Eng. Sci 26, pp. 1203-1221.

ANGAL, S. and DEAN, P.D.G. (1977). "The effect of matrix on the binding of albumin to immobilized Cibacron Blue" Biochem. J. 167, p. 301.

ANGAL, S. and DEAN, P.D.G. (1978). "The Use of Immobilized Cibacron Blue in Plasma Fractionation" FEBS Lett. 96, 346.

ARNOLD, F.H., BLANCH, H.W. and WILKE, C.R. (1985a). "Analysis of Affinity Separations I: Predicting the Performance of Affinity Adsorbers" The Chem. Eng. J. 30, B9-B23.

ARNOLD, F.H., BLANCH, H.W. and WILKES, C.R. (1985b). "Analysis of Affinity Separations II: The Characterization of Affinity Columns by Pulse Techniques" The Chem. Eng. J. 30, pp. B25-B36.

ARNOLD, F.H., SCHOFIELD, S.A. and BLANCH, H.W. (1986). "Analytical Affinity Chromatography I: Local Equilibrium Theory and Measurement of Association and Inhibition Constants. J. Chromatogr. 355, pp. 1-12.

AXEN, R., PORATH, J. and ERNBACK, S. (1967). "Chemical Coupling of Peptides and Proteins to Polysaccharides by Means of Cyanogen Halides" Nature 214, pp. 1302-1304.

BEISSNER, R.S. and RUDOLPH, F.B. (1978). "Immobilized Anthraquinone Dyes for Affinity Chromatography" J. Chromatogr. 161, pp. 127-135.

BETHELL, G.S., AYERS, J.S., HANCOCK, W.S. and HEARN, M.T.W. (1979). "A novel method of activation of cross-linked agaroses with 1,1'-carbonyl diimidazole which gives a matrix for Affinity Chromatography devoid of additional charged groups" J. Biol. Chem. 254(8), pp. 2572-2574.

BIRKENMEIER, G. and KOPPERSCHLAGER (1982). "Application of Dye-ligand Chromatography to the Isolation of -1-Proteinase Inhibitor and -1-acid Glycoprotein" J. Chromatography 235, pp. 237-240.

BISCHOFF, K.B. and LEVENSPIEL, O. (1962). "Fluid Dispersion-generalization and comparison of mathematical models I: Generization of Models. Chem. Eng. Sci. 17, pp. 245-255.

BOHART, G.S. and ADAMS, E.E. (1920). "Some aspects of the behaviour of charcoal with respect to chlorine" J. Am. Chem. Soc. 42, pp. 543-545.

BOHME, H-J., KOPPERSHLAGER, SCHULZ, J. and HOFMANN, E. (1972). "Affinity Chromatography of Phosphofructokinase using Cibacron Blue 3GA" J. Chromatogr. 69, pp. 209-214.

BONNERJEA, J. Oh, S., HOARE, M. and DUNNILL, P. (1986). "Protein Purification: The Right Step at the Right Time" Biotech. 4, pp. 954-958.

BRUNAUER, S., EMMETT, P.H. and TELLER, E. (1938). "Adsorption of gases in multimolecular layers" J. Am. Chem. Soc. 60, p. 309.

CERRO, R.L. and SMITH, J.M. (1970). "Chromatography of non adsorbable gases" A.I.ch.E. J. 16(6), pp. 1034-1038.

CHAMBERS, G.K. (1977). "Determination of Cibacron Blue 3GA Substitution in Blue Sephadex and Blue Dextran Sepharose" Anal. Biochem. 83, pp. 551-556.

CHASE, H.A. (198a). "Prediction of the Performance of Preparative Affinity Chromatography" J. Chromatogr. 297, pp. 179-202.

CHASE, H.A. (1984b). "Affinity Separations Utilising Immobilised Monoclonal Antibodies - A New Tool for the Biochemical Engineer" Chem. Eng. Sci. 39(7/8), pp. 1099-1125.

CHASE, H.A. (1984c). "Scale-up of Immunoaffinity Separation Processes" J. Biotech. 1, pp. 67-80.

CHASE, H.A. (1985). "Factors important in the design of fixed-bed adsorption processes for the purificationi of proteins", in: Discovery and Isolation of Microbial Products (Verrall, M.S., Ed.) Ellis Horwood Ltd., Chichester, pp. 129-147.

CHASE, H.A. (1986). "Automated Affinity Separation Processes" J. Chem. Tech. and Biotech. 36(8), pp. 351-356.

CHEN, L.F. and TSAO, G.T. (1976). "Physical Characteristics of Porous Cellulose Beads as Supporting Material for Immobilized Enzymes" Biotech. Bioeng. 18, p. 1507-1516.

CHEN, L.F. and TSAO, G.T. (1977). "Chemical Procedures for Enzyme Immobilization on Porous Cellulose Beads" Biotech. Bioeng. 19, pp. 1463-1473.

CLEMENTS, W.C.J.Y. (1969). "A note on determination of the parameters of the longitudinal dispersion model from experimental data" Chem. Eng. Sci. 24, pp. 957-963.

CIBA-GEIGY (1976) Handbooks on: Cibacron Dyes Exhaust Methods. Cibacron Dyes Pad Methods.

COHN, E.J., STRONG, L.E., HUGHES, W.L., MULFORD, D.J., ASHWORTH, J.N., MERLIN, M. and TAYLOR, H.L. (1946). "Preparation and Properties of Serum and Plasma Proteins IX: A System for the Separation into Fractions of the Protein and Lipoprotein Components of Biological Tissues and Fluids" J. Am. Chem. Soc. 68, pp. 459-475.

CUATRECASAS, P. WILCHECK, S. and ANFINSEN, C.B. (1968). "Selective Enzyme Purification by Affinity Chromatography" Proc. Nat. Acad. Sci. (U.S.A.) 61, p. 636.

CUATRECASAS, P. (1970a). "Agarose derivatives for purification of protein by Affinity Chromatography" Nature 228, pp. 1327-1328.

CUATRECASAS, P. (1970b). "Protein Purification by Affinity Chromatography: Derivatization of Agarose and Polyacrylamide Beads" J. Biol. Chem. 245, pp. 3059-3065.

CURLING, J.M. (1978). "Industrial Scale Gel Filtration and Ion Exchange Chromatography with Special Reference to Plasma Fractionation" in: Chromatography of Synthetic and Biological Polymers, (Epton, R., Ed.) Ellis Horwood Ltd. Ch. 6, pp. 75-87.

DANCKWERTS, P.V. (1953). "Continuous Flow Systems" Chem. Eng. Sci. 2, pp. 1-13.

DELANEY, M. and O'CARRA, P. (1974). "Lactate Dehydrogenase: Affinity Chromatographic Studies of the Relationshipo between Abortive Complex Formation and Oxaloacetate Inhibition. Biochem. Soc. Trans 2, pp. 1311-1313.

DWYER, J.L. (1984). "Scale-up of Bioproduct Separation with High Performance Liquid Chromatography" Biotech. 2, p. 957.

EVELEIGH, J.W. and LEVY, D.E. (1977). "Immunochemical Characteristics and Preparative Application of Agarose-Based Immunosorbents". J. Solid-Phase Biochem. 2(1), pp. 45-78.

FAN, L.T., CHEN, G.K.C. and ERICKSON, L.E. (1971). "Efficiency and Utility of Collocation Methods in Solving the Performance Equations of Flow Chemical Reactions with Axial Dispersion" Chem. Eng. Sci. 26, pp. 379-387.

FERGUSON, N.B. and FINLAYSON, B.A. (1970). "Transient Chemical Reaction Analysis by Orthogonal Collocation" Chem. Eng. J. 1, pp. 327-335.

FINLAYSON, B.A. (1969). "Applications of the method of weighted residuals and variational methods. 1". Brit. Chem. Eng. 14(1), pp. 53-57.

FINLAYSON, B.A. (1972). "The Method of Weighted Residuals and Variational Principles" Academic Press.

FINLAYSON, B.A. (1980). "Non linear analysis in Chemical Engineering" McGraw-Hill Int. Book Company.

FREUNDLICH, H. (1926). "Colloid and Capillary Chemistry", Methuen and Co. London.

FURUSAWA, T., SUZUKI, M. and SMITH, J.M. (1976). "Rate Parameters in Heterogeneous Catalysis by Pulse Techniques" Catal. Rev. Sci. Eng. 13(1), pp. 43-76.

GRAHAM, E.E. and FOOK, C.F. (1982). Rate of Protein Adsorption and Desorption on Cellulosic Ion Exchangers. A.I. Ch.E.J. 28(2), pp. 245-250.

GANGWAL, S.K., HUDGINS, R.R., BRYSON, A.W. and SILVESTON, P.L. (1971). "Interpretation of Chromatographic Peaks by Fourier Analysis" Canada J. Chem. Eng. 49, pp. 113-119.

HANFORD, R., MAYCOCK, W. d'A, VALLET (1978). "Separation of Human Albumin by Affinity Chromatography" in Chromatography of Synthetic and Biological Polymers (Epton, R., Ed.) Ellis Horwood Ltd., Ch. 23, pp. 288-291.

HANSEN, K.W. (1971). "Analysis of Transient Models for Catalytic Tubular Reactors by Orthogonal Collocation". Chem. Eng. Sci. 26, pp. 1555.

HASHIMOTO, N. and SMITH, J.M. (1973). "Macropore diffusion in molecular sieve pellets by Chromatography" Ind. Eng. Chem. Fundam. 12(3), pp. 353-359.

HAUGHEY, D.P. and BEVERIDGE, G.S. (1969). "Structural Properties of Packed Beds - A Review" Canad. J. Chem. Eng. 47, pp. 131-140.

HEYNS, W. and DEMOOR, P. (1974). "A 3(17) -hydroxysteroid dehydrogenase in Rats Erythrocytes Conversion of 5 -dihydro-stestrone into 5 -androstane-3 ,17 diol and purification of Enzyme by Affinity Chromatography" Biochemica et Biophysica Acta 358, pp. 1-13.

HIESTER, N.K. and VERMEULEN, T. (1952). "Saturation Performance of Ion-Exchange" Chem. Eng. Prog. 48(10), pp. 505-516.

HJERTEN (1962). "Chromatographic Separations according to Size of Macromolecules and Cell Particles on Columns of Agarose Suspensions" Arch. Biochem. Biophys. 99, pp. 466-475.

JANSON, J.C. and HEDMAN, P. (1982). "Chromatography of Proteins" in Advances in Biochem. Eng. (Fiechter, A., Ed.), Vol. 25, Springer Verlag, pp. 43-99.

JANSON, J-C (1984). "Large-Scale Affinity Purification - State of the Art and Future Prospects. Trends Biotech. 2(2), pp. 31-38.

JANSON, J-C. and HEDMAN, P. (1987). "On the Optimization of Process Chromatography of Proteins" Biotech. Prog. 3(1), pp. 9-13.

KAMIYANAGI, K. and FURUSAKI, S. (1985). "Analysis of Chromatography by Means of Transfer Functions" Int. Chem. Eng. 25(2), pp. 301-307.

KARANTH, N.G. and HUGHES, R. (1974). "Simulation of an Adiabatic Packed Bed Reactor" Chem. Eng. Sci. 29, pp. 197-205.

KATOH, S., KAMBAYASHI, T., DEGUCH, R. and YOSHIDA, F. (1978). "Performance of Affinity Chromatography Column" Biotech. Bioeng. 20, pp. 267-280.

KOPPERSCHLAGER, G., BOHME, H-J and HOFFMANN (1982). "Cibacron Blue F36-A and related Dyes as Ligands in Affinity Chromatography. In: Advances in Biochem. Eng. (Fiechler, A., Ed.), Vol. 25, pp. 101-138.

KUCERA, E. (1965). "Contribution to the theory of Chromatography Linear non-equilibrium elution Chromatography". J. Chromatog. 19, pp. 237-248.

LANGER, G., ROETHE, A.P., ROETHE, K.P. and GELBIN, D. (1978). "Heat and Mass Transfer in Packed Beds III: Axial Mass Dispersion". Int. J. Heat Mass Trans. 21, pp. 751-759.

LANGMUIR, I. (1918). "The adsorption of gases on plane surfaces of glass, mica, and platinum. J. Am. Chem. Soc. 60, p. 309.

LEATHERBAROW, R.J. and DEAN, P.D.G. (1980). "Studies on the Mechanism of Binding of Serum Albumins to Immobilized Cibacron Blue F3GA" Biochem. J. 189, pp. 27-34.

LEVENSPIEL, O. (1979). The Chemical Reactor Omnibook: Ch. 63, OSU Book Stores Inc. p.6.

LEVENSPIEL, O. (1972). "Chemical Reaction Engineering", 2nd Ed. Ch. 9, Wiley International, p. 276.

LIAPIS, A.I. and RIPPIN, W.T. (1978). "The Simulation of Binary Adsorption in Activated Carbon Columns Using Estimates of Diffusional Resistance Within Carbon Particles Derived from Batch Experiments". Chem. Eng. Sci. 33, pp. 593.

LIAPIS, A.I. and LITCHFIELD, (1980). "Ternary Adsorption in Columns". Chem. Eng. Sci. 35, p. 2366.

LKB (Trade Literature) (1983). "Utrogel^{R}, Magnogel^{R} and Trisacryl^{R} - Practical guide for use in Affinity Chromatography and Related Techniques". Reactifs IBF-Societe Pointet-Girard 35, Avenue Jean-Jaure's, 92390 Villeneuve-La-Garenne, France.

LOWE, C.R. and DEAN, P.D.G. (1974). "Affinity Chromatography" John Wiley and Sons Ltd.

LOWE, C.R., SMALL, D.A.P. and ATKINSON, A. (1981). "Some preparative and analytical application of Triazine dyes" Int. J. Biochem. 13, pp. 33-40.

LOWE, C.R. and STEAD, C.V. (1985). "The use of reactive dyestuffs in the isolation of Proteins" In: Discovery and Isolation of Microbial Products (Verrall, M.S., Ed.) Ellis Horwood Ltd., Chichester, pp. 149-158.

LOWRY, O.H., ROSEBROUGH, N.J., FARR, A.L., RANDALL, R.J. (1951). "Protein measurement with the Folin phenol Reagents" J. Biol. Chem. 193, pp. 265-275.

McCORMICK, D. (1987). "Currents in Chromatography" Biotech. 5, pp. 246-250.

MANDARO, R.M., ROY, S. and HOU, K.C. (1987). "Filtration Supports for Affinity Separation". Biotech. 5, pp. 928-932.

MARRAZZO, W.N., MERSON, R.L. and McCOY, B.J. (1975). "Enzyme Immobilized in a packed bed reactor: Kinetic parameters and Mass Transfer Effects" Biotech. Bioeng. XVII, pp. 1515-1528.

MARTIN, A.J.P. and SYNGE, R.L.M. (1941). "A new form of Chromatography employing two Liquid Phases". Biochem. J. 35, p. 1358.

MITRA, G. and NG, P.K. (1986). "Practice of Ultrafiltrationi-Diafiltration. In: The Plasma Fractionation Industry". In. Membrane Separations in Biotechnology (McGregor, W.C., Ed.) Marcel Dekker Inc., N.Y.

MOSBACH, K., GUILFOR, H., OHLSSEN, R. and SCOTT, M. (1972). "General Ligands Affinity Chromatography".

NISHIWA, A.H. (1975). "Affinity Purification of Enzymes" Chemtech. (Sept. 1974), pp. 564-571.

O'CARRA, P. and BARRY, S. (1972). "Affinity Chromatography of Lactate Dehydrogenase (LDHI)" FEBS Lett. 21(3), pp. 281-285.

OSTERGAARD, K. and MICHELSEN, M.L. (1969). "On the use of the imperfect tracer pulse method for determination of HOLD-UP and AXIAL MIXING" Canad. J. Chem. Eng. 47, pp. 107-112.

PARIKH, I. and CUATRECASAS P. (1985). "Affinity Chromatography" C and EN pp. 17-32.

PESKA, J., STAMBERG, J., HRADIL, J. and ILAVSKY, M. (1976). "Cellulose in Bead Form - Properties Related to Chromatographic Uses" J. Chromatogr. 125, pp. 455-469.

PHARMACIA FINE CHEMICALS (Trade literature) (1983). "Affinity Chromatography - Principles and Methods" Pharmacia Fine Chemicals Ltd., Uppsala, Sweden.

PORATH, J. and FLODIN, P. (1959). "Gel Filtration: A method for Desalting and Group Separations" Nature 183, pp. 1657-1659.

PORATH, J., AXEN, R. and ERNBACK, (1967). "Chemical Coupling of Proteins to Agarose" Nature 215, pp. 1491-1492.

RAGHAVAN, N.S. and RUTHVEN, D.M. (1983). "Numerical Simulation of a Fixed-Bed Adsorption Column by the Method of Orthogonal Collocation" Alch. E. J. 29, No. 6, pp. 922-925.

RAMACHANDRAN, P.A. (1974). "A General Model for the Packed Bed Encapsulated Enzyme Reactor" J. Appl. Chem. Biotechnol. 24, pp. 265-275.

ROBINSON, P.J., DUNNILL, P. AND LILLY, M.D. (1972). "Factors Affecting Scale-up of Affinity Chromatography of β-galactosidase" biochiem. Biophys. Acta 285, pp. 28-35.

ROBINSON, P.J., WHEATLEY, M.A., JANSON, J-C., DUNNILL, P. and LILLY, M.D. (1974). "Pilot Scale Affinity Chromatography: Purification of -galactosidase" Biotech. Bioeng. 16, pp. 1103-1112.

RIVITO, B.J. and KITTRELL, J.R. (1973). "Film and Pore Diffusion Studies with Immobilized Glucose Oxidase" Biotech. Bioeng. XV, pp. 143-161.

SADA, E., KATOH, S., SUKAI, K., TOHMA, M. and KONDO, A. (1986). "Adsorption Equilibrium in Immuno-Affinity Chromatography with Polyclonal and Monoclonal Antibodies. Biotech. Bioeng. XXVIII, pp. 1497-1502.

SCHNEIDER, P. and SMITH, J.M. (1968). "Adsorption Rate Constants from Chromatography" AlchE.J. 14(5), pp. 762-771.

SEINFIELD, J.H. and LAPIDUS, L. (1974). "Process Modelling, Estimation and Identification", In: Mathematical Methods in Chemical Enginering, Vol. 3. Prentice-Hall Inc., New Jersey.

SIROTTI, D.A. and EMERGY, A. (1983). "Mass Transfer Parameters in An Immobilized Glucoamylase Column by Pulse Response Analysis" Biotech. Bioeng. XXV, 1773-1779.

SMALL, D.A.P., ATKINSON, A. and LOWE, C.R. (1983). "Preparative High-Performance Liquid Affinity Chromatography". J. Chromatogr. 266, pp. 151-156.

SODERMAN, D.D., GERMERSHAUSEN, J. and KATZEN, H.M. (1973). "Affinity Binding of Intact Fat Cells and their Ghosts to Immobilized Insulin" Proc. Nat. Acad. Sci. (USA) 70(3), pp. 792-796.

SOUTHERN, D. and HOLLIS, D. (1986). "Fast Affinity Chromatography" BioTech. 4, pp. 519-521.

SPORTSMAN, J.R., LIDDLL, J.D. and WILSON, G.S. (1983). "Kinetic and Equilibrium Studies of Insulin Immunoaffinity Chromatogrphy" Anal. Chem. 55(4), pp. 771-775.

STEAD, C.V. (1987). "The Use of Reactive Dyes in Protein Separation Processes" J. Chem. Tech. Biotechnol. 37, pp. 55-71.

SUZUKI, M. and SMITH, J.M. (1972). "Axial Dispersion in Beds of Small Particles. Chem. Eng. J. 3, pp. 256-264.

THOMAS, H.C. (1944). "Heterogeneous Ion Exchange in A Flowing System" J. Amer. Chem. Soc. 66, pp. 1664-1666.

THOMAS, H.C. (1948). "Chromatography: A problem of Kinetics" Ann. N.Y. Acad. Sci. 49(1), pp. 161-182.

TRAYER, I.P., HOLROYDE, M.J., SMALL, D.A.D., TRAYER, H.R. and WRIGHT, C.L. (1978). "Design of Affinity Chromatography Systems from Free Solution Kinetics" In: Chromatography of Synthetic and Biological Polymers. Vol. 2 (Epton, R., Eds.)

TSOU, H. and GRAHAM, E.E. (1985). "Prediction of Adsorption and Desorption of Protein on Dextran based Ion-Exchange Resin" A.I.Ch.E. J. 31(12), pp. 1959-1966.

URBAN, J.C. and GOMEZPLATA, A. (1969). "Axial Dispersion Coefficient in Packed Beds at Low Reynolds Numbers". Canadian J. Chem. Eng. 47, pp. 353-359.

VAN DER LAAN, E.T. (1958). "Notes on the Diffusio-type Model for Longitudinal Mixing in Flow. Chem. Eng. Sci. 7, pp. 187-191.

VERMEULEN, T. (1958). "Separation by Adsorption Methods". In: Advances in Chemical Engineering, Vol. 2 (Brew, T.B., and Hoopes Jr, J.W., Eds.) Academic Press Inc., N.Y., pp. 147-208.

VERMEULEN, T., KELEIN, G. and HEISTER, N.K. (1963). "Adsorption and Ion Exchange" In: The Chemical Engineers Handbook (Perry, R.H. and Hilton, C.H., Eds) 5th Edition, McGraw-Hill, N.Y.

VERMEULEN, T. and LE VAN, M.D. (1984). "Adsorption and Ion-Exchange", In: Chemical Engineers' Handbook, 6th Ed., Chp. 16,

Perry, R.H., Green, D.W. and Maloney, J.O., Eds.) McGraw-Hill, N.Y.

VILLADSEN, J. (1970). "Selected Approximation Methods for Chemical Engineering Problems" Instituttet Kemiteknik, Denmarks tekniske Hojskole.

VILLADSEN, J.V. and STEWART, W.E. (1967). "Solution of Boundary-Value Problems by Orthogonal Collocation" Chem. Eng. Sci. 22, pp. 1483-1501.

VILLADSEN, J. and MICHELSEN, M.L. (1978). "Solution of Differential Equation Models by Polynomial Approximation", Prentice-Hall Inc., New Jersey.

WALTERS, R.R. (1985). "Affinity Chromatography" Anal. Chem. 57(11), pp. 1099A-1113A.

WAKAO, N., TANAKA, K. and NAGAI, H. (1976). "Measurements of particle-to-gas mass transfer coefficients from chromatographic adsorption experiments" Chem. Eng. Sci. 31, pp. 1109-1113.

WAKAO, N. and KAGUEI, S. (1982). "Heat and Mass Transfer in Packed Beds" Chp. 2, Gorden and Breach Science Publishers, p. 78.

WANKAT, P.C. (1974). "Theory of Affinity Chromatography Separations" Anal. Chem. 46(11), pp. 1400-1408.

WEBER, T.W. and CHAKRAVORTI, R.K. (1974). "Pore and Solid Diffusion Models for Fixed-Bed Adsorbers" A.I.Ch.E.J. 20(2), pp. 228-238.

WEHNER, J.F. and WILHELM, R.H. (1956). "Boundary Conditions of Flow Reactors" Chem. Eng. Sci. 6, p. 89.

WILSON, E.J. and GEANKOPLIS, C.J. (1966). "Liquid mass transfer at very low Reynolds numbers in packed beds" Ind. Eng. Chem. Fund. 5, p. 9.

YANG, C-M. and TSAO, G.T. (1982). "Packed Bed Adsorption Theories and their application to Affinity Chromatography" In: Adv. Biochem. Eng. Vol. 25, (Fiechter, A., Ed.) Springer-Verlag, N.Y., pp. 1-42.

YOUNG, M.E., CARROAD, P.A. and BELL, R.L. (1980). "Estimation of Diffusion Coefficients of Proteins" Biotech. Bioeng. XXII, pp. 947-955.

NOMENCLATURE

Symbol	Description	Units
A	Cross sectional area of bed	cm^2 , m^2
A	Molecule of adsorbate	(-)
$\bar{A}$	Collocation constant for the derivative for bulk liquid	(-)
A_A	Area covered by complex between adsorbate and ligand	$cm^2/\mu mole$
AB	Complex between adsorbate and adsorbent	(-)
A_{ij}, A'_{ik}	Collocation constant for the derivative for the bulk liquid	(-)
a_i	Coefficient of polynomial	(-)
a_v	External surface area of particle per unit volume of bed	m^{-1}
B	Biospecific binding site on adsorbent	(-)
B, $\bar{B}$	Laplacian collocation constant for	
B_{ij}, B_{ik}	bulk liquid and particle respectively	(-)
B_o	Original concentration of ligand (Wankat's equation)	$cm^3/\mu mole$
$\bar{C}$, C_{ji}	Matrix (equation 5.17 and 5.22)	(-)
$C_{(N)}$	Constant in equation 95.10)	(-)
c	Concentration of adsorbate in solution	mg/ml or kg/m^3
c*	Equilibrium concentration of adsorbate in solution	"

Symbol	Description	Units
Δc_{max}	Concentration difference between max. and min.	mg/ml or kg/m^3
$\bar{c}$	Dimensionless concentration of adsorbate in solution	(-)
$\bar{c}$	Concentration vector (equation 5.15)	(-)
c(p,x), c(p,ℓ)	Laplace transform of adsorbate concentration in solution, c	(-)
$\bar{c}'$	Laplace transform of dimensionless concentration, c	(-)
c_a	Macropore fluid phase concentration of adsorbate	kg/m^3
c_i	Micropore fluid phase concentration of adsorbate	kg/m^3
c_o	Initial concentration of adsorbate	"
c_p	Dimensionless pore fluid phase concentration	(-)
D_a	Macropore diffusivity	m^2/s
D_e	Effective pore diffusivity	"
D_i	Micropore diffusivity	"
D_L	Axial diffusivity	"
D_m	Free solution diffusivity	"
$\bar{D}, D_{ji}$	Matrix in equation (5.15)	(-)
e	Exponential	(-)
F	Differential equation operator in Eqn. (5.1)	(-)
f(t)	Pulse function	(-)
G	Differential equation operator in eqn. (5.2)	(-)
I_N	Integral (N = 0, 1, 2....)	(-)

Symbol	Description	Units
j_D	Colburn and Chilton Factor	(-)
K	Kelvin temperature	K
k	Film mass transfer coefficient	m/s
k'	Volumetric mass transfer coefficient	s^{-1}
k_A	Dimensionless forward rate constant	(-)
k_{AB}	Dissociation constant (Wankat's equation, 4.2a)	$mole/cm^3$
k_B	Dimensionless backward rate constant	
k_E	Dimensionless dissociation constant (k_d/c_0)	(-)
k_F	Constant in equation 4.1 (Freundlich equation)	m^3/kg
k_a	Adsorption rate constant (equation 4.26)	$m^3/kg.s$
k_d	Dissociation constant	kg/m^3
k_f	Dimensionless film mass transfer coefficient	(-)
k_m	Adsorption equilibrium constant (eqn. 4.11, 4.15 and appendix 3) for linear isotherm	m^3/kg
k_1	Forward rate constant	$m^3/kg.h$
k_2	Backward rate constant	s^{-1}
L	Laplace transform operator	(-)
ℓ	Length of bed (or reference length)	m
ℓ_i	Lagrange interpolation polynomial	(-)
M	Degree of orthogonal polynomial (lower degree)	(-)
Ma	Mass	kg
M.Wt.	Molecular weight	Dalton
M1	Reciprocal of Peclet number	(-)
m	Total number of collocation points for non-symmetrical system	(-)
N	Degree of orthogonal polynomial (higher degree) or number interior collocation points	(-)

Symbol	Description	Units
N_D	Dispersion number	(-)
N_O, N_F	Flux per unit area	$kg/m^2 s$
N_1	Dimensionless parameter $\left(\frac{D_e}{R^2} \cdot \frac{\ell}{u}\right)$	(-)
n	Number of interior collocation points	(-)
Pe	Peclet number	(-)
P_{i-1}	Orthogonal polynomial	(-)
$P_M(x)$	Orthogonal polynomial of degree M in x	(-)
$P_N(x)$	Orthogonal polynomial of degree N in x	(-)
p	Laplace transform parameter	(-)
Q	Volumetric flow rate	kg/m^3
$Q, Q_{ji}, \bar{Q}$	Matrix in equations 5.15 and 5.16	(-)
$Q^{-1}, \bar{Q}^{-1}$	Matrix in equation 5.17	(-)
q	Solid phase concentration of adsorbate	kg/m^3 or kg/kg
$\bar{q}$	Dimensionless solid phase concentration of adsorbate	"
$\bar{q}'$	Laplace transform of q' (appendix 3)	(-)
q*	Equilibrium concentration of q	kg/m^3 or kg/kg
q_a	Macropore solid phase concentration	kg/m^3
q_b	Solid phase concentration in terms of bed volume	kg/m^3 of bed
q_i	Micropore solid phase concentration	kg/m^3
q_m	Maximum solid phase concn for adsorbate	kg/m^3 or kg/kg
q_p	Solid phase concentration of adsorbate in terms of particle vol.	kg/m^3 of particle

Symbol	Description	Units
q_w	Solid phase concn. of adsorbate in terms of dry wt. of adsorbent	kg/kg
R	Particle radius	m)
R_h	Hydraulic radius	m
R_a,R_v, $R_a(c)$, $R_v(c)$	Rate expression for adsorption	(-)
Re_p	Particle Reynolds number	(-)
r	Radial coordinate in particle	m
r_a	Macropore radius	m
r_i	Micropore radius	m
Sc	Schmidt number	(-)
Sh	Sherwood number	(-)
t	Time	h,min,s
$\bar{t}$	Residence time	"
$\bar{t}_b$	Bed retention time	"
$\bar{t}_{BD}$	Retention time for blue dextran	"
t_{BSA}	Retention time for BSA	"
t_i	ith time	"
Δt_i	ith time interval	"
u_o	Superficial velocity	m/s
u	interstitial velocity	m/s
V	Batch or bed volume	m^3
V_o	Void volume of bed	m^3
V_i	Internal void volume of bed	m^3
V_t	Total bed volume	m^3

Symbol	Description	Units
W(t),	Weight factor	(-)
w(x)	Weight factor	(-)
x	Axial position along bed	m
x_j	Collocation point along the length of column	m
$\bar{x}$	Vector of x	(-)
Y,Y(x)	Approximating polynomial	(-)
Y_N	Trial polynomial	
y	Dimensionless radial position	
y_i	Ordinate point	
y_k	Collocation point in radial position	
z	Dimensionless distance x/ℓ	

Greek Letters

α, β	Index of Legendre and Jacobi polynomial	(-)
β	Dimensionless concentration (q_m/c_o)	(-)
δ_{NM}	Kronecker delta	(-)
ϵ	External voidage	(-)
ϵ_a	Macropore voidage	(-)
ϵ_i	Internal voidage	(-)
ρ	Fluid density	kg/m^3
ρ_s	Bed packing density	kg/m^3
μ	Viscosity of fluid	kg/ms
μ_1	First absolute moment	s
μ_2'	Second central moment	s
ϕ_n	Polynomial function	(-)
τ	Tortuosity	(-)
θ	Dimensionless time	(-)
∇	Differential operator	(-)

APPENDICES

APPENDIX 1

(a) Polyacrylamide Gel Electrophoresis

PREPARATION OF REAGENTS

(1) Acrylamide/Bis-Acrylamide

16 g of acrylamide and 0.5 g of bisacrylamide were dissolved in 100 mls of distilled water.

(2) Tris-HCl-Temed Buffer, pH 8.9

36.3 g Tris was added to about 48 mls of 1 M HCl to give a pH of 8.9. The solution was mixed with 0.46 ml TEMED and the resulting solution made up to 100 mls with distilled water.

(3) Reservoir Buffer, pH 8.9

6 g of Tris and 28.8 g glycine were added to about a litre of distilled water. The pH was adjusted to 8.9 with NaOH and the solution made up to 1 litre.

(4) TEMED Solution

Prepared on the day of use by mixing 0.1 ml TEMED with 9.9 ml of distilled water.

(5) Persulphate Solution

0.245 g of ammonium persulphate was prepared on the day of use by adding to 25 mls of distilled water.

(6) Fixing Solution

12 g of trichloroacetic acid was added to 86 mls of distilled water to give a 12% solution.

(7) Staining Solution

50 mg of amido black was added to 15% acetic acid in distilled water.

(8) Destaining Solution

7 mls of acetic acid was mixed with 93 ml of water to give a 7% solution.

(9) Sucrose Solution

2.5 g of sucrose was added to 22.5 ml of distilled water to give a 5% solution.

(10) Bromophenol Blue

5 mg of bromophenol blue was added to 50 mls of water to give an 0.01% solution.

(c) PREPARATION OF GELS

The capacity of the gel racks is twelve and the following recipe usually gave enough gels for the twelve tubes.

The gel was prepared by adding the following stock solutions in a 100 ml beaker in the order shown below.

3.5 ml of water, 8.5 ml of acrylamide/Bis, 1.6 Tris-HCl buffer/TEMED, 1 ml TEMED solution and 1.4 ml persulphate solution.

A hypodermic syringe was used to fill the 7.5 mm x 5 mm tubes which were stoppered at the bottom with size 5 rubber bungs. With polyacrylamide soution care was taken not to entrap air bubbles in

the gel by filling slowly through the wall sides from the tube top. Each tube was filled to about 5 mm from its top. To ensure a flat smooth gel end, water was used to fill up the tubes completely before the polymerization reaction was completed. Before the filling operation, the tubes were fitted in the apparatus reading for use leaving the top of the tubes some 10 mm from the base of the upper chamber. Gelling usually took some 1½-2 hrs.

(d) PREPARATION OF SAMPLES

The sample for electrophoresis was prepared by pipetting 100 µl of a 1 g/l sample into 0.8 ml of 5% sucrose solution. The resulting solution was mixed with 4 drops of the bromophenol blue.

The bromophenol blue acts as a marker of the advancing front of the sample while the sucrose is used to weigh down the sample when applying it to the top of the tubes.

(e) ELECTROPHORESIS OPERATION

The top and bottom sections of the electrophoresis apparatus (see Fig. 3.11) were filled to appropriate levels with 1:10 diluted reservoir buffer. The bottom section was filled up to the level so that about 20 mm of the bottom of the tubes were immersed when the top section was positioned and the top section filled to the level so that the top electrode was fully immersed when placing the top lid in position.

A 100 µl autopipette, equipped with disposable tips was used, to add very carefully, 200 µl of sample to the top of the tubes. Each sample was added with a new tip in order to avoid cross

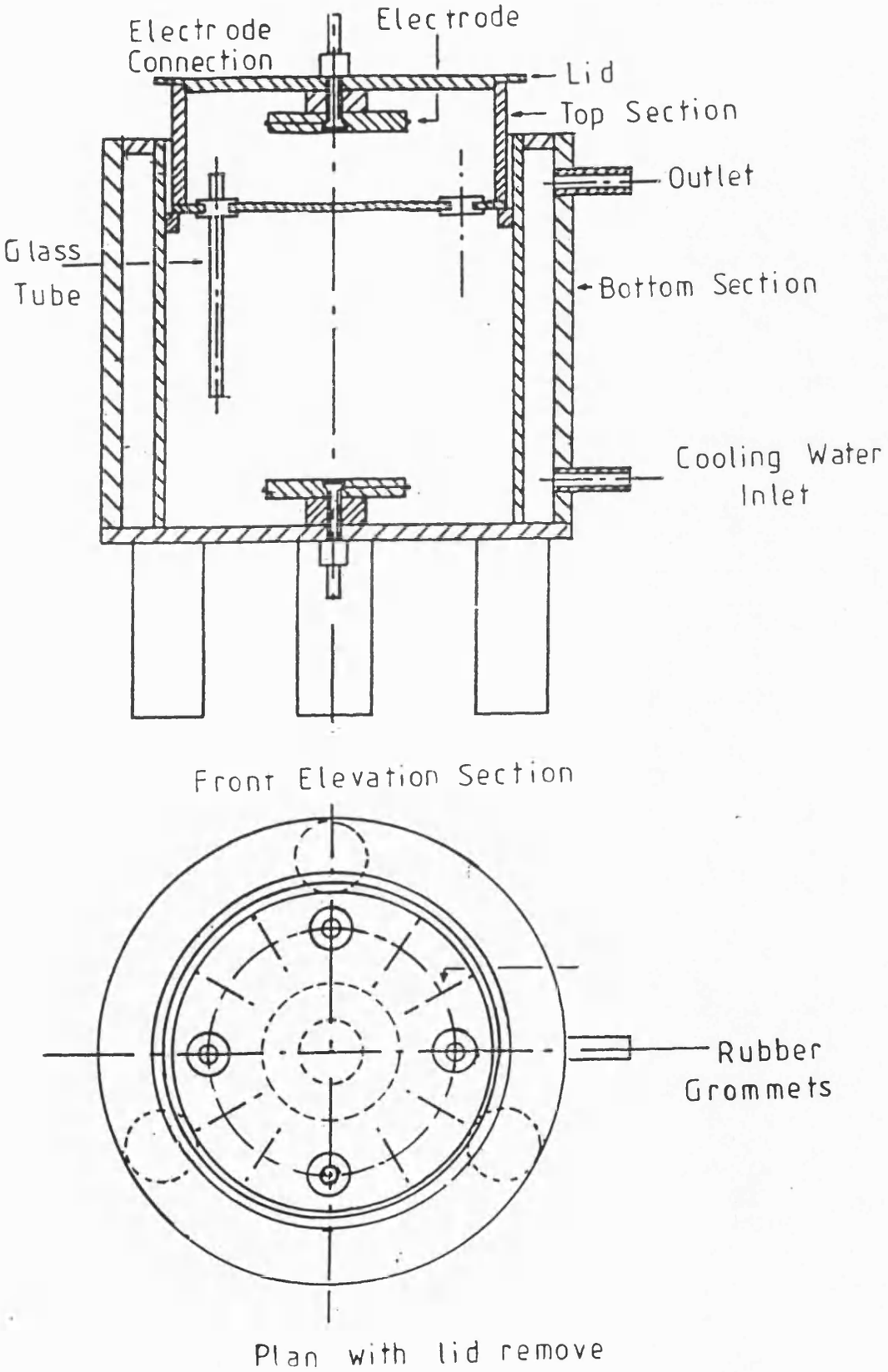

Fig. A1. Electrophoresis Apparatus.

contamination.

After the lid had been put in place and the electrodes connected to a Shandon power supply - positive electrode to the base and negative electrode at the top - the power supply was switched on. The power supply unit was operated in the variable current mode. Each run was performed at 4 mA per tube (48 mA for full loading of apparatus) and at room temperature. Constant current supply was maintained by adjusting the current with a dial and the progress of the marker front watched until the marker reached the tube bottom. The power was then switched off.

(f) GEL TREATMENT

On completion of the electrophoresis run, the tubes were removed and placed in an ice bucket so that the gels contracted. The gels were removed by injecting ice cold water, with a hypodermic syringe, around the inner periphery of the tube. The tube was rotated at the same time as the injection of water, using the needle to probe around the tube periphery.

After rinsing the gels with distilled water, it was placed in TCA solution for 30 to 45 minutes to fix the protein in the gel.

After fixing, and rinsing with distilled water, the gels were stained with amido black solution for 1 hr.

The gels were then destained by soaking in 7% acetic acid solution for at least 6 hrs.

The gels were then placed in the SP400 spectrophotometer densitometer and scanned at an absorbance of 540 nm and a chart speed of 20 cm/s.

(b) Some Physical Properties of the Blue Sponge Related to Use as an Adsorbent

(i) Density

The density of the blue sponge for batch operations was determined as follows:

Blue sponge was cut into very small pieces and then soaked overnight in distilled water. Thoroughly wet blue sponge was placed in 10 cm^3 density bottle and weighed. The sponge was then removed and dried in an oven at 120°C for 2 hrs. Density was measured as g dry weight of sponge/volume. The value obtained with three measurements was

$$0.05103 \pm 0.0002 \text{ g dry wt/cm}^3$$

(ii) Voidage

Voidage or porosity was defined as volume fraction of solvent in the swollen sample. From (i) the average swollen sample weight was 9.868 g and the dry weight was 0.5103 g. Assuming the density of water to be 1 g/cm^3, the volume fraction of water in swollen sponge was

$$(9.8679 - 0.5103)\ cm^3 = 9.3576\ cm^3$$

therefore,

$$\text{porosity or voidage} = \frac{9.3576\ cm^3}{10\ cm^3} \simeq 0.94$$

(iii) Microsopic structure of sponge

Photograph A1 shows the microscopic structure of the sponge at two different magnifications.

Microscopic structure of sponge at low magnification.

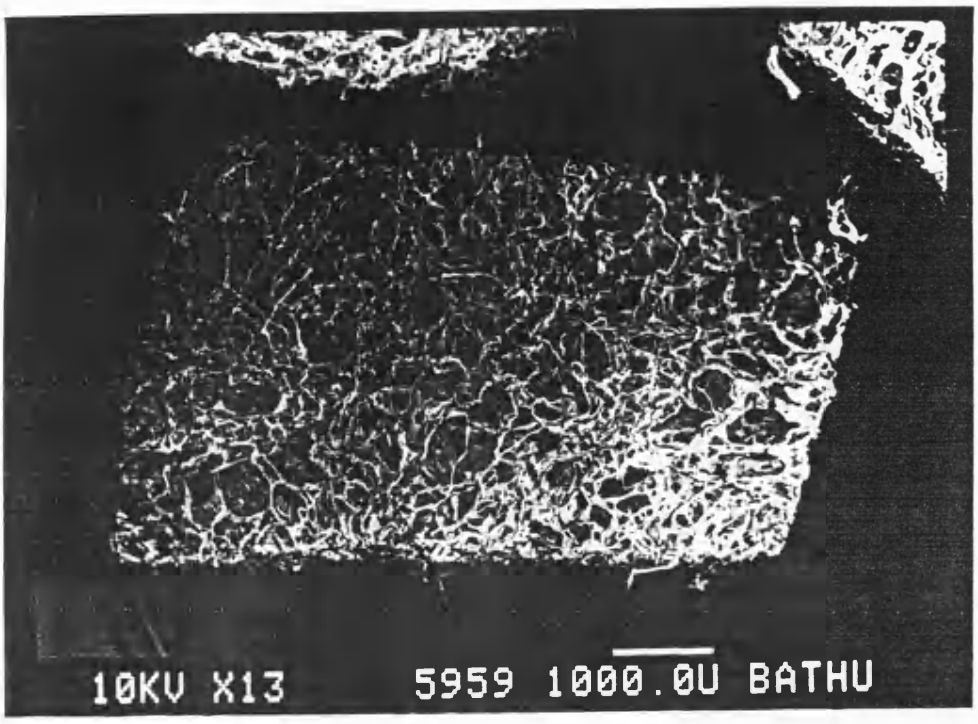

Photograph A1.

APPENDIX 2

AXIALLY DISPERSED PLUG FLOW MODELS FOR PACKED BEDS

I. CONTINUITY EQUATIONS

A. Non-Porous Particle Model

The model to be used to describe the affinity membrane according to the axially dispersed model for flow of adsorbate solutions through a bed of non-porous particles is depicted in Fig. 1. The bulk liquid has a solute concentration c with a volumetric flow rate Q through a bed of length L, with cross-sectional area, A and void fraction, ε. The solute concentration in the solid phase is q and the interstitial velocity u ($= Q/A\varepsilon$)

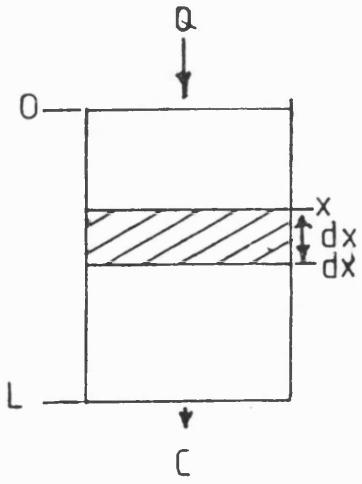

Fig. 1. Model of sponge column

A material balance on the mobile phase in Fig. 1 on the elemental volume of height dx is given by the general mass conservation of the form

$$(\text{flux in}) - (\text{flux out}) + \left(\begin{matrix}\text{Rate of solid}\\ \text{phase}\\ \text{accumulation}\end{matrix}\right) = \left(\begin{matrix}\text{Net rate of accumulation}\\ \text{in the fluid phase}\end{matrix}\right)$$

flux of solute into boundary dx = $uAc\varepsilon + N_F A\varepsilon$

(bulk flow) (diffusion)

flux of solute out of boundary x+dx = $(uAc\varepsilon + AN_F\varepsilon) + \frac{\partial}{\partial x}(uAc\varepsilon + AN_F\varepsilon)dx$

Rate of uptake of solute by adsorption = $- R_a A (1-\varepsilon) dx$

Accumulation of A inside the fluid = $\frac{\partial}{\partial t} (Ac\varepsilon dx)$

where N_F = diffusional flux/unit area = $- D_L \frac{\partial c}{\partial x}$

and R_a = rate of mass transfer onto adsorbent = $\frac{\partial q}{\partial t}$

Assuming that the diffusion coefficient D_L and velocity u are constant and substituting into the mass conservation relation gives:

$$\varepsilon A\, dx \frac{\partial c}{\partial t} = (uAc\varepsilon + AN_F\varepsilon) - [(uAc\varepsilon + AN_F\varepsilon) + \frac{\partial}{\partial x}(uAc\varepsilon + AN_F\varepsilon)\, dx - (1-\varepsilon)R_a A dx$$

$$\varepsilon A\, dx \frac{\partial c}{\partial t} = - \frac{\partial}{\partial x}(uAc\varepsilon + AN_F\varepsilon)\, dx - R_a\, dx\, A(1-\varepsilon)$$

$$\varepsilon \frac{\partial c}{\partial t} = - \frac{\partial}{\partial x}(uc\varepsilon + N_F\varepsilon) - R_a(1-\varepsilon) \qquad ...(1a)$$

Since $N_F = - D_L \frac{\partial c}{\partial x}$ equation (1a) becomes;

$$\varepsilon \frac{\partial c}{\partial t} = D_L \varepsilon \frac{\partial^2 c}{\partial x^2} - \varepsilon u \frac{\partial c}{\partial x} - R_a(1-\varepsilon)$$

or

$$\frac{\partial c}{\partial t} = D_L \frac{\partial^2 c}{\partial x^2} - u \frac{\partial c}{\partial x} - \frac{1-\varepsilon}{\varepsilon} \frac{\partial q_p}{\partial t} \qquad ...(1)$$

define q = dry weight solid phase concentration (kg/kg dry wt.)

$q_p = \frac{q\rho_s}{1-\varepsilon}$ = solid phase concentration based on particle volume (kg/m^3)

$q_b = q_p(1-\varepsilon)$ = solid phase concentration based on bulk volume of bed (kg/m^3)

Equation (1) can be re-written as

$$\frac{\partial c}{\partial t} = D_L \frac{\partial c}{\partial x^2} - u \frac{\partial c}{\partial x} - \frac{\rho_s}{\epsilon} \frac{\partial q}{\partial t} \quad \ldots(1b)$$

$$\frac{\partial c}{\partial t} = D_L \frac{\partial^2 c}{\partial x^2} - u \frac{\partial c}{\partial x} - \frac{1}{\epsilon} \frac{\partial q_b}{\partial t} \quad \ldots(1c)$$

Where ρ_s is the bulk volume density (kg/m^3)

B. Porous Particle Model

If the assumptions of the non-porous model that infinite intraparticle mass diffusivity exists and hence no intraparticle solute concentration gradients are relaxed. Assuming that the sponge particles are porous sponge packing can be depicted as in Fig. 2.

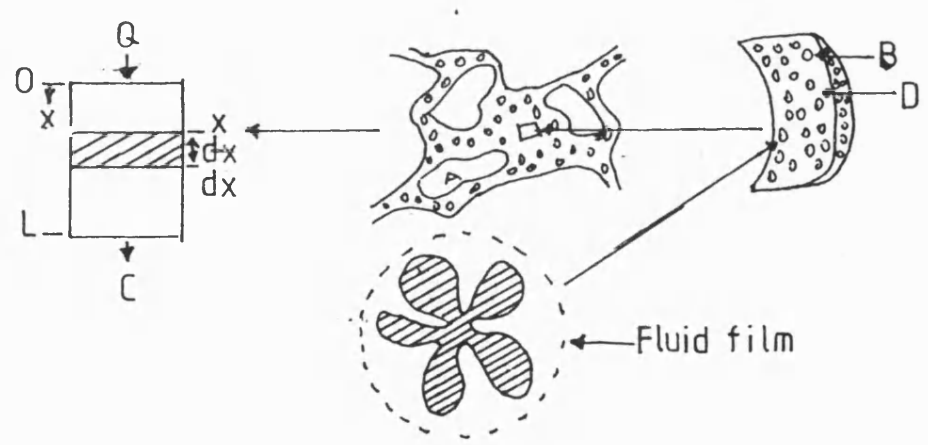

A = macropore

B = micropore

D = sponge particle

Fig. 2. Porous particle model to describe sponge affinity column.

The bulk liquid has a solute concentration (c (x,t))with a volumetric flow rate,Q (m^3/s) through a bed of length ℓ, with cross-sectional area A(m^2) and external void fraction, ε. The average solid phase concentration is $\bar{q}$ (ncludes pore concentration), the superficial velocity,(u_0) is given by $u_0 = Q/A$.

For individual particles, they are assumed to be approximately spherical with radius R, internal voidage ε_i, the particle concentration is $q_i(r, x, t)$ and the pore solute concentration is $c_i(r, x, t)$.

(i) Exernal Field Mass balance

A mass balance over a secion of the column dx yields the continuity relation as for the non-porous particle mass balance which can be written as

$$\varepsilon \frac{\partial c}{\partial t} = D_L \frac{\partial^2 c}{\partial z^2} - u_0 \frac{\partial c}{\partial z} - 1 - \varepsilon \quad \frac{\partial \bar{q}}{\partial t} \qquad \ldots(2a)$$

but the rate of change in the average particle concentration $(1-\varepsilon \frac{\partial \bar{q}}{\partial t})$ = flux of solute into the pores. That is,

$$(1-\varepsilon) \frac{\partial \bar{q}}{\partial t} = \frac{3(1-\varepsilon)}{R} N_0$$

$$= a_v N_0$$

$$= a_v D_e \frac{\partial c_i}{\partial r} \Big|_{r=R}$$

where $a_v = \frac{3(1-\varepsilon)}{R}$ = Surface area of particles per unit bed volume (m^{-1})

N_0 = solute flux per unit surface area of the particles

and

D_e = effective pore diffusion coefficient ($m^2 s^{-1}$) (based on entiure particle volume).

Equation (2a) becomes;

$$\varepsilon \frac{\partial c}{\partial t} = D_L \frac{\partial^2 c}{\partial x^2} - u_o \frac{\partial c}{\partial} - \frac{3(1-\varepsilon)}{R} D_e \frac{\partial c_i}{\partial r}\Big|_{r=R} \quad \ldots(2)$$

(ii) Single Particle Mass Balance

Assuming that approximate spherical sponge particles are about equal in size, average pore is representative of all pores in the particle and that diffusional mass transfer is governed by Fick's Law, a mass balance on a spherical shell as shown in Fig. 3 over elemental shell bounded by r and r + dr is as follows

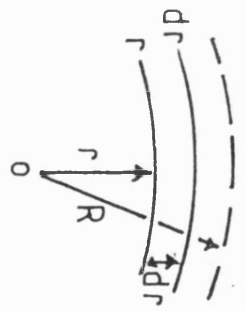

Fig. 3. Particle mass balance over a spherical shell.

Using the same form of mass conservation as for external field mass balance, namely:

Net rate of solute accumulation in pore fluid	=	Solute flux into the system	−	Solute flux out of system	+	Rate of solute uptake by adsorption

flux in at boundary, r = $AN_F = A\left(-D_e \frac{\partial c_i}{\partial r}\right)$

flux out at boundary r + dr = $A\left(-D_e \frac{\partial c_i}{\partial r}\right) + \frac{\partial}{\partial r}\left(-D_e A \frac{\partial c_i}{\partial r}\right)dr$

flux in - flux out = $A\left(-D_e \frac{\partial c_i}{\partial r}\right) - \left\{A\left(-D_e \frac{\partial c_i}{\partial r}\right) + \frac{\partial}{\partial r}\left(-D_e A \frac{\partial c_i}{\partial r}\right)dr\right\}$

$$= -\frac{\partial}{\partial r}\left(-D_e A \frac{\partial c_i}{\partial r}\right) dr$$

Net rate of solute accumulation in the pore fluid

$$= \frac{\partial}{\partial} \left(\varepsilon_i A\, c_i\right) dr$$

Rate of solute accumulation on solid surface = $R_v A\, dr$

but $A = 4\pi r^2$ and $R_v = \partial q_i / \partial t$

$$\varepsilon_i \cancel{4\pi} r^2 \cancel{dr} \frac{\partial c_i}{\partial t} = -\frac{\partial}{\partial r}\left(D_e \cancel{4\pi r^2} \frac{\partial c_i}{\partial r}\right)\cancel{dr} - R_v \cancel{4\pi} r^2 \cancel{dr}$$

$$\varepsilon_i \frac{\partial c_i}{\partial t} = -\frac{1}{r^2} \frac{\partial}{\partial r}\left(-D_e r^2 \frac{\partial c_i}{\partial r}\right) - \frac{\partial q_i}{\partial t} \qquad \ldots(3)$$

The continuity equations for the porous particle model in an axially dispersed plug flow is summarised as follows

External field equation

$$\varepsilon \frac{\partial c}{\partial t} = D_L \frac{\partial^2 c}{\partial x^2} - u_o \frac{\partial c}{\partial x} - \frac{3(1-\varepsilon)}{R} D_e \frac{\partial c_i}{\partial r}\Big|_{r=R} \qquad \ldots(2)$$

Particle equation

$$\varepsilon_i \frac{\partial c_i}{\partial t} = \frac{1}{r^2} \frac{\partial}{\partial r}\left(D_e r^2 \frac{\partial c_i}{\partial r}\right) - \frac{\partial q_i}{\partial t} \qquad \ldots(3)$$

APPENDIX 3

AXIALLY DIPERSED PLUG FLOW MODEL FOR PACKED BEDS

II. PARAMETER ESTIMATION BY METHOD OF MOMENTS

Non-Porous Particle Model

The fundamental equation according to the dispersed plug flow model (appenxix 2) is

$$D_L \frac{\partial^2 c}{\partial x^2} - u \frac{\partial x}{\partial x} - \frac{\partial c}{\partial t} - \frac{(1-\epsilon)}{\epsilon} \frac{\partial q}{\partial t} = 0 \qquad \ldots(1)$$

Where

D_L = coefficient of axial dispersion (m^2/s)

ϵ = voidage of the bed (-)

u = fluid interstitial velocity (m/s)

q = concentration of adsorbate in solid phase (uniform throughout a particle) (kg/m^3 of particle)

c = concentration of adsorbate in fluid phase (kg/m^3)

Assuming that the fluid to solid mass transfer of the adsorbate is governed by a linear driving force (difference between fluid phase concentration c and the equilibrium concentration of fluid phase on the particle surface c* and that the diffusivity within the particles is very large, so that the film mass transfer resistance is rate limiting, then the rate equation is given by

$$\frac{dq}{dt} = ka_v (c - c^*) \qquad \ldots(2a)$$

where

k = fluid phase film mass transfer coefficient (m/s)

a_v = specific surface area of the packing (m^2/m^3)

$\overline{ka_v}$ = volumetric mass transfer coefficient

Equation (2a) can be re-written as:

$$\frac{dq}{dt} = k' \quad (c - c^*) \qquad \ldots(2)$$

where k' = mass transfer coefficient measured in units of (s^{-1})

On a further assumption of the adsorption process being governed by a linear isotherm relationship (implicit in the method of moment), that is

$$q = k_m c^* \qquad \ldots(3)$$

where k_m is the equilibrium constant

Equation (2), rate equation becomes:

$$\frac{dq}{dt} = k' \quad (c - q/k_m) \qquad \ldots(4)$$

The continuity equation for fluid phase mass balance and the rate equation are

$$D_L \frac{\partial^2 c}{\partial x^2} - u \frac{\partial c}{\partial x} - \frac{\partial c}{\partial t} - \frac{(1-\varepsilon)}{\varepsilon} \frac{\partial q}{\partial t} = 0 \qquad \ldots(1)$$

$$\frac{dq}{dt} = k' (c - 1/k_m) \qquad \ldots(4)$$

BOUNDARY AND INITIAL CONDITIONS

For a bed of finite length (the system used in this work is a differential bed) the Danckerts boundary condition (Danckwerts, 1953; Wehner and Wilhelm, 1956) is widely used and is given by

at x = 0 (bed inlet)

$$uc - D_L \frac{dc}{dx} = f(t) \qquad \ldots(5)$$

and x = ℓ (bed outlet)

$$\frac{dc}{dx} = 0 \qquad \ldots(6)$$

where f(t)= t; the impulse function for an ideal application of tracer

Defining the following dimensionless variables

$$c' = \frac{c}{c_0} \; ; \quad z = \frac{x}{L} \; ; \quad q' = \frac{q}{q_m} \; , \quad \theta = \frac{t}{\bar{t}} \text{ and } \bar{t} = \frac{\ell}{u}$$

$$Pe = \frac{u\ell}{D_L} \; ; \quad \beta = \frac{q_m}{c_0} \text{ and } k_f = k'\bar{t}$$

Equations (1), (4), (5) and (6) become respectively

$$\frac{1}{Pe}\frac{\partial^2 c'}{\partial x^2} - \frac{\partial c'}{\partial z} - \frac{\partial c'}{\partial \theta} - \frac{(1-\varepsilon)}{\varepsilon}\beta\frac{\partial q'}{\partial \theta} = 0 \qquad \ldots (7)$$

$$\beta\frac{dq'}{d\theta} = k_f(c' - \beta q/k_m) \qquad \ldots(8)$$

<u>at z = 0</u>

$$c' - \frac{1}{Pe}\frac{dc'}{dz} = \delta(\theta) \qquad \ldots(9)$$

<u>at z = 1</u>

$$\frac{dc'}{dz} = 0 \qquad \ldots(10)$$

where c_0 = initial fluid phase concentration (kg/m^3)

ℓ = total bed length (m)

q_m = maximum solid phase concentration (kg/m^3)

Pe = Peclect number (-) (defined on the basis of length rather than size because the particle size is not important due to uniform solid phase concentration assumption. Only the void, ε is important.

The solution to equations (7), (8), (9) and (10) express the systems parameters in terms that can be related to experimentally determinable moments. The solution scheme essentially involves computing the Laplace transforms of equations (7-10) for $\bar{c}$ and then

using the Van der Laan (1957) expression to relate this to moments determined experimentally from which the required system parameters can be computed. The solution scheme is given as follows:

The L.T. of equations 7-10 are respectively

$$\frac{1}{Pe}\ \frac{\partial^2\bar{c}'}{\partial z^2} - \frac{\partial\bar{c}'}{\partial z} - p\bar{c}' - \frac{(1-\varepsilon)}{\varepsilon}\ \beta\, p\ \bar{q}' = 0 \qquad \ldots(11)$$

$$\beta\, p\bar{q}' = k_f\bar{c}' - \beta k_f\, \bar{q}'/k_m \qquad \ldots(12)$$

$$\bar{c}' - \frac{1}{Pe}\ \frac{d\bar{c}'}{dz} = 1 \quad \text{at } z = 0 \qquad \ldots(13)$$

(Since L $\{\delta(\theta)\}$ = 1.0, general for delta functions which represents the pulse input)

$$\frac{d\bar{c}'}{dz} = 0 \quad \text{at } z = 0 \qquad \ldots(14)$$

From equations (11) and (12)

$$\bar{q}' = \frac{k_f\bar{c}'}{\beta p + 3k_f/k_m}$$

$$\frac{1}{Pe}\ \frac{\partial^2\bar{c}'}{\partial z^2} - \frac{\partial\bar{c}'}{\partial z} - p\bar{c}' - \frac{(1-\varepsilon)}{\varepsilon}\ \frac{k_f\bar{c}'p}{(p + k_f/k_m)} = 0 \qquad \ldots(15)$$

Where p is the Laplace transform parameter from the general L.T. relation $L\{\bar{c}(\theta)\} = \int_0^\infty e^{-p\theta}\,\bar{c}(\theta)\,d\theta$

Re-arranging equation(15) and collecting items in $\bar{c}$ for the 3rd and 4th terms gives

$$-p\bar{c}' - \frac{(1-\varepsilon)}{\varepsilon}\ \frac{pk_f\bar{c}'}{(p+k_f/k_m)} = \frac{-p\bar{c}'[1 + k_f(1-\varepsilon)]}{(p + k_f/k_m)\,\varepsilon}$$

Simplifying gives:

$$\frac{-\,p\,\bar{c}'\,[\varepsilon + (p + k_f/k_m) - (1-\varepsilon)\,pk_f\bar{c}' + p\bar{c}'(1 + k_f(1-\varepsilon))]}{(p + k_f/k_m)\,\varepsilon} = 0$$

$$= \frac{-\,p\,\bar{c}'(\,p + k_f/k_m + k_f/\varepsilon - k_f/\varepsilon\,)}{(\,p + k_f/k_m\,)} = g\,\bar{c}'$$

By letting

$$\frac{p[\,p + k_f(1/k_m + 1/\varepsilon - 1)\,]}{p + k_f/k_m} = g \qquad \ldots(16)$$

The mass balance equation, equation (11) becomes:

$$\frac{1}{Pe}\,\frac{d\bar{c}'}{dz^2} - \frac{dc'}{dz} - g\,\bar{c}' = 0 \qquad \ldots(17)$$

Where

$$g = f(p)$$

The Laplace transform (L.T.) of the boundary condition equations (13) - (14) gives:

$$\bar{c}' = -\,\frac{1}{Pe}\,\frac{d\bar{c}'}{dz} = 1 \quad \text{at } z = 0 \qquad \ldots(18)$$

and

$$\frac{d\bar{c}'}{dz} = 0 \quad \text{at } z = 1 \qquad \ldots(19)$$

As given earlier.

Applying the general solution technique for second order ordinary differential equation of the general form:

$$a\frac{d^2y}{dx^2} + b\frac{dy}{dx} + dy = f(x) \qquad \ldots(20a)$$

The solution (general) to the auxillary parts of equation (20a)

$$a\frac{d^2y}{dx^2} + b\frac{dy}{dx} + cy = 0 \text{ is given by}$$

$$y = A\,e^{m_1 x} + Be^{m_2 x} \qquad \ldots(20b)$$

where m_1 and m_2 are roots of the equation

$$a\,m^2 + bm + c = 0 \text{ (auxillary equation)}$$

and A and B are 2 arbitrary constants.

The general solution to equation(17) is as follows

For equation 17,

$$\frac{1}{Pe}\frac{d^2\bar{c}'}{dz^2} - \frac{d\bar{c}'}{dz} - g\,\bar{c}' = 0 \qquad \ldots$$

auxillary equation is:

$$m^2 - Pe\,m - g\,Pe = 0$$

Solving for the roots by using the relation:

$$\text{roots} = \frac{-b \pm \sqrt{(b^2 - 4ac)}}{2a}$$

gives

$$\frac{Pe \pm \sqrt{\{(-Pe)^2 - [4 \times g \times (-Pe)]\}}}{2} = \frac{Pe}{2} + \frac{Pe^2 - 4gPe}{4}$$

$$m_1 = \frac{Pe}{2} + \frac{Pe^2}{4} + g\ Pe$$

and

$$m_2 = \frac{Pe}{2} - \frac{Pe^2}{4} + g\ Pe$$

The general solution for the 2nd order O.D.E. generated by the L.T. of our original continuity equation (P.D.E) given by equation (17) is

$$\bar{c}' = A \exp\left(\frac{Pe}{2} + \frac{Pe^2}{4} + g\ Pe\right)z + B \exp\left(\frac{Pe}{2} - \frac{Pe^2}{4} + g\ Pe\right) z \qquad ..(21a)$$

and letting $Pe^2/4 + g\ Pe = q$ equation (21a) becomes:

$$\bar{c}' = A \exp\left(\frac{Pe}{2} + q\right)z + B \exp\left(\frac{Pe}{2} - q\right) z \qquad ...(21)$$

Using the boundary conditions, equations (18) - (19) the arbitrary constants A and B in equation (21) are determined as follows

at $z = 1$, $\frac{d\bar{c}'}{dz} = 0$

and from equation (21a)

$$\frac{d\bar{c}'}{dz} = \frac{Pe + q^{1/2}}{2} A \exp\left(\frac{Pe + q^{1/2}}{2}\right)z + \left(\frac{Pe - q^{1/2}}{2}\right) B \exp\left(\frac{Pe-q^{1/2}}{2}\right)z$$

Since $\frac{d\bar{c}'}{dz} = 0$ when $z = 1$,

$$A = \frac{-B\left[(Pe/2) - q^{1/2}\right] \exp(-2\,q^{1/2})}{\left[(Pe/2) + q^{1/2}\right]} \qquad ...(22)$$

<u>At z = 0</u> when $z = 0, \bar{c}' - 1/Pe \frac{d\bar{c}'}{dz} = 1$

$$A + B - \frac{1}{Pe}\left(\frac{Pe + q^{1/2}}{2}\right) A - \frac{1}{Pe}\left(\frac{Pe - q^{1/2}}{2}\right) B = 1 \qquad ...(23)$$

Substituting for A from equation (22) into equation (23) and solving for A and B gives the following results:

$$B = \frac{Pe\ (\frac{Pe}{2} + q^{\frac{1}{2}})}{[\exp(-2q^{\frac{1}{2}}) - 1][\frac{Pe^2}{4} - q] - Pe\ \exp\ (-2q^{\frac{1}{2}})(\frac{Pe}{2} - q^{\frac{1}{2}}) + Pe(\frac{Pe}{2} + q^{\frac{1}{2}})} \qquad (24)$$

$$A = \frac{-\ Pe(\frac{Pe}{2} - q^{\frac{1}{2}})\ \exp\ (-2q^{\frac{1}{2}})}{[\exp\ (-2q^{\frac{1}{2}}) - 1]\ [\ \frac{Pe^2}{4} - q\ ] - Pe\ \exp\ (-2q^{\frac{1}{2}})(\frac{Pe}{2} - q^{\frac{1}{2}}) + Pe(\frac{Pe}{2} + q^{\frac{1}{2}})} \qquad (25)$$

Expressions for the arbitrary constants could be substituted into equation (21) and the solution inverted to give $\bar{c}$ in terms of time parameter instead of the L.T. parameter p but this is very difficult and instead the known property of the L.T. which is

$$\int_0^\infty t^k\ c(t)\ dt = (-1)^k \lim_{p \to 0} \frac{d^k \bar{c}(p)}{dp^k} \qquad \ldots(26)$$

Can be used to relate the solution to moment of the impulse response, namely

$$\mu_1 = - \lim_{p \to 0} \frac{d\bar{c}'}{dz} \qquad (27)$$

and

$$\mu_2' = \lim_{p \to 0} \frac{d^2 \bar{c}'}{dz^2} - \mu_1^2 \qquad (28)$$

which were the expressions according to Van der Laan (1957) using the method of moment.

Where μ_1 and μ_2' are the first moment (mean) and second central moment respectively.

From equations (21), (24) and (25).

$$\bar{c}' = \frac{2\ Pe\ q^{\frac{1}{2}}\ \exp\ (\frac{Pe}{2} - q^{\frac{1}{2}})}{[\exp(-2q^{\frac{1}{2}}) - 1]\ [\frac{Pe^2}{4} - q\ ] - Pe\ \exp\ (-2q^{\frac{1}{2}})(Pe/2 - q^{\frac{1}{2}}) + Pe(\frac{Pe}{2} + q^{\frac{1}{2}})}$$

Since g = f(p) that is, $g = \dfrac{p\ [p + k_f\ (1/k_m + 1/\epsilon\ - 1)]}{p + k_f/k_m}$

$$q = \frac{Pe^2}{4} + g\ Pe$$

As $p \to 0$, $g \to 0$ $\qquad q^{1/2} \to \frac{Pe}{2}$

Treating $\bar{c}'$ as a quotient of the form $y = u/v$

So that $\bar{c}' = f(u,v)$, $u = f(q)$ and $v = f(q)$ to give

$$\frac{d\bar{c}'}{dq} = v\frac{du}{dq} - u\frac{dv}{dq}$$ according to

well known quotient formula.

But $\frac{du}{dq} = Pe\ \exp\ (\frac{Pe}{2} - q^{1/2})(q^{-1/2}-1)$

and

$$\frac{dv}{dq} = [1 + q^{1/2}\ \exp\ (-2q^{1/2}) - \exp\ (-2q^{1/2}) + \frac{Pe^2}{4q^{1/2}}\ \exp\ (-2q^{1/2}) - \exp\ (-2q^{1/2})\ Pe$$

$$+ \exp\ (-2q^{1/2})\ \frac{Pe}{2q^{1/2}} + \frac{Pe}{2q^{1/2}}\ ]$$

$q^{1/2} \to \frac{Pe}{2}$ as $p \to 0$ therefore $u = Pe^2$ and $v = Pe^2$

$$\therefore \frac{d\bar{c}'}{dq} = \frac{du - dv}{Pe^2} \quad \text{or} \quad \frac{1}{Pe^2}\ (\frac{du}{dq} - \frac{dv}{dq})$$

$$= \frac{1}{Pe^2}\ (2 - Pe - 2) = -\frac{1}{Pe} \qquad \ldots(29)$$

Since, as $q^{1/2} \to \frac{Pe}{2}$ then $\frac{dv}{dq} = 0$ and $\frac{du}{dq} = 2 - Pe$ $\qquad \ldots(30)$

and $\quad q = \frac{Pe^2}{4} + g\ Pe$

$$\therefore \frac{dq}{dp} = Pe\ \frac{dg}{dp}\ ; \qquad \frac{d\bar{c}'}{dp} = \frac{d\bar{c}'}{dq} \times \frac{dq}{dp} \qquad \ldots(31)$$

From equation (16)

$$g = \frac{p\,[p + k_f(1/k_m + 1/\epsilon - 1)]}{p + k_f/k_m}$$

$$\frac{dg}{dp} = [(p + k_f/k_m)\,\{2p + k_f(1/k_m + 1/\epsilon - 1)\}]/\,(k_f/k_m)^2$$

As $p \to 0$ then,

$$\frac{dg}{dp} = \frac{1}{k_m} + \frac{1}{\epsilon} - 1 = 1 + k_m\,\frac{(1-\epsilon)}{\epsilon}$$

From equation (31)

$$\lim_{p \to 0} \frac{dc'}{dp} = -1/Pe \;.\; Pe\,\frac{dg}{dp}$$

For a non-adsorbing tracer input,

$$\text{From the relation } g = \frac{p^2 + pk_f(1/k_m) + 1/\epsilon - 1)}{p + k_f/k_m}$$

$$g = p$$

$$\frac{dg}{dp} = 1$$

Also $\frac{d\bar{c}'}{dp} = -\frac{1}{Pe} \;.\; Pe \;.\; 1 = -1$

Since $\mu_1 = \;; \frac{d\bar{c}}{dp}$ $\quad \therefore \mu_1 = -\frac{d\bar{c}'}{dp} = -1(-1) = 1$

that is, the first absolute moment

$$\mu_1 = 1 \qquad \ldots(32)$$

This is the same result given by Bischoff and Levenspiel (1962).

To obtain μ_2' for non-adsorbing tracer input; noting that according to Van dar Laan

$$\mu_2' = \lim_{p \to 0} \frac{d^2 \bar{c}}{dz^2} - \mu_1^2$$

and that $\frac{d^2 g}{dp^2} = 2 \frac{k_m}{k_f} (1 - 1/\epsilon)$ as $p \to 0$

and using the same manipulations used to obtain equation (29) for $\frac{d\bar{c}'}{dq}$ gives

$$\frac{d^2 \bar{c}'}{dp^2} = \frac{d^2 \bar{c}'}{dq^2} \left(\frac{dq}{dp}\right)^2 + \frac{d^2 q}{dp^2} \frac{d\bar{c}'}{dq}; \quad \frac{d^2 q}{dp^2} = Pe \frac{d^2 g}{dp^2}$$

$$\frac{d^2 \bar{c}'}{dp^2} = \frac{d^2 \bar{c}'}{dq^2} \cdot Pe \cdot \left(\frac{dg}{dp}\right)^2 + Pe \cdot \frac{d^2 g}{dp^2} \cdot \frac{d\bar{c}'}{dq}$$

$$= \left(\frac{dg}{dp}\right)^2 \left[\frac{2}{Pe} - \frac{2}{Pe^2} + \frac{2}{pe^2} \exp(-Pe) + 1 \right] - \frac{d^2 g}{dp^2}$$

For non-adsorbing tracer input $g = p$, and $\frac{dg}{dp} = 1$

$$\frac{d^2 g}{dp^2} = 0 \quad \text{giving:}$$

$$\frac{d^2 \bar{c}'}{dp^2} = \frac{2}{Pe} - \frac{2}{Pe^2} + \frac{2}{Pe^2} \exp(-Pe) + 1$$

As $p \to 0$, $\mu_2' = \frac{d^2 \bar{c}'}{dp^2} - 1^2$

$$\therefore \quad \mu_2' = \frac{2}{Pe} - \frac{2}{Pe^2} + \frac{2}{Pe^2} \exp(-Pe) \qquad \ldots(33)$$

Equations (32) and (33) are the same as those given by Levenspiel (1972) for non-ideal flow in closed vessels of chemical reactions.

APPENDIX 4

FORMULATION OF SOLUTION SCHEME

(a) NON-POROUS PARTICLE MODEL

According to the axially dispersed plug flow model for non-porous particles packed in a column (appendix 2) the continuity equation for mass of fluid phase adsorbate is given by the equation

$$\frac{\partial c}{\partial t} = D_L \frac{\partial^2 c}{\partial x^2} = u \frac{\partial c}{\partial x} - \frac{\rho_s}{\varepsilon} \frac{\partial q}{\partial t} \qquad \ldots(1)$$

where c = concentration of adsorbate in the fluid phase (kg/m^3)

ε = bed voidage (-)

u = fluid interstitial velocity (m/s)

D_L = axial dispersion coefficient (m^2/s)

ρ_s = packingdensity (kg/m^3)

q = concentration of adsorbate in the solid phase (kg/kg)

Assuming that the rate of transfer of the adsorbate from the solution into the solid phase is slow compared with film mass transfer rate and therefore competes with diffusion as the rate limiting step. The rate equation is given by

$$\frac{\rho_s}{\varepsilon} \frac{\partial q}{\partial t} = k_1 . c . (q_m - q) - k_2 q \qquad \ldots(2)$$

where q_m = maximum solid phase adsorption capacity (kg/kg)

k_1 = forward rate constant

k_2 = backward rate constant

Derivation of the Boundary Conditions

Assuming that dispersion is significant at the bed's entrance. In Fig. 1 a mass balance on the elemental volume of length dx

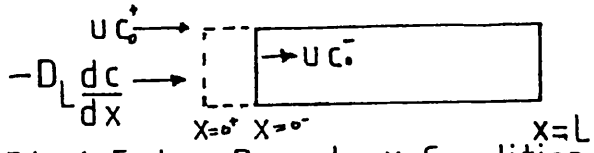

Fig 1: Entry Boundary Condition

for flux of material into the entrance and exit of the element bounded by $x = 0$ and any plane upstream of inlet where $c = c_o^+$

By conservation of mass

Input = output

Input at $x = 0^+$

(i) Bulk fluid at $x = 0^+ = uc_o^+$

(ii) Diffusional flux $= D_L \left.\frac{dc}{dx}\right|_{x=0^+}$

Output

(i) Bulk flux out $= uc_0^-$

Substituting into the conservation of mass equation gives

$$Uc_o^+ = D_L \left.\frac{dc}{dx}\right|_{x=0^+} = Uc_o^-$$

$$D_L \frac{dc}{dx} = uc_{o^+} - uc_{o^-}$$

$$D_L \frac{dc}{dx} = u\,(c_o^+ - c_0^-) \qquad \ldots(3)$$

at $x = \ell$

The concentration gradient is zero

$$\frac{dc}{dx} = 0 \qquad \ldots(4)$$

Initial Condition

Assuming that the bed was initially devoid of adsorbate

$$c = 0 \quad \text{and} \quad q = 0 \quad \text{at} \quad t = 0 \qquad \ldots(5)$$

Dimensionless form of model equation

Defining the variables in equations (1) - (5) in a dimensionless form, so that

$$\bar{c} = \frac{c}{c_o}\ ;\ \bar{q} = q/q_m;\ z = x/\ell;\quad \theta = \frac{ut}{\ell}$$

$$Pe = u\ell/D_L; \quad k_A = k_1\,\ell/u ; \quad k_B = k_2/c_o .\ \ell/u$$

wquations (1) - (5) become respectively

Equation 1

This equation can be re-written by substituting for $\frac{\rho_s}{\varepsilon}\ \frac{\partial q}{\partial t}$

from equation (2), namely,

$$\frac{\partial c}{\partial t} = D_L \frac{\partial^2 c}{\partial x^2} - u\ \frac{\partial c}{\partial x} - k_1.c.\ (q_m - q) - k_2 q$$

so that

$$\frac{u}{\ell}\quad c_0.\ \frac{\partial \bar{c}}{\partial \theta} = \frac{D_L c_0}{\ell_2}\ .\ \frac{\partial^2 \bar{c}}{\partial z^2} - c_0.\ \frac{u}{\ell}\ \frac{\partial \bar{c}}{\partial z} - \{k_1.c.c_0 q_m(1-\bar{q}) - k_2 q_m \bar{q}\}$$

$$\frac{\partial \bar{c}}{\partial \theta} = \frac{D_L}{\ell^2}\ .\ c_0'\ .\ \frac{\ell'}{u}\ .\ \frac{1}{c_0'}\ \frac{\partial^2 c}{\partial \epsilon^2} - \frac{c_0'}{c_0'}\ .\ \frac{u'}{\ell'}\ .\ \frac{\ell'}{u'}\ \frac{\partial \bar{c}}{\partial z} - \frac{\ell}{u}\ .\ \frac{1}{c_0}$$

$$\{\ k_1.\bar{c}.c_0 q_m(1-\bar{q}) - k_2 q_m \bar{q}\ \}$$

$$\frac{\partial \bar{c}}{\partial \theta} = \frac{1}{Pe}\ \frac{\partial^2 \bar{c}}{\partial z^2} - \frac{\partial \bar{c}}{\partial z} - \{k_1.\ \frac{\ell}{u}\ .q_m \bar{c}(1-\bar{q}) - \frac{k_2}{c_0}\ .\ \frac{\ell}{u}\ q_m \bar{q}\}$$

$$\frac{\partial \bar{c}}{\partial \theta} = \frac{1}{Pe}\ \frac{\partial^2 \bar{c}}{\partial z^2} - \frac{\partial \bar{c}}{\partial z} - q_m\{\ k_A \bar{c}(1-\bar{q}) - k_B \bar{q}\} \qquad \ldots(7)$$

Equation 2

$$\frac{u}{\ell}\ .\ q_m'\ \frac{\rho_s}{\varepsilon}\ \frac{\partial \bar{q}}{\partial \theta} = k_1.\bar{c}.c_0 q_m'\ (1-\bar{q}) - k_2 q_m' \bar{q}$$

$$\frac{\partial \bar{q}}{\partial \theta} = k_1.\ \frac{\ell}{u}\ .\ c_0.\ \frac{\varepsilon}{\rho_s}\ .\ \bar{c}.\ (1-\bar{q}) - k_2.\ \frac{\ell}{u}\ .\ \frac{\varepsilon}{\rho_s}\ .\ \bar{q}$$

$$\frac{\partial \bar{q}}{\partial \theta} = \frac{\varepsilon}{\rho_s}.\ c_0\ \{k_1.\ \frac{\ell}{u}.\ \bar{c}.(1-q) - \frac{k_2}{c_0}\ .\ \frac{\ell}{u}\ .\ \bar{q}\ \}$$

$$\frac{\partial \bar{q}}{\partial \theta} = \frac{\varepsilon}{\rho_s} \cdot c_0 \{ k_A.\bar{c}.(1-\bar{q}) - k_B\bar{q} \} \quad ...(8)$$

Boundary and initial conditions become

$$\frac{\partial \bar{c}}{\partial z} = Pe\ (\bar{c} - 1) \qquad \text{at } z = 0 \quad ...(9)$$

$$\frac{\partial \bar{c}}{\partial z} = 0 \qquad \text{at } z = 1 \quad ...(10)$$

and

$$\bar{c} = 0;\ \bar{q} = 0 \qquad \text{at } \theta = 0 \quad ...(11)$$

Alternatively equation (1) can be written in terms of solid phase concentration measured in terms of kg/(m^3 of bed) so that equation (1c) of appendix 2 is used, namely

$$\frac{\partial c}{\partial t} = D_L \frac{\partial^2 c}{\partial x^2} - u \frac{\partial c}{\partial x} - \frac{1}{\varepsilon} \frac{\partial q_b}{\partial t}$$

or

$$\frac{\partial c}{\partial t} = D_L \frac{\partial^2 c}{\partial x^2} - u \frac{\partial c}{\partial x} - \frac{1}{\varepsilon} k_1.c(q_m - q) - k_2 q \quad ...(12)$$

the rate equation becomes

$$\frac{\partial q_b}{\partial t} = k_1.c.(q_m - q) - k_2 q \quad ...(13)$$

As for the previous case, the dimensionless form of equations 12a and 13a are respectively

Fluid phase equation

$$\frac{\partial c}{\partial \theta} = \frac{\partial^2 \bar{c}}{\partial z^2} - \frac{\partial c}{\partial z} - \frac{1}{\epsilon} \{k_1 . c_0 . \frac{\ell}{u} q_m \bar{c} (1-\bar{q}) - k_2 . \frac{\ell}{u} q_m\}$$

so that

$$\frac{\partial c}{\partial \theta} = \frac{\partial^2 \bar{c}}{\partial z^2} - \frac{\partial c}{\partial z} - \frac{\beta}{\epsilon} \{k_A \bar{c}(1-\bar{q}) - k_B \bar{q}\} \quad ...(12)$$

where $k_A = k_1 . c_0 . \frac{\ell}{u}$ and $k_B = k_2 . \frac{\ell}{u}$

Rate equation

$$\frac{u}{\ell} q_m \frac{d\bar{q}}{d\theta} = k_1 . c_0 . \bar{c} . q_m (1-\bar{q}) - k_2 q_m \bar{q}$$

so that

$$\frac{d\bar{q}}{d\theta} = k_1 . \frac{\ell}{u} . c_0 \bar{c} (1-\bar{q}) - k_2 . \frac{\ell}{u} \bar{q}$$

$$= k_A \bar{c} (1-q) - k_B \bar{q} \quad ...(13)$$

The initial and boundary conditions remain the same as for the previous case.

The computer code was based on the above version. Equations 12 and 13 when expressed in collocation form at collocation point z_j are as follows

$$\frac{d\bar{c}_j}{d\theta} = \frac{1}{P_e} \sum_{i=1}^{m} B_{ji} c_i - \sum_{i=1}^{m} A_{ji} c_i - \frac{\beta}{\epsilon} \{k_A \bar{c}_j (1-\bar{q}_j) - k_B \bar{q}_j\} \quad ...(12)$$

$$\frac{d\bar{q}_j}{d\theta} = \{k_A \bar{c}_j (1-\bar{q}_j) - k_B \bar{q}_j\} \quad ...(13)$$

at $z = z_0 = 0$

$$\sum_{i=1}^{m} A_{1i} c_i = Pe \ (c_1 - 1) \qquad \ldots(14a)$$

at $z = z_1 = 1$

$$\sum_{i=1}^{m} A_{mi} c_i = 0 \qquad \ldots(15a)$$

where N = number of interior collocation points

m = N + 2

A = Gradient Collocation matrix

B = Laplacian Collocation matrix

The boundary conditions - equations (14) and (15) are used to eliminate c_1 and c_m in equations (1) as follows:

<u>At z = 1</u>

Expanding equation (15a) gives

$$\sum_{i=2}^{m-1} A_{mi} c_i + A_{m1} c_1 + A_{mm} c_m = 0$$

$$C_m = - \frac{A_{m1} C_1}{A_{mm}} - \sum_{i=2}^{m-1} \frac{A_{mi}}{A_{mm}} c_i \qquad \ldots(15b)$$

<u>At z = 0</u>

Expanding equation (14a) and substitutiong equation (15b) into it gives:

$$\sum_{i=2}^{m-1} A_{1\,i} c_i + A_{11} c_1 + A_{1\,m} c_m = Pe \ (c_1 - 1)$$

$$\sum_{i=2}^{m-1} A_{1i} c_i + A_{11} c_1 + A_{1m} \{ - \sum_{i=2}^{m-1} \frac{A_{mi} c_i}{A_{mm}} - \frac{A_{m1} c_1}{A_{mm}} \} = Pe \ c_1 - Pe$$

$$\sum_{i=2}^{m-1} A_{1i}c_i + A_{11}c_1 - \sum_{i=2}^{m-1} \frac{A_{mi}A_{1m}}{A_{mm}} c_i - \frac{A_{1m}A_{m1}}{A_{mm}} c_1 = Pe\ c_1 - Pe$$

Collecting terms in c_1 and solving for c_1 gives:

$$A_{11}c_1 - Pec_1 - \frac{A_{1m}A_{m1}}{A_{mm}} c_1 = - Pe - \sum_{i=2}^{m-1} A_{1i}c_i + \sum_{i=2}^{m-1} \frac{A_{mi}A_{1m}}{A_{mm}} c_i$$

$$c_1 \left(A_{11} - Pe - \frac{A_{1m}A_{m1}}{A_{mm}}\right) = - Pe - \sum_{i=2}^{m-1} \left(A_{1i} - \frac{A_{mi}A_{1m}}{A_{mm}}\right) c_i$$

$$\therefore \quad c_1 = \frac{-Pe - \sum_{i=2}^{m-1} \left(A_{1i} - \frac{A_{mi}A_{1m}}{A_{mm}}\right)c_i}{A_{11} - Pe - \frac{A_{1m}A_{m1}}{A_{mm}}} \qquad \ldots(16)$$

The expression of equation 12 yields:

$$\frac{dc_j}{d\theta} = \sum_{i=2}^{m-1} M1B_{ji}c_i + M1B_{j1}c_1 + M1B_{jm}c_m - \left(\sum_{i=2}^{m-1} A_{ji}c_i + A_{j1}c_1 + A_{jm}c_m\right)$$

$$- \frac{\beta}{\epsilon} \left(k_A \bar{c}_j(1-\bar{q}_j) - k_B \bar{q}_j\right)$$

Rearranging

$$\frac{dc_j}{d\theta} = \left\{\sum_{i=2}^{m-1} M1B_{ji}c_i - \sum_{i=2}^{m-1} A_{ji}c_i\right\} + \left\{M1B_{j1}c_1 - A_{j1}c_1\right\} +$$

$$\left\{M1B_{jm}c_m - A_{jm}c_m\right\} - \frac{\beta}{\epsilon} \left\{k_A c_j(1-\bar{q}_j) - k_B \bar{q}_j\right\}$$

where M1 = 1/Pe

Simplifying:

$$\frac{dc_j}{d\theta} = \sum_{i=2}^{m-1} (M1B_{ji} - A_{ji})c_i + (M1B_{j1} - A_{j1})c_1 + (M1B_{jm} - A_{jm})c_m$$

$$- \frac{\beta}{\epsilon} \left(k_A c_j(1-q_j) - k_B q_j\right) \qquad \ldots(17)$$

Summary:

$$\frac{dc_j}{d\theta} = \sum_{i=2}^{m-1} (M1B_{ji} - A_{ji})c_i + (M1B_{j1} - A_{j1})c_1 + (M1B_{jm} - A_{jm})c_m$$

$$- \frac{\beta}{\varepsilon} [\, k_A c_j (1-q_j) - k_B q_j \,]$$

$$\frac{d\bar{q}_j}{d\theta} = k_A \bar{c}_j (1-\bar{q}_j) - k_B \bar{q}_j \qquad \ldots(18)$$

$$c_1 = \frac{- Pe - \sum_{i=2}^{m-1} (A_{1i} - \frac{A_{mi}A_{1m}}{A_{mm}})c_i}{A_{11} - Pe - \frac{A_{m1}A_{1m}}{A_{mm}}} \qquad \ldots(19)$$

$$c_m = - \frac{A_{m1}c_1}{A_{mm}} - \sum_{i=2}^{m-1} \frac{A_{mi}}{A_{mm}} c_i \qquad \ldots(20)$$

APPENDIX 5

CALCULATION OF COLLOCATION CONSTANTS

The calculation procedure for the non-symmetrical system is given here. The same procedures however, applies to the symmetric problem though with a slightly different algorithm to take care of the even order polynomials involved and the number of total collocation points. The full algorithm for the symmetric program has been given by Villadsen and Stewart (1967).

(a) Power Series Method

The discretization matrices A and B were computed by writing equations 5.515 - 5.17 for the function $y = x^0$, $y = x^1$ .... $y = x^{N+1}$ and solving the resulting systems of equations for the arrays of A_{ji} and B_{ji}, where N is the number of interior collocation points.

The algorithm for the computation can be summarised compactly in matrix form as follows:

$$Q_{ji} = x_i^{i-1} = \begin{bmatrix} 1 & x_1^2 & . & . & x_1^{N+1} \\ & & & & \\ & & & & \\ 1 & x_{N+2}^2 & . & . & x_{N+2}^{N+1} \end{bmatrix} \qquad \ldots(1)$$

$$A_{ji} = (i-1)x_j^{i-2}.Q_{ji}^{-1}\left(C_{ji}.Q_{ji}^{-1}\right) \begin{bmatrix} \frac{dx^0}{dx}\Big|_{x_1} & \cdots & \frac{dx^{N+1}}{dx}\Big|_{x_1} \\ \\ \frac{dx^0}{dx}\Big|_{x_{N+2}} & \cdots & \frac{dx^{N+1}}{dx}\Big|_{x_{N+2}} \end{bmatrix}^{-1} Q \quad \ldots(2)$$

$$B_{ji} = D_{ji}.Q_{ji}^{-1} = (i-1)(i-2)x_j^{i-3}.Q_{ji}^{-1}$$

$$\begin{bmatrix} \nabla^2(x^0)|_{x_1} & \cdots & \nabla^2(x^{N+1})|_{x_{N+1}} \\ \\ \nabla^2(x^0)|_{x_{N+2}} & \cdots & \nabla^2 x^{N+1}|_{x_{N+2}} \end{bmatrix}^{-1} \begin{bmatrix} \\ Q \\ \\ \end{bmatrix} \quad \ldots(3)$$

The collocation oints $x_1 \ldots\ldots x_{N+1}$ are the roots of $P_N(x) = 0$;

$x_{N+2} = 1.$

The explicit formula for the power series representation of the polynomial $P_N^{(\alpha,\beta)}(x)$ is as follows

$$P_N^{(\alpha,\beta)}(x) = a_i x^i - a_{i-1}x^{i-1} + a_{i-2}x^{i-2} - \ldots + (-1)^i \equiv \sum_{i=0}^{N} (-1)^{N-i} a_i x^i \quad \ldots(4)$$

There are various ways of calculating the coefficients, a_i .
These have been discussed by Villadsen and Michelsen (1978). The simplest recursive expression of a_i is given by the expression:

$$a_i = \frac{N-i+1}{i} \quad \frac{N+i+\alpha+\beta}{i+\beta} \quad a_{i-1} \qquad \ldots(5)$$

with $a_0 = 1$ and $i = 1, 2, \ldots\ldots N$

However, Villadsen and Michelsen (1978) have argued that while equation (5) is excellently suited for a calculation of the coefficient in the explicit expression of equation (4) for P_N, it is not at all suitable for machine computation of P_N and a specific x-value. a_{Ni} are rapidly increasing with N and since the terms in equation (4) occur with alternating sign a significant loss of digits is unavoidable.

Hence the authors recommended another computational scheme to obtain $P_N(x)$. The following recurrence relation was recommended.

$$P_N = (F_N x - G_N)\, P_{N-1} - H_N P_{N-2} \qquad \ldots(6)$$

where F_N, G_N and H_N are functions of N, α, and β .
Viladsen(1970) has shown that the three-term recurrence relation above holds for any family of orthogonal polynomials and the functions F_N, G_N and H_N can be calculated by an application of the fundamental definition of the orthogonal family given by the expression:

$$\int_0^1 x^{\beta}(1-x)^{\alpha}\, P_j(x)\, P_N(x)\, dx = 0 \quad j = 0, 1, \ldots N-1 \qquad \ldots(7)$$

Villadsen and Michelsen (1978) gave the following recurrence formula for the rescaled polynomials $P_N = P_N/G_{NN}$ for this case in the following equations:

$$P_N = [\, x - g_N(N,\alpha,\beta)\,]\, P_{N-1} - h_N(N,\alpha,\beta)\, P_{N-2} \qquad \ldots(8)$$

$$g_1 = \frac{\beta + 1}{\alpha + \beta + 2} \qquad g_N = \frac{1}{2}\left[1 - \frac{\alpha^2 - \beta^2}{(2N + \alpha + \beta - 1)^2 - 1}\right] \qquad \ldots(9)$$

for $N > 1$

$$h_1 = 0, \quad h_2 = \frac{(\alpha+1)(\beta+1)}{(\alpha+\beta+2)^2(\alpha+\beta+3)}$$

$$h_N = \frac{(N-1)(N+\alpha-1)(N+\beta-1)(N+\alpha+\beta-1)}{(2N+\alpha+\beta-1)(2N+\alpha+\beta-2)^2(2N+\alpha+\beta-3)} \qquad \ldots(10)$$

for $N > 2$

The recursive evaluation of $P_N(x_k)$ is started with $N = 1$, $P_{-1}(x_k)$ arbitrary, and $P_0(x_k) = 1$.

For the computation of the zeros of orthogonal polynomial using equation (6), the numbers $P_0[x_k^{(i)}] \equiv 1, P_1[x_k^{(i)}], \ldots\ldots P_N[x_k^{(i)}]$ form a so called Sturm sequence (Villadsen and Michelsen,1978). The Newton iteration scheme based on equation (8) is:

$$P_j = [x_k^{(i)} - g_j] P_{j-1} - h_j P_{j-2}$$

$$P_j^{(1)} = [x_k^{(i)} - g_j] P_{j-1}^{(1)} - h_j P_{j-2}^{(1)} + P_{j-1} \qquad j = 1, 2, \ldots N \qquad \ldots(11)$$

$$P_0 = 1, \quad P_0^{(1)} = 0, \quad p_{-1} = P_{-1}^{(1)} \quad \text{arbitrary}$$

A Newton iterration starting from $x = 0$ will produce a sequence $x_1^{(1)}, x_1^{(2)}, \ldots$ that converges to x_1 from below. The reason being that $P_N^{(1)}(x)$ is monotonously decreasing in $(-\infty, x_1)$.

In the program Colmat, two subroutines are used to calculate the collocation points (or roots of the Legendre polynomial) and the matrices A and B. The main program is for Input/Output of the collocation constants.

In the subroutine roots which calculates the roots of the Legendre polynomial, or Jacobi polynomials the parameters have the following meanings:

n: number of the interior collocation points
no and n1 may be given the value 0 and 1 so that
nT = n + no + n1.

no: decides whether x = 0 is included as a collocation point. no must be set equal to 1 (including x = 0) or 0 (excluding this point).

n1: As for no, but for thepoint x = 1.

al, be: The values of α and β; for Legendre polynomial both are zero but unity and zero respectively for Jacobi polynomials.

nn3: dimensions of the vector root which holds the roots of the polynomial.

The subroutine consists of essentially two parts: First the values of the coefficients g_i and h_i, i = 1, 2, ... N, of the recurrence formula of equation (8) are computed according to equations (9) and (10). The 2N coefficients are stored temporarily in DIF1 and DIf2.

Next the zeros of P_N are determined using equation (11) by Newton's method with root suppression. The smallest zero x_1 is stored in root (1), x_2 in root (2), and x_n in root (n).

If $x_0 = 0$ is included as a collocation point (no = 1), the n zeros are shofted one position so that root (1) = 0, root (2) = x_1 and root (N+1) = x_N. Finally, an extra element root (nt) = 1 is added to root if n1 = 1. The vector root now contains the zeros of the polynomials in ascending order.

Fig. A2. Listing of Program Colmat for calculation of Collocation Constants.

```
c*****************************************************
      program colmat
c*****************************************************
c THIS PROGRAM CAL. THE COLLOCATION MATRICES A & B
c
c IT CALLS THE SUBROUTINES ROOTS & MATCOL THAT CAL.
c THE ROOTS OF THE POLYNOMIAL & THE DERIVATIVES and
c THE A & B MATRICES RESPECTIVELY
c*****************************************************
c
      implicit double precision(a-h,o-z)
      dimension root(4),r(4),a(4,4),b(4,4),s(4,4)
      data n,nn3,al,be/2,4,0.0d0,0.0d0/
      data n1,n0/4,4/
c  OPEN THE OUTPUT FILE FOR THE COLLOCATION CONSTANTS
      open(6,form='formatted',status='new',file='col')
      call roots(n,nn3,al,be,root)
      do 1000 i=1,n0
      r(i)=root(i)
 1000 continue
      write(6,1)
    1 format(//       ' THE PROGRAM COLMAT OUTPUT IS: '      //)
      write(6,2)
    2 format('      THE ROOTS  ARE     ')
      write(6,2000)(root(i),i=1,n0)
      call matcol(n1,n0,r,s,a,b)
      write(6,3)
    3 format('     THE A MATRIX IS      ')
      write(6,2000)((a(i,j),j=1,n0),i=1,n0)
      write(6,4)
    4 format('     THE  B  MATRIX  IS      ')
      write(6,2000)((b(i,j),j=1,n0),i=1,n0)
        stop
 2000 format(4(/1x,4d11.3/))
      end
c*********************************************************
c*******************************************************
c
      subroutine roots(n,nn3,al,be,root)
      implicit double precision(a-h,o-z)
      dimension dif1(4),dif2(4),root(nn3)
c
c  EVALUATION OF THE ROOTS AND THE DERIVATIVES OF THE
c JACOBI POLYNOMIALS, PN(AL<BE).
c  FIRS EVALUATION OF THE COEFF. IN THE RECURSION FORMULAE
c TO BE STORED IN THE DEF1 &DEF2
c
c
c     INPUT:
c         n       =NO OF THE INTERIOR COLLO CATION POINTS
c       (AL,BE)  =(0,0)- LEGENDRE POLYNOMIALS
c                =(1,0)- JACOBI POLYNOMIALS
c
```

```
c*******************************************************
c
c  NEXT 3 THREE STATERMENTS FOR THIS CASE
c
      n0=1
      n1=1
      nt=n+n0+n1

      ab=al+be
      ad=be-al
      ap=be*al
      dif1(1)=(ad/(ab+2.0d00)+1.0d00)/2.0d00
      dif2(1)=0.0d00
      if(n.lt.2) go to 15
      do 10 i=2,n
      z1=dble(i-1)
      z=ab+2.0d00*z1
      dif1(i)=(ab*ad/z/(z+2.0d00)+1.0d00)/2.0d00
      if(i.ne.2) go to 11
      dif2(i)=(ab+ap+z1)/z/z/(z+1.0d00)
      go to 10
   11 z=z*z
      y=z1*(ab+z1)
      y=y*(ap+y)
      dif2(i)=y/z/(z-1.0d00)
   10 continue
c
c   ROOT DETERMINATION BY THE NEWTON METHOD WITH THE SUPRESSION
c   OF THE PREVIOUSLY DETERMINED ROOTS
c
   15 x=0.0d00
       do 20 i=1,n
   25  xd=0.0d00
       xn=1.0d00
       xd1=0.0d00
       xn1=0.0d00
         do 30 j=1,n
         xp=(dif1(j)-x)*xn-dif2(j)*xd
         xp1=(dif1(j)-x)*xn1-dif2(j)*xd1-xn
         xd=xn
         xd1=xn1
         xn=xp
   30    xn1=xp1
      zc=1.0d00
      z=xn/xn1
      if(i.eq.1) go to 21
        do 22 j=2,i
   22   zc=zc-z/(x-root(j-1))
   21 z=z/zc
      x=x-z
      if(dabs(z).gt.1.0d-09) go to 25
      root(i)=x
      x=x+.00010d00
   20 continue
c
c  ADD EVENTUAL COLLOCATION PONITS AT x=0 and x=1
c
c
      if(n0.eq.0) go to 35
      do 31 i=1,n
      j=n+1-i
   31 root(j+1)=root(j)
      root(1)=0.0d00
  35 if(n1.eq.1) root(nt)=1.0d00
c
      return
      end
c*******************************************************
```

```
      subroutine matcol(n1,n0,r,s,a,b)
c
c*****************************************************
c
      implicit double precision (a-h,o-z)
      dimension wkspce(31),c(4,4),d(4,4),q(4,4)
      dimension a(n1,n0),b(n1,n0),s(n1,n0),r(n0)
      do 100 j=1,n0
      do 100 i=1,n0
         nn1=i-1
         n2=i-2
         n3=i-3
           if(i.eq.1) q(j,i)=1.0d00
           if(i.eq.1) c(j,i)=0.0d00
           if(i.eq.1) d(j,i)=0.0d0
           if(i.eq.1) go to 100
         if(i.eq.2) q(j,i)=r(j)
         if(i.eq.2) c(j,i)=1.0d00
         if(i.eq.2) d(j,i)=0.0d00
         if(i.eq.2) go to 100
c
         if(i.eq.3) q(j,i)=r(j)*r(j)
         if(i.eq.3) c(j,i)=2.0d0*r(j)
         if(i.eq.3) d(j,i)=2.0d0
         if(i.eq.3) go to 100
c
         q(j,i)=(r(j)**nn1)
         c(j,i)=(i-1)*(r(j)**n2)
         d(j,i)=(i-1)*(i-2)*(r(j)**n3)
  100 continue
c
c
      ifail=1
      call f01aaf(q,n1,n0,s,n1,wkspce,ifail)
      do 180 i=1,n0
         do 180 j=1,n0
         a(i,j)=0.0d00
         b(i,j)=0.0d00
          do 180 k=1,n0
           a(i,j)=a(i,j)+c(i,k)*s(k,j)
           b(i,j)=b(i,j)+d(i,k)*s(k,j)
  180 continue
      write(6,4)
    4 format('    THE Q INVERT IS      ')
      write(6,1000)((s(i,j),j=1,n0),i=1,n0)
 1000 format(4(/1x,4d11.3/))
c
      return
      end
```

THE PROGRAM COLMAT OUTPUT IS:

THE ROOTS ARE

0.000D+00 0.211D+00 0.789D+00 0.100D+01

THE Q INVERT IS

0.100D+01 0.000D+00 0.000D+00 0.000D+00

-0.700D+01 0.820D+01 -0.220D+01 0.100D+01

0.120D+02 -0.186D+02 0.126D+02 -0.600D+01

-0.600D+01 0.104D+02 -0.104D+02 0.600D+01

THE A MATRIX IS

-0.700D+01 0.820D+01 -0.220D+01 0.100D+01

-0.273D+01 0.173D+01 0.173D+01 -0.732D+00

0.732D+00 -0.173D+01 -0.173D+01 0.273D+01

-0.100D+01 0.220D+01 -0.820D+01 0.700D+01

THE B MATRIX IS

0.240D+02 -0.372D+02 0.252D+02 -0.120D+02

0.164D+02 -0.240D+02 0.120D+02 -0.439D+01

-0.439D+01 0.120D+02 -0.240D+02 0.164D+02

-0.120D+02 0.252D+02 -0.372D+02 0.240D+02

The subroutine matcol calculates the matrices A and B using the roots calculated in subroutine roots, which are in the vector, r. The roots of vector, r, is an input via the main program. The input parameters have the following meanings:

no, n1: dimensions of the matrices A, B, C, D and Q and vector, r.

r: vector of the roots

Output

S: inverse of matrix Q (i.e. Q^{-1})

a: First derivative discretization matrix (A)

b: Laplacian discretization matrix (B)

The subroutine consists of essentially three parts. First matrices q, c and d are calculated according to equations (1) to (3).

Next the matrix Q is inverted using the NAG matrix inversion subroutine folaaf The inverted matrix is output in the matrix s.

Finally the matrices A and B are computed using equations (1) to (3). ifail, wkspce are special parameters of the NAG inversion routine.

The main program supplies the necessary input parameters to subroutines roots and Matcol, and outputs the roots of the polynomials, plus the matrices A and B.

(b) LAGRANGE INTERPOLATION POLYNOMIAL METHOD

The alternative method for calculting the A and B matrices has been proposed by Michelsen and Villadsen (1972). This method is based on Lagrange interpolation polynomials and involves neither the matrix inversion nor the explicit expression of the power series representation of the polynomials as in the previous method. According to the authors, this method

is faster and more accurate than that involving matrix inversion. The previous method is very reliable for $N < 10$ with only a few digits lost in the inversion routine; for larger N the process is slow, however, and may give serious distortions of A and B since the Kth column of Q tends to zero for large N and $k \simeq N$. Hence Q becomes nearly singular and the matrices A and B are poorly matched with the collocation abscissae $\bar{x}$

The Nth order Lagrange interpolation polynomial is given by

$$P_N(x) = (x - x_1)(x - x_2) \ \ldots\ldots\ (x-x_N) \qquad \ldots (12a)$$

$$= \prod_{1}^{N} (x - x_i)$$

where x_i are the interpolation points which in this case will be the same as the collocation points.

The Lagrange interpolation formula for any function $\emptyset_N(x)$ can be expressed in terms of the ordinates y_i at the selected interpolation points x_i.

$$\emptyset_N(x) = \sum_{i=0}^{N} \ell_i(x)\, y_i \qquad \ldots(12b)$$

where

$$\ell_i(x) = \frac{P_N(x)}{P_N^{(1)}(x_i)(x-x_i)} \qquad \ldots(12c)$$

$P_N^{(1)}(x_i)$ is the first derivative of $P_N(x)$ at the interpolation point x_i.

$P_N(x)$ is called the node polynomial and $\ell_i(x)$ are the Lagrange polynomials.

For the non-symmetrical problem discussed in Section 5.1.2 there are two extra interpolation points between the interval

(0, 1). This gives a polynomial of N+2th degree in x so that equation (12a) becomes

$$P_{N+2}^{(x)} = (x = x_0)(x - x_1)(x - x_2) \ldots\ldots (x - x_N)(x - x_{N+1})$$
$$= (x = x_0)(x - x_{N+1})\ P_N(x) \qquad \ldots.(12d)$$

Where N is the number of interior interpolation points.

Recall approximating operator or trial function, Y for non-symmetrical problem in general form:

$$Y = a(t) + b(t)\ x + x(1-x) \sum_{i=1}^{N} a_i(t)\ P_{i-1}(x)$$

and ordinate representation of the form:

$$Y = \sum_{i=1}^{N+2} d_i(t)\ P_{i-1}(x)$$

In the same manner, the linear operator for the Lagrange interpolation polynomial of equation (12d) can be represented using equations (12b) and (12c) as follows:

$$Y(x) = \sum_{i=0}^{N+1} \ell_i(x) y_i = \sum_{i=1}^{N+2} {}_i(x) y_i \qquad \ldots(12)$$

and

$$\ell_i(x) = \frac{1}{x - x_i} \cdot \frac{P_{N+2}(x)}{P^{(1)}_{N+2}(x_i)} \qquad \ldots(13)$$

Note that in equation (12d) the interior interpolation points, N are taken as the zeros of the orthogonal polynomial $P_N(x)$, normalized so that leading coefficient is 1.

Also, $x_0 = 0$ and $x_{N+1} = 1$, therefore equation (12d) becomes

$$P_{N+2}(x) = x(x-1)\ P_N(x)$$
$$= \prod_{0}^{N+1} (x - x_i) \qquad \ldots(14)$$

The interior zeros of $P_N(x)$ are $x_1, x_2, \ldots x_N$. The polynomial $P_N(x)$ satisfies the usual orthogonal relationship

$$\int_0^1 w(x)\, P_N(x)\, P_M(x) = C_N\, \delta_{NM} \quad M = 1, \ldots N-1$$

To compute the matrices A and B, the first and second derivatives of the linear operator Y (x) of equation (13) are required, namely.

$$\frac{d^{(k)}}{dx^{(k)}} [\, Y(x)] = \sum_{i=0}^{N+1} \frac{d\ell_i(x)}{dx}\, y(x_i) = [\bar{I}^{(k)}]^T\, \bar{Y} \quad \ldots\ldots(15)$$

Where the superscript (k) denotes kth derivative.

$\bar{Y}$ and $\bar{I}$ are vectors

According to equation (13):

$$(x - x_i)\ \ell_i(x) = \frac{P_{N+2}(x)}{P^{(1)}_{N+2}(x_i)}$$

and differentiating with respect to x gives

$$\frac{P^{(1)}_{N+2}(x)}{P^{(1)}_{N+2}(x_i)} = (x - x_i)\ \ell_i^{(1)}(x) + \ell_i(x) \qquad \ldots(16)$$

$$\frac{P^{(2)}_{N+2}(x)}{P^{(1)}_{N+2}(x_i)} = (x - x_i)\ \ell_i^{(2)}(x) + 2\, \ell_i^{(1)}(x) \qquad \ldots(17)$$

where superscripts (1) and (2) denoted first and second derivatives respectively or in general:

$$\frac{P^{(k)}_{N+2}(x)}{P^{(1)}_{N+2}(x_i)} = (x - x_i)\, \ell^{(k)}(x) + k\, \ell_i^{(K-1)}(x) \qquad \ldots(18)$$

Let j represent the jth collocation point and i represent any given interpolation point Equation (18) gives different values depending on whether $i \neq j$ or $i = j$.

To interpolate at $x = x_i$ equation (18) gives the Lagrange polynomial differential as

$$\ell_i^{(k-1)}(x_i) = \frac{1}{k} \cdot \frac{P_{N+2}^{(k)}(x_i)}{P_{N+2}^{(1)}(x_i)} \qquad \ldots(19)$$

Since the first term drops out and for $x = x_j \neq x_i$

$$\ell_i^{(k)}(x_j) = \frac{1}{x_j - x_i} \left[\frac{P_{N+2}^{(k)}(x_j)}{P_{N+2}^{(1)}(x_i)} - k.\ \ell_i^{(k-1)}(x_j) \right] \qquad \ldots(20)$$

So that for first and second differentials of $\ell_i(x)$ are as follows

(a) At $x = x_i$ equation (19) gives:

$$\ell_i^{(1)}(x_i) = \frac{1}{2} \frac{P_{N+2}^{(2)}(x_i)}{P_{N+2}^{(1)}(x_i)} \qquad \ldots(21)$$

and

$$\ell_i^{(2)}(x_i) = \frac{1}{3} \frac{P_{N+2}^{(3)}(x_i)}{P_{N+2}^{(1)}(x_i)} \qquad \ldots(22)$$

(b) At $x = x_j$ equation (20) gives:

$$\ell_i^{(1)}(x_j) = \frac{1}{x_j - x_i} \frac{P_{N+2}^{(1)}(x_j)}{P_{N+2)}^{(1)}(x_i)} \quad [\text{since } \ell_i(x_j) = 0] \qquad \ldots(23)$$

$$\ell_i^{(2)}(x_j) = \frac{1}{x_j - x_i} \quad \frac{P_{N+2}^{(2)}(x_j)}{P_{N+2}^{(1)}(x_i)} - 2\,\ell_i^{(1)}(x_j) \qquad \ldots(24a)$$

Substituting for $P_{N+2}^{(1)}(x_i)$ in equation (24a) gives

$$\ell_i^{(2)}(x_j) = \ell_i^{(1)}(x_j) \quad \frac{P_{N+2}^{(2)}(x_j)}{P_{N+1}^{(1)}(x_j)} - 2\,\frac{1}{x_j - x_i} \qquad \ldots(24b)$$

Put $\ell_j^{(1)}(x_j) = \frac{1}{2} \quad \frac{P_{N+2}^{(2)}(x_j)}{P_{N+2}^{(1)}(x_j)}$ (see equation 19)

Eauation (24b) becomes

$$\ell_i^{(2)}(x_j) = 2\,\ell_i^{(1)}(x_j)\left[\ell_j^{(1)}(x_j) - \frac{1}{x_j - x_i}\right] \qquad \ldots(24)$$

All the coefficients $\ell_i^{(1)}(x_j)$ and $\ell_i^{(2)}(x_j)$, i = 1, 2, ...N+2 and j = 1, 2, ...N+2 can therefore be calculated from the three derivatives of $P_{N+2}(x_j)$ $P_{N+2}^{(1)}(x_j)$, $P_{N+2}^{(2)}(x_j)$, and $P_{N+2}^{(3)}(x_j)$, j = 1, 2, ... N+2

The vector of derivatives

$$\bar{Y}^{(1)} = \left[\left(\frac{dy}{dx}\right)_{x=x_i}, \left(\frac{dy}{dx}\right)_{x=x_2}, \ldots, \left(\frac{dy}{dx}\right)_{x=x_N}\right]^T \qquad \ldots(25)$$

may be expressed as:

$$\frac{d(\bar{Y})}{dx} = \bar{A}\,\bar{Y} \qquad \ldots(26)$$

Where $A_{ji} = \ell_i^{(1)}(x_j)$ and similarly

$$\frac{d^2}{dx^2}(\bar{Y}) = \bar{B}\,\bar{y} \qquad \ldots(27)$$

Where $B_{ji} = \ell_i^{(2)}(x_j)$.

However, to calculate $\ell_i^{(1)}(x_j)$ and $\ell_i^{(2)}(x_j)$ the derivatives of the node polynomial $P_{N+2}(x)$ at given interpolation points (say x_i) are required. Villadsen and Michelsen (1978) have given a recurrence formula for the node polynomial:

$$P_{n+2}(x) = \prod_{j=1}^{N+2} (x - x_j)$$

As $P_0(x) = 1$

and $$P_j(x) = (x - x_j)\, P_{j-1}(x) \quad j = 1, 2, \ldots N+2 \quad \ldots(28)$$

Differentianting the recurrence formula of equation (28) w.r.t.x gives:

$$p_j^{(1)}(x) = (x - x_j)p_{j-1}^{(1)}(x) + P_{j-1} \quad \ldots(29)$$

$$p_j^{(2)}(x) = (x - x_j)P_{j-1}^{(2)} + 2\, P_{j-1}^{(1)}(x) \quad \ldots(30)$$

$$p_j^{(3)}(x) = (x - x_j)p_{j-1}^{(3)}9x) + 1\, p_{j-1}^{(2)}(x) \quad \ldots(31)$$

with $p_0^{(1)}(x) = P_0^{(2)}(x) = p_0^{(3)}(x) = 0$

where x_j is the jth zero of $P_{N+2}(x)$.

Values of $P_{N+2}^{(k)}(x_i)$ may thus be found by simultaneous evaluation of equations (28) to (31) with x_i inserted for x. Reduction in computing time is obtained when the interpolation points are re-ordered such that the x_i value at which $P_{N+2}^{(k)}(x)$ is to be evaluated is always placed first:

$$x_i, x_1, x_2 \ldots\ldots, x_{i-1}, x_{i+1}, \ldots\ldots, x_{N+1}$$

Starting from $p_0(x_i) = 1$, $p_0^{(K)}(x_i) = 0$, K = 1, 2, 3 to obtain from equations (28) to (31).

$$p_1(x_i) = (x_i - x_i)p_0(x_i) = 0$$
$$p_1^{(1)}(x_i) = (x_i - x_i)p_0^{(1)}(x_i) + p_0(x_i) = 1$$
$$p_1^{(2)}(x_i) = (x_i - x_i)p_0^{(2)}(x_i) + 2p_0^{(2)}(x_i) = 0$$
$$p_1^{(3)}(x_i) = (x_i - x_i)p_0^{(3)}(x_i) + 3p_0^{(2)}(x_i) = 0$$

$p_j(x_1)$ remains zero for all $j > 1$, and equations (29) to (31) become:

$$p_j^{(1)}(x_i) = (x_i - x_j) \qquad ...(32)$$

$$p_j^{(2)}(x_i) = (x_i - x_j)p_{(j-1)}^{(2)}(x_i) + 2p_{(j-1)}^{(1)}(x_i) \qquad ...(33)$$

$$p_j^{(3)}(x_i) = (x_i - x_j)P_{(j-1)}^{(3)}(x_i) + 3p_{(j-1)}^{(2)}(x_i) \qquad ...(34)$$

with j = 2, 3, ... i-1, i+1, ..., N+2 and starting from

$$p_1^{(1)}(x_i) = 1, \quad p_1^{(2)}(x_i) = p_1^{(3)}(x_i) = 0 \qquad ...(35)$$

Equations (21) to (24) and (32) to (34) are valid for any choice of distinct interpolation points x_i (Valladsen and Michelsen, 1978).

The listing of the program (program Lang which calculates the discretization matrices A and B using the equations (21) to (24), (32) to (34) and (26) to (27) is shown on the next page.

In addition to the calculation of the roots of the polynomial as in program COLMAT; the subroutine roots also calculates the first three derivatives of the node polynomial

Fig. A3. Listing of Program Lang for Calculation of Collocation Constants.

```
c*************************************************************
c
      program lang
c
c*************************************************************
      implicit double precision(a-h,o-z)
      dimension w(4,4),a(4,4),b(4,4)
      dimension dif1(4),dif2(4),dif3(4),root(4)
      dimension v1(4),v2(4)
      data nn3,n/4,2/
      open(6,file='result',form='formatted',status='new')
      call roots(nn3,dif1,dif2,dif3,root)
c
c seyt up the A and B matrices
      do 2000 i=1,4
      call dfopr(4,2,1,1,i,1,dif1,dif2,dif3,root,v1)
      call dfopr(4,2,1,1,i,2,dif1,dif2,dif3,root,v2)
      do 3000 j=1,4
      a(i,j)=v1(j)
      b(i,j)=v2(j)
 3000 continue
 2000 continue
      write(6,1)
    1 format(//  '   THE PROGRAM LANG OUTPUT IS: ' //)
      write(6,2)
    2 format(/  '  THE ROOTS OF THE POLYNOMIAL ARE:  '  /)
      write(6,1000)(root(i),i=1,4)
      write(6,3)
    3 format(/  '  THE A MATRIX IS: '  /)
      write(6,1000)((a(i,j),j=1,4),i=1,4)
      write(6,4)
    4 format(/  ' THE B MATRIX IS: ' /)
      write(6,1000)((b(i,j),j=1,4),i=1,4)
 1000 format(4(1x,d11.3))
      stop
      end
c*************************************************************
      subroutine roots(nn3,dif1,dif2,dif3,root)
c*************************************************************
      implicit double precision(a-h,o-z)
      dimension dif1(4),dif2(4),dif3(4),root(nn3)
c
c  EVALUATION OF THE ROOTS AND THE DERIVATIVES OF THE
c JACOBI POLYNOMIALS, PN(AL<BE).
c  FIRS EVALUATION OF THE COEFF. IN THE RECURSION FORMULAE
c TO BE STORED IN THE DEF1 &DEF2
c
c
c     INPUT:
c         n       =NO OF THE INTERIOR COLLO CATION POINTS
c        (AL,BE)  =(0,0)- IEGENDRE POLYNOMIALS
c                 =(1,0)- JACOBI POLYNOMIALS
c
c*************************************************************
c
c  NEXT 3 THREE STATERMENTS FOR THIS CASE
c
      n=2
      al=0.0d00
      be=0.0d00
```

```
      n0=1
      n1=1
      nt=n+n0+n1
      ab=al+be
      ad=be-al
      ap=be*al
      dif1(1)=(ad/(ab+2.0d00)+1.0d00)/2.0d00
      dif2(1)=0.0d00
      if(n.lt.2) go to 15
      do 10 i=2,n
      z1=dble(i-1)
      z=ab+2.0d00*z1
      dif1(i)=(ab*ad/z/(z+2.0d00)+1.0d00)/2.0d00
      if(i.ne.2) go to 11
      dif2(i)=(ab+ap+z1)/z/z/(z+1.0d00)
      go to 10
   11 z=z*z
      y=z1*(ab+z1)
      y=y*(ap+y)
      dif2(i)=y/z/(z-1.0d00)
   10 continue
c
c   ROOT DETERMINATION BY THE NEWTON METHOD WITH THE SUPRESSION
c   OF THE PREVIOUSLY DETERMINED ROOTS
c
   15 x=0.0d00
       do 20 i=1,n
   25  xd=0.0d00
       xn=1.0d00
       xd1=0.0d00
       xn1=0.0d00
         do 30 j=1,n
         xp=(dif1(j)-x)*xn-dif2(j)*xd
         xp1=(dif1(j)-x)*xn1-dif2(j)*xd1-xn
         xd=xn
         xd1=xn1
         xn=xp
   30    xn1=xp1
      zc=1.0d00
      z=xn/xn1
      if(i.eq.1) go to 21
        do 22 j=2,i
   22   zc=zc-z/(x-root(j-1))
   21 z=z/zc
      x=x-z
      if(dabs(z).gt.1.0d-09) go to 25
      root(i)=x
      x=x+.00010d00
   20 continue
c
c  ADD EVENTUAL INTERPOLATION POINTS AT x=0,AND x=1
c
c
      if(n0.eq.0) go to 35
      do 31 i=1,n
      j=n+1-i
   31 root(j+1)=root(j)
      root(1)=0.0d00
  35 if(n1.eq.1) root(nt)=1.0d00
c
```

```
c   EVALUATES DERIVATIVES OF POLYNOMIAL
c
      do 40 i=1,nt
      x=root(i)
      dif1(i)=1.0d00
      dif2(i)=0.0d00
      dif3(i)=0.0d00
         do 40 j=1,nt
         if(j.eq.i) go to 40
         y=x-root(j)
         dif3(i)=y*dif3(i)+3.0d00*dif2(i)
         dif2(i)=y*dif2(i)+2.0d00*dif1(i)
         dif1(i)=y*dif1(i)
   40 continue
      return
      end
c*************************************************************
      subroutine dfopr(nd,n,n0,n1,i,id,dif1,dif2,dif3,root,vect)
c*************************************************************
c
      implicit double precision(a-h,o-z)
      dimension dif1(nd),dif2(nd),dif3(nd),root(nd),vect(nd)
c
c this subroutine evaluates the discretization matrices and
c guassian quadrature weights,normalised to sum 1
c
c   ID=1;DISCRETION MATRIX FOR Y(1)
c   ID=2:    ,,        ,,   ,, y(2)
c   id=3: guassian quadrature weights
c
      nt=n+n0+n1
      if(id.eq.3) go to 10
      do 20 j=1,nt
      if(j.ne.i) go to 21
      if(id.ne.1) go to 5
      vect(i)=dif2(i)/dif1(i)/2
      go to 20
    5 vect(i)=dif3(i)/dif1(i)/3
      go to 20
   21 y=root(i)-root(j)
      vect(j)=dif1(i)/dif1(j)/y
      if(id.eq.2)vect(j)=vect(j)*(dif2(i)/dif1(i)-2/y)
   20 continue
      go to 50
   10 y=0.0d00
      do 25 j=1,nt
      x=root(j)
      ax=x*(1-x)
      if(n0.eq.0)ax=ax/x/x
      if(n1.eq.0)ax=ax/(1-x)/(1-x)
      vect(j)=ax/dif1(j)**2
   25 y=y+vect(j)
      do 60 j=1,nt
   60 vect(j)=vect(j)/y
   50 return
      end
```

THE PROGRAM LANG OUTPUT IS:

THE ROOTS OF THE POLYNOMIAL ARE:

0.000D+00 0.211D+00 0.789D+00 0.100D+01

THE A MATRIX IS:

-0.700D+01	0.820D+01	-0.220D+01	0.100D+01
-0.273D+01	0.173D+01	0.173D+01	-0.732D+00
0.732D+00	-0.173D+01	-0.173D+01	0.273D+01
-0.100D+01	0.220D+01	-0.820D+01	0.700D+01

THE B MATRIX IS:

0.240D+02	-0.372D+02	0.252D+02	-0.120D+02
0.164D+02	-0.240D+02	0.120D+02	-0.439D+01
-0.439D+01	0.120D+02	-0.240D+02	0.164D+02
-0.120D+02	0.252D+02	-0.372D+02	0.240D+02

$$P_{NT}(x) = P_{N+2}(x) = x^{NO} P_N(x)(x-1)^{N1} \qquad ...(14)$$

Subroutine roots evaluate the derivatives at the interpolation points according to equations (32) to (34) after putting $p_1^{(1)}(x_i) = 1$, $p_1^{(2)}(x_i) = p_1^{(3)}(x_i) = 0$ as in equation (35). The derivatives are stored in the vectors Dif1, Dif2 and Dif3 for the first, second and 3rd derivatives respectively.

In addition to the above, subroutine Dfopr accepts the input of derivatives, of the polynomials and the roots (interpolation points) from subroutine roots via the main program. The first and second derivatives of the Lagrange polynomials $\ell_i(x_i)$ are computed with equations (21) to (24); their values are stored in the vector vect.

A call of subroutine Dfopr from the main program passes the derivative of the Lagrange polynomials for the computation of A and B, matrices via the vectors V1 (for A matrix) and V2 (for B matrix) using equations (26) to (27) in the main program. The I.D. input parameter in subroutine Dfopr indicates the call for $\ell_i^{(1)}$ [V1] (I.D. = 1) or $\ell_i^{(2)}$ [V2] for I.D. = 2.

APPENDIX 6

SIMULATION OF BREAKTHROUGH CURVE: COMPUTER PROGRAM

(a) Non porous particle model equation.

The simulation of the breakthrough curve (B.T.C.) was carried out using the orthogonal collocation scheme as formulated in Appendix 4 (equations (17) - (20)). The ISIM interactive simulator for ordinary differential equations (O.D.E.) using the 4th order Runge-Kutta integration method was used.

To formulate the model equations suitable for use with ISIM the model equations referred to above were re-written as follows:

Fluid phase equation:

$$\frac{dc_j}{d\theta} = \sum_{i=1}^{m-1} (M1\ B_{ji} - A_{ji})c_i - \frac{\beta}{\epsilon}\left[K_A c_j(1-q_j) - k_B q_j\right]$$

$$= \sum_{i=1}^{m-1} (M1\ B_{ji} - A_{ji})c_i - BT\ \left[K_A c_j(1-q_j) - K_B q_j\right] \qquad \ldots(1a)$$

where $M1 = 1/Pe$; $BT = \beta/\epsilon$

$m-1 = N$ = number of interior collocation points

$j = 2, \ldots. N$

The first and last collocation points are given by c_1 and c_m respectively and have been derived from the boundary conditions. There are therefore N O.D.E.'s to solve. Equation (1a) was reduced further by substituting x_j for

$$\sum_{i=1}^{m-1} (M1\ B_{ji} - A_{ji})c_i$$

so that the O.D.E.8s are of the form

$$\frac{dc_j}{d\theta} = x_j - BT\left[K_A c_j(1-q_j) - k_B q_j\right] \qquad \ldots(1)$$

The Rate Equation

This is in the form

$$\frac{dq_j}{d\theta} = K_A c_j(1-q_j) - k_B q_j \qquad \ldots(2)$$

First and last collocation points

$$c_1 = \frac{-Pe - \sum_{i=2}^{m-1} \left(A_{i1} - \frac{A_{mi}A_{1m}}{A_{mm}}\right) c_i}{A_{11} - Pe - \frac{A_{m1}A_{1m}}{A_{mm}}} \qquad \ldots(3a)$$

$$= \frac{-Pe\, A_{mm} - \sum_{i=2}^{m-1} (A_{ij}A_{mm} - A_{mi}A_{1m})c_i}{(A_{11}-Pe)\, A_{mm} - A_{m1}\, A_{1m}} \qquad \ldots(3)$$

$$c_m = \sum_{i=1}^{m-1} \left(\frac{A_{mi}}{A_{mm}}\right) c_i \qquad \ldots(4)$$

The general flow sheet for the simulation has been given in Figure 5.3. Figure 1 shows the Listing of the ISIM program for the simulation of the adsorption breakthrough curve using equations (1) to (4). the sequence of computation as shown in the program is

c_1

$\frac{dc_j}{d\theta}$ = c_j' in the ISIm program

$\frac{dq_j}{d\theta}$ = q'_j in the ISIM program

$c_m = c_7$ in the ISIM program

Five interior collocation points (or 7 total) were used for all simulations.

Fig. A4. Listing of Computer Program for Non-Porous Model.

```
CONSTANT ALGO=1,TFIN=200,CINT=.02,NOCI=50
constant n=1,e=.721
constant ax=.16909e-4
constant u=1.478,lc=.05,pe=10
DIMENSION A(7,7),B(7,7)
CONSTANT A=-31.0,-13.09609,3.73216,-1.875
CONSTANT 1.11962,-0.64458,1.0,34.69972,10.13408
CONSTANT -7.62512,3.36805,-1.94084,1.10353
CONSTANT -1.70788,-5.03152,3.87973,1.51671
CONSTANT -4.04306,1.85712,-0.98752,1.50942
CONSTANT 2.13333,-1.44628,3.41215,0.0
CONSTANT -3.412125,1.44628,-2.13333,-1.50942
CONSTANT 0.98752,-1.85712,4.04306,-1.51671
CONSTANT -3.87973,5.03152,1.70788,-1.10353
CONSTANT 1.94084,-3.36805,7.62512,-10.13408
CONSTANT -34.69972,-1.0,0.64458,-1.11962
CONSTANT 1.8750,-3.73216,13.09609,31.0
CONSTANT B=480.0,292.91504,-21.02473,7.5
CONSTANT -6.30728,14.41697,60.0,-671.96836
CONSTANT -390.42093,59.8168,-14.86704,11.26125
CONSTANT -24.80217,-102.3049,268.3469,120.83914
CONSTANT -66.91239,30.03371,-12.53116,22.74946
CONSTANT 89.65971,-123.73334,-35.6975,35.6975
CONSTANT -45.333,35.69749,-35.69749,-123.7333,89.65971
CONSTANT 22.74946,-12.53116,30.03371,-66.9124
CONSTANT 120.83915,268.34691,-102.3045,-24.80217
CONSTANT 11.26125,-14.86704,59.81681,-390.42094
CONSTANT -671.9680,60.0,14.41697,-6.30728
CONSTANT 7.50,-21.02472,292.91503,480.0
INITIAL
PRINT" LYSOZYME BREAKTHROUGH CURVE"
PRINT" B.T.C NUMBER,N            =",N
PRINT"TYPE OF COLUMN USED IS 1/4 INCH"
PRINT"DIMENSINLESS FORWARD RATE CONT.,KA,=",KA,"(-)"
PRINT"MAX ADSORBENT CONC. ,QM     =",QM," (KG/M3)"
PRINT"ADSORBATE CONC.(INLET),C0   =",C0," (KG/M3)"
PRINT"PECLECT NUMBER          PE  =",PE," (-)"
PRINT"BED LENGHT              ,LC =",LC," (M)"
PRINT"DISSOCIATION CONSTANT ,KD   =",KD," (KG/M3)"
PRINT"INTEGRATION STEP LENGHT,CINT=",CINT,"(H)"
PRINT"FORWARD RATE CONST.  ,K1=",K1, "(M3/KG/H)"
PRINT"AXIAL VELOCITY       ,U=",U," (M/H)"
C1=0;C2=0;C3=0;C4=0;C5=0;C6=0;C7=0
Q1=0;Q2=0;Q3=0;Q4=0;Q5=0;Q6=0;Q7=0
DYNAMIC
:COMPUTE THE  KINETICS CONSTANT
tbar=lc/u;bt=qm/(c0*e)
KA=K1*C0*TBAR
kb=k1*kd*tbar
TR=T*TBAR;MIN=TR*60
BV=LC*AX
```

```
VT=U*AX*TR;EBV=VT/BV
M1=1/PE;PJ=A(7,7)*PE
PIE=((A(1,1)-PE)*A(7,7))-(A(1,7)*A(7,1))
PI=1/PIE;B1=A(7,1)/A(7,7)
D2=(M1*B(2,1))-(A(2,1))
D3=(M1*B(3,1))-(A(3,1))
D4=(M1*B(4,1))-(A(4,1))
D5=(M1*B(5,1))-(A(5,1))
D6=(M1*B(6,1))-(A(6,1))
:COMPUTE THE JM CONSTANT
E2=(M1*B(2,7))-(A(2,7))
E3=(M1*B(3,7))-(A(3,7))
E4=(M1*B(4,7))-(A(4,7))
E5=(M1*B(5,7))-(A(5,7))
E6=(M1*B(6,7))-(A(6,7))
:COMPUTE THE POINT 1  CONSTANTS
A2=(A(1,2)*A(7,7))-(A(7,2)*A(1,7))
A3=(A(1,3)*A(7,7))-(A(7,3)*A(1,7))
A4=(A(1,4)*A(7,7))-(A(7,4)*A(1,7))
A5=(A(1,5)*A(7,7))-(A(7,5)*A(1,7))
A6=(A(1,6)*A(7,7))-(A(7,5)*A(1,7))
:COMPUTE THE C7 CONSTANTS
B2=A(7,2)/A(7,7);B3=A(7,3)/A(7,7)
B4=A(7,4)/A(7,7);B5=A(7,5)/A(7,7)
B6=A(7,6)/A(7,7)
S2=(M1*B(2,2))-(A(2,2))
S3=(M1*B(2,3))-(A(2,3))
S4=(M1*B(2,4))-(A(2,4))
S5=(M1*B(2,5))-(A(2,5))
S6=(M1*B(2,6))-(A(2,6))
:COMPUTE POINT 3 CONSTANTS
P2=(M1*B(3,2))-(A(3,2))
P3=(M1*B(3,3))-(A(3,3))
P4=(M1*B(3,4))-(A(3,4))
P5=(M1*B(3,5))-(A(3,5))
P6=(M1*B(3,6))-(A(3,6))
:COMPUTE POINT 4 CONSTANTS
M2=(M1*B(4,2))-(A(4,2))
M3=(M1*B(4,3))-(A(4,3))
M4=(M1*B(4,4))-(A(4,4))
M5=(M1*B(4,5))-(A(4,5))
M6=(M1*B(4,6))-(A(4,6))
:COMPUTE POINT 5 CONSTANTS
N2=(M1*B(5,2))-(A(5,2))
N3=(M1*B(5,3))-(A(5,3))
N4=(M1*B(5,4))-(A(5,4))
N5=(M1*B(5,5))-(A(5,5))
N6=(M1*B(5,6))-(A(5,6))
:COMPUTE POINT 6 CONSTANTS
T2=(M1*B(6,2))-(A(6,2))
T3=(M1*B(6,3))-(A(6,3))
T4=(M1*B(6,4))-(A(6,4))
T5=(M1*B(6,5))-(A(6,5))
T6=(M1*B(6,6))-(A(6,6))
C1=PI*(-PJ-(C2*A2+C3*A3+C4*A4+C5*A5+C6*A6))
X2=C2*S2+C3*S3+C4*S4+C5*S5+C6*S6+D2*C1+E2*C7
C2'=X2-BT*((KA*C2*(1-Q2)-(KB*Q2)))
Q2'=(KA*C2*(1-Q2))-(KB*Q2)
X3=C2*P2+C3*P3+C4*P4+C5*P5+C6*P6+D3*C1+E3*C7
C3'=X3-BT*((KA*C3*(1-Q3)-(KB*Q3)))
Q3'=(KA*C3*(1-Q3))-(KB*Q3)
```

```
X4=C2*M2+C3*M3+C4*M4+C5*M5+C6*M6+C1*D4+C7*E4
C4'=X4-BT*((KA*C4*(1-Q4)-(KB*Q4)))
Q4'=(KA*C4*(1-Q4))-(KB*Q4)
X5=C2*N2+C3*N3+C4*N4+C5*N5+C6*N6+D5*C1+E5*C7
C5'=X5-BT*((KA*C5*(1-Q5)-(KB*Q5)))
Q5'=(KA*C5*(1-Q5))-(KB*Q5)
X6=C2*T2+C3*T3+C4*T4+C5*T5+C6*T6+D6*C1+C7*E6
C6'=X6-BT*((KA*C6*(1-Q6)-(KB*Q6)))

 Q6'=(KA*C6*(1-Q6))-(KB*Q6)
 C7=-(C1*B1+C2*B2+C3*B3+C4*B4+C5*B5+C6*B6)
 terminate c7.gt.1
 PREPARE MIN,EBV,C7,Q6
 OUTPUT MIN,EBV,C7,Q6
 $ VAL K1       =   3.6200
 $ VAL KD       =  0.56000
 $ VAL QM       =   11.200
 $ VAL C0       =   1.0000
 $ VAL CINT     =  0.40000E-01
 $ VAL NOCI     =   25.000
```